

POLYMERS AND COATINGS DERIVED FROM NOVEL BIO-BASED VINYL ETHER

MONOMERS

A Dissertation
Submitted to the Graduate Faculty
of the
North Dakota State University
of Agriculture and Applied Science

By

Deep Jyoti Kalita

In Partial Fulfillment of the Requirements
for the Degree of
DOCTOR OF PHILOSOPHY

Major Department:
Coatings and Polymeric Materials

March 2018

Fargo, North Dakota

North Dakota State University
Graduate School

Title

POLYMERS AND COATINGS DERIVED FROM NOVEL BIO-BASED
VINYL ETHER MONOMERS

By

Deep Jyoti Kalita

The Supervisory Committee certifies that this *disquisition* complies with North Dakota
State University's regulations and meets the accepted standards for the degree of

DOCTOR OF PHILOSOPHY

SUPERVISORY COMMITTEE:

Dr. Dean C. Webster

Chair

Dr. Bret J. Chisholm

Dr. Andriy Voronov

Dr. Dilpreet Bajwa

Approved:

04/06/2018

Date

Dr. Dean. C. Webster

Department Chair

ABSTRACT

To fulfill the demand for household, industrial, light weight transportation, health, and cosmetic products etc., production of polymeric materials has been increasing every year. However, limited resource of fossil fuel is threatening the sustainability of the raw materials used to produce these products. These products have very low to no biodegradability, thereby staying in the ecosystem for long time causing serious threats. Increasing environmental concerns and strict regulations has made renewable based materials suitable for the development of environmental friendly polymers with sustainability.

Novel plant oil based vinyl ether (POVE) monomers were derived from plant oil such as soybean, linseed and camelina oil. Polymers varying in molecular weight (MW) were derived from these monomers and studied for air-drying coatings. Study of the coating and free film properties showed that at a given MW, Tensile (Young's modulus, and tensile strength), viscoelastic (T_g , XLD), physical (hardness, solvent resistance, and impact resistance) properties increased with increasing unsaturation in the parent PO. Polymers derived from distilled POVE monomers resulted essentially colorless poly(POVEs) which were evaluated as a binder for artist paint in comparison to linseed oil. Colorless poly(POVE)s showed significantly faster dry/cure along with dramatically lower yellowness than linseed oil.

Novel, vinyl ether monomers, were also synthesized from cardanol (CEVE) and eugenol (EEVE) and coatings produced from their homopolymers and copolymers with cyclohexyl vinyl ether were studied in comparison to commercial alkyds. Glass transition temperatures of these homopolymers were increased with CHVE incorporation. However, incorporation of 25% CHVE resulted in cured coatings and free films with better mechanical, viscoelastic and physical properties than commercial alkyds. Incorporation of CHVE > 50wt.% in the copolymer resulted

in low crosslinked networks with reduced properties such as percent elongation, chemical resistance and impact resistance. Epoxidized poly(E EVE) resins varying in percent epoxide (30%, 50% and 70%) were synthesized and studied for two component amine cured coatings in comparison to BPA based epoxy resin. Results obtained from high throughput experimentation showed the ability of Epoly(E EVE) resins with 50% or higher epoxide to form harder, higher crosslinked coatings with tunability based on type of curative than BPA based resin.

ACKNOWLEDGEMENTS

I would like to express my deepest appreciation to my advisor Dr. Dean C. Webster and my mentor Dr. Bret J. Chisholm, for their guidance and support during the course of this research. Without their guidance and persistent help this dissertation would not have been possible. I am grateful to my committee members Dr. Andriy Voronov and Dr. Dilpreet Bajwa for their time and guidance during my graduate tenure at North Dakota State University.

I would like to thank all the former members of Dr. Chisholm's group especially to Harjyoti, Ihor, Olena, Sneha, Taehyun, Rriddhiman, Samim, Satyabrat, Andry, Jim, Shane, Lyndsiy for their help and sharing their expertise during research. I would like to thank all the members from Dr. Webster's group for giving me accommodation and helping me out whenever I struggled with my research. Since science cannot be done without instrumentation, I would like to thank Heide, Chunju, Greg and Fred for sharing their expertise in various instruments.

I cannot be more grateful to my family members especially to my parents and my lively wife Priyanka Kalita for their constant support and encouragements throughout my graduate study. Their blessings have helped me to achieve my goals.

My immense gratitude to all the faculty members of Coatings and Polymeric Materials who had shared their knowledge and experiences in the polymer and coating field.

Finally, I would like to thank National Science Foundation EPSCoR Program (grant IIA-1355466) for providing financial support for my research.

DEDICATION

To my parents Jiban Chandra Kalita, Anima Kalita; to my lovely wife Priyanka Kalita.

TABLE OF CONTENTS

ABSTRACT	iii
ACKNOWLEDGEMENTS	v
DEDICATION	vi
LIST OF TABLES	xv
LIST OF FIGURES	xviii
CHAPTER 1. INTRODUCTION	1
1.1. Development of linear chain growth polymers from renewables: early challenges and recent successes	1
1.2. Polymers derived using acrylic functionality	5
1.3. Polymers derived using vinyl ether functionality	17
1.4. Polymers derived using vinyl ester and allyl ester functionality.....	26
1.5. Polymers derived using cyclic imino ether, norbornene, aromatic functionality.....	29
1.6. Summary and outlook	36
1.7. Need statement	37
1.8. Research objectives	38
1.9. Organization of this dissertation	38
1.10. References	39
CHAPTER 2. BIOBASED POLY(VINYLEETHER)S DERIVED FROM SOYBEAN OIL, LINSEED OIL, AND CAMELINA OIL: SYNTHESIS, CHARACTERIZATION, AND PROPERTIES OF CROSSLINKED NETWORKS AND SURFACE COATINGS	46
2.1. Abstract	46
2.2. Introduction	47
2.3. Experimental	54
2.3.1. Materials	54
2.3.2. Synthesis of monomer	56

2.3.3. Synthesis of polymers.....	57
2.3.4. Preparation of coatings and crosslinked free films.....	59
2.3.5. Methods and instrumentation	59
2.3.5.1. Nuclear magnetic resonance (NMR) spectroscopy.....	59
2.3.5.2. Gel permeation chromatography (GPC)	59
2.3.5.3. Dynamic mechanical analysis (DMA).....	60
2.3.5.4. Tensile testing	60
2.3.5.5. Dynamic viscosity.....	60
2.3.5.6. Drying time measurement.....	61
2.3.5.7. Coating property	61
2.4. Results and discussion.....	61
2.4.1. Synthesis and characterization	61
2.4.1.1. Monomer synthesis and characterization.....	61
2.4.1.2. Polymer synthesis and characterization.....	62
2.4.1.3. Viscosity measurement	64
2.4.1.4. Drying time measurements	66
2.4.2. Viscoelastic properties of crosslinked free-films	68
2.4.3. Mechanical properties of cured films	70
2.4.4. Properties of surface coatings.....	72
2.5. Conclusion.....	75
2.6. References	77
CHAPTER 3. PLANT OIL-BASED COATINGS WITH FAST DRYING/CURING AND LOW YELLOWNESS	83
3.1. Abstract	83
3.2. Introduction	84
3.3. Materials and methods	87

3.3.1. Materials	87
3.3.2. Synthesis of colorless plant oil vinyl ether (POVE) monomers from soybean oil (2-VOES), linseed oil (2-VOEL) and palm oil (2-VOEP).....	88
3.3.3. Synthesis of poly(2-VOEL), poly(2-VOES), and poly(2-VOEP).....	90
3.3.4. Synthesis of copolymers from 2-VOEL, 2-VOES, and 2-VOEP.....	91
3.3.5. Preparation of coatings	93
3.3.6. Instrumentations and methods.....	94
3.3.6.1. Differential scanning calorimetry (DSC).....	94
3.3.6.2. Gel permeation chromatography (GPC)	94
3.3.6.3. Nuclear magnetic resonance (NMR) spectroscopy.....	94
3.3.6.4. Fourier transform infrared (FT-IR) spectroscopy	95
3.3.6.5. Drying time measurements	95
3.3.6.6. Ultraviolet-visible spectrometer (UV-VIS)	95
3.3.6.7. Viscosity measurement	95
3.3.6.8. Tristimulus colorimeter.....	96
3.3.6.9. Coating properties	96
3.4. Results and discussion.....	96
3.4.1. Characterization of POVE monomers	96
3.4.2. Characterization of homopolymers and copolymers	98
3.4.3. Visual and spectroscopic confirmation of removal of color impurities	101
3.4.4. Thermal properties of homopolymers and copolymers.....	103
3.4.5. Viscosity vs molecular weight (MW) of 2-VOES homopolymers	105
3.4.6. Characterization of coatings	106
3.4.6.1. Drying time measurements of polymers	106
3.4.6.2. Drying time measurements of polymers with pigment.....	108
3.4.6.3. Qualitative and quantitative color evaluation of pigmented coatings.....	111

3.4.6.4. Evaluation of physical properties of cured coatings	114
3.5. Conclusions	117
3.6. References	117
CHAPTER 4. NOVEL BIO-BASED COATING RESINS PRODUCED FROM CARDANOL USING CATIONIC POLYMERIZATION AND THEIR POTENTIAL FOR ALKYD TYPE COATINGS.....	121
4.1. Abstract	121
4.2. Introduction	122
4.3. Materials and methods	125
4.3.1. Materials	125
4.3.2. Synthesis of monomer	126
4.3.3. Synthesis of polymers.....	127
4.3.3.1. Synthesis of CEVE homopolymer	127
4.3.3.2. Synthesis of CHVE homopolymer.....	129
4.3.3.3. Synthesis of copolymer.....	130
4.3.4. Commercial soy based alkyds for coating performance comparison	131
4.3.5. Preparation of cured free films and coatings.....	132
4.3.6. Methods and instrumentation	133
4.3.6.1. Nuclear magnetic resonance (NMR) spectroscopy.....	133
4.3.6.2. Fourier transform resonance (FTIR) spectroscopy	133
4.3.6.3. Gel permeation chromatography (GPC)	133
4.3.6.4. Dynamic viscosity.....	134
4.3.6.5. Dynamical mechanical analysis (DMA).....	134
4.3.6.6. Differential scanning calorimetry (DSC).....	134
4.3.6.7. Tensile testing	135
4.3.6.8. Swelling ratio	135

4.3.6.9. Drying time measurement.....	135
4.3.6.10. Coating property measurement	135
4.4. Results and discussion.....	136
4.4.1. Synthesis and characterization of monomer and polymer.....	136
4.4.2. Thermal properties of polymers	141
4.4.3. Drying time measurement	144
4.4.4. Viscoelastic properties of crosslinked free-films	144
4.4.5. Swelling study of crosslinked films	149
4.4.6. Mechanical properties of cured films	150
4.4.7. Coatings properties.....	154
4.5. Conclusions	157
4.6. References	158
CHAPTER 5. POLY (VINYL ETHER)S BASED ON EUGENOL AND THEIR APPLICATION AS SURFACE COATINGS	161
5.1. Abstract	161
5.2. Introduction	162
5.3. Experimental	164
5.3.1. Materials.....	164
5.3.2. Synthesis of 2-eugenoxylethyl vinyl ether (EEVE)	165
5.3.3. Synthesis of poly (2-eugenoxylethyl vinyl ether), poly(EEVE).....	166
5.3.4. Synthesis of EEVE and cyclohexyl vinyl ether (CHVE) copolymers	168
5.3.5. Synthesis of CHVE homopolymer	169
5.3.6. Commercial soy-based alkyds for coating performance comparison.....	169
5.3.7. Preparation of cured free films and coatings.....	170
5.3.8. Methods and instrumentation	171
5.3.8.1. Nuclear magnetic resonance (NMR) spectroscopy.....	171

5.3.8.2. Fourier transform resonance (FTIR) spectroscopy	171
5.3.8.3. Gel permeation chromatography (GPC)	171
5.3.8.4. Dynamical mechanical analysis (DMA)	172
5.3.8.5. Differential scanning calorimetry (DSC).....	172
5.3.8.6. Tensile testing	172
5.3.8.7. Thermogravimetric analysis (TGA).....	173
5.3.8.8. Gel content	173
5.3.8.9. Drying time measurement.....	173
5.3.8.10. Coating property measurement	173
5.4. Results and discussion.....	174
5.4.1. Synthesis and characterization of monomer and polymer.....	174
5.4.2. GPC analysis	180
5.4.3. Thermal properties of EEVE monomer and polymers	181
5.4.4. Study of autoxidation of poly(EEVE)	183
5.4.5. Drying time measurements	185
5.4.6. Viscoelastic properties of crosslinked free-films	186
5.4.7. Mechanical properties of cured films	191
5.4.8. Coatings properties	194
5.5. Conclusions	200
5.6. References	200
CHAPTER 6. A HIGH THROUGHPUT APPROACH TO STUDY THE EFFECT OF CURATIVES AND LEVELS OF EPOXIATION ON THE PROPERTIES OF THE COATINGS DERIVED FROM EUGENOL.....	205
6.1. Abstract	205
6.2. Introduction	206
6.3. Experimental	209

6.3.1. Materials	209
6.3.2. Synthesis of 2-eugenoxylethyl vinyl ether (EEVE)	209
6.3.3. Synthesis of poly (2-eugenoxylethyl vinyl ether), poly(EEVE).....	211
6.3.4. Synthesis of epoxidized poly (2-eugenoxylethyl vinyl ether), Epoly(EEVE).....	212
6.3.5. Preparation of thermosets	214
6.3.6. Methods and instrumentation	215
6.3.6.1. Dye extraction.....	215
6.3.6.2. Nanoindentation.....	217
6.3.6.3. Differential scanning calorimetry	217
6.3.6.4. Thermogravimetric analysis (TGA).....	218
6.3.6.5. Nuclear magnetic resonance (NMR) spectroscopy.....	218
6.3.6.6. Gel permeation chromatography (GPC)	218
6.3.6.7. Fourier transform resonance (FTIR) spectroscopy	219
6.3.6.8. König pendulum hardness.....	219
6.3.6.9. Measurement of epoxy equivalent weight	219
6.4. Results and discussion.....	219
6.4.1. Synthesis and characterization of EEVE and poly(EEVE)	219
6.4.2. Synthesis and characterization of Epoly(EEVE).....	222
6.4.3. Thermal properties of EEVE, poly(EEVE) and Epoly(EEVE).....	224
6.4.4. Molecular weight and polydispersity index analysis.....	226
6.4.5. Properties of cured coatings	227
6.4.5.1. Dye extraction.....	228
6.4.5.2. Differential scanning calorimetry (DSC).....	230
6.4.5.3. König pendulum hardness (KPH).....	232
6.4.5.4. Nanoindentation.....	235

6.5. Conclusions	239
6.6. References	240
CHAPTER 7. CONCLUSIONS AND FUTURE DIRECTIONS	246
7.1. Conclusions	246
7.2. Future research directions	248

LIST OF TABLES

<u>Table</u>	<u>Page</u>
1.1. Conditions and results for the ATRP of cardanyl acrylate and its copolymers at varying initiator ratio. “Data from reference 21”	12
1.2. Tensile properties of latex films (at room temperature) from OVM and SBM with MMA. “Data from reference 33”	14
1.3. Curing of epoxide containing polycardanol and its hardness. “Data from reference 64”	34
2.1. FA composition and IV of SBO, ⁴ LO, ⁴ and CMO, ⁴⁹ as determined previously.....	54
2.2. A description of the chemicals used for the study.	55
2.3. Composition of the polymerization mixtures used to produce POVE polymers.	58
2.4. T _g , plateau modulus, and XLD obtained from DMA measurements.....	70
2.5. Young’s modulus, tensile strength, and elongation at break for cross-linked networks derived from POVE polymers that varied with respect to composition and MW. Each value represents the average and standard deviation from five test specimens.	72
2.6. Properties of coatings derived from various POVE polymers. Values for pendulum hardness and solvent resistance represent the average and standard deviation from five replicates.	75
3.1. A description of the starting materials used for the study.	88
3.2. Compositions of the polymerization mixtures used to produce POVE homo and copolymers.	92
3.3. Mn and PDI of the homopolymers and copolymers produced from POVEs.	101
3.4. Drying time poly(2-VOES) and linseed oil in presence of TiO ₂	109
3.5. L*, a*, b* values of the coatings prepared with TiO ₂ containing paint films cured at RT and at 120 °C for 5h. (color was measured after 2 months).	112
3.6. L*, a*, b* values showing the color difference between TiO ₂ pigmented produced from pure poly(2-VOES), pure linseed oil and their blend at different weight ratios.....	114
3.7. The drying time of the ultramarine blue-containing paint films.....	114

3.8.	The physical properties of coatings produced from poly(2-VOES), 6.9k and linseed oil with TiO ₂ pigment cured at RT for 60 Days without drier catalyst.	115
3.9.	The physical properties of coatings produced from homopolymers (except poly(2-VOEP) and copolymers with ultramarine blue pigment without drier package.	116
4.1.	A description of the starting materials used for the study.	126
4.2.	Composition of the polymerization mixtures used to produce poly(CEVE-co-CHVE) copolymers.	130
4.3.	Descriptions of the BECKOSOL 1272 and BECKOSOL 10-539 as specified in the data sheet.	132
4.4.	Mn and PDI of the synthesized polymers and commercial alkyd resins measured using GPC.	140
4.5.	Drying time measurement data for polymers with drying catalyst.	144
4.6.	Properties showing the T _g and XLD of the cured films produced from commercial alkyd resin, poly(CEVE), and poly(CEVE-co-CHVE) copolymer.	147
5.1.	A description of the starting materials used for the study.	165
5.2.	Composition of the polymerization mixtures used to produce poly(EEVE-co-CHVE) copolymers and poly(CHVE).	168
5.3.	Descriptions of the commercial alkyds as specified in the data sheet.	170
5.4.	Mn and PDI of the synthesized polymers and commercial alkyd resins.	181
5.5.	Drying time measurement data for polymers with drying catalyst.	186
5.6.	Properties showing the T _g , XLD and gel content of the cured films produced from commercial alkyd resin, poly(EEVE), and poly(EEVE-co-CHVE) copolymer. One set of networks was produced by curing at ambient conditions for 4 weeks, while the other set was cured by heating for an hour at 120 °C and an hour at 150 °C then allowing the coatings to stand at ambient conditions for 4 weeks.	187
5.7.	Young's modulus, tensile strength and elongation of the networks derived from the commercial alkyd resin, poly(EEVE), and poly(EEVE-co-CHVE) copolymer. One set of networks was produced by curing at ambient conditions for 4 weeks, while the other set was cured by heating for an hour at 120 °C and an hour at 150 °C then allowing the coatings to stand at ambient conditions for 4 weeks.	193
5.8.	Properties of coatings derived from the commercial alkyd resin, poly(EEVE), and poly(EEVE-co-CHVE) copolymer.	198
6.1.	A description of the starting materials used for the study.	209

6.2. Compositions for the reaction mixtures used to produce Epoly(E EVE) resins with epoxidation levels of 30, 50 and 70% and their percent conversion evaluated from titration and ^1H NMR.....	214
6.3. List of amine curatives used to study structure-property relationships.	215
6.4. Mn and PDI of the synthesized poly(E EVE) homo-polymers and its epoxy functionalized polymers with three levels of epoxidation. All values are expressed relative to polystyrene standards.....	227

LIST OF FIGURES

<u>Figure</u>	<u>Page</u>
1.1. Transesterification and polymerization scheme of HEA and MO using lipase catalyst. ²⁶	9
1.2. Schematic of the atom transfer radical polymerization of cardanyl acrylate. ²¹	11
1.3. Typical DMTA cure curve of poly(cardanyl acrylate) catalyzed by benzoyl peroxide (4 wt.%), at a heating rate of 3 °C/min in dual cantilever mode. “Reproduced from reference 21”	12
1.4. Synthesis of soy-based acrylic monomer via direct transesterification reaction of triglycerides of soybean oil with N-(hydroxyethyl)acrylamide. ³²	13
1.5. Proposed mechanism for the amidation of triglycerides with amino alcohols using ethanol amine as example and the importance of secondary nature of amino group to achieve H-bonding. “Reproduced from reference 35”	15
1.6. Schematic illustration for the coupling of PS-b-PSBA-b-PS triblock copolymer by bis-TAD. (a) “Click coupling” with 5 mol% of bis-TAD leads to the formation of gel. (b) A slightly “click coupled” (with 1 mol% bis TAD) sample can be well dissolved in THF. (c) Monotonic stress–stain curves of PS49-b-PSBA82-b-PS49 “click coupled” with 1 mol%, 2 mol%, and 5 mol% of bis-TAD respectively. (d) Representative cyclic stress–strain curves of PS49-b-PSBA82-b-PS49 “click coupled” with 1 mol%. For clarity, the curves are shifted on the strain axis. “Reproduced from reference 37”	17
1.7. A schematic illustrating the difference in molecular architecture between a plant oil triglyceride and a synthetic polymer containing a fatty pendent group in the repeat unit. ³⁸	18
1.8. A schematic illustrating the synthesis of cardanol ethyl vinyl ether. ⁴⁶	25
1.9. Synthesis of soy-based 2-oxazoline monomer (SoyOx). ⁶⁸	30
1.10. Oxazoline polymerization via cationic ring opening. ⁶⁸	30
1.11. Proposed mechanism for the formation of cyclic imino ethers derived from N-hydroxyalkyl fatty amides. ³⁵	31
1.12. Representation to the sphere to rice grain morphological transition. ⁷²	32
1.13. Oxidative polymerization of cardanol. ³¹	33
1.14. Oxidative polymerization of cardanol via two different routes. ⁷⁴	34

1.15. Derivatization of triglycerides into N-hydroxyalkyl fatty amides and corresponding ring opening metathesis polymerization of norbornene monomers. ³⁵ ...	35
2.1. Synthesis of a POVE polymer from a PO triglyceride.	52
2.2. ¹ H NMR spectra of 2VOES (bottom), 2VOEL (middle), and 2VOEC (top).	62
2.3. Representative GPC chromatograms using the polymers derived from 2VOEC. The values in the legend correspond to number-average MWs determined using GPC. Chromatograms of polymers with MWs above 15,000 g/mole (A) were obtained using two TSKgel SuperHM columns, while those with MWs below 15,000 g/mole (B) were obtained using two TSKgel SuperH3000 columns.	63
2.4. ¹ H NMR spectra of representative POVE polymers [poly(2VOEC) (bottom), poly(2VOEL) (middle), and poly(2VOES) (top)].	64
2.5. Viscosity at 23 °C as a function of polymer MW for the three series of POVE polymers.	65
2.6. Log (Viscosity) vs Log (Mn) plots for the three series of POVE polymers.	66
2.7. The viscoelastic properties of crosslinked networks derived from POVE polymers that varied with respect to composition and MW. Both the storage modulus response (A and B) and tangent delta response (C and D) are provided.	70
2.8. Plots of tensile stress as a function of elongation for cross-linked networks derived from POVE polymers that varied with respect to composition and MW.	71
2.9. Plots showing correlation of XLD with Young's modulus with XLD.	72
2.10. Plots showing correlation of XLD with pendulum hardness and MEK double rubs.	73
2.11. Plots showing correlation of plateau modulus with pendulum hardness.	74
3.1. Schematic illustrating the synthesis of POVE monomer (2-VOES, 2-VOEL and 2-VOEP).	90
3.2. Schematic illustrating the synthesis of poly(POVE)s.	92
3.3. ¹ H NMR spectrum of the 2-VOES, 2-VOEL and 2-VOEP monomers.	97
3.4. ¹ H NMR spectrum of the poly(2-VOES) and poly(2-VOEL) homo-polymers.	99
3.5. ¹ H NMR spectrum of the poly(2-VOES-co-VOEL)-50/50, poly(2-VOES-co-VOEP)-50/50 and poly(2-VOEL-co-2-VOEP)-50/50 copolymers.	99
3.6. Characteristic FT-IR spectra of linseed oil, 2-VOEL and poly(2-VOEL).	100

3.7. Images that provide a comparison of the color difference between the (C) and (D) two poly(2-VOES) samples produced with purified 2-VOES to (A) linseed oil as well as a (C) poly(2-VOES) produced using non- purified 2-VOES.	102
3.8. Images providing visual confirmation of the synthesis of essentially colorless homopolymers and copolymers from distilled POVE monomers.	102
3.9. UV-VIS spectra of the linseed oil, non-distilled 2-VOES monomer, distilled 2-VOES and poly(2-VOES) from distilled monomer.....	103
3.10. DSC thermograms for linseed oil, poly(2-VOEL), 18k, poly(2-VOES), 18.9k, and poly(2-VOES-co-2-VOES), 17k.....	104
3.11. Viscosity at 23 °C as a function of MW for the poly(2-VOES) homo-polymers.....	105
3.12. Drying time measurements of poly(2-VOES) homo-polymers (a) without drier package and (b) with drier package.	106
3.13. Drying time measurements of homo-polymers from 2-VOES, 2-VOEL and 50/50 wt.% co-polymers from 2-VOES, 2-VOEL and 2-VOEP (a) without and (b) with drier package.....	108
3.14. The drying/curing time for white paints based on blends of poly(2-VOES) and linseed oil as the binder.....	109
3.15. Drying time measurements of homo-polymers from 2-VOES, 2-VOEL and 50/50 wt.% co-polymers from 2-VOES, 2-VOEL and 2-VOEP with TiO ₂ without drier package.	110
3.16. Drying time measurements of homo-polymers from 2-VOES, 2-VOEL and 50/50 wt.% co-polymers from 2-VOES, 2-VOEL and 2-VOEP with ultramarine blue pigment without drier package.....	111
3.17. Images that provide a comparison of the color difference between a white paint produced with poly(2-VOES) synthesized from 2-VOES that was purified by distillation to an analogous paint based on linseed oil.....	112
3.18. Images that provide a comparison of the color difference between a white paint produced with pure poly(2-VOES), pure linseed oil, or a blend of the two materials incorporated at different ratios.	113
4.1. Natural compounds present in the cashew nut shell liquid anacardic acid (71.7%), cardanol (4.7%), traces of cardol (18.7%), 2-methylcardol (2.7%), and the remaining 2.2% is unidentified polymeric material. ¹³ The side chain may be saturated, mono-olefinic, di-olefinic or tri-olefinic with a high percentage of the components having one or two double bonds per molecule of CNSL. ⁵	124
4.2. Schematic illustrating the synthesis of CEVE.	127

4.3. Schematic illustrating the synthesis of poly(CEVE).	129
4.4. Schematic illustrating synthesis of poly(CHVE).	130
4.5. Schematic illustrating the synthesis of poly(CEVE-co-CHVE).	131
4.6. ¹ H NMR spectrum of the cardanol, CEVE and poly(CEVE).	137
4.7. ¹ H NMR spectrum of the poly(CHVE).	138
4.8. ¹ H NMR spectrum of the characteristic poly(CEVE-co-CHVE) i.e. poly(CEVE-co-CHVE)-75/25 along with poly(CHVE) and poly(CHVE).	138
4.9. FTIR spectrums of cardanol, CEVE, poly(CEVE) and poly(CEVE-co-CHVE)-75/25.	139
4.10. GPC chromatograms for (a) poly(CEVE), poly(CHVE) and poly(CEVE-co-CHVE) co-polymers and (b) BECKOSOL 1272, BECKOSOL10-539.	140
4.11. DSC thermograms for (a) poly(CEVE); (b) poly(CHVE), poly(CEVE-co-CHVE)-75/25 and poly(CEVE-co-CHVE)-50/50; (c) BECKOSOL 1272 and BECKOSOL10-539.	143
4.12. Representative storage modulus plots derived from (a)BECKOSO1272, (b) BECKOSOL 110-539, (c) poly(CEVE), (d) poly(CEVE-co-CHVE)-75/25 and (e) poly(CEVE-co-CHVE)-50/50 cured at RT, 120 for 1 h, and 150 °C for 1 h.	145
4.13. Representative tan δ thermogram plots derived from (a) BECKOSO1272, (b) BECKOSO10-539, (c) poly(CEVE), (d) poly(CEVE-co-CHVE)-75/25 and (e) poly(CEVE-co-CHVE)-50/50 cured at RT, 120 for 1 h, and 150 °C for 1 h.	146
4.14. Plots showing linear relationship between Tg and XLD of the networks produced from CEVE based polymers and commercial alkyds.	149
4.15. Representative stress-strain curves obtained for the fifteen different crosslinked networks derived from (a) poly(CEVE), (b) poly(CEVE-co-CHVE)-75/25, (c) poly(CEVE-co-CHVE)-50/50, (d) BECKOSO1272, and (e) BECKOSO10-539 cured at RT, 120 for 1 h and 150 °C for 1 h.	152
4.16. Average values of (a) Young's modulus, (b) elongation at break, and (c) toughness for the fifteen crosslinked networks produced for the study.	153
4.17. Plots describing the properties of coatings derived from the polymers of interest (a) Cross hatch adhesion, (b) pendulum hardness, (c) chemical resistance and (d) pencil hardness.	155
5.1. The chemical structure of eugenol.	164
5.2. Synthesis of 2-eugenoxylethyl vinyl ether (EEVE).	166

5.3. Synthesis of poly(E EVE).....	167
5.4. Schematic illustrating the synthesis of poly(E EVE-co-CHVE) copolymers.....	168
5.5. Schematic illustrating synthesis of poly cyclohexyl vinyl ether [poly(CHVE)].	169
5.6. ¹ H NMR spectra of (a) EEVE and (b) poly(E EVE).	175
5.7. FTIR spectra of (a) eugenol, (b) EEVE, (c) poly(E EVE) and (d) poly(E EVE-co-CHVE)-50/50.....	177
5.8. ¹ H NMR spectra of the three copolymers of EEVE and CHVE.....	178
5.9. ¹ H NMR spectra of (a) CHVE and (b) poly(CHVE).	179
5.10. GPC chromatograms for poly(E EVE), (a) poly(CEVE-co-CHVE) copolymers, and (b) three commercial alkyds.....	180
5.11. DSC thermogram of 2-vinyloxy ethyl vinyl ether (EEVE).	181
5.12. DSC thermograms obtained for all the (a) polymers produced and (b) commercial alkyds.	182
5.13. TGA thermograms for all of the polymers produced.....	183
5.14. Illustration of resonance stabilization of a radical generated by hydrogen abstraction by singlet oxygen.....	184
5.15. FTIR spectra of poly(E EVE) with catalyst taken at different time intervals along with difference spectra from the one taken at zero time.....	185
5.16. Representative storage modulus thermogram plots derived from (a) BECKOSO1272, (b) BECKOSO 10-539, (c) BECKOSO 10-539 (c), (d) poly(E EVE), (e) poly(E EVE-co-CHVE)-75/25 and (f) poly(E EVE-co-CHVE)-50/50 cured at RT, 120 for 1 h, and 150 °C for 1 h.	189
5.17. Representative tan δ plots derived from (a) BECKOSO 1272, (b) BECKOSO 10-539, (c) BECKOSO 10-539 (c), (d) poly(E EVE), (e) poly(E EVE-co-CHVE)-75/25 and (f) poly(E EVE-co-CHVE)-50/50 cured at RT, 120 for 1 h, and 150 °C for 1 h... ..	190
5.18. Plots showing variation in XLD with temperature during the DMA analysis for the films produced from (a) BECKOSO 10-060, (b) BECKOSO 10-539, (c) poly(E EVE), (d) poly(E EVE-co-CHVE)-75/25 and (e) poly(E EVE-co-CHVE)-50/50 cured at RT, 120 for 1 h, and 150 °C for 1 h.	191
5.19. Stress as a function of elongation for representative crosslinked networks derived from the commercial alkyd resins, poly(E EVE), and poly(E EVE-co-CHVE) copolymers. All samples were cured at ambient conditions for 4 weeks before testing.....	192

5.20. A comparison of the solvent resistance as a function of time for coatings derived from the commercial alkyd resin, poly(E EVE), and poly(E EVE-co-CHVE) copolymer. Solvent resistance was measured according to ASTM method D5420 (i.e. MEK double rub test).	195
5.21. Picture of (a) Coatings exposed to 3% NaOH solution, (b) BECKOSOL 1272 coating after 15 min, (c) BECKOSOL 10-060 coating after 15 min, (d) BECKOSOL 10-539 coating after 15 min, (e) poly(E EVE) coating after 24 h, (f) poly(E EVE-co-CHVE)-75/25 coating after 24 h, (g) poly(E EVE-co-CHVE)-50/50 coating after 24 h, and (h) poly(E EVE-co-CHVE)-25/75 coating after 24 h.	199
6.1. Synthesis of 2-eugenolxyethyl vinyl ether (E EVE).....	210
6.2. Synthesis of poly(E EVE).....	212
6.3. Schematic illustrating the synthesis of epoxy poly(2-eugenolxyethyl vinyl ether) i.e. E poly(E EVE).	213
6.4. Illustration of the dye extraction method.....	216
6.5. ¹ H NMR spectrum of (a) E EVE (bottom) and (b) poly(E EVE) (top).	220
6.6. FTIR spectra of (a) eugenol (bottom), (b) E EVE (middle) and (c) poly(E EVE) (top).....	222
6.7. ¹ H NMR spectrum of E poly(E EVE)-50%.	223
6.8. FTIR spectra of (a) poly(E EVE) and (b) E poly(E EVE).....	224
6.9. DSC thermogram of E EVE.....	225
6.10. DSC thermograms of poly(E EVE), E poly(E EVE)-30%, E poly(E EVE)-50% and E poly(E EVE)-70%.	226
6.11. GPC chromatograms for a) poly(E EVE), E poly(CHVE)-30%, E poly(CHVE)-50%, and E poly(CHVE)-70%.	227
6.12. Dye extraction” heat maps” for perylene incorporated coatings; E poly(E EVE)-30% (a), E poly(E EVE)-50% (b), E poly(E EVE)-70% (c) and EPON 828 (d). A three scale color coding was used.	230
6.13. Glass transition temperature (°C) heat maps (a) E poly(E EVE)-30%, (b) E poly(E EVE)-50%, (c) E poly(E EVE)-70% and d) EPON 828. A three-scale color-coding was used for individual map. Another icon scale is used where each 20 % increment in value is represented with an additional black quarter of the circle.....	232

- 6.14. König pendulum hardness (sec.) heat maps (a) Epoly(E EVE)-30%, (b) Epoly(E EVE)-50%, (c) Epoly(E EVE)-70% and d) EPON 828. A three-scale color-coding was used for individual map to perceive the variation in a better way. Another icon scale is used where each 20 % increment in value is represented with an additional black quarter of the circle..... 235
- 6.15. “Heat maps” for hardness (GPa) values of (a) Epoly(E EVE)-30%, (b) Epoly(E EVE)-50%, (c) Epoly(E EVE)-70% and (d) EPON 828. Coatings of Epoly(E EVE) cured for 6h. was not included in the experiment. 238
- 6.16. “Heat maps” for elastic modulus (GPa) values of (a) Epoly(E EVE)-30%, (b) Epoly(E EVE)-50%, (c) Epoly(E EVE)-70% and (d) EPON 828. Coatings of Epoly(E EVE) cured for 6 hours was not included in the experiment..... 239

CHAPTER 1. INTRODUCTION

1.1. Development of linear chain growth polymers from renewables: early challenges and recent successes

Recent advances in scientific discoveries have led to the expansion of the scientific horizon leaving more space for creative technology. These new technologies demand for additional resources that can only be fulfilled using renewable resources,¹ which can be directly implemented into the polymer field where of the demand for thermoplastics and thermosets is increasing rapidly. Petrochemical feedstock was considered the primary source for polymers and coatings until the limited availability and adverse impacts on the environment and health became a concern.² Synthesis of sustainable polymeric materials from fully or partially renewable biomass could potentially reduce this dependency on fossil fuel.³ Renewable biomass, with its availability, low price, and structural advantages could serve as precursor materials to provide similar or potentially more useful chemicals which are usually derived from petroleum feedstock.^{4,5} Recently, there is a huge drive to utilize renewables to reduce the environmental impact from petroleum. Plant oils have been used extensively since the early 18th century, with the raw form being used as a binding material for paints and flooring.⁶⁻⁸ The ability to incorporate polymerizable groups and undergo autooxidation utilizing the inherent unsaturation in the fatty chains makes plant oils ideal candidates for developing novel polymeric systems using various polymerization techniques such as cationic, free radical polymerization etc.⁹ Guner et al. reported that between 2001 to 2005 almost 15% of all soybean oil had been consumed for industrial purposes.¹⁰ With remarkable synthetic chemistry development other bio-renewables such as carbohydrates,¹¹ starch,⁶ furan,¹² cellulose,¹³ wood derivatives,^{14, 15} and proteins have been explored for the synthesis of inexpensive, biodegradable polymeric materials. Unfortunately with all of the ongoing effort, less than five

percent of the petroleum based market has been replaced by renewables to date.^{16, 17} This slow replacement of petrochemicals by renewable materials may be a result of, established technology that utilizes fossil fuels, politically-motivated ignorance on the depletion of fossil fuel resources, and the lower cost of petrochemical derived products. Currently, the average American consumes 21,000 pounds of fossil fuels per year. A single flight from Atlanta to Athens results in the loss of 500 pounds of fuel (mass equivalent of 23,000 PET bottles).¹⁶ Extensive use of these fossilized carbon materials results in significant environmental impact with the increase in emission of greenhouse gases, and accumulation of non-biodegradable waste on earth.¹⁸ So, even the replacement of a small fraction of the petroleum market with renewable material would make a significant difference in slowing the rate of environmental degradation. The replacement of 100 water bottles made with renewables from 200 bottles per American, per year can lead to the elimination of 660 million pounds of fossil fuels.¹⁹ Additionally, the potential price volatilization as the availability of fossil fuel supplies declines heightens the importance of the incorporation of renewable materials which expected to have stable market.¹⁶ Recent commercial success of renewable material utilization includes products such as “Ingeo PLA” from Natureworks, “I’m Green Polyethylene” from Braskem, and “Plant Bottle PET” from Coca Cola.³ Given the need for high performance/multifunctional materials, scientists are constantly searching for polymers having properties like thermal stability, flexibility, chemical resistance, biocompatibility, biodegradability, adhesion to metallic substances, gas permeability, electrical conductivity and non-flammability. These properties are direct reflections of the chemical nature of the monomer and the network formed due to crosslinking.¹⁰ A huge portion of the coatings market such as UV-curable coatings, inks, low surface energy coatings, and adhesives require that the polymers can be easily processed and later crosslinked resulting in better gloss and adhesion properties.²⁰ There

has been a constant effort to develop linear polymers fully or partially from renewable resources with decent solubility in common solvents that can be converted into thermosets via chain growth polymerization.²¹

However, the challenge is to develop monomers with proper functionality, which can undergo chain growth polymerization in the presence of other reactive groups which are capable of forming crosslinked networks.³ Chain growth polymerization is one of the most prevalent polymerization processes from a commercial perspective, and is broadly applicable to a wide range of monomers, especially those containing carbon-carbon double bonds. In comparison with step-growth polymerization, chain growth polymerization can lead to much higher molecular weights and in much shorter times, although the resulting distributions of molecular weight are comparably broad unless the polymerization is living polymerization. There are three essential reaction steps in a chain-growth polymerization: initiation of the chain, propagation or growth of the chain, and termination of the chain. Although, a fourth process, chain transfer, may also be involved. Among several mechanisms by which chain growth polymerization can take place, the prominent ones are radical and ionic (cationic and anionic). For free radical initiated chain growth polymerization a wide variety of free radical initiators are available that can undergo dissociation or degradation generating highly active species under the influence of physical agencies such as heat, light, radiation etc.; the most common act by thermally-induced cleavage of a peroxide or azo linkage. Propagation occurs by addition of a monomer to a growing polymer radical, and is typically very rapid. Termination occurs by reaction between two radicals, either by direct combination or by disproportionation. Compared to free radical, ionic chain growth polymerization is selective and not all olefinic monomers can undergo ionic polymerization. Also, ionic chain growth polymerization requires stringent reaction conditions including high purity of the monomer and is

also effected by the polarity of the solvent. Monomers with electron releasing substituents can undergo cationic chain growth polymerization where the end carbon of the growing chain bears a positive charge also called carbonium ion. However, to undergo anionic chain growth polymerization the monomer should possess electron withdrawing groups as the end growing polymer chain contains a negative charge also called carbanion. For ionic chain growth polymerization, chain initiation usually carried out using acidic or basic compounds for example, complexes of Lewis acids (BF_3 , AlCl_3 , SnCl_4 etc.) with water, tertiary oxonium salt or strong protonic acid (HCl , H_2SO_4) for cationic chain growth polymerization or alkali metals and their organic compounds for anionic polymerization.

Recently, more research groups have focused on developing monomers from renewables that can undergo chain growth polymerization to produce soluble linear polymers or copolymers with the ability to form thermosets via post curing.¹⁰ In this chapter, previous research will be addressed where attempts have been made to synthesize monomers partially or fully from bio-renewables which can undergo polymerization via chain growth polymerization. Special attention has been paid to include the research that successfully resulted in synthesized soluble linear polymers, where, the pendent groups equipped with functionalities that can be utilize for further derivatization or post curing to form thermosets. The presence or incorporation of suitable functional group in the monomer that can undergo polymerization selectively in presence of other functional moiety without forming gel has been considered very crucial for the synthesis of cross-linkable linear polymer. Keeping this in mind this chapter has been organized based on the functional moieties utilized for synthesizing linear polymers discussing any issues that occurred during polymerization, their solutions and finally the properties of those synthesized linear polymers and the cured coatings or free films derived from them.

1.2. Polymers derived using acrylic functionality

As an early work, Bufkin et al.²² reported the synthesis of fatty acrylate (FA) monomers from linolenic, linoleic, oleic and lauroleic acid. Each fatty acid for example linolenic acid was first reacted with bromine to obtain hexabromostearic acid which then reduced to linoleic acid using zinc dust. Linolenyl alcohol was produced when linolenic acid was added to an anhydrous ether suspending with lithium aluminium hydride. The alcohol was purified of and further reacted with acryloyl chloride in presence of triethylamine producing linolenyl acrylate. Copolymers of fatty acrylate monomers [linolenyl acrylate (LA3), linoleyl acrylate (LA2), oleyl (OA), lauryl acrylate (LA)] were synthesized with varying amount of methyl methacrylate and ethyl acrylate (10, 50, and 90 mol%) using 1% AIBN at 60 °C to study the reactivity ratios. Reactivity ratio product (r_1r_2) of LA3, LA2 and OA with MMA were found to be 0.52, 1.44, and 1.71 and with EA were 0.75, 1.05, and 1.2 respectively. As concluded, long chain fatty acrylates showed stronger tendency towards copolymerization than do the short chain acrylates. In a separate study, emulsion polymers of these fatty acrylate monomers were prepared with both MMA and EA as comonomers using a pre-emulsion system.²³ Four emulsion polymers were prepared from each fatty acrylate monomer where the percent incorporation of monomers in the formulation (FA/MMA/EA) were varied from 2/58.8/39.2, 4/57.6/38.4, 6/56.4/37.6 and 8/55.2/36.8. Each polymerization showed conversion > 98% with any coagulation. Glass transition temperature (T_g) of the synthesized emulsion polymers were found to decrease with increasing the amount and unsaturation of the fatty acrylate monomer which was concluded first due to internal plasticization provided by long side chain increasing segmental mobility and then weakening of the intermolecular forces due to unsaturation, imposing kinks or bends reducing side chains fitting with each other. The ability of the emulsion polymers to undergo autoxidation was studied by preparing films from 4 % linoleic

acrylate incorporated emulsion polymer with and without cobalt drier catalyst and confirmed that films prepared with drier catalyst showed higher gel content, hardness, tensile strength and elongation than the film prepared without drier catalyst after being cured for 2, 4, and 6 days at room temperature. Films were also produced from each emulsion polymer and were cured using different curing regimes; 2 weeks at RT, 4 weeks at RT, 1 hour at 100 °C and 2 hours at 100 °C. Cured films were evaluated for tensile properties (tensile strength, elongation), gel content, swelling ratio, water and base stability. Results concluded that curing for 2 weeks at RT or 1 hour at 100 °C was sufficient to result in well crosslinked films as physical properties did not improve for longer periods of curing (4 weeks at RT or 2 hours at 100 °C). Also, film properties increased with increasing incorporation of FA monomer and the fatty acid unsaturation, however, the increase in tensile strength with FA monomer amount was only prominent for LA3 as the higher crosslink density provided by this monomer compared to LA2 and OA could only compensate for the plasticization provided by its long fatty chain.

Thames et al.²⁴ disclosed the synthesis of crosslinkable monomers from semi drying and non-drying oils. Acrylate and methacrylate derivatized fatty acid monomer from oleic acid was synthesized by reacting oleyl alcohol with acryloyl chloride and methacryloyl chloride respectively in presence of triethylamine using an ice bath for 2 hours. As synthesized oleyl acrylate and methacrylate monomers were stabilized from self-polymerization by addition of hydroquinone. Emulsion polymers were prepared from both monomers using butyl acrylate as comonomer with ammonium persulfate as the initiator. The emulsion polymers showed low minimum film forming temperatures (MFT) ranging from about -5 to about 10 °C and the polymers cured to films having glass transition temperatures (T_g s) higher than 25 °C in the presence of a cobalt drier catalyst.

Incorporation of drying oils in to emulsion polymers always presents a challenge because of their hydrophobicity limiting their transportation through the aqueous phase to the polymerization site. Although, poor transport could be overcome using phase transport catalysts, a further issue is that the allylic protons associated with the oil carbon-carbon double bonds typically results in extensive chain transfer, poor rates of polymerization, and high gel content. In order to eliminate these issues Thames et al. development functionalized castor oil or castor acrylated monomer (CAM). Latexes synthesized from CAM copolymerized with conventional emulsion monomers (methyl methacrylate, butyl acrylate) exhibited good film formation and high gloss. However, film properties were found to be poor due to the low unsaturation levels in castor oil which were only effective in interior flat coatings formations. Booth et al.²⁵ reported the synthesis of acrylic macromonomers containing urethane functionality to obtain hydrogen bonding along with crosslinking through fatty chain unsaturation in the latex films. As termed urethane fatty acid acrylate monomers (UFAAM) were synthesized from safflower (USfAM), soybean (USAM), and linseed oil (ULiAM) to also study the chain transfer behavior due to fatty unsaturation. Monomers were synthesized by converting each oil to diglyceride via reacting with glycerol at 1:1 molar ratio which further reacted with isophorone diisocyanate (IPDI) and dibutyl tin dilaurate followed by addition of hydroxyethyl acrylate (HEA) at 70 °C. Latexes from these UFAAM monomers were produced with MMA and butyl methacrylate comonomers using a single stage polymerization where, allylic protons were found to be susceptible to abstraction during latex synthesis. Preservation of fatty unsaturation was significantly dependent on reaction temperature, decreasing when the reaction temperatures was increased above 65 °C. Films were produced from USfAM, USAM, and ULiAM-based latexes and cured for 3 days, 1, 2, and 4 weeks at RT to evaluate their chemical resistance (MEK resistance) improvements versus time indicating the

extent of auto-oxidative reactions thereby increasing films' crosslink density. Films produced from ULiAM latex showed a 330% increase in solvent resistance after 4 weeks of drying compared to USfAM and USAM based latex films which was attributed to the high level of unsaturation preserved during latex synthesis for ULiAM.

Chao et al.²⁶ successfully synthesized 2-(acryloyloxy) ethyl oleate (AEO) monomer via transesterification between 2-hydroxy ethyl acrylate and methyl oleate using Novozyme 435 as a catalyst. This enzymatic way is still considered one of the safest synthetic pathways compared to the chemical route. The synthesized acrylic functional monomers were both homo-polymerized and copolymerized with methyl methacrylate (MMA) via free radical polymerization, using benzoyl peroxide as an initiator. The polymerization scheme representing the synthesis of poly(AEO) and poly(AEO-co-MMA) is shown in **Figure 1.1**. Synthesized linear polymers had molecular weights in the range from 20 kDa to 30 kDa. Coatings prepared from poly(AEO) cured using 2-butanone peroxide (MEKPO) for 3 days resulted in a pencil hardness of 1H. However, coatings derived from poly(MMA-co-AEO) with 14.13% AEO monomer resulted in harder coatings (pencil hardness 3H) under the same curing conditions, although the content of the double bonds, i.e. the crosslinking sites of poly(AEO), was higher.

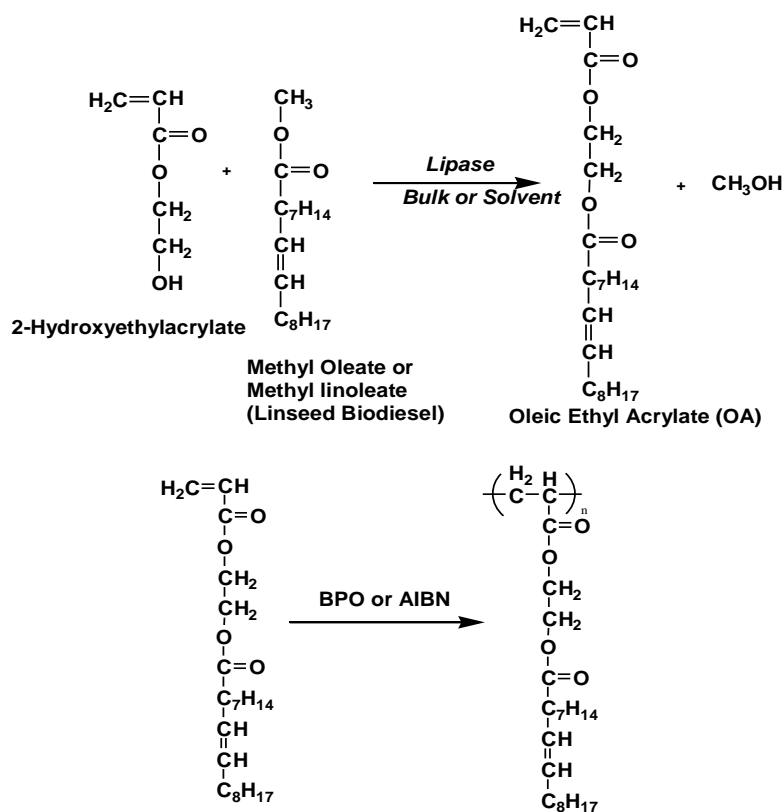


Figure 1.1. Transesterification and polymerization scheme of HEA and MO using lipase catalyst.²⁶

Palmese et al.²⁷ disclosed the synthesis of glycidyl methacrylate fatty acid monomer, by reacting glycidyl methacrylate with fatty acid with AMC-2 and $\text{SbPh}_3/\text{PPh}_3$ catalysts evaluated separately. The synthetic routes allowed preservation of the fatty acid double bonds for post curing purposes with polymerization through the incorporated methacrylate bond. Barandiaran et al.²⁸ followed this work to synthesize methacrylate derivatize oleic acid monomer (MOA) with retention of fatty acid double bonds using AMC-2 and Nacure XC-9206 (instead of $\text{SbPh}_3/\text{PPh}_3$) catalysts with autoxidative properties separately. At 0.5 wt.% optimal catalyst concentration AMC-2 showed full conversion after 240 min compared to 420 min for Nacure XC-9206. Latexes were synthesized from MOA via mini-emulsion polymerization using two types of initiators, a thermal initiator KPS and a redox initiator TBHP/AsA. Polymerization carried out with monomers using redox pair initiator TBHP/AsA, showed a faster polymerization rate than the thermal initiator

KPS. The rate of polymerization was found to be higher for TBHP/AsA initiated system than for KPS. The lower rate of polymerization with KPS was attributed to the hydrophilic nature of the sulfate radicals and the extremely low concentration of the MOA monomer in the aqueous phase causing radical termination over propagation and particle entry. Free films were prepared from the latexes and cured via autoxidation at RT and at 120 °C for an hour without drier catalyst. However, the films prepared from latexes where, the MOA was synthesized using AMC-2 catalyst showed better mechanical properties over the films derived from lattices produced from MOA synthesized using Nacure XC-9206, for both RT curing and curing at 120 °C for one hour. For example, AMC-2 derived MOA films showed Young's modulus, tensile strength and hardness of 7.8 MPa, 0.7 MPa and 6 kg respectively, compared to 1 MPa, 0.2 MPa and 1.9 kg for the films prepared with Nacure XC-9206 derived MOA. The observed higher mechanical properties were attributed from the higher auto-oxidative character of the Cr(III) based AMC2 catalyst used to synthesize MOA promoting higher crosslinking through the fatty unsaturation than Zn-based Nacure XC-9206 catalyst. The green color of the Cr(III) containing monomer as well as the yellowish color of the monomer disappeared during the polymerization, yielding a transparent and glossy film. Although very effective in the formation of linear polymers via crosslinking through acrylic double bonds, a small portion of gel formation due to side reactions through fatty double bonds was reported when fatty chains with high unsaturation were used.²⁹

An acrylate functionalized monomer from cardanol was synthesized by John et al.³⁰ via base catalyzed reaction of cardanol with acryloyl chloride. The synthesis of a copolymer from cardanyl acrylate and MMA was attempted via conventional free radical polymerization using AIBN or benzoyl peroxide by suspension technique. Instead of a linear copolymer, formation of a crosslinked network was reported. The crosslinked network was suspected to form due to the

ability of the initiator to abstract the labile proton from the alkyl chain which can undergo recombination with another radical. This in turn generated a reactive pendent radical, bearing the potential to crosslink via combination with another radical. Kattimuttathu et al.²¹ was able to overcome this issue and synthesized linear polymer from cardanyl acrylate (PCA) and four copolymers (PCAMMA1 to PCAMMA4, reported in Table 1.1) with methyl methacrylate (MMA) with varying the monomer to initiator ratio ($[M]_0/[I]_0$) via atom transfer radical polymerization (ATRP) using pentamethyl diethylene triamine (PMDETA) as a ligand and cuprous bromide (CuBr) as a catalyst for 5 h at 95 °C in bulk as shown in Figure 1.2. DOWEX 50 (Fluka) ion exchange resin was added at the end of the reaction to deactivate the catalyst.

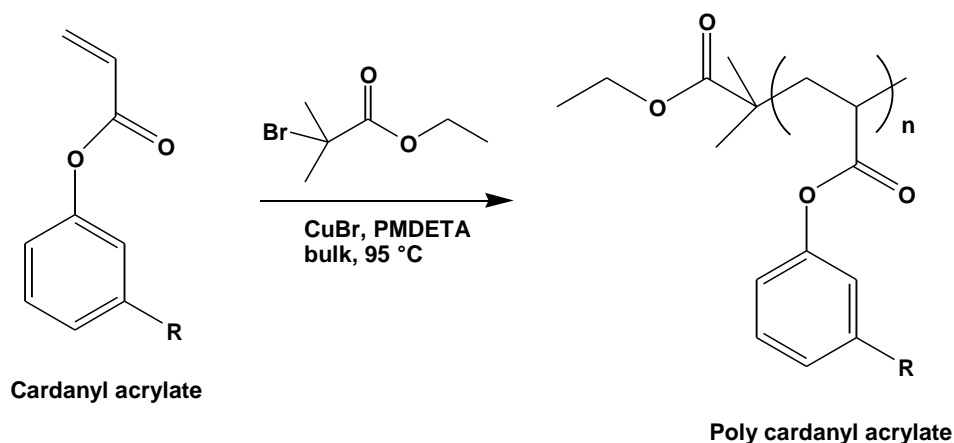


Figure 1.2. Schematic of the atom transfer radical polymerization of cardanyl acrylate.²¹

The study of the effect of initiator concentration on the copolymerization, as reported in **Table 1.1**, confirmed that with increasing initiator concentration, both molecular weight and polydispersity was decreased. This behavior satisfied the general requirement for living radical polymerizations at lower monomer to initiator ratio. This ability to synthesize a linear polymer comes from the fact that in the case of atom transfer radical polymerization, unlike conventional free radical polymerization, the concentration of active radicals remains very low reducing the probability of radical attack at the alkyl chain unsaturation.²⁰

Table 1.1. Conditions and results for the ATRP of cardanyl acrylate and its copolymers at varying initiator ratio. “Data from reference 21”

Sample Code	[M] ₀ /[I] ₀	Conversion %	Mn (Theory)	GPC		Mn _{GPC} /Mn _{Theory}
				Mn	PDI	
PCAMMA1	200	32	8,314	8,911	2.0	1.07
PCAMMA2	80	45	4,834	6,205	1.43	1.28
PCAMMA3	50	46	3,116	3,844	1.26	1.23
PCAMMA4	30	60	2,429	3,356	1.27	1.38
PMMA	80	41	3,280	4,832	1.36	1.47
PCA	30	62	6,112	18,654	1.48	3.05

The curing kinetics of poly(cardanyl acrylate) was studied using a dynamic mechanical thermal analyzer (DMTA) (model: Rheometric IV machine) in dual cantilever mode and the obtained curves are shown in **Figure 1.3**. DMTA showed an increase in the storage modulus with temperature, except at about 90 °C, where a slight decrease of storage modulus and a shoulder for tan delta was observed. This was due to the T_g of PCA. Similar behavior was observed by Ikeda et al.³¹ for oxidative polymerization of cashew nut shell liquid (CNSL). Curing of PCA with benzoyl peroxide (4 wt.%) at 100 °C for 4 hours resulted in the formation of a crosslinked network. Also, incorporation of 10% cardanyl acrylate as a co monomer with PMMA improved the thermal stability by ~35 °C.³⁰

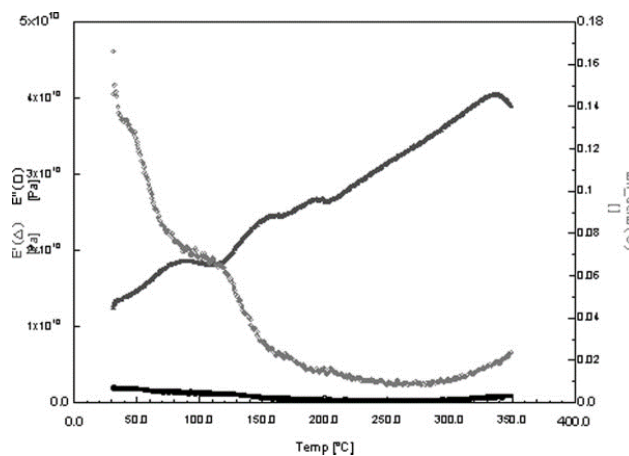


Figure 1.3. Typical DMTA cure curve of poly(cardanyl acrylate) catalyzed by benzoyl peroxide (4 wt.%), at a heating rate of 3 °C/min in dual cantilever mode. “Reproduced from reference 21”

Synthesis of a soy-based acrylic monomer (SBA) [(acryloylamino)ethyl soyate] via a one-step transesterification process was reported by Tarnavchyk et al.³² As shown in **Figure 1.4**, soybean oil triglyceride was reacted with N-(hydroxyethyl)acrylamide using NaOH as a catalyst.

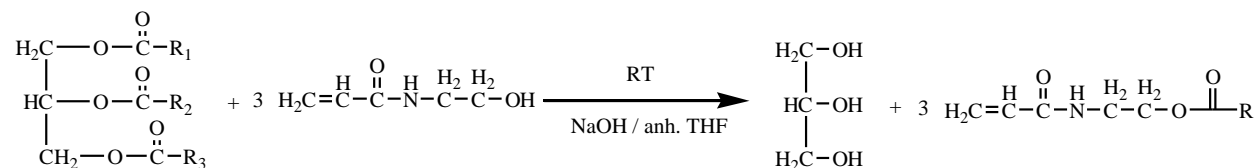


Figure 1.4. Synthesis of soy-based acrylic monomer via direct transesterification reaction of triglycerides of soybean oil with N-(hydroxyethyl)acrylamide.³²

Free radical polymerization of 2-(acryloylamino) ethyl soyate resulted in a homopolymer with $M_n = 26,380$ g/mol, PDI = 1.8 with ~85% conversion. ¹H NMR spectroscopy confirmed the formation of the backbone linkage exclusively through a vinyl group of the N-acryloyl fragment while completely retaining the fatty acid unsaturation. Q-e parameters of (acryloylamino)ethyl soyate monomer were determined by studying instantaneous copolymerization behavior of SBA with styrene and methyl methacrylate and the values were calculated to be $Q = 0.39$ and $e = 0.58$.

Demchuk et al.³³ recently extended the work done by Tarnavchyk et al.³² and studied the effect of parent oil composition, reaction temperature, and initiator concentration on the polymerization of a series of N-acryloyl monomers derived by transesterification of soybean (SBM), sunflower (SFM), linseed (LSM) and olive oil (OVM). A study of the rate of polymerization concluded that the rate constantly decreased with increasing unsaturation in the monomer. For example, LSM, with highest unsaturation, showed a rate constant of 2.08×10^5 , mol L⁻¹s⁻¹ while OVM, with the lowest unsaturation, showed 12.2×10^5 mol L⁻¹s⁻¹. Increasing the reaction temperature from 70 to 85 °C increased the rate constant from 2.08 to 11.2×10^5 , mol L⁻¹s⁻¹ for LSM and 12.2 to 62.3×10^5 mol L⁻¹s⁻¹ for OVM. This study concludes that the increase in the reaction rate with temperature is more prominent for monomers with lower unsaturation. In

subsequent work, these acrylic monomers LSM, SBM, OVM and SFM were copolymerized with MMA or VAc using emulsion and miniemulsion polymerization for making latexes.³⁴ Synthesized linear copolymers with MMA showed a decrease in molecular weight, however, an increase in latex particle size with increasing of the unsaturation of the monomer. However, both T_g and conversion showed very little difference (97-96 °C and 97-98 % respectively) with varying unsaturation. Similar but more prominent trends were observed in case of VAc as the comonomer than for MMA. Tensile properties of the films from these latexes cured via autoxidation showed that the incorporation of more plant oil-based monomers made the MMA and VAc copolymer networks tougher with a brittle to ductile transition. Tensile properties of the free films prepared, cured at RT for selected composition are reported in **Table 1.2**. Incorporation of these hydrophobic plant oil-based monomers into polyvinyl acetate (PVA) provided excellent water resistance (350->400 water double rubs) to the cured films. This improvement was significant as PVA has very poor water resistance.

Table 1.2. Tensile properties of latex films (at room temperature) from OVM and SBM with MMA. “Data from reference 33”

	$G'(\omega)$, MPa	E , MPa	σ , MPa	ϵ_b , %	Toughness, $\times 10^{-4}$, J/m ³
15OVM	1634	1429 \pm 166	10.3	0.95	3.8
35OVM	697	542 \pm 48	9.5	17.5	23
45OVM	342	131 \pm 30	3.3	243.0	180
20SBM	1615	1159 \pm 6	11.3	1.3	5.2
35SBM	916	407 \pm 26	6.6	3.2	5.8
40SBM	263	171 \pm 38	3.1	68.1	6.7

$G'(\omega)$, is the storage modulus, E is Young’s modulus, σ is the tensile strength at break, and ϵ_b is the elongation at break. The numbers associated with the monomer in the first column are the wt.% of the plant oil monomer in the copolymer.

The synthesis of a methacrylate functionalized monomer via N-hydroxyalkyl fatty amide as intermediate was reported by Yuan et al.³⁵ A robust, novel methodology was used for the

synthesis of N-hydroxyalkyl fatty amides via transesterification of plant oil triglyceride with amino alcohol in the presence of sodium methoxide. As shown in Figure 1.5, the O-acyl product from transesterification undergoes O–N intramolecular acyl migration. Both primary and secondary amino alcohols (ethanolamine, 3-amino-1-propanol, and N-methyl ethanolamine) were used for the synthesis of N-hydroxyalkyl fatty amides to study the effect of hydrogen bonding on the physical and thermal properties of the polymers.

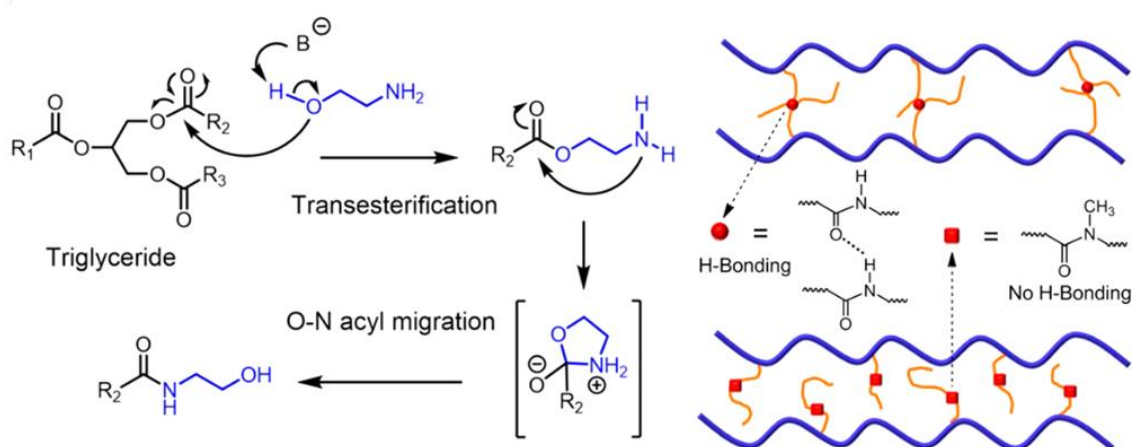


Figure 1.5. Proposed mechanism for the amidation of triglycerides with amino alcohols using ethanol amine as example and the importance of secondary nature of amino group to achieve H-bonding. “Reproduced from reference 35”

Initially, methacrylate functionality was incorporated via reacting the N-hydroxyalkyl fatty amide with methacryloyl chloride. This often led to crosslinking during polymerization and was due to the formation of dimethacrylate from methacryloyl chloride acting as a di-functional crosslinker. Because of the formation of crosslinked polymer while using methacryloyl chloride based monomers, the synthesis of the methacrylate functionalized monomer via transesterification reaction between N-hydroxyalkyl fatty amide and methacrylic anhydride using catalytic 4-dimethylaminopyridine (DMAP) was carried out. Free radical polymerization of the methacrylate fatty amide monomers with varying amide group (secondary or tertiary) resulted in linear polymers

with retention of the fatty unsaturation that were soluble in common solvents. T_g of the synthesized linear polymers were strongly dependent on the secondary or tertiary nature of the amide group and varied from -6 to -54 for tertiary (3°) amide containing monomers, while T_g s were higher and varied from 20 to 60 °C with secondary (2°) amide containing monomers.³⁶ As reported, films prepared from the polymers with secondary amide groups resulted free standing films without chemical crosslinking, with higher T_g s above room temperature and better thermal stability than the one with tertiary amide, which remained tacky because it was unable to form H-bonding.³⁵

In a recent report,³⁷ copolymers of acrylate or methacrylate functionalized N-hydroxyalkyl fatty amide (PSBA or PSBMA) with styrene (PS) were synthesized using ATRP, resulting in poly(PS-b-PSBA-b-PS) and poly(PS-b-PSBMA-b-PS) triblock copolymers. Triazolinedione (TAD) based click chemistry was used to achieve chemical crosslinking between the double bonds on PSBA or PSBMA block and bis-TAD. Poly(PS-b-PSBA-b-PS) resulted in films with tensile strength of 0.9 MPa due to poor chain entanglement. Incorporation of crosslinking to only 1% of the double bonds improved the tensile strength to 1.8 MPa. Increasing the “click coupling” i.e. crosslinking to 5% of double bonds resulted in films with tensile strength 6.2 MPa and free-standing gel insoluble in THF as shown in **Figure 1.6**.

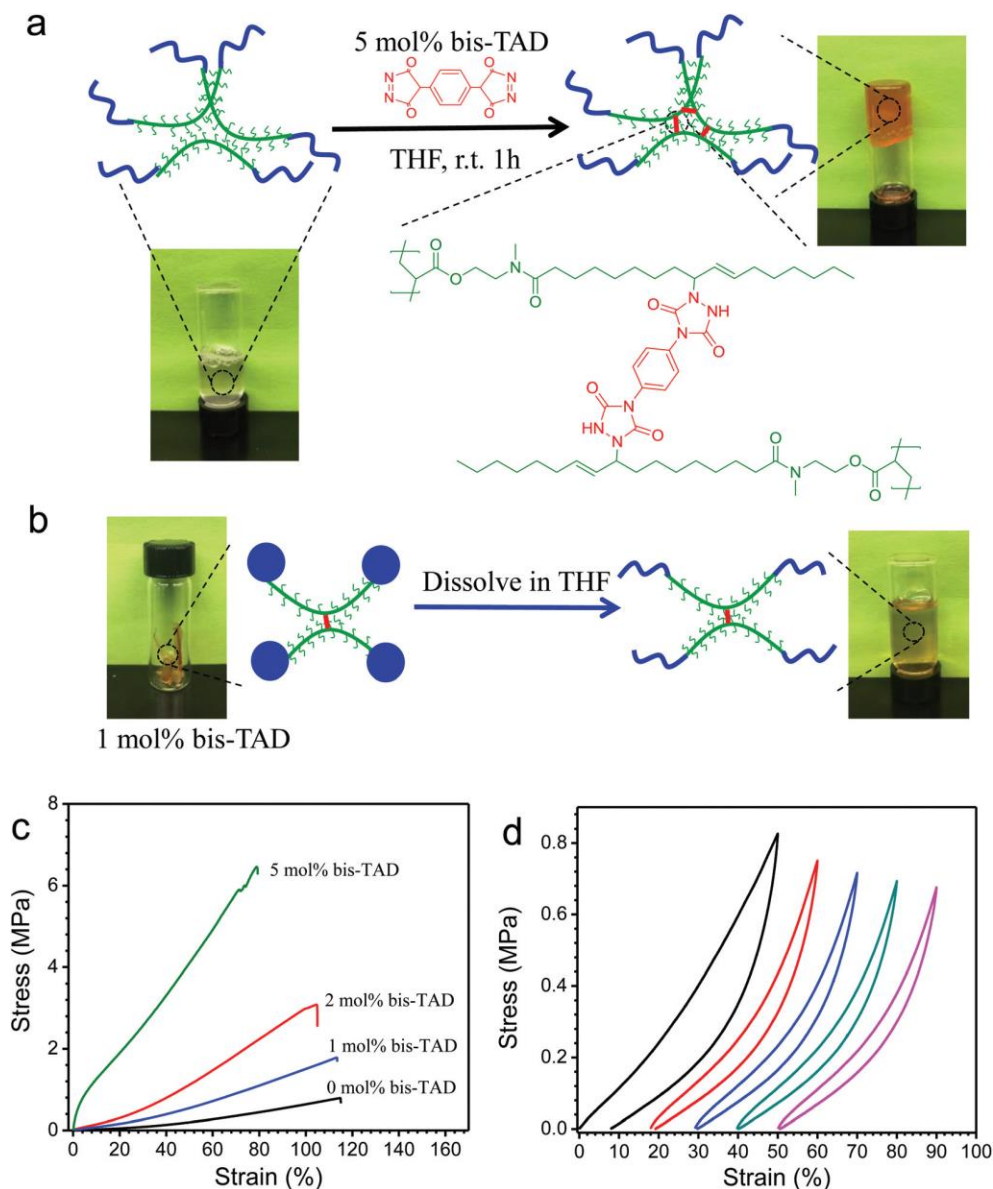


Figure 1.6. Schematic illustration for the coupling of PS-b-PSBA-b-PS triblock copolymer by bis-TAD. (a) “Click coupling” with 5 mol% of bis-TAD leads to the formation of gel. (b) A slightly “click coupled” (with 1 mol% bis TAD) sample can be well dissolved in THF. (c) Monotonic stress–strain curves of PS49-b-PSBA82-b-PS49 “click coupled” with 1 mol%, 2 mol%, and 5 mol% of bis-TAD respectively. (d) Representative cyclic stress–strain curves of PS49-b-PSBA82-b-PS49 “click coupled” with 1 mol%. For clarity, the curves are shifted on the strain axis. “Reproduced from reference 37”

1.3. Polymers derived using vinyl ether functionality

Alam et al.³⁸ reported the synthesis of a vinyl ether monomer from soybean oil (VESFA) via base catalyzed transesterification of soybean oil (SBO) with ethylene glycol vinyl ether. This

vinyl ether monomer was then utilized to develop a linear polymer with an architecture as shown in **Figure 1.7**. Compared to the triglyceride, for example, in the case of soybean oil which contains 4.5 double bonds on average, the linear polymer derived from soybean oil could possess hundreds of double bonds depending on the degree of polymerization. Homopolymerization of VESFA was carried out via cationic polymerization using 1-isobutoxyethyl acetate (IBEA) as cationogen previously reported by Aoshima and Higashimura et al.³⁹ and ethylaluminum sesquichloride solution (25 wt.% in toluene) as co-initiator. ¹H NMR confirmed that the polymerization went exclusively through the vinyl ether functionality leaving the fatty unsaturation intact. Compared to the DSC thermogram of SBO which showed two strong melting endotherms at -39 °C and -35 °C, the thermogram of polyVESFA showed a T_g around -98 °C with a very diffuse, weak endotherm around -28 °C. PolyVESFA showed two orders of magnitude higher viscosity than SBO at a shear rate below 2000 s⁻¹ and reduced tack free time by 4 to 8 orders of magnitude using low to high levels of cobalt catalyst.

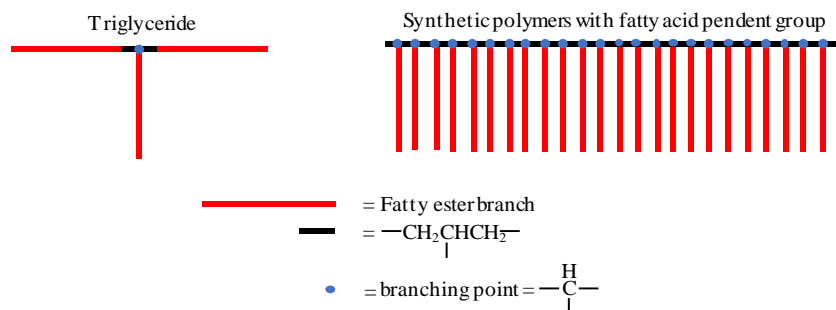


Figure 1.7. A schematic illustrating the difference in molecular architecture between a plant oil triglyceride and a synthetic polymer containing a fatty pendent group in the repeat unit.³⁸

The fatty unsaturation in polyVESFA and SBO was further derivatized to epoxy (E-polyVESFA and E-SBO) and acrylate (A-polyVESFA and A-SBO) functionality to study their curing behavior. Curing study of E-polyVESFA with triethylenetetramine (TETA) by measuring the shear modulus with time at 120 °C showed a sharp increase after 25 minutes and fully cured

networks after 4 hours, which was very rapid compared to 15 hours for the E-SBO/TETA blend. Similar trends were observed for the coatings E-polyVESFA, E-SBO and their 30 wt.% blends with 3-ethyl-3-hydroxymethyl-oxetane (EHMOx) cured by cationic photopolymerization monitored by real-time FTIR and photo DSC. T_g for cationically photocured E-polyVESFA ($T_g = 26\text{ }^\circ\text{C}$) and its blends with EHMOx showed higher values than its E-SBO analog. A-polyVESFA also showed faster curing behavior in place of A-SBO in free-radical photocure systems. Because of the chemical nature of the bis-allylic protons, epoxy and acrylic functional groups in both polyVESFA and SBO were similar, the observed variation in the curing behavior was attributed to higher number of functional groups per molecule associated with the use of polyVESFA as opposed to SBO.

Although conversion of soybean oil triglyceride to a linear polymer significantly increases the functionality thereby resulting in highly crosslinked cured films, surprisingly, the crosslinked networks produced from E-poly(VESFA) and A-poly(VESFA) resins showed sub-ambient T_g s which were attributed to the very low T_g of poly(VESFA) homopolymer. In a recent study, to increase the T_g of polymer synthesized from 2-vinyloxy ethyl soyate [poly(2-VOES)], cyclohexyl vinyl ether (CHVE) was copolymerized with 2-VOES via cationic polymerization. Due to rigidity provided by the ring structure of CHVE, the poly(CHVE) homopolymer resulted in a T_g around $50\text{ }^\circ\text{C}$.⁴⁰ Increase of the T_g from $-98\text{ }^\circ\text{C}$ to $-34\text{ }^\circ\text{C}$ was observed for poly(2-VOES-co-CHVE) copolymer with 25 wt.% CHVE repeat units, however, the T_g of the copolymer with 50 wt.% CHVE was not distinct because of having a distribution of chemical composition resulting in a broadening of the segments' mobility. Cured films at RT with 25 and 50 wt.% CHVE repeat units improved the T_g s by 12.5 and 18.5 $^\circ\text{C}$, respectively, compared to poly(2-VOES) cured film. This significant increase in T_g was attributed to the increased rigidity of the polymer segments as

incorporation of CHVE repeat units reduced the reactive functionality thereby crosslink density. T_g of the cured films increased up to ~25 % when cured at elevated temperatures (120 °C or 150 °C for an hour compared to films cured at RT although the crosslink density increased by only 1.5 percent. Compared to poly(2-VOES) cured films which showed brittle character in stress-strain curves, CHVE incorporated films had ductile nature with higher elongation mainly due to reduced crosslink density. An increased Young's modulus was observed as an outcome of pushing the T_g s above RT with increasing CHVE content, thereby making the cured films behave more glassy at RT at which the tensile measurements were done. Incorporation of CHVE comonomer also improved the coatings' hardness and adhesion, however, due to the reduced crosslink density the chemical resistance was sacrificed.

Copolymers were also synthesized using menthol vinyl ether (MVE) as a comonomer with soybean oil ethyl vinyl ether.⁴¹ Unlike CHVE, menthol is a naturally occurring terpene increasing the overall biomass content of the copolymers. MVE was synthesized by reacting menthol with vinyl acetate in presence of sodium carbonate and $[\text{IrCl}(\text{cod})]_2$ as catalyst at 100 °C for 4 hours previously reported by Okimoto et al.⁴² The homopolymer of MVE was synthesized using carbocationic polymerization using the procedure reported by Alam et al.³⁸ The resulting homopolymer had a T_g of ~68 °C. Copolymers of 2-VOES synthesized incorporating 25 and 50 wt.% of MVE showed broad inflections during DSC experimentation with T_g s around -78 and -45 °C respectively which was in agreement with the T_g calculated from the Fox equation.⁴³ Films produced from copolymers with 25 and 50 wt.% incorporation of MVE cured at RT, resulted in an increase in T_g s up to 20 and 31 °C respectively compared to poly(2-VOES) film cured at RT, with T_g s even increased for the coatings cured at elevated temperatures compared to RT mainly due to increasing crosslink density. Incorporation of 50 wt.% MVE resulted in cured films having

ductile nature with 70 to 90 % elongation compared to poly(2-VOES) cured films showing only 10 to 20 % elongation with brittle failure. Significant improvement in adhesion and pendulum hardness was achieved with increasing MVE repeat units. An improvement in pendulum hardness was small for 25 wt.% MVE incorporated coatings compared to 50 wt.% MVE as the T_g for 50 wt.% MVE incorporated coatings were above RT, making them glassier during pendulum hardness experimentation at RT.⁴⁴

The synthesis of amphiphilic copolymers from 2-VOES monomer as the hydrophobic component with tri(ethylene glycol) ethyl vinyl ether (TEGEVE) as the hydrophilic component was reported by Alam et al.⁴⁵ which showed good dispersibility in water and surface activity without the need for a surfactant.⁴⁵ Kalita et al.⁴⁶ took the advantage of this ability to form emulsions from the plant oil based amphiphilic copolymer and synthesized three copolymers from 2-VOES and penta (ethylene glycol) ethyl vinyl ether by incorporating 50, 85 and 90 wt.% 2-VOES monomer. Coatings were prepared by casting 30 wt.% aqueous dispersions of these amphiphilic copolymers in the presence of a drier package. Coatings showed decent tack free times ranging from 7 hours to 3.5 hours with increasing the 2-VOES incorporation from 30 to 50 wt.%. Cured films had excellent optical clarity, which can be attributed to the lack of surfactant in the films.

Kalita et al.⁴⁷ reported the synthesis of vinyl ether monomer and polyurethane networks thereafter from palm oil (PO), which is mostly used as a food ingredient, in cooking oil and in cosmetics due to its low unsaturation and ability to resist oxidation. Synthesized 2-(vinylloxy)ethyl palmitate (2-VOEP) monomers were polymerized using cationic polymerization previously reported by Alam et al.³⁸ and Chernykh et al.⁴⁸, resulting in a linear homopolymer with a $M_n \sim 16,000$ g/mol and PDI ~ 1.15 . Polyols were derived from poly(2-VOEP), PO and SBO to produce

analogous polyurethane networks via first epoxidizing using peroxy acetic acid and then ring opening with methanol. Curing study of synthesized polyols with hexamethylene diisocyanate trimer (HDT) at 100 °C by monitoring the dynamic viscosity concluded that, irrespective of having the same concentration of hydroxyl groups and isocyanate groups, polyol derived from poly(2-POVE) cured much faster reaching a dynamic viscosity of 10,000 Pa.s within ~11 minutes, however, the polyol from PO (HO-PO) reached the same viscosity in 48 minutes. This is due to the polymeric structure of HO-poly(2-POVE), resulting in an average number of hydroxyl groups per molecule (polymer chain) as high as 38, while the average number of hydroxyl groups for HO-PO in its triglyceride structure was 1.8. SBO polyol (HO-SBO)/HDT mixture showed slightly faster curing than HO-poly(2-VOEP)/HDT which was due to much higher concentration of hydroxyl groups and isocyanate groups. In addition, since the number of functional groups per molecule for both HO-SBO and HDT is 3 or higher, every reaction leading to the formation of a urethane group should contribute to the crosslink density. Similar advantages of this polymeric structure have been observed in the viscoelastic properties of the cured polyurethane films, where the crosslink density calculated from the plateau modulus was reported to be $9.06 \times 10^{-4} \text{ mol/cm}^3$ for HO-poly(2-VOEP), much higher than HO-PO which was $2.21 \times 10^{-4} \text{ mol/cm}^3$ and surprisingly similar to HO-SBO. Despite this high crosslink density, T_g for the HO-poly(2-VOEP) polyurethane network showed only a 3 °C increase compared to the HO-PO network, which was mainly due to the presence of tri-saturated and mono-unsaturated triglycerides which do not contribute to the crosslinking; rather they act as plasticizers. Both the tensile and mechanical properties of the HO-poly(2-VOEP) polyurethane networks showed values closer to OH-SBO and much higher than OH-PO. For example, Young's modulus and chemical resistance HO-poly(2-VOEP) was reported to be $12.2 \pm 0.4 \text{ MPa}$ and 230 ± 10 double rubs which is closer to that of OH-

SBO having numbers 17.8 ± 2.7 MPa and 180 ± 8 double rubs than OH-PO with values only 3.2 ± 0.3 MPa and 130 ± 8 double rubs respectively.

Samanta et al.⁴⁹ reported the synthesis of nonisocyanate polyurethane thermosets from poly(2-VOES) linear polymer, which could potentially replace the use of isocyanates that possess potential health hazards. As referenced, commercially available epoxidized soybean oil (EEW = 245 g/mol) was reacted with supercritical carbon dioxide in presence of TBAB catalyst in a high-pressure reactor for 48 hours at 140 °C, maintaining a pressure of 12.4 MPa. 99.18 mol % conversion of epoxy groups to cyclic carbonates was observed with a carbonate equivalent weight of 289 g/mol. However, due to gelling issues during carbonization reaction, epoxidized poly(2-VOES) (EEW = 255 g/mol) was diluted with toluene and the reaction was stopped at 85.3 % conversion resulting in a polymer with a carbonate equivalent weight of 293 g/mol. Three thermoset networks were prepared from each cyclic carbonate-functionalized soybean oil (CSBO) and cyclic carbonate-functionalized poly(2-VOES) [Cpoly(2-VOES)] polymers by curing with 1,6-hexamethylenediamine (HMDA), 1,9-nonanediamine (NDA), and 1,13-tridecanediamine (TDA) curatives at 100 °C for 16 hours. Cpoly(2-VOES) showed an exponential increase in dynamic viscosity reaching up to 4000 Pa-s in 361 seconds while curing with HMDA, however CSBO resulted in similar dynamic viscosity value around 978 seconds while curing with HDMA. These results correlate with the findings from Alam et al.³⁸ and were attributed to the presence of higher functionality [increasing with degree of polymerization (DP) of polymer] in the case of linear polymers compared to its parent oil having only three fatty chains per triglyceride. Cpoly(2-VOES) cured films showed a higher T_g , Young's modulus and crosslink density and less brittleness than films produced from CSBO.

The effect of crosslinker chain length on the crosslink density and thereby on the tensile properties have been studied. Increasing the chain length of the crosslinker from hexamethylene to tridecane reduces the crosslink density from 447 to 335 mol/m³ for CSBO and 1310 to 700 mol/m³ for Cpoly(2-VOES). Similarly, Young's modulus decreased from 7.2 to 3.7 MPa for CSBO and 17 to 5.8 MPa for Cpoly(2-VOES) however, elongation increased from 13% to 28% for Cpoly(2-VOES) with changing the crosslinker from hexamethylene to tridecane diamine. In the case of CSBO, thermosets with HMDA showed the highest elongation at 156% with the highest Young's modulus, confirming it to be the toughest among all three CSBO thermosets. This observed phenomenon is a result of the highest concentration of urethane groups, which resulted in intermolecular hydrogen bonding thereby converting mechanical energy into heat by the breaking and forming of hydrogen bonds.⁵⁰⁻⁵⁴

Recently, attention has been given to natural resources with aromatic functionality. Cardanol, mainly derived via decarboxylation of anacardic acid which is the major component of cashew nut shell liquid, is a byproduct of cashew nut processing.⁵⁵ Cardanol ethyl vinyl ether (CEVE), was synthesized via reacting cardanol with 2-chloroethyl vinyl ether using the Williamson Ether Synthesis process as shown in **Figure 1.8**.⁴⁶ Using cationic polymerization, the homo-polymer of CEVE was synthesized which showed a $T_g \sim -78$ °C which was determined using DSC. This low T_g of CEVE was attributed to the presence of the long (C₁₅) alkyl chain at the pendent moiety. Free films and coatings were prepared from poly(CEVE) in presence of a drier package. Curing at RT for two weeks resulted in cured films with a T_g around 5 °C, and a Young's modulus and elongation around 18.9 MPa and 20.3% respectively. Cured coatings also resulted in excellent adhesion, impact resistance and mandrel bend along with decent hardness and solvent resistance of 37 s and 120 double rubs. In most cases, these numbers increased for curing at 120

and 150°C for an hour. T_g increased to 11 and 15°C for 120 and 150°C cured coatings. Curing at 150°C significantly increased the Young's modulus up to 47 MPa while decreasing the elongation up to 16% due to increase in crosslink density. These elevated temperature-cured coatings showed better hardness and solvent resistance along with excellent physical properties.

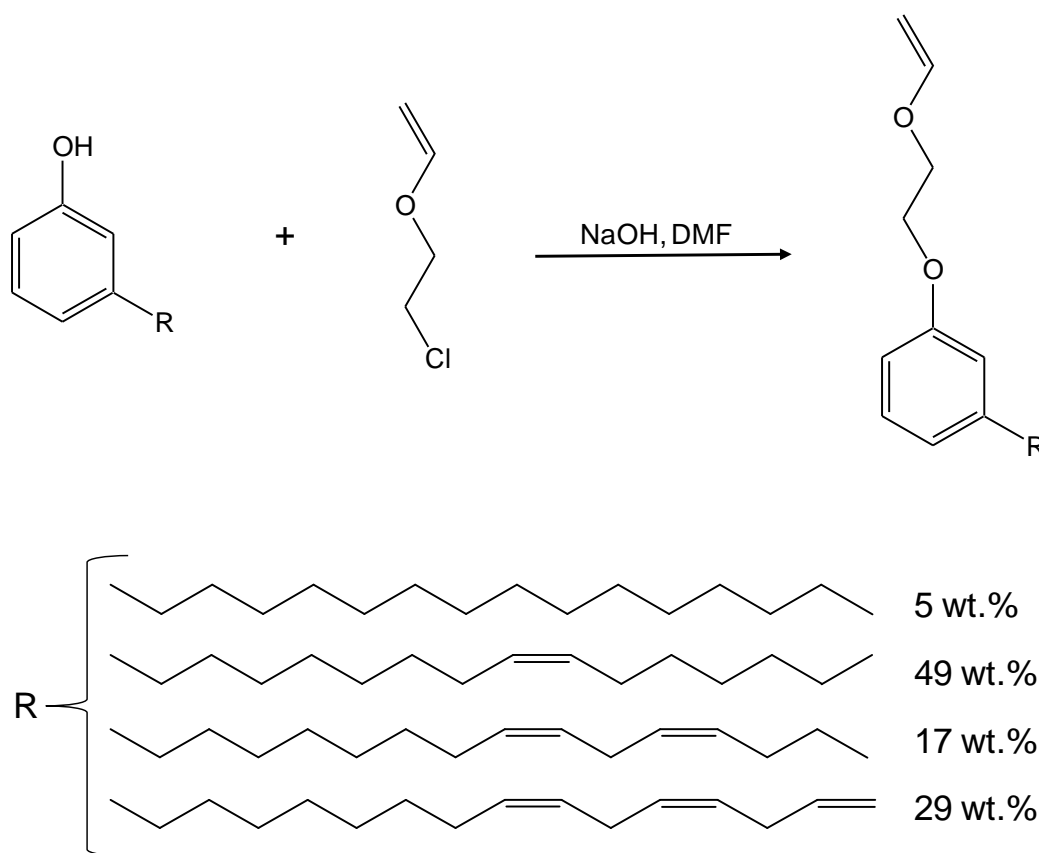


Figure 1.8. A schematic illustrating the synthesis of cardanol ethyl vinyl ether.⁴⁶

In another study,⁵⁶ the ability of 2-VOES monomers to undergo free radical copolymerization was shown using maleic anhydride (MA) as a comonomer in the presence of AIBN as initiator, resulting in an alternating copolymer. Compared to poly(2-VOES) with a T_g ~98°C, the synthesized poly(2-VOES-alt-MA) copolymer resulted in a T_g ~54°C which was unexpectedly higher and may be attributed to the cyclic nature of MA in the backbone thereby providing high rigidity and reducing the mobility of the polymer segments. Due to this high T_g ,

coatings cast from poly(2-VOES-alt-MA) solution in toluene became tack free as soon as the solvent evaporated. Free films cured at RT in the presence of a drier catalyst for 3 weeks showed a $T_g \sim 100^\circ\text{C}$ which was 107°C higher than the coatings derived from poly(2-VOES). This higher T_g indicates the films behave glassier at RT which might contribute to the significantly higher Young's modulus $\sim 711 \pm 26$ MPa compared to 11 ± 2 MPa for poly(2-VOES) cured films. Films cured at 120 and 150°C for an hour showed even further increases in their thermal and mechanical properties. Similar observations were made for physical properties tested on coatings cast on steel panels. Compared to RT cured coatings with a pendulum hardness of 62 ± 2 s and chemical resistance at 330 ± 5 MEK double rubs, coatings cured at 120°C displayed a Konig hardness value of 108 s and 640 ± 5 MEK double rubs. These values surprisingly increase to 131 s and >1500 double rubs for coatings cured at 150°C . Both the mandrel bend and crosshatch adhesion were excellent at 32% and 5B respectively for all the coatings, which may result from the flexibility of the pendent fatty chains. Although air dried, these coatings showed properties that can be compared to 2K epoxy coating systems rather than alkyd.

1.4. Polymers derived using vinyl ester and allyl ester functionality

Swern et al.⁵⁷ synthesized a series of allyl containing esters of oleic acid via direct esterification with 2-chloroallyl, allyl and, methally alcohol. As reported, homo-polymerization of these allyl eaters with 1% benzoyl peroxide resulted viscous insoluble materials rather than linear soluble polymers. Formation of crosslinked polymers was due to the participation of the 9, 10 double bond in oleic acid in olefinic copolymerization reaction. Allyl ester monomers were also copolymerized with vinyl acetate using 0.5% benzoyl peroxide. However, instead of linear soluble copolymers, soft gels were obtained when incorporation of allyl ester monomers was 30% or more below which the copolymers were insoluble hard, glassy material.

Toussaint et al.⁵⁸ in early 1942 disclosed the synthesis of vinyl oleate by reacting vinyl acetate with oleic acid using mercuric acetate and sulfuric acid as catalysts, which mainly involved vinyl exchange (transvinylation). An excess of vinyl acetate at higher temperature (limited to the boiling point of vinyl acetate) was required for efficient vinyl exchange to the fatty acid.

Harrison et al.⁵⁹ studied the free radical polymerization of vinyl and allyl esters of stearate, oleate and linoleate fatty acids using 2% benzoyl peroxide as initiator at 80°C. In the case of vinyl and allyl linoleate, the slowest polymerization rate was observed along the slowest conversion comparing to stearate and oleate due to the presence of easily abstractable bis-allylic protons by the peroxy radical. This observed trend in conversion was also confirmed from the intrinsic viscosity of the resultant polymers showing a decrease in viscosity of the polymer with increasing the fatty acid unsaturation of the vinyl or allyl ester monomer. Frank et al.⁶⁰ and Wilson et al.⁶¹ also observed similar retarded polymerization behavior with unsaturated fatty acids, however they did not report any explanation for this behavior. As concluded by Harrison et al.⁵⁹ the free radical initiator could add to the 9 and 12 double bonds of the linoleate and the vinyl or allyl groups in the monomer. In the scenario where the radical adds to the allyl or vinyl groups it readily propagates to another double bond. However, the radicals formed at the fatty unsaturation are relatively stable, thereby rather than propagating it undergoes termination by combination. In the case of linoleate, the propagation mostly occurs through the vinyl or allyl group which may react with the 9 or 12 double bonds, resulting in ultimate chain termination and therefore observed low conversion. Although this research attempted synthesizing linear chain growth polymers, they all had issues for the preservation of fatty unsaturation which is important for further crosslinking.

Lincoln et al.⁶² developed a ruthenium catalyst for trans-vinylation to synthesize vinyl esters and showed a performance advantage over previously reported mercury⁵⁸ and palladium⁶³

catalysts. Unlike the mercury catalyst which has toxicity and volatility issues and palladium catalyst which has low thermal stability resulting from inactive palladium (0) near the boiling point of vinyl acetate, the ruthenium catalyst showed desirable physical and chemical properties suitable for commercial purposes.⁶⁴ Hideto et al.⁶⁵ disclosed the use of catalytic amounts of $[\text{Ir}(\text{cod})\text{Cl}]_2$ or $[\text{Ir}(\text{cod})_2]\text{BF}_4$ for the synthesis of a vinyl ester by reacting carboxylic acid with terminal alkynes resulting in 1-alkenyl ester. Following this work, Gandini et al.²⁹ used iridium catalyst $[\text{Ir}(\text{cod})\text{Cl}]_2$ for the synthesis of fatty acid vinyl esters by the transvinilation of oleic and linoleic acids with vinyl acetate. Fatty acid was reacted with 10 eq. excess of vinyl acetate (VAc) in the presence of catalyst ($[\text{Ir}(\text{cod})\text{Cl}]_2$, 0.01 eq), along with sodium acetate (0.03 eq), under magnetic stirring at 100°C resulting in vinyl oleate (VO) and vinyl linoleate (VL) in 90% and 50% yield, respectively. Homopolymers and copolymers of vinyl oleate (VO) and vinyl linoleate (VL) with different ratios of vinyl acetate were carried out free radically using benzoyl peroxide as initiator at 85 °C. Homo-polymerization of vinyl oleate resulted in linear polymers only through the vinyl double bond and was confirmed by NMR via the disappearance of vinyl proton resonances (δ 4.5, 4.8 and 7.3 ppm) and appearance of the backbone protons CH and CH₂ with the retention of fatty chain double bond proton at δ 5.3 ppm. However, in case of vinyl linoleate the backbone proton resonance was not clear in addition to the low intensity signals from the vinyl proton, implying polymerization occurred both through the vinyl and fatty acid double bond. The yield for polyvinyl linoleate was lower (<10%) compared to polyvinyl oleate (>50%) which confirmed the involvement of the fatty acid double bond during polymerization resulting in a higher termination rate. Copolymerization with vinyl acetate showed similar behavior for both vinyl oleate (VO) and vinyl linoleate (VL). Thermal analysis showed that irrespective of the type/amount of fatty acid vinyl ether (FAVE) monomers and quantity of radical initiator, vinyl acetate copolymers showed

a two-step pathway degradation profile around 340–350 °C (Td1) corresponding to the deacetylation of the pendent group and 440–450 °C (Td2), associated with the depropagation of the polyolefin backbone. Oxidative drying of the copolymer films was confirmed by FT-IR study at different time intervals viz 1, 3, 19, 26, 68 and 140 h. at RT. FT-IR spectra of poly(VAc-co-VL) copolymer with 13% VL obtained over 140 h. of curing exhibited two new bands around 3430 cm^{-1} and 1633 cm^{-1} assigned to hydroperoxide moieties and conjugated double bonds. Also, peaks at 3010 and 723 cm^{-1} confirmed the disappearance of the fatty double bond and occurrence of oxygen induced polymerization. Similar drying behavior was observed by Lazzari et al.⁶⁶, during the study of the drying behavior of linseed oil. In the case of the vinyl ester of fatty acids, it is difficult to synthesize linear chain growth polymers of highly unsaturated vinyl esters like linoleate or linolenate that carry bis-allylic protons due to the affinity of the radical towards both vinyl and fatty double bonds in addition to the increasing affinity of the fatty double bond radical to recombine with another fatty radical rather than attacking the vinyl double bond.

1.5. Polymers derived using cyclic imino ether, norbornene, aromatic functionality

Oxazoline rings with 2-alkyl substitution have been utilized as a platform to synthesize functional monomers having applications in many fields.⁶⁷ In 1964, Beck et al.⁶⁸ from Henkel corporation, took the advantage of the easy replacement of the hydrogen atom located on the α carbon of an alkyl group in the 2 position to synthesize soy based 2-oxazoline monomer (SoyOx). The synthetic route as shown in **Figure 1.9** was carried out via a two-step condensation reaction where the first step was the condensation between ethanol amine and fatty acid at 120-140°C and the second step involved ring closure using titanium acetylacetonate as a catalyst. Both gel permeation chromatography (GPC) and gas chromatograph-mass spectrometry (GC-MS) confirmed a mixture of 2-oxazolines with 15 or 17 carbon atoms with 0 to 2 double bonds in the

fatty side chain.⁶⁹ Lewis acid catalyzed ring opening polymerization of SoyOx monomer shown in **Figure 1.10** was carried out using boron trifluoro etherate.⁶⁸

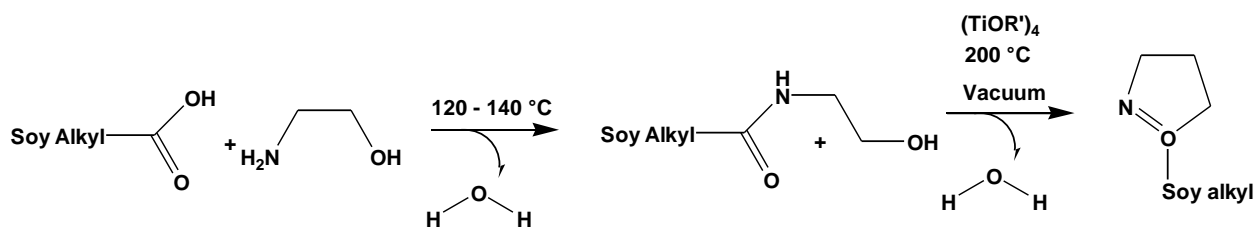


Figure 1.9. Synthesis of soy-based 2-oxazoline monomer (SoyOx).⁶⁸

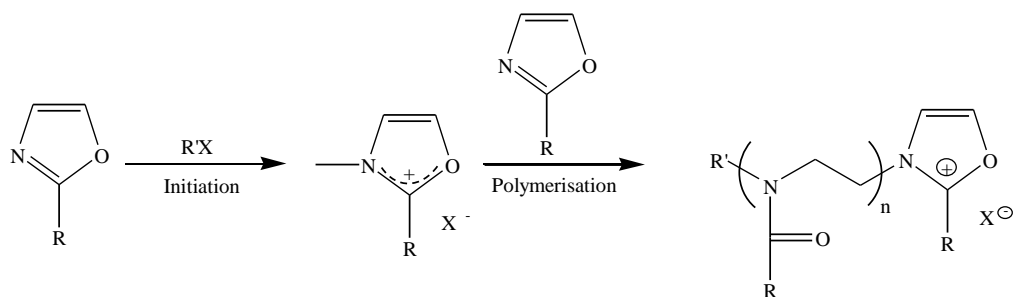


Figure 1.10. Oxazoline polymerization via cationic ring opening.⁶⁸

Recently, Yuan et al.³⁵ reported the synthesis of five or six-membered cyclic imino ether functionalized monomers from N-hydroxyalkyl fatty amides. Compared to previously reported techniques involving the condensation between alkyl acids or nitriles with amino alcohols in the presence of titanium catalyst at $\sim 200^{\circ}\text{C}$ ⁷⁰, the direct dehydration of N-hydroxyalkyl fatty amide shown in **Figure 1.11** was carried out with the assistance of p-toluenesulfonyl chloride, triethylamine and DMAP at RT using dichloromethane as solvent. These cyclic imino ethers are reactive monomers for making poly(N-acylalkylenimine)s.

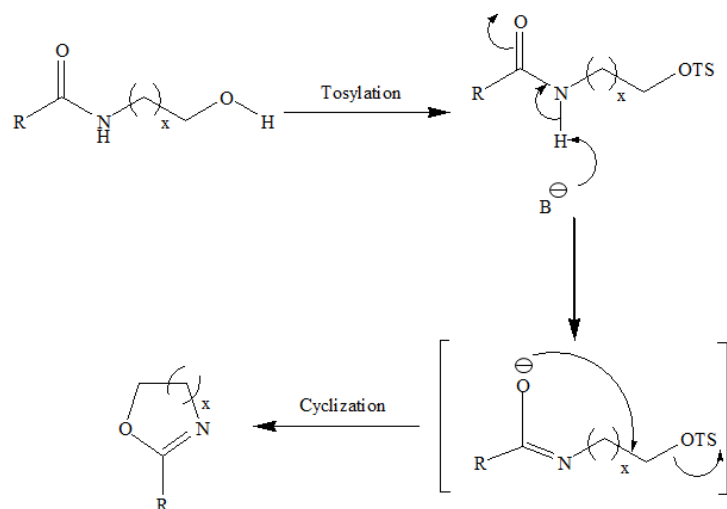


Figure 1.11. Proposed mechanism for the formation of cyclic imino ethers derived from N-hydroxyalkyl fatty amides.³⁵

Hoogenboom et al.⁷¹ took a cleaner approach and synthesized poly(SoyOx) via microwave-assisted cationic polymerization. A polymerization kinetic study confirmed that the bulk polymerization had a living nature and full conversion was rapidly achieved with the double bonds unaffected.⁶⁹ Huang et al.⁷² reported the synthesis of amphiphilic poly(2-ethyl-2-oxazoline-block-2-“soy alkyl”-2-oxazoline) di-block copolymer (PEtOx-PSoyOx) for the preparation of core-crosslinked spherical micelles in aqueous medium. A microwave assisted ring opening polymerization technique was used where 2-ethyl-2-oxazoline and methyl tosylate were first stirred under microwave irradiation at 140 °C for 13.33 min in acetonitrile. SoyOx was added to the reaction mixture under an inert atmosphere and polymerization was continued for another 3.33 min. Micelles were prepared by first dissolving the synthesized PEtOx₆₈-PSoyOx₁₈ copolymer in acetone at a concentration of 1 g/L and followed by the dropwise addition of water to trigger micellization. Taking advantage of fatty chain unsaturation, UV-cross-linking of the micelles was performed under stirring. Interestingly, these micelles resulted in sphere (in water) to rice grain (in acetone) transition as shown in **Figure 1.12**, due to the swelling of the core. This ability of the micelles to undergo morphological change due to core swelling/deswelling could be used to

encapsulate and/or release molecules of interest or stimuli-sensitive templating medium for the creation of smart surfaces.

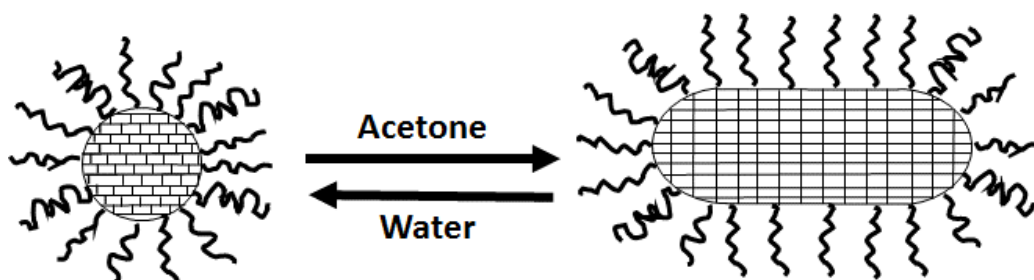


Figure 1.12. Representation to the sphere to rice grain morphological transition.⁷²

Ikeda et al.³¹ reported the synthesis of soluble polyphenol with crosslinkable unsaturated alkyl side groups from cardanol via enzyme catalysis and oxidative polymerization. As shown in **Figure 1.13**, polymerization was initially targeted using either soybean peroxidase (SBP), horseradish peroxidase (HRP) in conjunction with hydrogen peroxide (H_2O_2). Polymerization was also carried out by non-enzymatic methods using iron-N,N'-ethylenebis(salicylideneamine) (Fe-salen) with H_2O_2 as a catalyst. Although previous work by Tonami et al.⁷³ reported the polymerization of short chain substituted m-phenol, HRP was inactive in the case of cardanol due to the large side chain at the para position. Polycardanol with SBP was synthesized and as reported the molecular weight varied from 4.8 kDa to 10 kDa depending on the solvent system used. Both the molecular weight and yield increased with increasing the amount of Fe-salen in 1,4-dioxane as solvent or addition of pyridine as a base while keeping the amount of Fe-salen catalyst the same. Curing of polycardanol was carried out with cobalt naphthenate (3 wt.%) and showed rapid curing resulting in cured films of pencil hardness H after curing for only 2 h. With the same curing conditions, cardanol resulted in significantly inferior films, which confirms the advantage of a linear polymer structure that provides macromonomers with multiple functionality depending on the molecular weight of the polymer. This advantage of a linear structure with multifunctionality

has also been reported by Alam et al.³⁸ with their work on vinyl ether monomers. Curing of polycardanol was observed even without drier catalyst whereas cardanol did not cure at all.

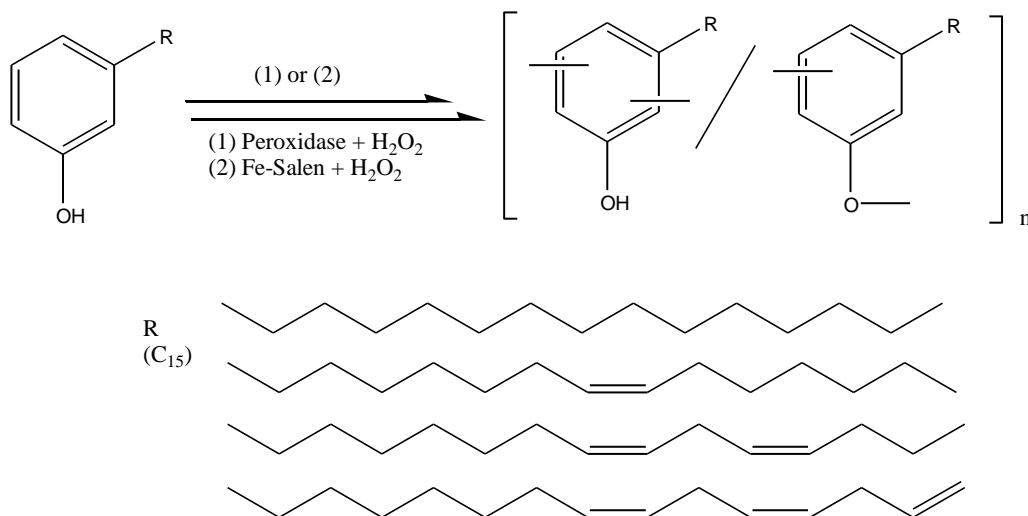


Figure 1.13. Oxidative polymerization of cardanol.³¹

In another study, Kim et al.⁷⁴ reported the synthesis of epoxy functionalized polycardanol using lipase along with acetic acid (5 mmol) and hydrogen peroxide (30%, 7.5 mmol) added continuously to the mixture for 6 h using a perfusion pump resulting in 95% epoxy conversion. Polymerization of both cardanol and epoxidized cardanol were carried out with *C. Cinereus* IFO 8371 peroxidase was reported for the first time. As shown in **Figure 1.14** two different pathways were carried out. Route A involved the synthesis of polycardanol first using peroxidase followed by epoxidation of the unsaturated groups in the side chain using lipase, whereas route B begins with the epoxidation followed by the peroxidase. Coatings from cardanol (1), epoxidized cardanol (2), polycardanol (3) and epoxidized polycardanol (4) were prepared and cured by thermal treatment at 150 °C for 4 different time intervals. Epoxidized polycardanol was also cured with phenalkamine (5) as a curing agent. Curing behavior was monitored at 150 °C by measuring pencil hardness at different time intervals with reported values in **Table 1.3**. Reported values show a trend of (1) < (2) < (3) < (4) < (5) in terms of increasing hardness, suggesting that epoxidized

cardanol as a part of linear polymer rather than alone resulted in increased hardness i.e. crosslinked networks. Additionally, clear films were obtained from 3, 4 and 5. In addition to the epoxy functionality, the presence of the aromatic group in cardanol enhanced the mechanical properties, like the hardness (9H), giving significantly higher values than commercially available general alkyd resins (4H). Curing epoxidized polycardanol in the presence of phenalkamine curative resulted in coatings with a hardness of 5H after curing for 2 h. These sufficiently high properties allow epoxide-containing polycardanol to perform as a potential alternative to the existing phenol-formaldehyde epoxy resin system.^{4, 74}

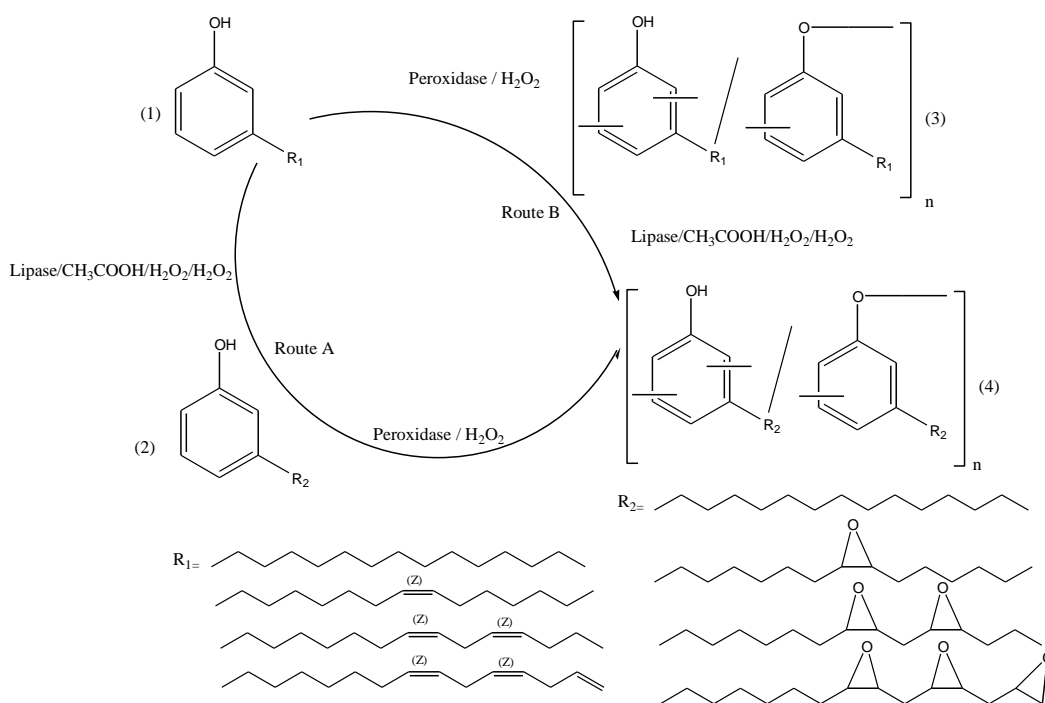


Figure 1.14. Oxidative polymerization of cardanol via two different routes.⁷⁴

Table 1.3. Curing of epoxide containing polycardanol and its hardness. “Data from reference 64”

	1h	1h	1h	1h
Cardanol	-	-	-	-
Epoxide-containing cardanol (2)	-	-	-	-
Polycardanol (3)	-	TF	2B	H
Epoxide-containing polycardanol (4)	TF	5B	H	9H
Epoxide-containing cardanol (4) + phenalkamine	2H	5H	7H	>9H

Yuan et al.³⁵ reported the synthesis of cyclic norbornene functionalized monomers derived from high oleic soybean oil. Monomers were synthesized via esterification between epoxidized N-hydroxyalkyl fatty amides and *exo*-5-norbornenecarboxylic acid catalyzed by DMAP with the assistance of trimethyl acetic anhydride. Prior to esterification, epoxidation of N-hydroxyalkyl fatty amides was carried out in order to eliminate possible interference during ring-opening metathesis polymerization using Grubbs III catalyst as shown in **Figure 1.15**. Depending on the primary or secondary nature of the ethanol amine used for the synthesis of N-hydroxyalkyl fatty amides, both molecular weight and T_g varied significantly. Linear polymers with secondary amino groups resulted in a $T_g \sim -27^\circ\text{C}$ which is higher than the tertiary amino containing polymer with $T_g \sim -32^\circ\text{C}$. This drop in T_g is due to the loss of H-bonding because of the tertiary nature of the amino group. These oxirane-containing linear polymers could be used for surface coatings via crosslinking with various amine curatives.

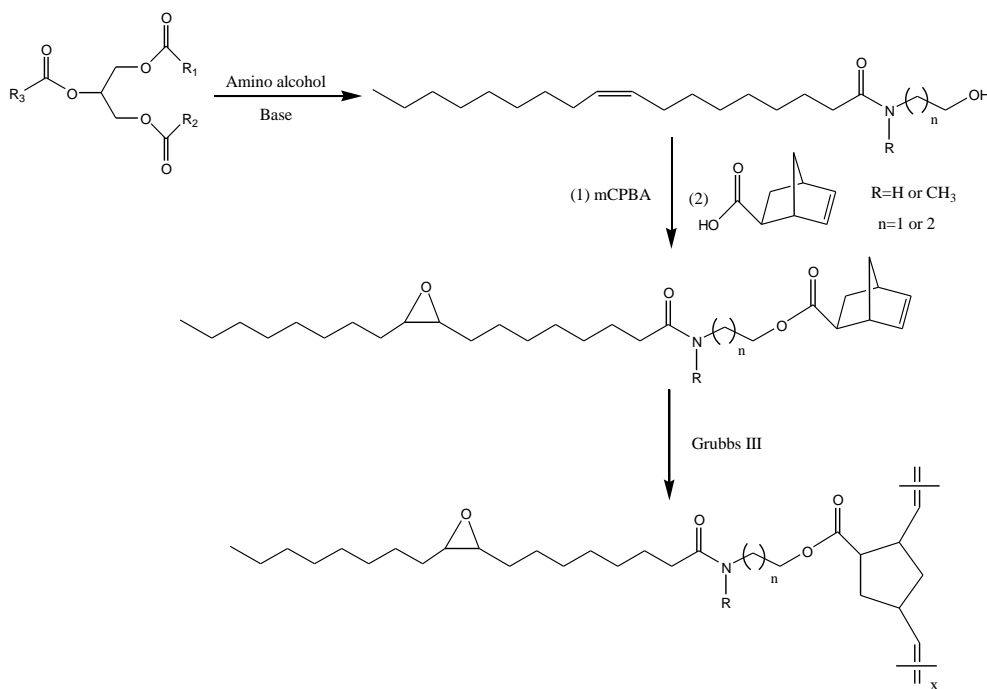


Figure 1.15. Derivatization of triglycerides into N-hydroxyalkyl fatty amides and corresponding ring opening metathesis polymerization of norbornene monomers.³⁵

1.6. Summary and outlook

Research work summarized in this chapter confirms the ongoing efforts to introduce renewable materials in the polymers and coatings industry. Linear chain growth polymers from renewables come with unique structural advantages of having multiple functional groups per molecule compared to conventional biobased materials produced by derivatizing from their monomeric or raw form. Most of the developments towards linear chain growth polymers are encouraging due to their ability to produce thermosets with a wide variety of curing chemistries with the potential to achieve faster curing and higher crosslink densities due to the multiple reactive functional groups per molecule. Results also show that cured coatings or free films produced from linear chain growth polymers having increased physical properties such as hardness, chemical resistance, modulus etc. Linear chain growth polymers derived from plant oil based monomers demonstrate properties comparable to alkyds or even better, with the advantages of overcoming some issues associated with conventional alkyd resins, such as the energy intensive polymerization process, risk of gelation during resin production, and poor film properties due to the presence of monomers and other low molecular weight species. Low yield and gelation has still been reported as a common issue for vinyl ester functionalized monomers derived from highly unsaturated fatty acids such as linolenic acid. There is a strong need to develop proper polymerization conditions for vinyl ester monomers which can lead to the polymerization selectively through the vinyl group. So far researchers have been able to develop linear chain growth polymers using renewable resources from monomers with acrylic, vinyl ether, cyclic imino ether, norbornene etc. functionality with suitable polymerization techniques. Vinyl ether monomers have shown tremendous potential to undergo polymerization both cationically and free radically with complete retention of the unsaturation that can be used for post polymerization crosslinking. This novel

technology could serve as a platform which can lead to the utilization of renewable resources in the polymer and coating industry to achieve higher end properties.

1.7. Need statement

Recent efforts towards the development of environmental friendly polymeric materials has led to the identification of several renewable resources such as plant oils, carbohydrates (sucrose, furan), cellulose, lignin etc. with great potential to provide unique chemicals to be used in the coating industry. However, there is a constant need for technologies that can incorporate the monomers derived from these chemicals into polymeric structures. Direct functionalization of these renewables in their polymeric or depolymerized form to develop thermoset coatings via crosslinking has been used extensively which also comes with several issues such as low solubility and the need for high functionality monomers or macromonomers (drying oils) to achieve a well crosslinked system. Although one of the oldest resins, alkyds, still provide unique features such as solubility in common organic solvents increasing the scope for applications. However, conventional alkyds have their drawbacks because of the synthesis procedures and their chemical structures as discussed earlier (**section 1.6**), there is a constant need for the development of soluble linear polymer with chemically stable backbone chain, having pendent groups that can provide crosslinking to produce surface coatings. Developments of the synthesis of vinyl ether functionalized monomer from renewables to synthesize linear polymers via chain growth polymerization technique for coating application is very recent and so far, only a few monomers have been developed mostly from plant oils. There is a need for expansion of the novel vinyl ether monomers using renewables that can introduce aromatic functionality. There is also a need to study the effect of individual functional groups present in the linear polymer on the coating properties.

1.8. Research objectives

This research has four main objectives:

- (1) Synthesis of novel vinyl ether monomers and their linear polymers exploring renewables other than plant oils;
- (2) Study of the thermal, mechanical and physical properties of the auto cured films and coatings and evaluation of their potential as a replacement to conventional alkyds;
- (3) Explore the ability of novel poly(vinyl ether)s to develop epoxy functionalized resins and evaluate the properties of their coatings; and
- (4) Use of high throughput methods to study coating properties.

1.9. Organization of this dissertation

This dissertation contains eight independent chapters. Chapter 1 (this chapter) provides an overview of the challenges and successes towards the development of linear chain growth polymers from renewable materials and summarizes objectives of this research. The rest of the chapters are presented in journal format and will be submitted to peer reviewed journals for publication with required modifications. Chapter 2 includes the synthesis of poly(vinyl ether)s derived from soybean oil, linseed oil, and camelina oil aimed at studying the properties of the crosslinked networks and cured surface coatings derived from these poly(vinyl ether)s. Chapter 3 reports the synthesis of various colorless poly(vinyl ether)s from soybean oil, linseed oil, and palm oil and studies their potential application as artist paint binder to provide fast drying/curing and minimal yellowness. Chapter 4 reports the synthesis of vinyl ether monomer from cardanol (CEVE) and its homopolymer and copolymers with cyclohexyl vinyl ether (CHVE). The chapter also includes the results obtained from the study of thermal, mechanical and physical properties of the coating and free films derived from them. Chapter 5 describes the synthesis of poly(vinyl

ether)s derived from eugenol and copolymers with CHVE. The properties of auto cured films and surface coatings are also studied and compared to cured coatings derived from commercial alkyds. Chapter 6 involves high-throughput evaluation of the coatings based on three epoxy resins derived from eugenol with twelve amine curatives as a potential biobased replacement for bisphenol A epoxy resins. Chapter 7 summarizes the overall conclusions and future directions of the current study.

1.10. References

1. L. Raymond, *Proceedings of the Institution of Mechanical Engineers: Automobile Division*, 1959, **13**, 19-42.
2. T. N. Inuan and E. H. Simonei, Bisphenol A, National Institute of Health, Research Triangle Park, North Carolina 2010.
3. Z. Wang, L. Yuan and C. Tang, *Accounts of Chemical Research*, 2017, **50**, 1762-1773.
4. S. Kobayashi and H. Uyama, *Chemtech*, 1999, **29**, 2-28.
5. R. Narayan, in *Emerging Technologies for Materials and Chemicals from Biomass*, American Chemical Society, 1992, **476**, 1-10.
6. D. R. Erickson, *Practical handbook of soybean processing and utilization*, Elsevier, St. Louis, MO/Champaign, IL, 2015.
7. F. N. Jones, W. Maa, P. D. Ziemer, F. Xiao, J. Hayes and M. Golden, *Progress in Organic Coatings* 2005, **52**, 9-20.
8. R. Ploeger and O. Chiantore, *Smithsonian Contributions to Museum Conservation*, Torino 2012, 89-95.
9. C. B. Croston, I. L. Tubb, J. C. Cowan and H. M. Teeter, *Journal of the American Oil Chemists Society*, 1952, **29**, 331-333.

10. F. S. Güner, Y. Yagci and A. T. Erciyes, *Progress in Polymer Science*, 2006, **31**, 633-670.
11. X. Pan, P. Sengupta and D. C. Webster, *Green Chemistry*, 2011, **13**, 965-975.
12. A. Gandini, T. M. Lacerda, A. J. F. Carvalho and E. Trovatti, *Chemical Reviews*, 2016, **116**, 1637-1669.
13. I. Delidovich, P. J. C. Hausoul, L. Deng, R. Pfützenreuter, M. Rose and R. Palkovits, *Chem. Rev.*, 2016, **116**, 1540–1599.
14. I. Faye, M. Decostanzi, Y. Ecochard and S. Caillol, *Green Chemistry*, 2017, **19**, 5236-5242.
15. D. Kalita, I. Tarnavchyk, D. Sundquist, S. Samanta, J. Bahr, O. Shafranska, M. Sibi and B. Chisholm, *INFORM*, 2015, **26**, 472-475.
16. H. Nakagawa, Y. Okimoto, S. Sakaguchi and Y. Ishii, *Tetrahedron Letters*, 2003, **44**, 103-106.
17. K. Yao and C. Tang, *Macromolecules*, 2013, **46**, 1689–1712.
18. M. Pagliaro, R. Ciriminna, H. Kimura, M. Rossi and C. D. Pina, *Eur. J. Lipid Sci. Technol.*, 2009, **111**, 788-799.
19. S. A. Miller, *ACS Macro Letters*, 2013, **2**, 550-554.
20. R. Nagelsdiek, M. Mennicken, B. Maier, H. Keul and H. Höcker, *Macromolecules*, 2004, **37**, 8923-8932.
21. K. I. Suresh and M. Jaikrishna, *Journal of Polymer Science Part A: Polymer Chemistry*, 2005, **43**, 5953-5961.
22. F. B. Chen and B. G. Bufkin, *Journal of Applied polymer science*, 1985, **30**, 4571-4582.
23. F.-B. Chen and B. G. Bufkin, *Journal of Applied polymer science*, 1985, **30**, 4551-4570.

24. S. F. Thames, K. G. Panjnani and O. S. Fruchey, The University of Southern Mississippi, *Hattiesburg, MS (US) Pat.*, 2001, US 6,174,948 B1.
25. G. Booth, D. E. Delatte and S. F. Thames, *Industrial Crops and Products*, 2007, **25**, 257-265.
26. H. G. Cho, S. Y. Park, J. Jegal, B. K. Song and H. J. Kim, *Journal of Applied polymer science*, 2010, **116**, 736-742.
27. G. R. Palmese, J. J. L. Scala and J. M. Sands, Drexel University, US Secretary of Army, US8372926B2, 2013.
28. M. Moreno, M. Goikoetxea and M. J. Barandiaran, *Journal of Polymer Science Part A: Polymer Chemistry*, 2012, **50**, 4628-4637.
29. C. Vilela, R. Rua, A. J. D. Silvestre and A. Gandini, *Industrial Crops and Products*, 2010, **32**, 97-104.
30. G. John, S. K. Thomas and C. K. S. Pillai, *Journal of Applied polymer science*, 1994, **53**, 1415-1423.
31. R. Ikeda, H. Tanaka, H. Uyama and S. Kobayashi, *polymer preprints*, 2000, **41**, 83-84.
32. I. Tarnavchyk, A. Popadyuk, N. Popadyuk and A. Voronov, *ACS Sustainable Chemistry & Engineering*, 2015, **3**, 1618-1622.
33. Z. Demchuk, O. Shevchuk, I. Tarnavchyk, V. Kirianchuk, A. Kohut, S. Voronov and A. Voronov, *ACS Sustainable Chemistry & Engineering*, 2016, **4**, 6974-6980.
34. Z. Demchuk, O. Shevchuk, I. Tarnavchyk, V. Kirianchuk, M. Lorenson, A. Kohut, S. Voronov and A. Voronov, *ACS Omega*, 2016, **1**, 1374-1382.
35. Z. Yang, L. Yuan, N. M. Trenor and C. Tang, *Macromolecules*, 2015, **45**, 1320-1328.
36. L. Yuan, Z. Wang, N. M. Trenor and C. Tang, *Polymer Chemistry*, 2016, **7**, 2790-2798.

37. Z. Wang, L. Yuan, N. M. Trenor, L. Vlaminck, S. Billiet, A. Sarkar, F. E. D. Prez, M. Stefika and C. Tang, *Green Chemistry*, 2015, **17**, 3806-3818.
38. S. Alam and B. J. Chisholm, *Journal of Coatings Technology and Research*, 2011, **8**, 671-683.
39. S. Aoshima and T. Higashimura, *Macromolecules*, 1989, **22**, 1009-1013.
40. H. Kalita, S. Alam, A. Jayasooriyamu, S. Fernando, S. Samanta, J. Bahr, S. Selvakumar, M. Sibi, J. Vold, C. Ulven and B. J. Chisholm *Journal of Coatings Technology and Research*, 2015, **12**, 633-646.
41. H. Kalita, S. Selvakumar, A. Jayasooriyamu, S. Fernando, S. Samanta, J. Bahr, S. Alam, M. Sibi, J. Vold, C. Ulven and B. J. Chisholm, *Green Chemistry*, 2014, **16**, 1974-1986.
42. Y. Okimoto, S. Sakaguchi and Y. Ishii, *Journal of the American Chemical Society*, 2002, **124**, 1590-1591.
43. T. G. Fox, *Bull. Am. Phys. Soc*, 1956, 123-124.
44. H. Kalita, S. Alam, D. Kalita, A. Chernykh, I. Tarnavchyk, J. Bahr, S. Samanta, A. Jayasooriyama, S. Fernando, S. Selvakumar, D. S. Wickramaratne, M. Sibi and Bret J. Chisholm, *European Coatings Journal*, 2015, **6**, 26-29.
45. S. Alam, H. Kalita, O. Kudina, A. Popadyuk, B. J. Chisholm and A. Voronov, *ACS Sustainable Chemistry & Engineering*, 2013, **1**, 19-22.
46. H. Kalita, D. Kalita, S. Alam, A. Chernykh, I. Tarnavchyk, J. Bahr, S. Samanta, Anurad Jayasooriyama, S. Fernando, S. Selvakumar, D. S. Wickramaratne, M. Sibi and Bret J. Chisholm, *Biobased and Environmentally Benign Coatings*, ed. A. Tiwari, A. Galanis, M. D. Soucek, Wiley-Scrivener Publishing, 2016, **1**, 1-16.

47. H. Kalita, A. Jayasooriyama, S. Fernando and B. J. Chisholm, *Journal of Palm Oil Research*, 2015, **27**, 39-56.
48. A. Chernykh, S. Alam, A. Jayasooriya, J. Bahr and B. J. Chisholm, *Green Chemistry*, 2013, **15**, 1834-1838.
49. S. Samanta, S. Selvakumar, J. Bahr, D. Suranga Wickramaratne, M. Sibi and B. J. Chisholm, *ACS Sustainable Chemistry and Engineering*, 2016, **4**, 6551-6561.
50. J. W. Wicks, F. N. Jones. S. P. Pappas, *Organic Coatings: Science and Technology*, John Wiley & Sons, Hoboken, NJ, 2007.
51. W. J. Blank, King Industries, Inc. Norwalk, *USA Pat.*, 1989, 4,820,830.
52. M. S. Kathalewar, P. B. Joshi, A. S. Sabnis and V. C. Malshe, *RSC Advances*, 2013, **3**, 4110-4129.
53. A. Ekin and D. C. Webster, *Macromolecules*, 2006, **39**, 8659-8668.
54. R. J. Pieper, A. Ekin, D. C. Webster, F. Cassé, J. A. Callow and M. E. Callow, *Journal of Coatings Technology and Research*, 2007, **4**, 453.
55. V. S. Balachandran, S. R. Jadhav, P. K. Vemula, and G. John, *Chem. Soc. Rev.*, 2013, **42**, 427-438.
56. H. Kalita, S. Alam, D. Kalita, A. Chernykh, I. Tarnavchyk, J. Bahr, S. Samanta, A. Jayasooriyama, S. Fernando, S. Selvakumar, A. Popadyuk, D. S. Wickramaratne, M. Sibi, A. Voronov, A. Bezbaruah and B. J. Chisholm, in *Soy-Based Chemicals and Materials*, American Chemical Society, 2014, **1178**, 371-390.
57. W. J. Toussaint, Preparation of vinyl esters, Carbide and Carbon Chemicals Corporation, New York, 2,299,862, 1942.

58. D. Swern, G. N. Billen and H. B. Knight, *Journal of the American Chemical Society*, 1947, **69**, 2439-2442.
59. S. A. Harrison and D. H. Wheeler, *Journal of the American Chemical Society*, 1951, **73**, 839-842.
60. R. L. Frank, C. E. Adams, J. R. Blegen, R. Deanin and P. V. Smith, *Industrial & Engineering Chemistry*, 1947, **39**, 887-893.
61. W. K. Wilson, Vinyl Resin Emulsion, Shawinigan Resins corporation, USA, US2508341A, 6.
62. R. E. Murray and D. M. Lincoln, *Catalysis Today*, 1992, **13**, 93-102.
63. A. Sabel, J. Smidt, R. Jira and H. Prigge, *Eur. J. Inor. Chem.* 1969, 102, 2939-2950.
64. R.E. Murray, Transvinilation reaction, Union Carbide Chemicals and Plastics Technology LLC, US4981973A, 1991.
65. H. Nakagawa, Y. Okimoto, S. Sakaguchi and Y. Ishii, *Tetrahedron Letters*, 2003, **44**, 103-106.
66. M. Lazzari and O. Chiantore, *Polymer Degradation and Stability*, 1999, **65**, 303-313.
67. J. A. Frump, *Chemical Reviews*, 1971, **71**, 483-506.
68. M. Beck, P. Birnbrich, U. Eicken, H. Fischer, W. E. Fristad, B. Hase and H. J. Krause, *Die Angewandte Makromolekulare Chemie*, 1994, **223**, 217-233.
69. R. Hoogenboom and U. S. Schubert, *green chemistry*, 2006, **8**, 895-899.
70. R. Hoogenboom, *European Journal of Lipid Science and Technology*, 2011, **113**, 59-71.
71. R. Hoogenboom, M. A. M. Leenen, H. Huang, C.-A. Fustin, J. F. Gohy and U. S. Schubert, *Colloid and Polymer Science*, 2006, **284**, 1313-1318.

72. H. Huang, R. Hoogenboom, M. A. M. Leenen, P. Guillet, A. M. Jonas, U. S. Schubert and J. F. Gohy, *Journal of the American Chemical Society*, 2006, **128**, 3784-3788.
73. H. Tonami, H. Uyama, S. Kobayashi and M. Kubota, *Macromolecular Chemistry and Physics*, 1999, **200**, 2365-2371.
74. Y. H. Kim, E. S. An, S. Y. Park and B. K. Song, *Journal of Molecular Catalysis B: Enzymatic*, 2007, **45**, 39-44.

CHAPTER 2. BIOBASED POLY(VINYLETHER)S DERIVED FROM SOYBEAN OIL, LINSEED OIL, AND CAMELINA OIL: SYNTHESIS, CHARACTERIZATION, AND PROPERTIES OF CROSSLINKED NETWORKS AND SURFACE COATINGS

2.1. Abstract

A series of novel plant oil (PO)-based poly(vinyl ether)s were produced that varied with respect to PO composition and molecular weight (MW). The POs investigated were soybean oil, linseed oil, and camelina oil. All of the polymers were liquids at room temperature and were used to produce crosslinked networks, both as free-standing films and as surface coatings on steel substrates. Crosslinking was achieved at ambient conditions through the process of autoxidation. Viscosity of the neat polymers as well as the viscoelastic and mechanical properties of crosslinked networks were highly dependent on parent PO composition. At a given polymer MW, viscosity decreased with increasing PO unsaturation, while glass transition temperature, Young's modulus, and tensile strength of crosslinked networks increased with increasing PO unsaturation. For polymers derived from the most highly unsaturated PO, linseed oil, the impact resistance of the coatings was poor, due to the relatively high crosslink density of these coatings. Overall, these results demonstrated that the viscosity and properties of crosslinked films based on these novel PO-based poly(vinyl ether)s could be tailored through selection of the parent PO and control of polymer MW. This class of highly bio-based polymers appears to have particular utility for the production of one-component, ambient-cured coatings. One component, ambient-cured thermoset coatings are highly desired because of their ease of use, lower waste production, and energy cost savings compared to other thermoset coating systems.

2.2. Introduction

Prior to the abundant access to crude oil, chemicals and materials were derived from renewable resources, such as plant oils (POs), cellulosic biomass, tree resins, and insect secretions.¹ Due to the high demand for fossil fuels and the tremendous infrastructure put in place to meet the demand, research and development of chemicals and materials from renewable materials was largely abandoned. At present, over ninety percent of all chemicals and materials are derived from oil and gas.² However, the finite supply of fossil resources, issues with climate change, and toxicity associated with many petrochemicals has caused a resurgence of interest in the development of chemicals and materials from renewable resources.¹ Research and development of chemicals and materials from renewable resources can be broadly divided into two categories based on chemical composition. One category involves the production of drop-in replacements from renewable sources, such as adipic acid, poly(ethylene), 1,4-butanediamine, and ethanol, while the other involves the production of new chemicals and materials that are more easily obtained from renewable resources than fossil resources. Replacing existing petroleum-based chemicals and materials with renewable-based offsets has the advantage that the markets and demand for these materials is already well known and established. The challenge with this approach is cost-competitiveness. For commodity petroleum-based chemicals and materials, most all of the production equipment has been fully depreciated and processes have been extensively optimized to minimize cost. With regard to the production of new chemicals and materials that are more easily obtained from renewable resources, the challenge is obtaining sufficient value from these new chemicals and materials to achieve commercial success. In general, the fact that the chemical or material is derived from a renewable resource is not sufficient to motivate a customer purchase. The chemical or material must also provide a performance and/or cost benefit.

Of the different renewable resources available for the development of chemicals and materials, plant oils (POs) are particularly attractive because they are relatively easy to isolate and their chemical components cannot be readily produced from oil and gas. POs are triglycerides of fatty acids (FA) and depending on the species of the plant, FA composition of the triglycerides can vary widely. For example, about 90 percent of the FAs from coconut oil triglycerides are saturated and are less than 18 carbons in length.^{3,4} As a result, coconut oil has a melting temperature of about 24 °C and relatively good oxidative stability.⁵ In contrast, linseed oil (LO) consists of FAs that are 18 carbons in length and about 90 percent contain unsaturation.⁴ As a result, LO has a melting point of about -24 °C and is relatively easily oxidized.⁶

With regard to industrial applications, POs have been used extensively for paint and coating applications.⁷ For example, prior to the widespread availability of petrochemicals, LO was the primary material used as a binder for paints and coatings.⁸ The polyunsaturation in LO provides the bis-allylic protons that enable oxidative polymerization of the oil to an insoluble solid film when exposed to air.^{9,10} The oxidative polymerization of an unsaturated PO is typically referred to as autoxidation and can be effectively catalyzed by select metal salts, such as cobalt carboxylates.¹¹ For the coatings industry, POs are categorized by their level of unsaturation defined by their iodine value (IV).¹² The IV is the number of grams of iodine needed to fully react with the double bonds of 100 grams of PO. Thus, in general, the higher the IV, the faster the rate of autoxidation. POs with IV above 130 have been termed “drying” oils because thin films of the oil can be converted to an insoluble, tack-free film in a reasonable time to be useful as a binder for paints or stains. In addition to LO, other drying oils include tung oil, poppy seed oil, perilla oil, walnut oil, and hemp seed oil.^{13,14} POs with IV between 115 and 130 are referred to as “semi-drying” oils, since they are capable of providing insoluble, tack-free films through autoxidation, but the time required for

this process is quite long for practical applications. Soybean oil (SBO), the most abundant PO produced in the United States, falls in the category of semi-drying oils. Oils with IV below 115 are termed “non-drying” oils.

As a result of the abundance and low cost of SBO, chemical modifications have been made to enable industrial applications. For example, the double bonds in SBO have been converted to epoxide groups to produce a polyepoxide that is used primarily as a plasticizer and stabilizer for poly(vinyl chloride).^{15,16} In addition, the epoxy-functional SBO has been used to produce commercially available polyols and polyacrylates through ring-opening reactions of the oxirane moieties.^{17,18} SBO-based polyols are used primarily for the production of polyurethane foams, while acrylate-functional SBO is primarily used for radiation-curable coatings.^{19,20,21}

Extensive work has been conducted to produce polymers from unsaturated FA-containing monomers using conventional free-radical polymerization techniques, such as solution free-radical polymerization and emulsion polymerization. A major challenge associated with the free-radical polymerization of unsaturated FA-based monomers is chain transfer reactions associated with the very easily abstractable bis-allylic and allylic protons.²² For example, Delatte et al. achieved relatively low yields (i.e. less than 50 percent) for solution copolymerizations of a soy-based fatty amide acrylate and methyl methacrylate.²³ Only when an extraordinarily high concentration of initiator was used (i.e. 4 mole percent based on monomer) was a higher monomer conversion of 85 percent achieved. Black et al. demonstrated this issue by conducting free-radical polymerizations of butyl acrylate and methyl methacrylate in the presence of various POs using solution free-radical polymerization.²⁴ Chain transfer reactions involving bis-allylic and allylic protons of the POs was directly observed using *in situ* infrared (IR) spectroscopy. As expected, the POs resulted in chain transfer reactions which limited polymer molecular weight (MW) and

reduced the concentration of the bis-allylic and allylic protons needed for subsequent crosslinking by autoxidation. Demchuk et al.²⁵ produced FA-containing acrylamide monomers by base-catalyzed transesterification of N-(hydroxyethyl)acrylamide with a PO triglyceride. Homopolymers were produced by solution free-radical polymerization from monomers derived from sunflower oil, LO, SBO, and olive oil. It was found that the MW of the homopolymers and the rate of polymerization decreased with increasing unsaturation of the parent PO. These results were due to chain transfer and termination reactions associated with bis-allylic and allylic protons in the unsaturated FA chain. Yuan et al.²⁶ described the synthesis and homopolymerization of three fatty amide methacrylate monomers produced by reacting high oleic SBO (HOSO) with three amino alcohols and subsequently reacting the hydroxyl-functional fatty amide with methacrylic anhydride. Homopolymers with number-average MWs ranging from 15,300 to 63,000 g/mole were obtained by free-radical solution polymerization with monomer conversions greater than 90 percent. The relatively high MWs and polymer yields obtained with this monomer may be due to the fact that HOSO was used as the PO source. Compared to other unsaturated POs previously discussed, HOSO has a relatively low concentration of bis-allylic protons, which are the most reactive toward free-radical abstraction.²⁷

For waterborne coatings based on acrylic latexes, it has long been expected that incorporation of unsaturated FA chains in a poly(acrylate) would be very beneficial from two aspects.²⁸ First, the long fatty chains may serve as plasticizers, thereby potentially enabling latex particle coalescence without the need for the addition of a coalescing agent. This is desirable because coalescing agents contribute to the volatile organic compound (VOC) content of a coating. Second, bis-allylic and allylic protons present in unsaturated FA chains are expected to enable crosslinking through autoxidation, which would improve properties such as scrub resistance,

hardness, and chemical resistance. In addition to issues associated with chain transfer and termination reactions, the highly hydrophobic nature of FA-based monomers is problematic for conventional emulsion polymerization since it requires transport of monomer molecules from monomer droplets to micelles. Miniemulsion polymerization largely overcomes this limitation and, thus, can be effectively used for the polymerization of highly hydrophobic monomers.²⁹ In fact, Bunker and Wool³⁰ successfully polymerized a saturated FA-containing monomer using miniemulsion polymerization. This monomer was produced by epoxidizing the carbon-carbon double bond in methyl oleate and subsequently ring-opening the oxirane moiety with acrylic acid. Miniemulsion polymerization was also used to produce acrylate copolymers derived from a SBO-based monomer derived from the reaction of hydroxy ethyl methylate with maleated SBO.³¹ PO-based acrylamide monomers derived from the reaction of the PO triglyceride with *N*-(hydroxyethyl)acrylamide were successfully copolymerized with common monomers, such as styrene, vinyl acetate, and methyl methacrylate, using miniemulsion polymerization.³² While miniemulsion polymerization was effective for enabling the free-radical polymerization of vinyl-functional, PO-based monomers, it is not widely used in industry because high-energy mixing, such as ultrasonication or high pressure homogenization, is generally required for obtaining the very small particle sizes needed.³³

Chisholm et al. have been investigating polymers produced from PO-based vinyl ether (POVE) monomers using cationic polymerization.³⁴⁻⁴⁵ **Figure 2.1** illustrates both POVE monomer synthesis and its homopolymerization. Using SBO as the parent PO, it was shown that a living polymerization could be produced by utilizing an initiating system and polymerization conditions that provide carbocations that are reactive enough to enable polymerization of the vinyl ether (VE) double bonds, but not reactive enough to react with double bonds associated with SBO-based FA

chains.³⁶ Unlike free radical polymerization of the PO-based monomers previously discussed, cationic polymerizations of the novel POVE monomers were essentially free of chain transfer and chain termination reactions, thereby enabling polymers that possessed narrow MW distributions and no reduction in the unsaturation or allylic/bis-allylic protons of the PO-based portion of the repeat units. In addition, polymerization yields were typically greater than 95 weight percent. Further, it was demonstrated that the living nature of the polymerization could be used to produce block copolymers using a simple sequential addition of monomers.^{37,44}

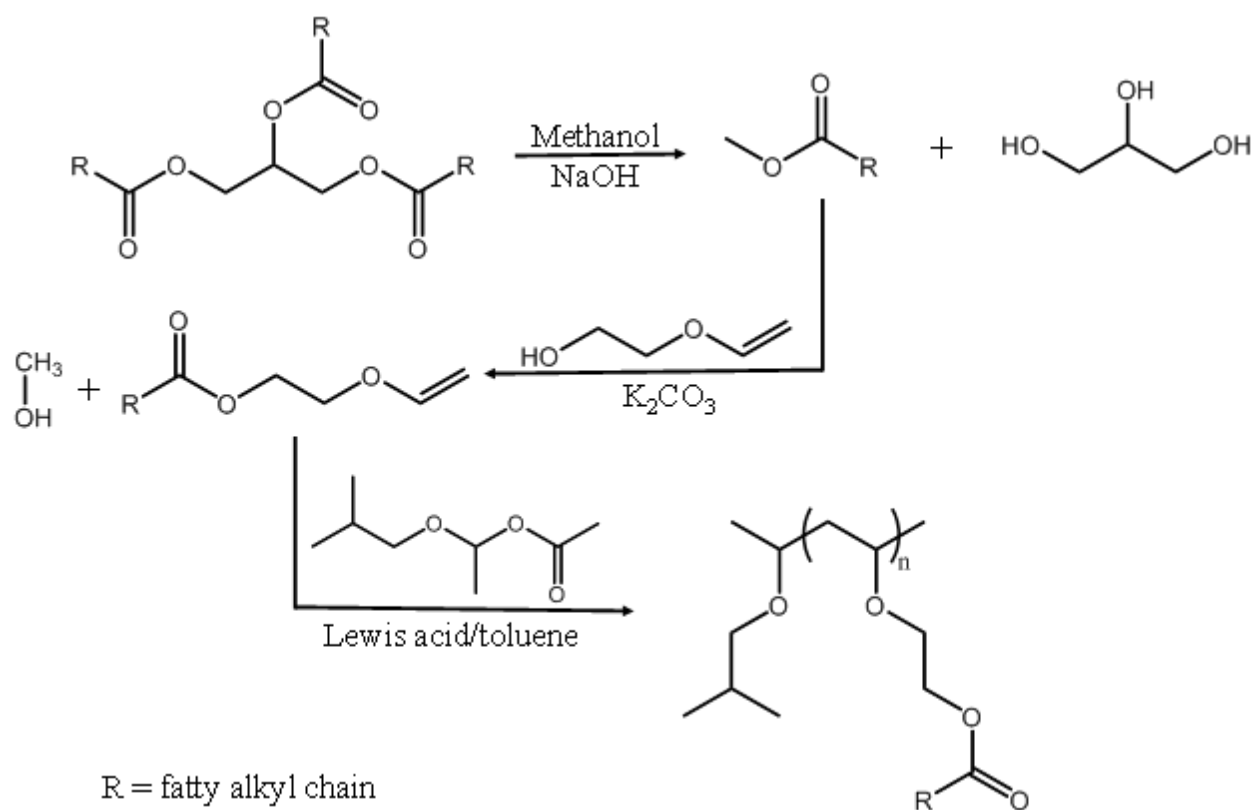


Figure 2.1. Synthesis of a POVE polymer from a PO triglyceride.

Since the VE/cationic polymerization approach readily produces polymers based on unsaturated POs in high yield that retain all of the allylic and bis-allylic protons present in the parent PO, these polymers are particularly useful for production of one-component, ambient-cured thermoset coatings. One component, ambient-cured thermoset coatings are highly desired because

of their ease of use and lower waste production compared to two-component, ambient-cured coatings. In addition, ambient-cured coatings eliminate energy costs associated with other curing methods, such as thermal and radiation curing. Compared to drying oils, such as LO, POVE polymers cure dramatically faster. The time associated with the conversion of a liquid film to a tack-free, insoluble coating, which is often referred to as the “drying time,” is illustrative. Using the same catalytic amount of metal carboxylates to promote autoxidation, the drying times for SBO, LO, and an SBO-based POVE polymer were 450, 280, and 6 hours, respectively.⁴⁶ The much shorter drying time for the SBO-based polymer can be attributed to its higher MW compared to the two triglycerides (i.e. LO and SBO). As a result of the higher MW of the polymer, the extent of autoxidation needed to reach the gel-point was much lower. Thus, converting SBO to its corresponding POVE polymer enabled a fast drying liquid polymer from a semi-drying PO.

The objective of the research described in this chapter was to synthesize a wide variety of POVE polymers that differ with respect to the chemical composition of parent PO and polymer MW and determine their properties with respect to application as surface coatings. The three POs were SBO, LO, and camelina oil (CMO). As shown in **Table 2.1**, the FAs comprising SBO and LO are mostly 18 carbons in length with a relatively small fraction of C16 FAs. The primary difference between SBO and LO is double bond content, as indicated by the considerably higher IV of LO. The primary difference between CMO and SBO or LO is that CMO contains about 22 weight percent of FA with hydrocarbon chains in excess of 18 carbons. The IV of CMO is in between that of LO and SBO, but the ratio of polyunsaturation to monounsaturation is lower for CMO than either LO or SBO.

CMO is a relatively new crop to the United States that is being positioned as an important feedstock for biodiesel/renewable diesel as well as biojet fuel.⁴⁷ According to Moser and Vaughn,⁴⁸

camelina has several beneficial agronomic attributes, which include: (1) a short growing cycle (85-100 days), (2) compatibility with existing farming practices, (3) tolerance of cold, drought, and semiarid conditions, (3) low input costs, such as fertilizer, irrigation, and pesticide, (4) tolerance of marginal lands, (5) relatively high value of the meal, and (6) high oil content (35 to 45 wt. %). Considering these factors, it was of interest to assess the utility of POVEs based on CMO.

Table 2.1. FA composition and IV of SBO,⁴ LO,⁴ and CMO,⁴⁹ as determined previously.

Fatty Acid	SBO	LO	CMO
Palmitic (C16:0) [wt. %]	9	5.5	5.3
Stearic (C18:0) [wt. %]	4	3.5	2.2
Oleic (C18:1) [wt. %]	28.5	22.1	16
Linoleic (C18:2) [wt. %]	49.5	20.5	18.4
Linolenic (C18:3) [wt. %]	8	47.5	32.4
Arachidic (C20:0) [wt. %]	----	----	1.6
Eicosenoic (C20:1) [wt. %]	----	----	14.9
Eicosadienoic (C20:2) [wt. %]	----	----	1.7
Erucic (C22:1) [wt. %]	----	----	3.7
Iodine value [g I ₂ /100 g oil]	130	177	147
Monounsaturated fatty acids (C:1) [wt. %]	28.5	22.1	34.6
Polyunsaturated fatty acids (C:2&3) [wt. %]	57.5	68	52.5
Ratio of polyunsaturated to monounsaturated fatty acids	2.02	3.08	1.52

2.3. Experimental

2.3.1. Materials

The chemicals and their sources used for this study are described in **Table 2.2**. Unless specified otherwise, all chemicals were used as received.

Table 2.2. A description of the chemicals used for the study.

Chemical	Designation	Vendor
Soybean oil	SBO	Bacher & Chefs
Linseed oil	LO	Cargill
Camelina oil	CMO	Making Cosmetics Inc.
Sodium hydroxide	NaOH	Sigma-Aldrich
Magnesium sulfate	MgSO ₄	Sigma-Aldrich
Ethylaluminum sesquichloride, 97%	Et ₃ Al ₂ Cl ₃	Sigma-Aldrich
Tin(IV) chloride, 98%	SnCl ₄	Sigma-Aldrich
Ethylene Glycol Monovinyl Ether	2VOE	TCI America
Methanol, 98%	Methanol	BDH Chemicals
Dichloromethane	CH ₂ Cl ₂	BDH Chemicals
Toluene	Toluene	BDH Chemicals
n-Hexane	n-Hexane	Sigma-Aldrich
Tetrahydrofuran, 99%	THF	J.T.Baker
Methyl ethyl ketone, 99%	MEK	Alfa Aesar
Cobalt 2-ethylhexanoate, 12% Co	Cobalt octoate	OMG Americas
Zirconium 2-ethylhexanoate, 18% Zr	Zirconium octoate	OMG Americas
Zinc carboxylate in mineral spirits, 8% Zn	Nuxtra® Zinc	OMG Americas

2.3.2. Synthesis of monomer

As illustrated in **Figure 2.1**, POVE monomers were produced via using base-catalyzed transesterification of 2VOE with the methyl ester of the parent PO. PO methyl esters were produced by base-catalyzed transesterification of the parent PO with methanol. 10 g of anhydrous NaOH was dissolved in 250 mL of methanol and vigorously stirred with 1 L of PO for 40 minutes using a three-neck, round-bottom flask equipped with a mechanical stirrer and a 30 °C water bath. The resulting two-phase mixture was transferred to a separatory funnel and the bottom layer removed before washing the top layer three times with 200 mL of deionized (DI) water. The water-washed methyl ester was then dried by stirring with MgSO₄ overnight. After drying, the MgSO₄ was removed by filtration.

The reactor system utilized for the synthesis of POVE monomers consisted of a three-neck, round-bottom flask equipped with an oil bath, reflux condenser, nitrogen bubbler, vacuum pump, and magnetic stirrer. The vacuum pump was attached to the set-up at the top of the condenser, and the condenser temperature set at 5 °C. The 2VOE was purified before use by vacuum distillation. 150 g of methyl ester, 135 g of distilled 2VOE, and 2.8 g of dry K₂CO₃ was charged to the reactor and the reaction allowed to proceed for 5 hours at 100-110 °C. The pressure in the reactor was adjusted to 200-300 mbar, which allowed the methanol generated from the reaction to pass through the condenser which then collected using a cold trap before reaching the vacuum pump, while the 2VOE was effectively condensed and returned to the reactor. After completion of the reaction, the excess 2VOE was removed by vacuum stripping at a temperature of 130 °C and pressure of 10 mbar. The reaction mixture was allowed to cool to room temperature before washing three times with 80 mL of DI water using a separatory funnel. The POVE monomer was then dried using

MgSO₄ and purified by fractional distillation using a thin-film evaporator operating at a pressure of 1 mTorr and a jacket temperature of 130 °C.

2.3.3. Synthesis of polymers

As illustrated in **Figure 2.1**, homopolymers of the three-different POVE monomers were produced by cationic solution polymerization using 1-isobutoxy-ethyl acetate (IBEA) as an initiator and SnCl₄ or Et₃Al₂Cl₃ as the Lewis acid coinitiator. IBEA was synthesized according to the method described by Aoshima and Higashimura.⁵⁰ All polymerizations were carried out inside a dry nitrogen-filled glove box equipped with a heptane bath for conducting sub-ambient polymerizations. POVE homopolymers designed to possess a MW below 10,000 g/mole were produced using SnCl₄ as the Lewis acid coinitiator and 1,4-dioxane as an electron donor,⁵¹ while those designed to possess a MW above 10,000 g/mole utilized Et₃Al₂Cl₃ as the Lewis acid coinitiator and no electron donor.³⁶ POVE polymers were produced in 40 mL vials partially submerged in the heptane bath cooled to 5 °C. For the relatively low MW POVE polymers, 15 ml of POVE monomer, 13 mL of CH₂Cl₂, and the appropriate amounts of IBEA and 1,4-dioxane were charged to the vial, mixed by vigorous shaking, and allowed to cool to the reaction temperature before initiating the polymerization by injecting the appropriate amount of a 0.10 M solution of SnCl₄ in CH₂Cl₂ and vigorously shaking the solution. The polymerization was allowed to proceed for 45 minutes before termination with a mixture of 0.5 mL of methanol and 0.4 g of sodium bicarbonate. The polymer solution was filtered, washed three times with methanol and dried at reduced pressure.

For relatively high MW POVE polymers, polymerizations were the same as that previously described by Chernykh and coworkers.³⁶ MW was varied by simply varying the molar ratio of monomer to initiator (i.e. IBEA), as indicated in **Table 2.3**

Table 2.3. Composition of the polymerization mixtures used to produce POVE polymers.

Polymer ID	Coinitiator	Monomer (g)	Initiator (g)	Coinitiator (g)	Electron Donor (g)	Mn g/mole	PDI
Poly(2VOES), 2K	SnCl ₄	20	1.429	0.053	1.101	2.07	1.13
Poly(2VOES), 6K	SnCl ₄	20	0.357	0.043	1.101	6.05	1.12
Poly(2VOES), 13K	Et ₃ Al ₂ Cl ₃ /	20	0.213	0.526	0	12.68	1.12
Poly(2VOES), 18K	Et ₃ Al ₂ Cl ₃	20	0.130	0.524	0	18.06	1.13
Poly(2VOES), 24K	Et ₃ Al ₂ Cl ₃	20	0.130	0.542	0	25.0	1.13
Poly(2VOES), 27K	Et ₃ Al ₂ Cl ₃	20	0.114	0.530	0	28.05	1.16
Poly(2VOES), 45K	Et ₃ Al ₂ Cl ₃	20	0.071	0.526	0	45.30	1.16
Poly(2VOEL), 2K	SnCl ₄	20	1.428	0.053	1.101	2.46	1.13
Poly(2VOEL), 4K	SnCl ₄	20	0.709	0.046	1.093	3.93	1.12
Poly(2VOEL), 6K	SnCl ₄	20	0.357	0.043	1.101	6.08	1.11
Poly(2VOEL), 12K	Et ₃ Al ₂ Cl ₃	20	0.213	0.526	0	11.90	1.10
Poly(2VOEL), 20K	Et ₃ Al ₂ Cl ₃	20	0.128	0.535	0	19.70	1.37
Poly(2VOEL), 30K	Et ₃ Al ₂ Cl ₃	20	0.089	0.524	0	29.74	1.39
poly(2VOEL), 39k	Et ₃ Al ₂ Cl ₃	20	0.071	0.526	0	38.88	1.49
Poly(2VOEC), 3K	SnCl ₄	20	1.429	0.053	1.101	2.67	1.14
Poly(2VOEC), 4K	SnCl ₄	20	0.709	0.046	1.093	4.34	1.15
Poly(2VOEC), 8K	SnCl ₄	20	0.357	0.043	1.101	7.51	1.11
Poly(2VOEC), 14K	Et ₃ Al ₂ Cl ₃	20	0.213	0.526	0	13.75	1.10
Poly(2VOEC), 21K	Et ₃ Al ₂ Cl ₃	20	0.128	0.533	0	21.49	1.33
Poly(2VOEC), 32K	Et ₃ Al ₂ Cl ₃	20	0.089	0.524	0	31.85	1.36
Poly(2VOEC), 40K	Et ₃ Al ₂ Cl ₃	20	0.071	0.526	0	40.11	1.44

2.3.4. Preparation of coatings and crosslinked free films

Crosslinked free-films and coating specimens on steel panels were produced from polymers representing a medium and high MW of those produced for the study. The MW range for the medium MW and high MW polymers was 13,000 to 14,000 g/mol and 39,000 to 45,000 g/mol, respectively. Prior to film casting 10 g of neat polymer was mixed with 8 mg of cobalt octoate, 40 mg of zirconium octoate, and 450 mg of Nuxtra® Zinc using a FlackTek mixer operating at 3500 rpm for 30 seconds. Coating specimens were produced by casting solutions of 70 wt.% polymer in toluene on steel panels (product number SP-105337 from Q-LAB) using a drawdown bar with an 8 mil gap. Free film specimens were produced by casting the same solutions over Teflon®-laminated glass panels. After curing, free film specimens were peeled from the Teflon® substrate. All samples were allowed to crosslink/cure at ambient conditions for four weeks before testing.

2.3.5. Methods and instrumentation

2.3.5.1. Nuclear magnetic resonance (NMR) spectroscopy

Spectra from proton nuclear magnetic resonance (^1H NMR) spectroscopy were obtained using a 400 MHz Bruker 400 NMR spectrometer. Data acquisition was accomplished using 16 scans and CDCl_3 was used as the lock solvent.

2.3.5.2. Gel permeation chromatography (GPC)

MW and MW distribution of the polymers produced were characterized using gel permeation chromatography. The instrument utilized was a EcoSEC HLC-8320GPC from Tosoh Bioscience and was equipped with a differential refractometer detector. Two different columns were used depending the expected MW of the polymers. For polymers with an expected MW below 15,000 g/mole, two TSKgel SuperH3000 columns were used, while two TSKgel SuperHM

columns were used for polymers with an expected MW above 15,000 g/mole. THF was used as the mobile phase, the flow rate was 0.35 ml/min, and the operating temperature of the columns and detector was 40 °C. Samples were prepared in THF at a nominal concentration of 1 mg/ml and the sample injection volume was 20µL. A calibration curve was produced using polystyrene standards (Agilent EasiVial PS-H 4mL).

2.3.5.3. *Dynamic mechanical analysis (DMA)*

The viscoelastic properties of crosslinked free films were characterized using dynamic mechanical analysis (DMA) utilizing a TA800 dynamic mechanical thermal analyzer from TA Instruments using tension-film clamps. For each cured system, specimens of 20 mm in length, 5 mm wide, and 0.07 to 0.10 mm thick were cut from free films. Temperature was ramped from -80 °C to 80 °C at a heating rate of 5 °C/min, strain rate of 0.1 %, and frequency of 1 Hz.

2.3.5.4. *Tensile testing*

The mechanical properties of cross-linked free films were determined from American Society for Testing and Materials (ASTM) method D638 type V test specimens die cut from the films cured on Teflon® coated glass panels. The tensile tester utilized was an Instron 5545 equipped with a 100N load cell. Measurements were conducted using a 4 mm/min displacement rate, and results were reported as the average of five replicates.

2.3.5.5. *Dynamic viscosity*

Polymer viscosities were determined with an ARES Rheometer from TA Instruments. Samples were placed in between two parallel plates with a 0.5 mm gap. Viscosity was measured by varying the shear rate from 1 to 100/min and the data at 10/min reported.

3.3.5.6. Drying time measurement

Drying time measurements of the neat polymers with/without drier package and with different pigments were performed according to D1640/D1640M–14 (Method A).

2.3.5.7. Coating property

Cured films cast on steel panels were used to measure coating hardness, chemical resistance, flexibility, and impact resistance. Hardness was determined using the König pendulum hardness test described in ASTM D4366. Chemical resistance was determined using the MEK double rub test detailed in ASTM D5402. Flexibility was characterized using the conical mandrel bend test as described in ASTM D522. Impact resistance was characterized using the falling weight impact tester and the method described in ASTM D2794. The uncoated side of the panel received the impact (i.e. reverse impact).

2.4. Results and discussion

2.4.1. Synthesis and characterization

2.4.1.1. Monomer synthesis and characterization

As illustrated in **Figure 2.1**, 2-(vinylloxy)ethyl soyate (2VOES), 2-(vinylloxy)ethyl linseedate (2VOEL), and 2-(vinylloxy)ethyl camelinate (2VOEC) were produced using base-catalyzed transesterification of the methyl ester of the PO triglyceride with 2VOE. **Figure 2.2** depicts the ¹H NMR spectra of the three monomers produced. The chemical shift and peak area integration data obtained from the spectra confirmed the successful synthesis of each monomer. For example, the relative area of the multiplet associated with bis-allylic protons (i.e. “k” in **Figure 2.2**) was determined to be 1.0/2.1/1.3 2VOES/2VOEL/2VOEC, which is consistent with the FA compositional information provided in **Table 2.1**. In addition, comparison of the peak areas associated with the two different methyl groups present in the monomers (“l” and “j” in **Figure**

2.2) is consistent with the relative concentrations of linolenic esters in the three different monomers. The relative area of “l” to “j” increases in the order 2VOES < 2VOEC < 2VOEL.

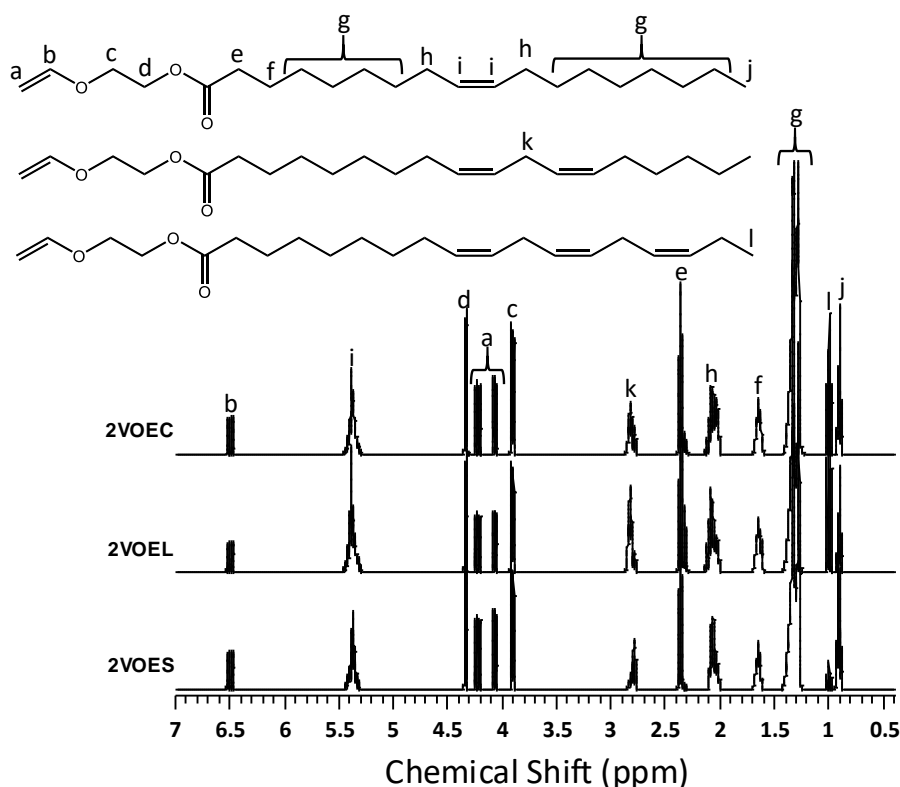


Figure 2.2. ^1H NMR spectra of 2VOES (bottom), 2VOEL (middle), and 2VOEC (top).

2.4.1.2. Polymer synthesis and characterization

For each POVE, a series of homopolymers was produced that varied with respect to MW. All of the polymers exhibited a relatively symmetrical, mono-modal GPC chromatographs with polydispersity index (PDI) ranging between 1.11 and 1.46 (Table 2.3). To illustrate, Figure 2.3 provides representative GPC chromatograms using the polymers derived from 2VOEC. Although these experiments were not conducted to determine if the polymerizations performed were living polymerizations, previous work has demonstrated the living polymerization of 2VOES using a VE/acetic acid adduct as an initiator, $\text{Et}_3\text{Al}_2\text{Cl}_3$ as the co-initiator, and toluene as the solvent.³⁶ The

relatively narrow MW distributions suggest that chain transfer and chain termination reactions were not prevalent in the polymerizations.

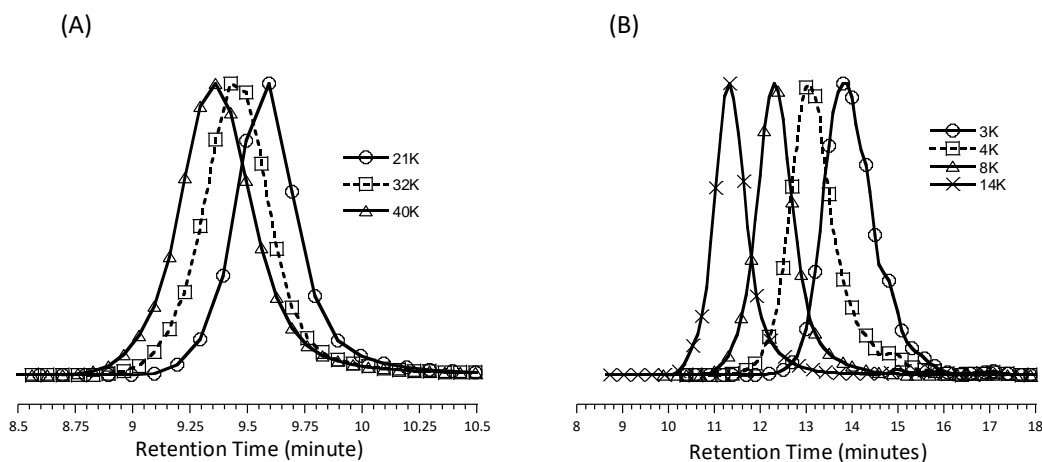


Figure 2.3. Representative GPC chromatograms using the polymers derived from 2VOEC. The values in the legend correspond to number-average MWs determined using GPC. Chromatograms of polymers with MWs above 15,000 g/mole (A) were obtained using two TSKgel SuperHM columns, while those with MWs below 15,000 g/mole (B) were obtained using two TSKgel SuperH3000 columns.

Figure 2.4 depicts the ^1H NMR spectra of representative poly(2VOES), poly(2VOEL), and poly(2VOEC) polymers. Signals associated with the bis allylic (“k” in Figure 4), allylic (“h” in Figure 4), and vinyl (“i” in Figure 4) protons of the fatty ester portion of the polymers are well resolved for relatively accurate peak integration. Using these peaks as well as those peaks associated with the methyl protons of the FA chains (“j” and “l”), information regarding the occurrence of side reactions during polymerization, such as hydride abstraction or addition to double bonds, was obtained. For these measurements, the methyl protons of the FA chains (“j” and “l”) were used for normalization purposes. By comparing normalized peak integration values for a given polymer to corresponding values obtained from its parent monomer, it was concluded that no significant side reactions involving the FA chains occurred during polymerization. As discussed previously, this result is significant since previous methods for producing unsaturated

FA-containing polymers by chain-growth polymerization methods were limited by chain transfer and termination reactions. The cationic polymerizations also resulted in over 95 % polymer yields.

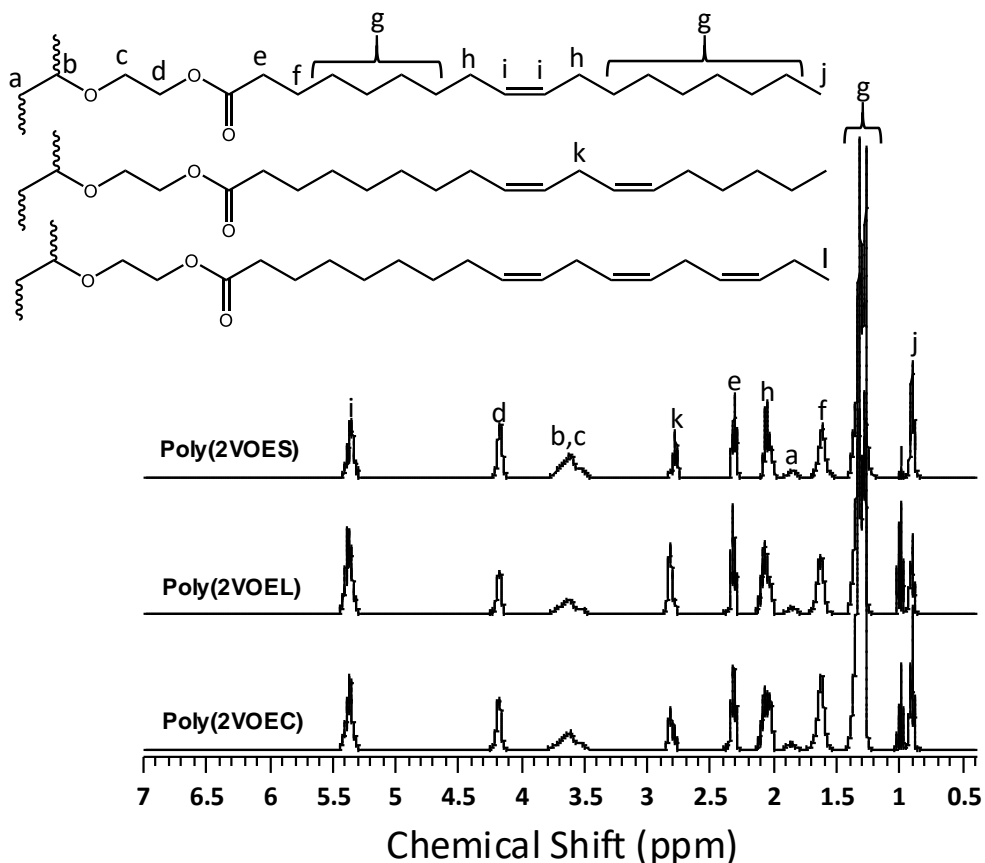


Figure 2.4. ^1H NMR spectra of representative POVE polymers [poly(2VOEC) (bottom), poly(2VOEL) (middle), and poly(2VOES) (top)].

2.4.1.3. Viscosity measurement

For surface coating applications, the relationship between polymer MW and viscosity is critical. While higher MW polymers are generally desired for obtaining the best film properties, regulations related to solvent emissions often result in an upper limit on polymer MWs that can be used for a given application. All of the POVE polymers were liquids at room temperature. **Figure 2.5** displays viscosity at 23 °C as a function of polymer MW for the series of homopolymers produced from the three types of POVE monomers. As shown in **Figure 2.5**, the variation in viscosity with MW was highly dependent on the composition of the parent PO used to produce the

polymer. Also, the magnitude of the difference in viscosity between the three polymers increased with increasing MW. For a given polymer MW, viscosity increased in the order, poly(2VOEL) < poly(2VOEC) < poly(2VOES). Considering the chemical composition of the three parent POs, there is a correlation between polymer viscosity and parent PO unsaturation, where polymer viscosity increases with decreasing unsaturation of the parent PO. This trend can be rationalized by considering the effect of FA side chain unsaturation on the ability of the side chains to form intermolecular interactions, such as van der Waals interactions. Since the unsaturation in these POs exists exclusively as *cis* double bonds, each of these double bonds introduce a “kink” in the fatty chain, which significantly reduces the ability of the fatty chain to form the necessary intermolecular interactions that enhance bulk viscosity. This explanation was proposed by Abramovic and Klofutar⁵² as well as Kim et al.⁵³ to explain the lower viscosities they observed for POs with higher levels of unsaturation. From a purely rheological point-of-view, these results indicated that poly(2VOEL) possessed a significant advantage over the other POVE polymers by enabling much lower viscosities at a given MW.

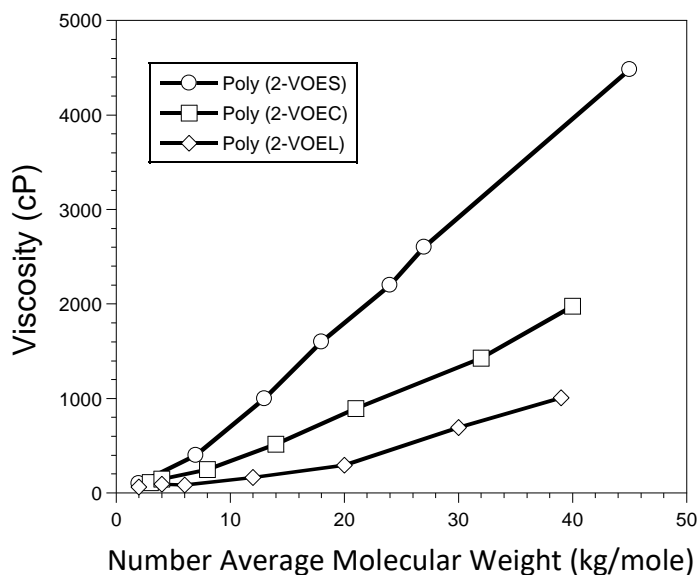


Figure 2.5. Viscosity at 23 °C as a function of polymer MW for the three series of POVE polymers.

Since it is known that the relationship between $\log(\text{viscosity})$ and $\log(\text{MW})$ of bulk polymers undergoes a shift from being a linear relationship to a 3.4 power relationship after a critical MW is exceeded, $\log(\text{viscosity})$ was plotted as a function of $\log(\text{MW})$.^{54, 55} For poly(2VOES), poly(2VOEC), and poly(2VOEL) the slope of the line (**Figure 2.6**) was 1.27, 1.02, and 1.01, respectively, and the correlation coefficient for each line was 0.94 or higher. This result suggested that the MW range used for the current study was below the critical MW, which has been associated with the minimum MW needed for the generation of polymer entanglements. Considering the exceptionally long side chains associated with the repeat units of these polymers, it's not surprising that the MW required for obtaining molecular entanglements would be above 45,000 g/mole.

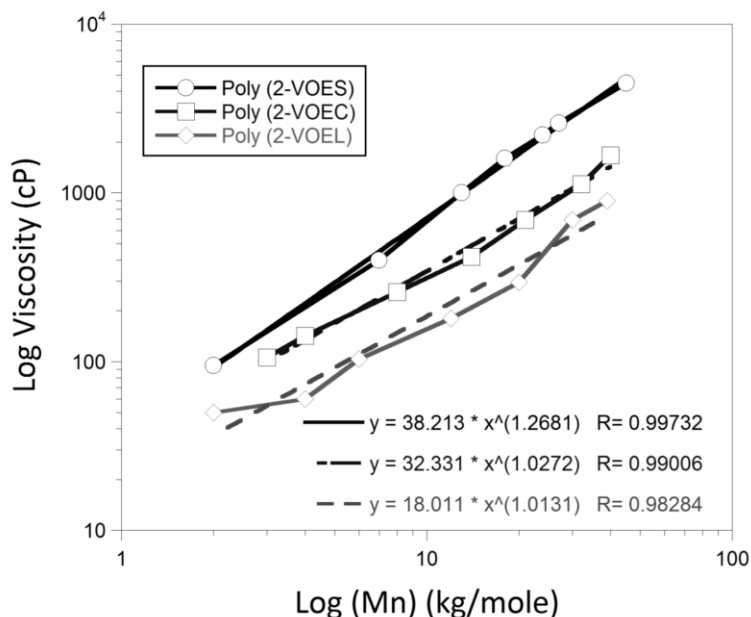


Figure 2.6. Log (Viscosity) vs Log (Mn) plots for the three series of POVE polymers.

2.4.1.4. Drying time measurements

The same compositions used to produce free film specimens were also used to produce coatings on steel panels. For coatings that cure/cross-link by autoxidation, an important property

is the tack-free time. According to ASTM D1640, a freshly cast coating is deemed “tack-free” when a tack-tester pressed against the surface of the coating for five seconds using a 300 g load is immediately released from the coating surface when the load is removed. For most coating applications, a short tack-free time is desired because with shorter the tack-free times the coated article or surface can be handled and/or put into service sooner. In addition, coatings that solidify to a tack-free film relatively quickly have less chance of accumulating surface defects from the adhesion of dust and other airborne debris.

For coatings derived from binders that have a T_g significantly above ambient temperature, tack-free time is essentially a function of the evaporation rate of the solvent. In contrast, for coatings derived from binders that have T_g well below ambient temperature, tack-free time is primarily a function of the rate of development of the cross-linked network and the influence of XLD on T_g . As shown in **Table 2.6**, at a given polymer MW, tack-free time increased in the order poly(2VOEL) < poly(2VOES) < poly(2VOEC). Since poly(2VOEC) possesses a higher level of unsaturation (i.e. higher IV) than poly(2VOES), it was surprising to observe that coatings derived from poly(2VOEC) took longer to achieve a tack-free surface than analogous coatings based on poly(2VOES). By considering differences in the nature of the unsaturation and the length of the FA side chains, a potential rationale for this observed trend was developed.

As shown in **Table 2.1**, CMO has a higher level of unsaturation than SBO, as expressed by the IV, but the ratio of polyunsaturated to monounsaturated FA esters is lower for CMO than SBO. It is well known that polyunsaturated FA oxidize much faster than monounsaturated FA. For example, linoleic acid and linolenic acid oxidize 41 and 98 times faster than oleic acid, respectively.⁵⁶ Thus, at the very early stages of the development of the cross-linked network, which is the situation when drying time measurements are made, it is possible that the XLD of a

poly(2VOES)-based coating may actually have been higher than for a coating based on an analogous poly(2VOEC).

In addition to the difference in the ratio of polyunsaturated to monounsaturated FA esters, a significant difference in the length of FA chains exists between poly(2VOEC) and poly(2VOES). As shown in **Table 2.1**, SBO contains no FA longer than 18 carbons, while approximately 22 percent of the FA identified in CMO are longer than 18 carbons. Most of these longer chain FA are monounsaturated and, as a result, incorporate relatively slowly into the cross-linked network. As a result, the longer tack-free times for poly(2VOEC)-based coatings as compared to poly(2VOES)-based coatings may have also been due to a difference in the relationship between XLD and coating T_g during the early stages of the development of the cross-linked network. Perhaps when the networks are relatively lightly cross-linked, as would be the case shortly after the coatings are cast, the T_g of networks based on poly(2VOEC) are lower than analogous networks based on poly(2VOES) due to plasticization by the longer chain FA in poly(2VOEC) that have yet to undergo oxidation. Obviously, as the XLD increases over the course of days and weeks allowing the monounsaturated FA chains to participate in the formation of oxidative crosslinks, this plasticization effect is no longer a factor.

2.4.2. Viscoelastic properties of crosslinked free-films

Crosslinked free-films derived from polymers representing a medium and high MW, within the MW range investigated, were characterized using DMA (**Figure 2.7**). The MW range for the medium MW and high MW polymers was 13,000 to 14,000 g/mole and 39,000 to 45,000 g/mole, respectively. Glass transition temperatures T_g s, expressed as the peak maximum of the tangent delta response, and plateau moduli, expressed as the storage modulus 60 °C above the T_g , are

provided in **Table 2.4**. Estimates of the crosslink density (XLD) were determined using the following equation, which is based on the theory of rubber elasticity (**Eq. 2.1**)^{57, 58}

$$\nu = E'/(3RT) \quad (2.1)$$

where, ν is the XLD defined as the moles of crosslinks per unit volume of material, R is the gas constant, E' is storage modulus in the rubbery plateau region, and T is the temperature corresponding to the storage modulus value.⁵⁹ All of the polymer networks possessed a T_g below room temperature. The data showed a trend between T_g , estimated XLD, and composition of the parent PO. T_g and estimated XLD increased in the order poly(2VOES) < poly(2VOEC) < poly(2VOEL), which is consistent with the trend in the level of parent PO unsaturation. Since crosslinking by autoxidation results from the bis-allylic and allylic protons of the FA chains, an increase in XLD with an increase in the level of unsaturation i.e. increasing number of bis-allylic was expected. This increase in XLD with increasing PO unsaturation inhibit the cooperative segmental motions of the networks resulting in an increase in T_g . For a given polymer composition, the XLD was higher for polymer networks derived from the higher MW polymer as it increases the number of functional groups per molecule. Increase MW i.e. higher pendent fatty chain also increases the possibility of having more unsaturated fatty chains per molecule. It also reduces the polymer end-groups that do not participate in the autoxidation process do not become incorporated into the elastic network and exist as dangling chains that may plasticize the network.^{34, 37}

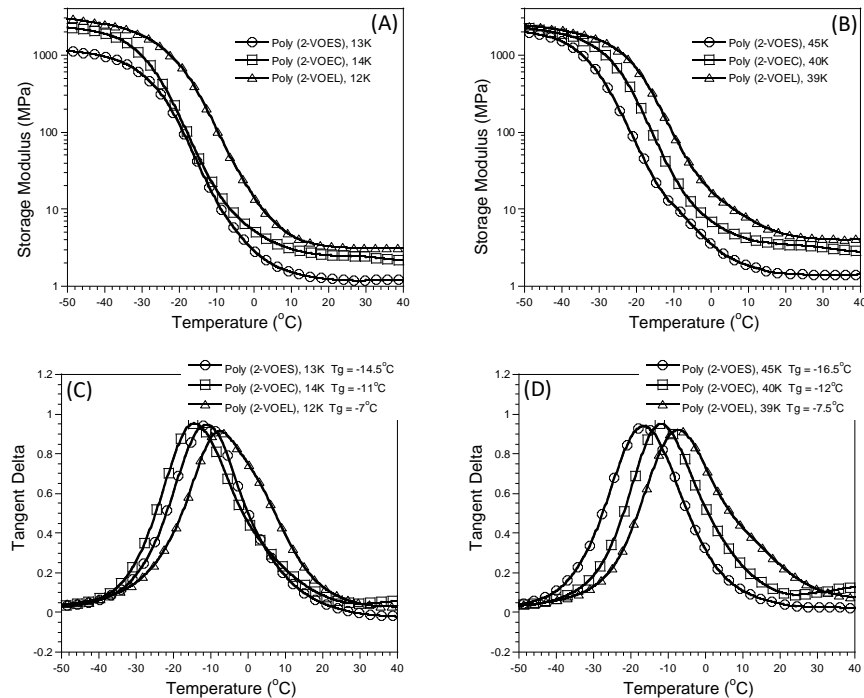


Figure 2.7. The viscoelastic properties of crosslinked networks derived from POVE polymers that varied with respect to composition and MW. Both the storage modulus response (A and B) and tangent delta response (C and D) are provided.

Table 2.4. T_g , plateau modulus, and XLD obtained from DMA measurements.

Sample ID	T_g (°C) [†]	Plateau Modulus (MPa) [*]	XLD (cm ³ /mole)
Poly(2VOES), 13K	-14.5	1.242	1.926 x 10 ⁻⁴
Poly(2VOES), 45K	-16.5	1.438	2.248 x 10 ⁻⁴
Poly(2VOEC), 14K	-11	2.182	3.339 x 10 ⁻⁴
Poly(2VOEC), 40K	-12	2.795	4.293 x 10 ⁻⁴
Poly(2VOEL), 12K	-7	3.138	4.730 x 10 ⁻⁴
Poly(2VOEL), 38K	-7.5	4.209	6.356 x 10 ⁻⁴

[†] T_g was reported as the peak maximum of the tangent delta curve. ^{*}Plateau modulus was taken as the storage modulus at a temperature 60 °C above the T_g .

2.4.3. Mechanical properties of cured films

Mechanical properties of the crosslinked free-films derived from polymers representing a medium and high MW, within the MW range investigated, were evaluated using tensile testing.

Figure 2.8 depicts tensile stress as a function of elongation for representative specimens, while

Table 2.5 provides the average and standard deviation from five replicate measurements. As shown in **Figure 2.8**, stress varied linearly with elongation for all samples, which is consistent with expectations for a cross-linked network of polymer chains that are in their rubbery state and largely free of molecular entanglements. For networks such as these, resistance to deformation is largely a function of XLD. Both Young's modulus and tensile strength correlated strongly with XLD estimated from DMA data (**Figure 2.9**) (correlation coefficient greater than 0.9), with both YM and TS increasing with increasing XLD. Thus, cross-linked networks based on poly(2VOEL) provided the highest YM and TS while networks based on poly(2VOES) displayed the lowest YM and TS. In addition, for a given polymer composition, the network based on the higher MW polymer gave a higher YM and TS. Elongations at break were similar and ranged from 14.6 to 20.0 percent and did not correlate with polymer composition or XLD.

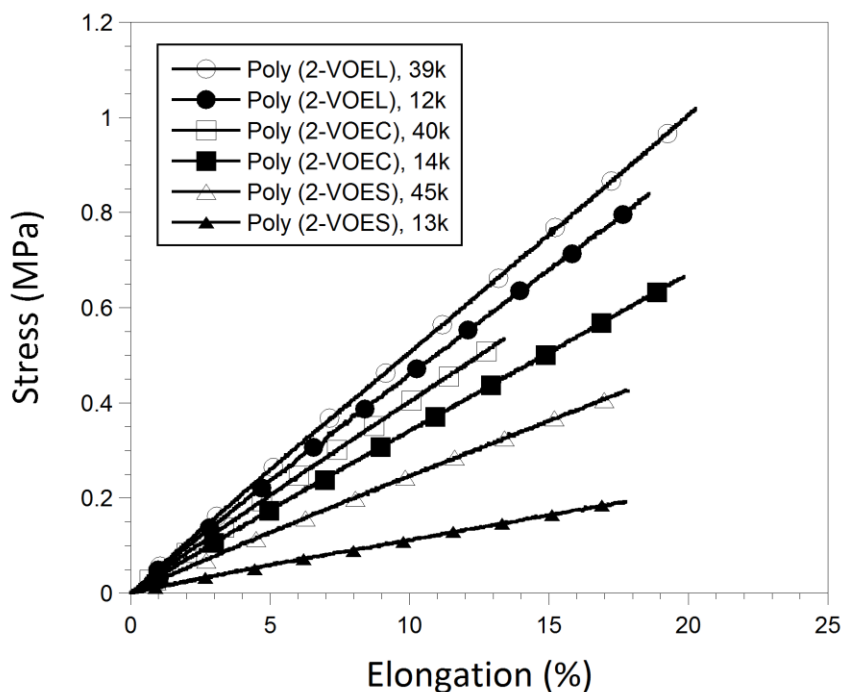


Figure 2.8. Plots of tensile stress as a function of elongation for cross-linked networks derived from POVE polymers that varied with respect to composition and MW.

Table 2.5. Young's modulus, tensile strength, and elongation at break for cross-linked networks derived from POVE polymers that varied with respect to composition and MW. Each value represents the average and standard deviation from five test specimens.

Sample ID	Young's modulus (MPa)	Tensile strength (MPa)*	Elongation at Break (%)
Poly(2VOES), 13K	1.37 ± 0.24	0.192 ± 0.028	17.6 ± 1.5
Poly(2VOES), 45K	2.60 ± 0.21	0.389 ± 0.027	15.3 ± 1.3
Poly(2VOEC), 14K	2.75 ± 0.51	0.358 ± .007	20.0 ± 2.4
Poly(2VOEC), 40K	4.07 ± 0.02	0.559 ± 0.069	14.6 ± 1.7
Poly(2VOEL), 12K	5.00 ± 0.11	0.736 ± 0.148	17.1 ± 2.0
Poly(2VOEL), 38K	5.36 ± 0.25	0.824 ± 0.139	15.7 ± 3.0

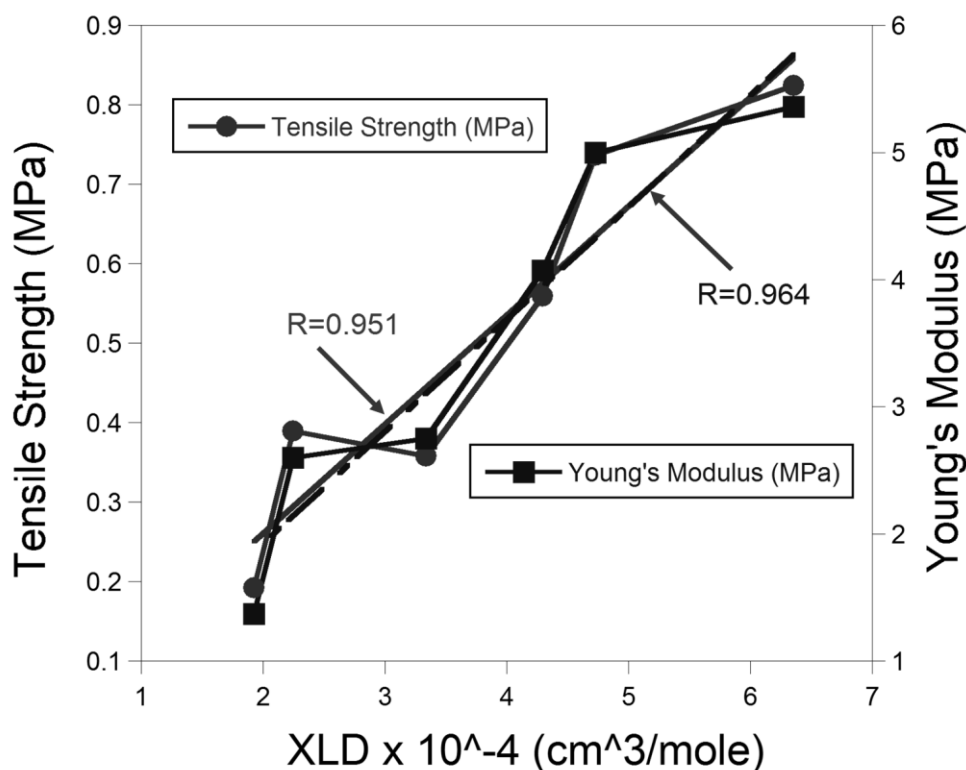


Figure 2.9. Plots showing correlation of XLD with Young's modulus with XLD.

2.4.4. Properties of surface coatings

Pendulum hardness according to ASTM D 4366 characterizes the hardness of a coating by setting two ball bearings rocking on the surface of a coating via a pendulum. For relatively soft coatings, the rocking motion of the ball bearings is dissipated more quickly than for a relatively

hard coating. Since the T_g s of the cross-linked free films were below room temperature, pendulum hardness was expected to be highly dependent on the XLD achieved during curing at ambient conditions. Pendulum hardness was plotted as a function of XLD (**Figure 2.10**) and a correlation coefficient of 0.79 was obtained. Since the DMA data provided in **Figure 2.7** showed that the high temperature portion of the temperature range associated with the T_g includes, for some samples, ambient temperatures (i.e. 20 to 24 °C), pendulum hardness was plotted as a function of the storage modulus (**Figure 2.11**) obtained at 23 °C. For this plot, the correlation coefficient was 0.99, which indicated that pendulum hardness was not only a function of XLD, but also the T_g of the coating.

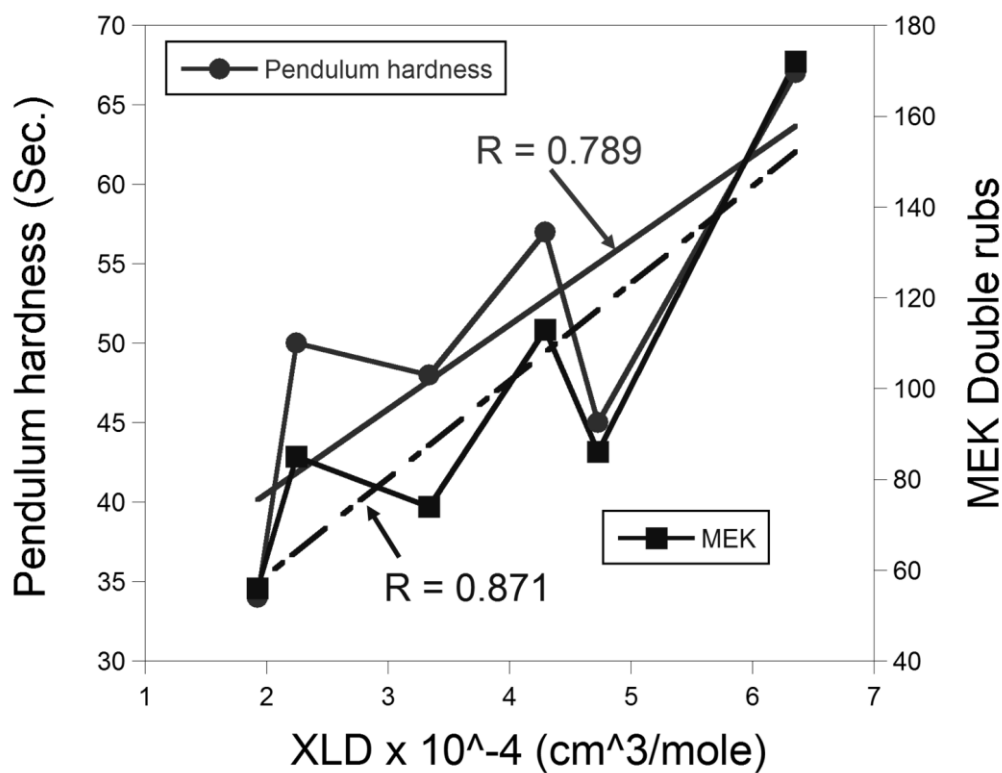


Figure 2.10. Plots showing correlation of XLD with pendulum hardness and MEK double rubs.

It is well known that the degree of swelling of a cross-linked network is directly related to XLD. As a result, it was expected that the solvent resistance of the coatings produced would be

largely a function of XLD, especially since the solubility parameters of the polymers would be expected to be essentially the same. Solvent resistance, expressed as the minimum number of MEK double rubs that result in a visible change in the coating, was plotted as a function of XLD (**Figure 2.10**) and a correlation coefficient of 0.87 obtained. As shown in **Table 2.6**, for a given polymer MW, solvent resistance increased in the order, poly(2VOES) < poly(2VOEC) < poly(2VOEL), and, for a given polymer, solvent resistance was higher for the coating based on the higher MW polymer.

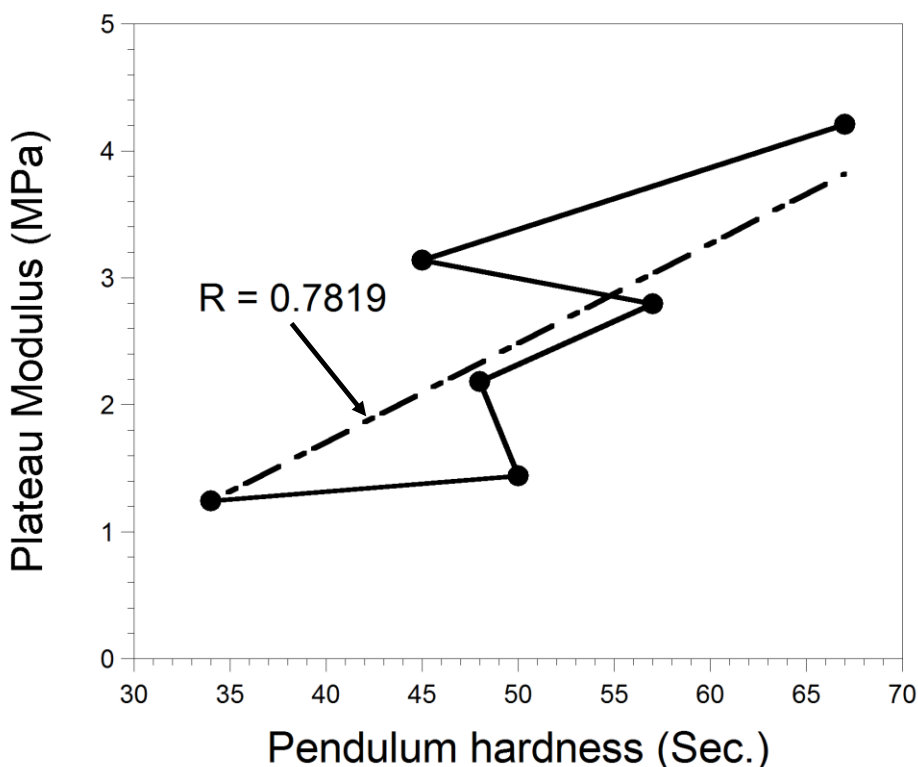


Figure 2.11. Plots showing correlation of plateau modulus with pendulum hardness.

The flexibility of the coatings was characterized using the conical mandrel bend test as specified in ASTM D522. All six of the coatings showed no cracking or delamination even at the highest strain associated with the test, which is 32 % elongation. This result indicated that all coatings possessed excellent flexibility. The impact resistance of the coatings was characterized

using the method described in ASTM D2794 by impacting the uncoated side of the panels (i.e. reverse impact). The maximum impact force that can be achieved with this test is 172 in-lbs. As shown in **Table 2.6**, coatings based on poly(2VOES) and poly(2VOEC) showed no coating damage or coating delamination when subjected to the highest possible impact force. In contrast, coatings based on poly(2VOEL) showed significantly lower impact resistance. The coating based on the lower MW poly(2VOEL) was 80 in-lb, while the value for the higher MW poly(2VOEL) was even lower at 60 in-lb. The lower impact resistance for the higher MW poly(2VOEL) was anticipated considering the higher XLD density associated with coatings based on this polymer.

Table 2.6. Properties of coatings derived from various POVE polymers. Values for pendulum hardness and solvent resistance represent the average and standard deviation from five replicates.

Polymer ID	Thickness (μm)	Tack-Free Time (min)	König Pendulum Hardness (s)	Solvent Resistance (MEK double rubs)	Reverse Impact Resistance (in-lbs)
Poly(2VOES), 13K	114± 2.1	373	34 ± 1.25	56 ± 1.73	172
Poly(2VOES), 45K	110± 2.7	72	50 ± 2.35	85 ± 4.36	172
Poly(2VOEC), 14K	108± 3.1	579	48 ± 1.35	74 ± 4.72	172
Poly(2VOEC), 40K	117± 2.5	400	57 ± 2.20	113 ± 7.63	172
Poly(2VOEL), 12K	109± 3.7	142	45 ± 0.58	86 ± 3.21	80
Poly(2VOEL), 38K	119± 3.2	35	67 ± 2.15	172 ± 4.72	60

2.5. Conclusion

The cationic polymerization processes used to produce POVE homopolymers enabled a series of polymers that varied systematically with respect to MW and composition of the FA side chains. Composition of the FA side chains was varied by producing three monomers, each of which was derived from a different PO, namely, SBO, LO, and CMO. Characterization of polymers using ¹H NMR and GPC indicated that the polymerizations were essentially free of chain transfer and termination reactions. Viscosity measurements of the polymers at 23 °C indicated that the MW

range used for the study was below the critical MW needed to obtain polymer entanglement. In addition, at a given MW, polymer viscosity was dependent on the composition of the parent PO. A trend was observed in which polymer viscosity decreased with increasing unsaturation of the parent PO. This trend was attributed to the influence of the *cis* double bonds in FA side chains on the ability of the side chains to form intermolecular van der Waals interactions. Each double bond effectively introduced a kink in the side chain that sterically limited the extent of intermolecular interactions between fatty chains.

The viscoelastic and tensile properties of cross-linked networks derived from select polymers representing relatively moderate and relatively high MW polymers were determined. T_g , XLD, YM, and TS varied as function of both the composition of the PO used to produce the polymer and polymer MW. At a given polymer MW, T_g , XLD, Young's modulus, and tensile strength all increased with increasing unsaturation in the parent PO. This result was due to the nature of the oxidative crosslinking mechanism involved in the formation of these networks. Unsaturated FA chains possess bis-allylic, allylic, and double bonds that contribute to the formation of crosslinks during the process of autoxidation. Thus, the higher the level of unsaturation in the parent PO, the higher the XLD in the cured films. In addition, for a given polymer chemical composition, increasing polymer MW also increased XLD. This trend was also consistent with expectations since a lower polymer end-group concentration reduces the number of dangling chains attached to the cross-linked network that may plasticize the network.

In addition to free films, cross-linked coatings on steel panels were produced and tested using industry standard testing methods. Trends in coating hardness, solvent resistance, and impact resistance with polymer composition were consistent with the viscoelastic property results obtained from cured free films, which, as previously discussed, could be rationalized based on

differences in the degree of FA side chain unsaturation and polymer MW. For example, at a given polymer MW, solvent resistance increased with increasing FA side chain unsaturation. For a given polymer composition, solvent resistance increased with an increase in polymer MW.

For tack-free time, coatings based on poly(2VOEC) showed a longer tack-free time than analogous coatings based on poly(2VOES). Although the total level of unsaturation for poly(2VOEC) was higher than poly(2VOES), the ratio of polyunsaturated to monounsaturated FA was lower for poly(2VOEC). As a result, the rate of crosslinking at the very early stages of cross-linked network formation may be higher for poly(2VOES) than for poly(2VOEC) resulting in a shorter tack-free time for the former. Poly(2VOEC) also possessed a substantial fraction of FA chains that were longer than those found in poly(2VOES). The presence of these longer FA chains may more effectively plasticize the cross-linked network, thus further contributing to longer tack-free times.

2.6. References

1. D. Kumar, *Paintindia*, 2015, **65**, 73-80.
2. B. Lochab, *Advances in Materials Physics and Chemistry*, 2012, **2**, 221-225.
3. P. D . Bates and J. Browse, *Frontiers in plant science*, 2012, **3**, 147-158.
4. V. Kostik, S. Memeti and B. Bauer, *Journal of Hygienic Engineering and Design*, 2013, **4**, 112-116.
5. R. S. Nasirullah, U. S. Shetty and R. S. Yella, *International Journal of Food Science and Technology*, 2010, **45**, 1395–1402.
6. C. G. J. Baker, M. D. Ranken and R. C. Kill, *Food industries manual*, Springer US, 24 edn., 1997.

7. P. Bazongo, I. H. N. Bassolé, S. Nielsen, A. Hilou, M. H. Dicko and V. K. S. Shukla, *Molecules*, 2014, **19**, 2684-2693.
8. M. Lazzari and O. Chintore, *Polymer Degradation and Stability*, 1999, **65**, 303-313.
9. R. Ploeger and O. Chintore, *Smithsonian Contributions to Museum Conservation*, 2012, 89-95.
10. J. Mallégo, J. Lameire and J. L. Gardette, *Progress in Organic Coatings*, 2000, **39**, 107–113.
11. S. Kasetaitė, J. Ostrauskaitė, V. Grazulevičienė, J. Svedienė and D. Bridziuvienė, *Journal of Applied polymer science*, 2014, **131**, 40683-40691.
12. Y. Xia and R. C. Larock, *Green Chem.*, 2010, **12**, 1893–1909.
13. W. M. Frank, N. Jones, P. D. Ziemer, F. Xiao, J. Hayes and M. Golden, *Progress in Organic Coatings*, 2005, **52**, 9-20.
14. H. S. Shin and S. W. Kim, *Journal of the American Oil Chemists' Society*, 1994, **71**, 619-622.
15. P. Karmalm, T. Hjertberg, A. Jansson and R. Dahl, *Polymer Degradation and Stability*, 2009, **94**, 2275–2281.
16. C. B. Ferrer, M. C. Garrigos and A. Jimenez, *Polymer Degradation and Stability*, 2010, **95**, 2207-2212.
17. M. Ionescu, Z. S. Petrovic and X. Wan, *Journal of Polymers and the Environment*, 2007, **15**, 237–243.
18. J. Lu, S. Khot and R. P. Wool, *Polymer*, 2005, **46**, 71-80.
19. X. Pan and D. C. Webster, *ChemSusChem*, 2012, **5**, 419 – 429.

20. S. N. Khot, J. J. Lascola, E. Can, S. S. Morye, G. I. Williams, G. R. Palmese, S. H. Kusefoglu and R. P. Wool, *Journal of Applied Polymer Science*, 2001, **82**, 703-723.
21. R. M. Pashlely, T. J. Senden and R. A. Morris, US Pat, 5360880, 1994.
22. G. Booth, D. E. Delatte and S. F. Thames, *Industrial Crops and Products*, 2007, **25**, 257-265.
23. D. Delatte, E. Kaya, L. G. Kolibal, S. K. Mendon, J. W. Rawlins and S. F. Thames, *Journal of Applied Polymer Science*, 2014, **131**, 40249-40259.
24. M. Black, J. Messman and J. Rawlins, *J. Appl. Polym. Sci.*, 2011, **120**, 1390-1396.
25. Z. Demchuk, O. Shevchuk, I. Tarnavchyk, V. Kirianchuk, A. Kohut, S. Voronov and A. Voronov, *ACS Sustainable Chemistry & Engineering*, 2016, **4**, 6974-6980.
26. L. Yuan, Z. Wang, N. M. Trenor and Chuanbing Tang, *Macromolecules*, 2015, **45**, 1320-1328.
27. H. Yin, L. Xu and Ned A. Porter, *Chem. Rev.*, 2011, **111**, 5944-5972
28. E. Kaya, S. K. Mendon, D. Delatte, J. W. Rawlins, and S. F. Thames, *Macromol. Symp*, 2013 **324**, 95-106.
29. K. Mullen and S. Kobayashi, *Encyclopedia of Polymeric Nanomaterials*, Springer-Verlag Berlin Heidelberg, New York, 2014.
30. S. P. Bunker and R. P. Wool, *J. Polym. Sci.: Part A: Polym. Chem.*, 2002, **40**, 451-458
31. C. Quintero, S. K. Mendon, O. W. Smith and S. F. Thames, *Prog. Org. Coat.*, 2006, **57**, 195-201.
32. Z. Demchuk, O. Shevchuk, I. Tarnavchyk, V. Kirianchuk, M. Lorenson, A. Kohut, S. Voronov and A. Voronov, *ACS Omega*, 2016, **1**, 1374-1382.
33. Y. Guo, V. L. Teo, S. R. S. Ting and P. B. Zetterlund, *Polym. Chem.*, 2012, **44**, 375-381.

34. S. Alam and B. J. Chisholm, *Journal of Coatings Technology and Research*, 2011, **8**, 671-683.
35. S. Alam, H. Kalita, O. Kudina, A. Popadyuk, B. J. Chisholm and A. Voronov, *ACS Sustainable Chemistry & Engineering*, 2013, **1**, 19-22.
36. A. Chernykh, S. Alam, A. Jayasooriya, J. Bahr and B. J. Chisholm, *Green Chemistry*, 2013, **15**, 1834-1838.
37. S. Alam, H. Kalita, A. Jayasooriya, S. Samanta, J. Bahr, A. Chernykh, M. Weisz and B. J. Chisholm, *European Journal of Lipid Science and Technology*, 2014, **116**, 2-15.
38. H. Kalita, S. Selvakumar, A. Jayasooriyamu, S. Fernando, S. Samanta, J. Bahr, S. Alam, M. Sibi, J. Vold, C. Ulven and B. J. Chisholm, *Green Chemistry*, 2014, **16**, 1974-1986.
39. A. Popadyuk, H. Kalita, B. J. Chisholm and A. Voronov, *International Journal of Cosmetic Science*, 2014, **36**, 547-555.
40. H. Kalita, S. Alam, A. Jayasooriyamu, S. Fernando, S. Samanta, J. Bahr, S. Selvakumar, M. Sibi, J. Vold, C. Ulven and B. J. Chisholm, *Journal of Coatings Technology and Research*, 2015, **12**, 633-646.
41. H. Kalita, D. Kalita, S. Alam, A. Chernykh, I. Tarnavchyk, J. Bahr, S. Samanta, A. Jayasooriyama, S. Fernando, S. Selvakumar, D. S. Wickramaratne, M. Sibi and Bret J. Chisholm, *European Coatings Journal*, 2015, **6**, 26-29.
42. H. Kalita, A. Jayasooriyama, S. Fernando and B. J. Chisholm, *Journal of Palm Oil Research*, 2015, **27**, 39-56.
43. S. Samanta, S. Selvakumar, J. Bahr, D. Suranga Wickramaratne, M. Sibi and B. J. Chisholm, *ACS Sustainable Chemistry and Engineering*, 2016, **4**, 6551-6561.

44. H. Kalita, S. Alam, D. Kalita, A. Chernykh, I. Tarnavchyk, J. Bahr, S. Samanta, A. Jayasooriyama, S. Fernando, S. Selvakumar, A. Popadyuk, D. S. Wickramaratne, M. Sibi, A. Voronov, A. Bezbaruah and B. J. Chisholm, *ACS Symposium Series*, 2014, **1178**, 731-790.
45. H. Kalita, D. Kalita, S. Alam, A. Chernykh, I. Tarnavchyk, J. Bahr, S. Samanta, Anurad Jayasooriyama, S. Fernando, S. Selvakumar, D. S. Wickramaratne, M. Sibi and Bret J. Chisholm, *Biobased and Environmentally Benign Coatings*, ed. A. Tiwari, A. Galanis, M. D. Soucek, Wiley-Scrivener Publishing, 2016, 1, 1-16.
46. D. Kalita, I. Tarnavchuk, D. Sundquist, S. Samanta, J. Bahr, O. Shafranska, M. Sibi, and B. Chisholm, *INFORM*, 2015, **26**, 472-475.
47. J. M. F. Johnson, M. D. Coleman, R. Gesch, A. Jaradat, R. Mitchell, D. Reicosky and W. W. Wilhelm, *The American Journal of Plant Science Biotechnology*, 2007, **1**, 1-28.
48. B. R. Moser and S. F. Vaughn, *Bioresource Technology*, 2010, **101**, 646-653
49. <http://www.makingcosmetics.com/certificate-of-analysis/coa-camelina-oil.pdf>, (accessed September, 2017)
50. S. Aoshima and Toshinobu Higashimura, *Macromolecules*, 1989, **22**, 1009-1013.
51. A. Kanazawa, Y. Hirabaru, S. Kanaoka, S. Aoshima, *Journal of Polymer Science: Part A: Polymer Chemistry*, 2006, **44**, 5795-5800.
52. H. Abramovic and C. Klofutar, *Acta Chimica Slovenica*, 1998, **45**, 69-77.
53. J. Kim, D. N. Kim, S. H. Lee, S. Yoo and S. Lee, *Food Chemistry*, 2010, **118**, 398-402.
54. G. C. Berry and T. G. Fox, *Adv. Polymer Sci.*, 1968, **5**, 261- 357.
55. L. J. Fetters, *Journal of Research of the National Bureau of Standards – A. Physics and Chemistry*, 1965, **69A**, 33-37

56. E. N. Frankel (Ed.), *Lipid Oxidation*, Woodhead Publishing Ltd, Sawston, Cambridge, UK, 2005.
57. N. G. Siatas, C. S. Kimbar, P. A. Tarantilis and M. G. Polissiou, *J. Am. Oil Chem. Soc.*, 2006, **83**, 53-57.
58. T. G. Fox, *Bull. Am. Phys. Soc.*, 1956, **1**, 123-124.
59. P. J. Flory, *Principles of Polymer Chemistry*. Cornell University Press. Ithaca, NY, 1953.

CHAPTER 3. PLANT OIL-BASED COATINGS WITH FAST DRYING/CURING AND LOW YELLOWNESS

3.1. Abstract

In this study, plant oil vinyl ether (POVE) monomers were synthesized from linseed, soy bean and palm oils via transesterification. Synthesized POVE monomers had color impurities which were removed via direct distillation resulting essentially colorless monomers. Linear polymers (homopolymers and copolymers) were produced from these purified POVE monomers via carbocationic polymerization. Being produced from fatty oils and essentially colorless these polymers were evaluated as binding media for artist paints where, color especially “yellowness” developed from the fatty binding media is a big concern. Molecular weight and composition of the POVE based polymers were varied in order to study their effect on drying behavior compared to linseed oil. Drying time evaluation showed that linear polymers derived from semi-drying/nondrying oils, such as soybean and palm oil were able to dry/cure faster than linseed oil which is a drying oil. Similar drying behavior was also observed when drying time was measured in presence either drying catalyst or pigment or both. Tailoring in drying time and viscosity was achieved with varying the molecular weight of the purified POVE based polymers. This tailoring in drying time with traditional fatty oils as binder can only be obtained by varying the oil type.

Compared to linseed oil as binder, polymers from purified POVE monomers as binder resulted significantly lower “yellowness” when coatings were made with TiO_2 as pigment. This lower value of “yellowness” was consistent when pigmented coatings were heat aged. Pigmented coatings derived from POVE based polymers also resulted better hardness, chemical resistance compared to pigmented coatings produced from linseed oil as binder.

3.2. Introduction

Artistic paintings provide a priceless look into the past. Materials (binders, colorants etc.) used for those paintings, until early 19th century, were mostly derived from plant oils.^{1,2} During the 16th century oil painting was practiced almost exclusively compared to other forms of paintings such as tempera, pastel painting etc. Oil based paints served as a much better binding medium for canvas and wood substrates.³ For these coatings, natural oils, particularly drying oils, such as linseed oil, tung oil, poppy oil, perilla oil, and walnut oil, were used as the binding media. These oils contain relatively high concentrations of linoleic and linolenic acid esters giving rise to a high “drying index” (Eq. 3.1). Oils having a “drying index” greater than 70 are classified as drying oils. Unfortunately, most of these oil binders are highly yellow in color and, as a result, it is difficult to produce soft colors such as white, pastels, and other pale colors. Prior to the advancement of analytical tools there was limited knowledge about the yellowing behavior of oil media.⁴ To avoid this yellowing issue artists usually used colorless or very low colored oils such as poppy oil, cottonseed oil, hemp oil, nut oil, and even castor oil. However, compared to linseed oil, tung oil or other drying oils these dries very slowly and even become rancid in a short time period.¹ Recently, most of the scientific literature that talks about application of paints are concerned with the binding media.⁵

$$\text{Drying index} = (\text{Percentage of fatty acids with 2 double bonds}) + 2 \times (\text{Percentage of fatty acids with 3 double bond}) \quad (3.1)$$

Autoxidation which is necessary to form a crosslinked network via oxidative polymerization, also results in side products mostly with keto functionality over time increasing “yellowness” of the coatings. In addition to increased yellowness a weight reduction of approximately 20% can also be observed depending on the oil. This weight loss is mainly attributed

to the rupture and fragmentation of triglycerides. These fragments form several low-molecular weight volatile compounds, mainly aldehydes and ketones, during aging. Evaporation of these volatile compounds along with water present in the oil matrix through the “linoxyn” layer leads to volume shrinkage and surface cracking. This “linoxyn” skin forming at the exposed surface has elastic behavior mainly due to the presence of saturated fatty acids which can act as lubricant. However, as the aging progresses due to the evaporation of the volatile side products, along with formation of small dicarboxylic acids, the “linoxyn” skin becomes very fragile aiding crack development.⁶ Despite proper conservation because of these inherent drawbacks, oil based binding medium paintings often go through a restoration process, which can alter its aesthetic value.¹ Due to these reasons synthetic binding media have been introduced in the art market as a replacement for traditional oil media.⁴

Most modern coating systems are based on petrochemicals like acrylics, which provide better durability transparency, rapid drying, and chemical stability.⁷ Although acrylics have better elasticity than the oil paints due to a slow rate of embrittlement, they are free of the issue of cracking. When compared to oil based paintings which usually suffer from fine hairline cracks called ‘craquelure’, modern paintings have shown even deeper cracks reaching down to the color coat. Recently, 25-35% of the 19th and 20th century oil paintings in the Metropolitan Museum of Art in New York were reported to suffer from cracking. Several reports from the popular press have described the occasional cracking of acrylic paintings.³ Other cracking issues might be generated due to wind damage, shipping at temperatures at or below 0-10 °C, relative humidity or by some defect in the paint composition (binder, pigments, other ingredients). Other factors such as inappropriate substrate, application conditions, and mishandling can also result in premature cracking of the paint.

From the beginning, acrylics has been criticized as “plastic paints” because of their inferiority in optical properties. Development of turbidity and lack of saturation in color have been the main critiques from artists using acrylic paints. According to Whitmore et al.⁸ this development of turbidity is mainly due to the formation of microscopic crystalline domains from polyethylene glycol type compounds that are used as surfactants during emulsion polymerization of acrylic binders. Studies done by Ziraldo et al.⁹ and Peer et al.¹⁰ concluded that due to the soft nature of the acrylic films (mainly due to T_g below room temperature) these hydrophilic surfactants tend to move to the air-film interface as the temperature rises above 20 °C or as relative humidity increases above about 40%. Tacky, liquid surfactant additives tend to accumulate and aggregate on the coating’s surface. Surfactants in acrylic paints tend to attract dust particles over time at a rate that is much higher than paintings with an oil medium.¹¹ Acrylic paintings from the 1960s are being cleaned more frequently since dust and pollutants take up to 50 years to become visible to the human eye.¹² It is well understood that these modern paintings have to undergo restoration over time, however, compare to traditional oil paintings where cultural heritage scientists have developed methods over five centuries, the experience with conservation of acrylic paintings is still underdeveloped. Due to the presence of surfactants and additives in acrylic films most of the cleaning and restoration methods that are used for oil paintings are not useful for acrylics.⁷

The modern acrylic artist paints, which can provide benefits like durability, low yellowness and rapid drying are not as well studied as traditional oil paint medium. Oil based media have been used for centuries allowing restoration experts to gather knowledge on how to best preserve these priceless works of art. Till now, a large portion of artists used traditional oil based media, where they liked the concept of using natural material and also the comfort of slow cure times.^{4, 13} Oil-based artisan paints are typically just a pigment or mixture of pigments dispersed in a drying oil.

In addition, depending on the viscosity of the oil and the requirements of the paint, a thickener may be added to the paint. Depending on the oil and the pigment, the drying/curing time can vary dramatically. In some cases, the paint does not become tack-free for over a month, which is undesirable. For the faster drying oils, such as linseed oil, the highly yellow color is problematic for white colors and other pale or soft colors.

Chisholm's group has patented and published several articles describing the synthesis and characterization of novel plant oil-based poly vinyl ethers (POVEs)¹⁴⁻¹⁹ It has been shown that compared to triglycerides, POVEs enable the number of double bonds per molecule to be dramatically increased and the can be controlled by controlling the molecular weight of the POVEs. The development of thermosets for coatings or cosmetic products has been the main focus of POVE research until now.²⁰⁻²⁵

It was, therefore, of interest to determine if binders from POVEs could be developed that could reduce or eliminate the yellowing issue while incorporating tunable drying behavior and superior durability. In this study, three different plant oils: linseed oil, soybean oil and palm oil were selected to synthesize POVEs. Linseed, soybean and palm oil are known as drying, semi-drying and non-drying oils, respectively. All the evaluations were carried out by considering unmodified drying linseed oil as a benchmark.

3.3. Materials and methods

3.3.1. Materials

The materials used for the study are described in **Table 3.1**. Unless otherwise specified, all materials were used as received.

Table 3.1. A description of the starting materials used for the study.

Chemical	Designation	Vendor
Soybean oil	SBO	Backers and Chefs
Linseed oil	LO	Sunnyside Co.
Palm oil	PAO	Malaysian Palm Oil Board
Ethylene glycol monovinyl ether (stabilized with KOH); >95%	EGVE	TCI America
Potassium hydroxide, reagent grade, 90%, flakes	KOH	Sigma-Aldrich
Magnesium sulfate, anhydrous, ReagentPlus®, >99%	MgSO ₄	Alfa Aesar
Ethylaluminum sesquichloride, 97%	Et ₃ Al ₂ Cl ₃	Sigma-Aldrich
Methanol, 98%	Methanol	BDH Chemicals
Toluene	Toluene	BDH Chemicals
n-Hexane, 99%	Hexane	BDH Chemicals
Methyl ethyl ketone, 99%	MEK	Alfa Aesar
Ultramarine blue pigment	blue pigment	Golden Artist Paint Co.
Titanium dioxide, rutile, tint strength 38.57	White pigment	Golden Artist Paint Co.
Cobalt 2-ethylhexanoate, 12% Cobalt	Cobalt octoate	OMG Americas
Zirconium 2-ethylhexanoate, 18% Zirconium	Zirconium octoate	OMG Americas
Zinc carboxylate in mineral spirits, 8%	Nuxtra® Zinc	OMG Americas

3.3.2. Synthesis of colorless plant oil vinyl ether (POVE) monomers from soybean oil (2-VOES), linseed oil (2-VOEL) and palm oil (2-VOEP).

All cationic polymerizations were carried out inside a glove box (MBruan, USA), equipped with cold well. Heptane was used as cooling medium and the cold well was connected to a chiller that can be operated at -30 °C as minimum temperature.

As illustrated in **Figure 3.1**, POVE monomers from soybean oil (SBO), linseed oil (LO) and palm oil (PAO) were produced using base-catalyzed transesterification of the triglyceride with ethylene glycol vinyl ether (EGVE) following the method described previously by Alam et al.¹⁷ An example is as follows: 50 g of the plant oil, 50 g of EGVE, and 1.41 g of anhydrous KOH were added into a 500 mL two-necked round bottom flask (rbf). Reaction mixture was then heated to

70 °C while stirring using magnetic stirrer bar under a nitrogen blanket. After 3 h, the reaction was stopped and cooled down to room temperature and diluted with 300 mL of hexane. The reaction mixture was then transferred to a separatory funnel and washed with 70 mL hydrochloric acid (HCl) solution (pH 4.0) and then multiple times with pure DI water until the pH was ~7. The organic layer was then dried over magnesium sulfate, filtered and transferred to a 250 mL one neck rbf. The product was recovered by removing the hexane with rotary evaporation and drying under vacuum (40-50 mm of Hg) at 25 °C overnight.

The synthesized monomers had a dark yellow color with an observed trend of 2-VOEL > 2-VOES > 2-VOEP. These monomers were then distilled via direct distillation to remove the small fraction of colored impurities. For the distillation, 100 g of colored POVE monomer was placed in a 250 mL single neck round bottomed (rbf) equipped with short path distillation head, receiving flask and magnetic stirring bar. Essentially colorless monomers started collecting when the temperature was raised to 200-205 °C, at a vacuum of 5 mbar with continuous stirring. After distillation of about 60 g of monomer, the vacuum decreased to 3 mbar and the temperature of the bath was increased to 210° C to distill the remaining monomer. About 99 g of purified (distilled) POVE monomer (i.e. 2-VOEL, 2-VOES and 2-VOEP) was collected in the receiving flask. Monomers were characterized by proton nuclear magnetic resonance (¹H NMR) spectroscopy, Fourier transform infrared spectroscopy (FT-IR), and ultraviolet-visible spectroscopy (UV-VIS).

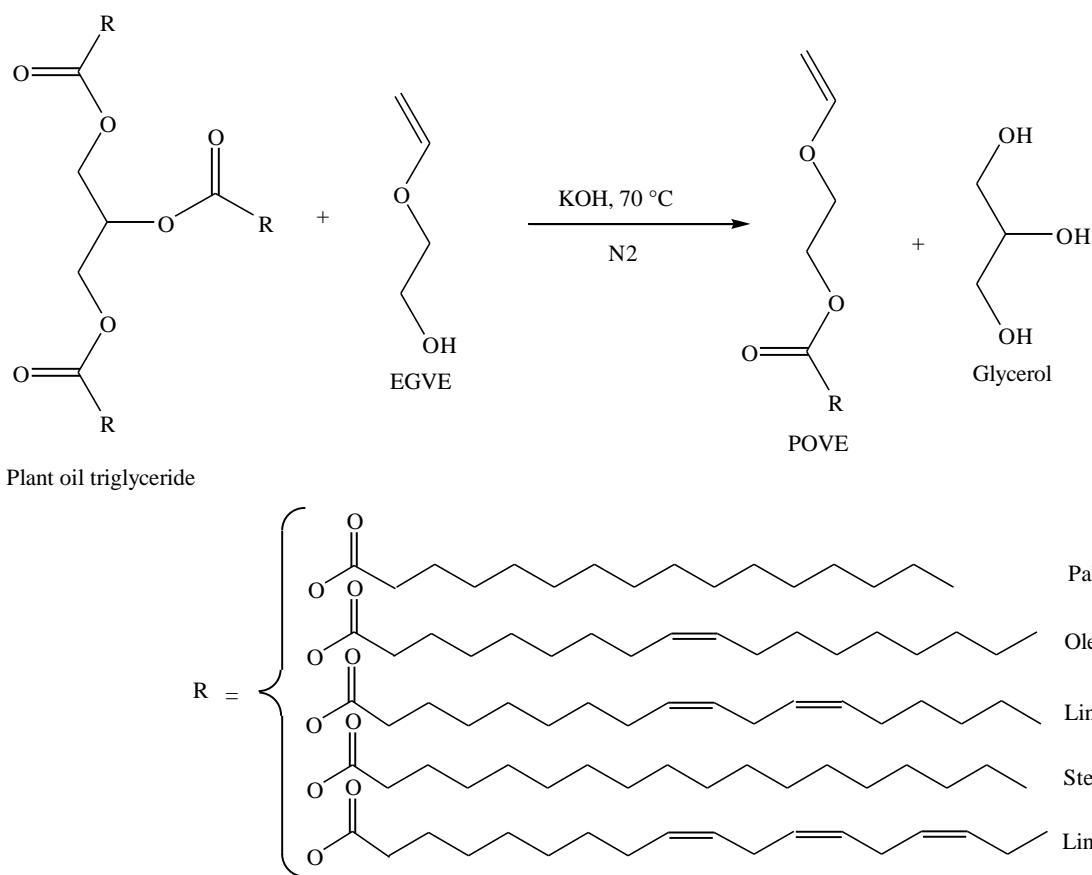


Figure 3.1. Schematic illustrating the synthesis of POVE monomer (2-VOES, 2-VOEL and 2-VOEP).

3.3.3. Synthesis of poly(2-VOEL), poly(2-VOES), and poly(2-VOEP)

Synthesis of homopolymers from the purified POVE monomers was carried out via cationic polymerization previously reported in the literature^{14-17, 21}. The cationogen, 1-isobutoxyethyl acetate (IBEA), was prepared using the procedure reported by Aoshima and Higashimura.²⁶ A generalized procedure of polymerization with a targeted molecular weight of 17 kDa, shown in **Figure 3.2** is described as follows. Initially, all glassware was baked at 200 °C for 2 h and then cooled down by purging with N₂ to avoid moisture condensation. Glassware was then transferred to a glove box where the polymerization was carried out. Initially, 50 g of dried purified POVE monomer was dissolved in 150 mL of dry toluene in a 250 mL three-necked round bottomed

flask and chilled to 0 °C. 0.457 g of initiator (i.e., IBEA), at monomer to initiator ratio of $[M]_0:[I]_0 = 50:1$, was added and chilled for another 30 min. The polymerization was initiated by the addition of 19 mL of the coinitiator, ethylaluminum sesquichloride solution (25 wt.% in toluene) ($[M]_0:[Et_3Al_2Cl_3]_0 = 50:7$). The reaction was terminated after 3 h by the addition of 100 mL of chilled methanol which caused the polymer to precipitate. The polymer was precipitated in ~150 mL of methanol and then washed three times with ~100 mL methanol. The purified polymer was collected as a viscous liquid. From gel permeation chromatography (GPC), the molecular weight was determined, and it was found to be 17 kDa.

In this study, a series of homo-polymers varying in molecular weight from ~6 kDa to ~55 kDa were synthesized to investigate the effect of molecular weight on drying time and viscosity by varying the $[M]_0:[I]_0:[Et_3Al_2Cl_3]_0$ ratios. In addition to the homopolymers made using purified monomers, poly(2-VOES) from non-distilled monomer was synthesized to compare the color difference to polymers synthesized from distilled monomer. The reaction mixtures used to synthesize homopolymers (i.e. quantities of $[M]_0$, $[I]_0$ and $[Et_3Al_2Cl_3]_0$) are reported in **Table 3.2**. The synthesized polymers were characterized by NMR, FT-IR, UV-VIS and GPC.

3.3.4. Synthesis of copolymers from 2-VOEL, 2-VOES, and 2-VOEP

Binders produced by mixing different types (i.e. drying, semidrying and non-drying oil) of oils is a common practice in artist paints to tune its drying behavior.²⁷ In this study, to investigate a similar tuning approach, three copolymers were synthesized by incorporating 50/50 wt.% of purified 2-VOEL/2-VOES, 2-VOEL/2-VOEP and 2-VOES/2-VOEP, using a similar carbocationic polymerization previously described. The compositions of the reaction mixtures are reported in **Table 3.2**. Copolymers were characterized using ¹H NMR, FT-IR, and GPC.

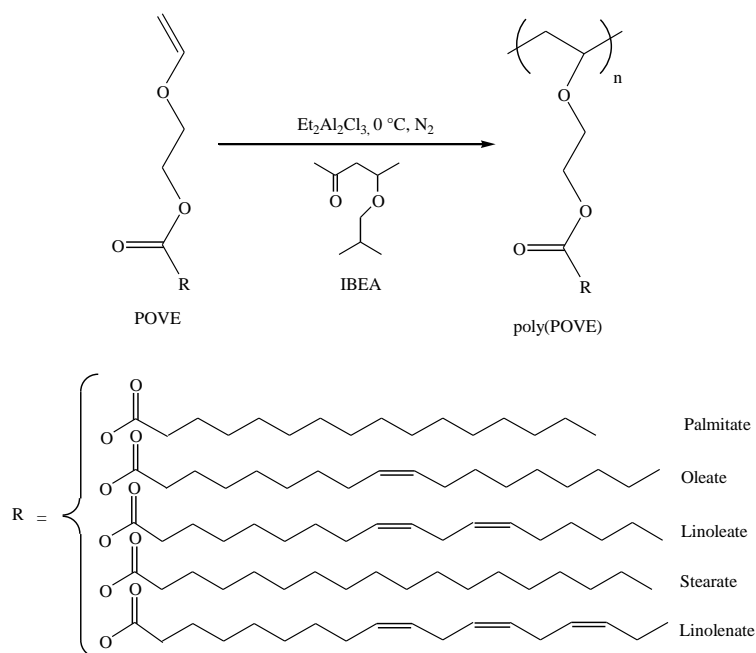


Figure 3.2. Schematic illustrating the synthesis of poly(POVE)s.

Table 3.2. Compositions of the polymerization mixtures used to produce POVE homo and copolymers.

Polymer	2-VOES	2-VOEL	2-VOEP	Initiator (IBEA)	Coinitiator (Et ₃ Al ₂ Cl ₃) 25wt.% in toluene	Targeted Mn (g/mole)
	g	g	g	G	mL	
poly(2VOES), 6.9k	40	-	-	1.06	49.19	6,000
poly(2VOES), 7.3k	40	-	-	0.92	42.69	7,000
poly(2VOES), 9.1k	40	-	-	0.71	32.94	9,000
poly(2VOES), 18.9k	40	-	-	0.36	16.70	18,000
poly(2VOES), 23.9k	40	-	-	0.26	12.06	25,000
poly(2VOES), 33k	40	-	-	0.18	8.35	35,000
poly(2VOES), 54k	40	-	-	0.12	5.56	55,000
poly(2VOES), 12k (non-distilled)	40	-	-	0.38	17.63	17,000
Poly(2VOEL), 18k	-	40	-	0.38	17.63	17,000
Poly(2VOEL-co-2-VOES), 17k	20	20		0.38	17.63	17,000
Poly(2VOEL-co-2-VOEP), 14k	-	20	20	0.38	17.63	17,000
Poly(2VOES-co-2-VOEP), 11.2k	20	-		0.38	17.63	17,000

3.3.5. Preparation of coatings

To study the drying behavior of polymers produced from purified POVEs and from linseed oil as comparison in presence of drier package, per 10 g of neat polymer or oil was mixed with 8 mg of cobalt octoate, 40 mg of zirconium octoate, and 450 mg of Nuxtra® Zinc. Blending was carried out using a FlackTek mixer operating at 3500 rpm for 30 seconds. To study the drying behavior of the neat polymers and linseed oil (reference) as a binder in pigmented coatings, 6.6 g of binder was blended with 4 g pigment using a pigment to binder ratio of 5:3. Same pigmented formulations were also prepared with the drier package used for neat polymers to study the drying behavior of the pigmented poly(POVE) binders in presence of drier catalyst. Mixing of the binder and pigment was done in a 2.75" mortar and pestle until no agglomerate from the pigments could be seen when a one mil thick coating was casted over LENETA (GARDCO) opacity charts using a drawdown bar. To evaluate the drying behavior formulations (both neat and pigmented binders) were casted on 4 × 8" BOROSIL® glass panels using a 1 mil drawdown bar. Pigmented formulations were also produced from blends of poly(2-VOES) and linseed oil based on linseed oil to poly(2-VOES) weight ratios at 90:10, 75:25, 50:50 and 25:75 using a pigment to binder ratio of 3:5. Pigmented coatings were casted over LENETA (GARDCO) opacity charts using a 8 mil drawdown bar and cured for 3 months at RT before color evaluation.

Pigmented formulations were also prepared from poly(POVE) polymers and linseed oil using the same pigment to binder ratio of 3:5 mixed using the mortar and pestle. Formulations were then coated on steel panels obtained from Q-LAB having product no SP-105337 (0.020 × 3 × 6", iron phosphate pretreated) using a 8 mil drawdown bar and cured for 2 months before properties were evaluated.

3.3.6. Instrumentations and methods

3.3.6.1. Differential scanning calorimetry (DSC)

Thermal properties of characteristic selected polymers were examined using differential scanning calorimetry DSC experiments were performed using Q2000 modulated differential scanning calorimeter (TA Instruments Inc.) with a cooling limit up to -200 °C. Helium 25mL/min was used as the purging gas. Sample sizes within the range of 7-10 mg were used and thoroughly dried prior to the measurement. At first, samples were equilibrated at 23 °C and then the cooled down to -170 °C (1st cooling cycle) using helium as purging gas; held at -170 °C for 2min, heated to 80 °C (1st heating cycle), held at 80 °C for 3min and cooled down to -170 °C (second cooling), held at -170 °C for 3 min, heated to 80 °C (2nd heating cycle). The heating/cooling rate for all the cycles were 10 °C min⁻¹.

3.3.6.2. Gel permeation chromatography (GPC)

Molecular weight and molecular weight distribution data was obtained using gel permeation chromatography (GPC). Symyx Rapid-GPC equipped with an evaporative light scattering detector (PL-ELS 1000) and 2Xpl gel mixed B column (10 µm particle size) was used to determine molecular weight. Samples were prepared in THF at a concentration of 2 mg/mL. The molecular weight data were expressed relative to polystyrene standards.

3.3.6.3. Nuclear magnetic resonance (NMR) spectroscopy

All proton NMR spectra were obtained using a Bruker 400 (400MHz) nuclear magnetic resonance spectrometer and CDCl₃ as the lock solvent. Data acquisition was completed using 32 scans.

3.3.6.4. Fourier transform infrared (FT-IR) spectroscopy

Fourier transform infrared (FT-IR) spectra were obtained using a Nicolet 8700 FT-IR spectrometer operated with OMNIC software. Thin polymer films were solution cast onto a KBr disc, subsequently dried, and then scanned from 500-4000 cm^{-1} using 64 scans and 1.93 cm^{-1} data spacing.

3.3.6.5. Drying time measurements

Drying time measurements of the neat polymers with/without drier package and with different pigments were performed according to D1640/D1640M-14 (Method A). According to ASTM D1640-14, a freshly cast coating is deemed “set to touch” when no coating material came off after lightly touching the test film with the tip of a finger. Dust free time was recorded using cotton fiber test method. Coating was considered as “tack free” when a “Zapon” tack-tester pressed against the surface of the coating for five seconds using a 300 g load is immediately released from the coating surface when the load is removed.

3.3.6.6. Ultraviolet-visible spectrometer (UV-VIS)

Removal of the colored impurities from the purified monomers were investigated measuring the absorbance over UV (220-380 nm) and visible range (380-750 nm) using UV quartz cuvette of type 1UV10.

3.3.6.7. Viscosity measurement

Polymer viscosities were determined with an ARES Rheometer from TA Instruments. Samples were placed in between two parallel plates with a 0.5 mm gap. Viscosity was measured by varying the shear rate from 1 to 100/min and the data at a shear rate of 10/min was reported for all polymers.

3.3.6.8. *Tristimulus colorimeter*

Quantification of the color difference was carried out using a Macbeth Color Eye 7000 colorimeter. L*, a*, b* values of the L*a*b* color space defined by the International Commission on Illumination was obtained.

3.3.6.9. *Coating properties*

Chemical resistance on the steel coated panels were performed with a modified version of ASTM D5402 in which double rubs were performed with a 2-lb ball peen hammer. The four folded cheese cloth was fastened to the ball end of the hammer with a wire. It was dipped in methyl ethyl ketone (MEK) solvent every 25 rubs. Hardness was determined using König pendulum hardness test described in ASTM D4366-16. Impact resistance of the steel coated panels were performed according to ASTM D2794-93. The uncoated side of the panel received the impact (i.e. reverse impact). Flexibility was characterized using the conical mandrel bend test as described in ASTM D522. Gloss and color of the coatings with pigments were carried out on matte black LENETA chart.

3.4. Results and discussion

3.4.1. Characterization of POVE monomers

Successful synthesis of 2-VOES, 2-VOEL, and 2-VOEP was confirmed using ^1H NMR and FT-IR. Normalized ^1H NMR spectrum of 2-VOES, 2-VOEL, and 2-VOEP are shown in **Figure 3.3**. Both the chemical shift and peak area integration data obtained from the spectra confirmed the successful synthesis of each monomer. Incorporation of the vinyl group was confirmed from the peaks assigned as “a” and “f” associated with vinyl group protons. The relative area of the multiplet assigned as “b” in **Figure 3.3** associated with the bis-allylic protons was calculated and found to be 4.20, 2.93 and 1.23 with $-\text{CH}_3$ protons as reference for 2-VOEL, 2-

VOES and 2-VOEP respectively, which is consistent with the approximate amount of double bonds i.e. 6.3, 4.5 and 1.8 per triglyceride for linseed, soybean and palm oils, respectively.^{15, 17} In addition, visual comparison of the area under the “p” peak associated with the methyl groups of linolenic esters showed consistency with the relative concentration of linolenic esters obtained from literature. Successful synthesis of 2-VOES, 2-VOEL, and 2-VOEP were also evaluated with FT-IR spectroscopy. In **Figure 3.6**, normalized characteristic FT-IR spectra of the 2-VOEL and linseed oil (reference) are shown. Successful synthesis of 2-VOEL is confirmed from the appearance of the medium, broad peak at 1615 cm^{-1} and a sharp peak at 1218 cm^{-1} confirming the incorporation of vinyl group along with the retention of the bands at 1615 and 1218 cm^{-1} associate with aliphatic $C=C$ fatty unsaturation.

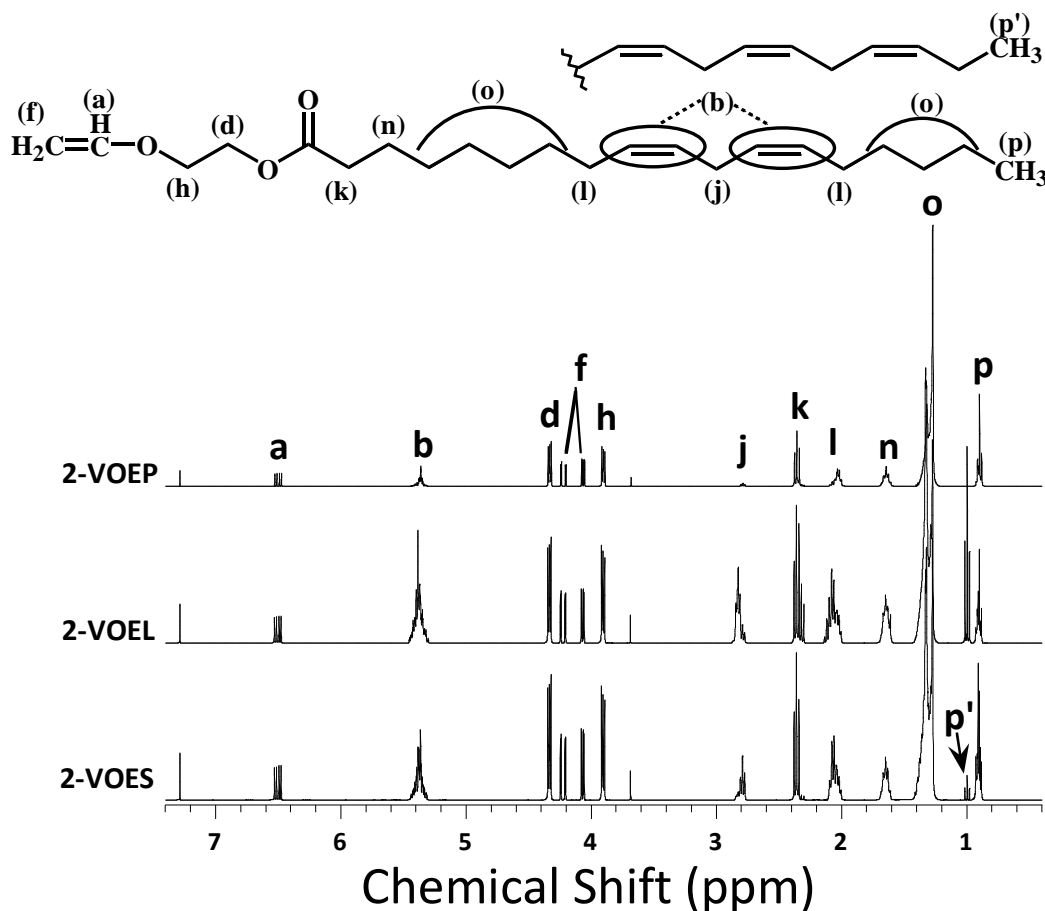


Figure 3.3. ^1H NMR spectrum of the 2-VOES, 2-VOEL and 2-VOEP monomers.

3.4.2. Characterization of homopolymers and copolymers

Successful synthesis of the homopolymers and copolymers along with variation in the composition of the fatty pendent chains was confirmed using ^1H NMR and FT-IR. ^1H NMR spectrum of the corresponding homopolymers and copolymers are shown in **Figure 3.4** and **Figure 3.5** respectively. Like the monomers, the relative peak intensity/area under the peaks assigned as “p” and “b” associated with the methyl protons of linolenic acid and bis-allylic protons clearly indicate a trend of $\text{poly}(2\text{-VOEL}) > \text{poly}(2\text{-VOES})$ for homopolymers and $\text{poly}(2\text{-VOES-co-VOEL})\text{-}50/50 > \text{poly}(2\text{-VOEL-co-VOEP})\text{-}50/50 > \text{poly}(2\text{-VOEL-co}2\text{-VOEP})\text{-}50/50$ for copolymers based on total unsaturation. So, compositional variation in the copolymer was achieved with varying the starting plant oil which might be advantageous to tune the curing behavior.

POVE homopolymers and copolymers were also evaluated with FT-IR spectroscopy. In **Figure 3.6**, normalized characteristic FT-IR spectrums of the $\text{poly}(2\text{-VOEL})$ along with its monomer and parent oil are shown for comparison. FT-IR spectra of rest of the polymers are not shown due to their similar nature with $\text{poly}(2\text{-VOEL})$. Successful synthesis of $\text{poly}(2\text{-VOEL})$ is confirmed from the disappearance of peaks at 1615 cm^{-1} ($\text{C}=\text{C}$, vinyl stretch) and a sharp peak at 1218 cm^{-1} (C-O-C , vinyl-alkyl stretch) and another two peaks at 987 and 825 cm^{-1} corresponding to the vinyl C-H bending. Retention of the bands at 2987 cm^{-1} and 1650 cm^{-1} associate with aliphatic $\text{C}=\text{C}$ unsaturation has been observed confirmed the retention of fatty unsaturation during polymerization.

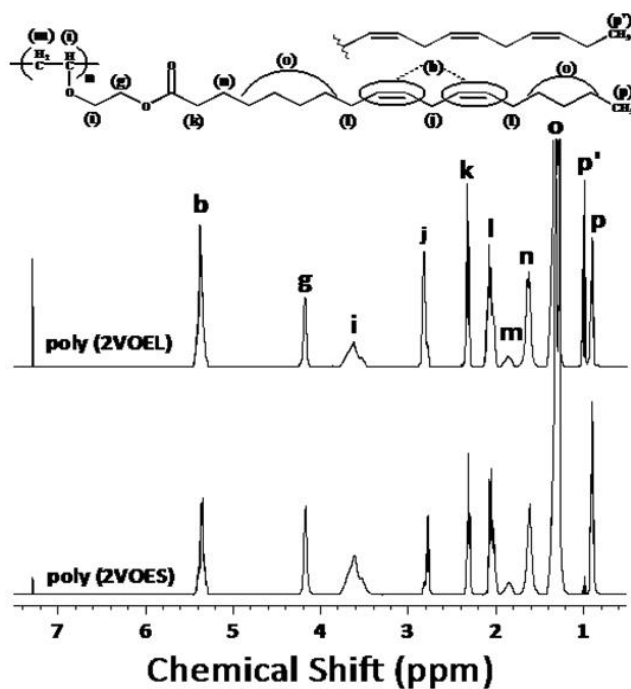


Figure 3.4. ^1H NMR spectrum of the poly(2-VOES) and poly(2-VOEL) homo-polymers.

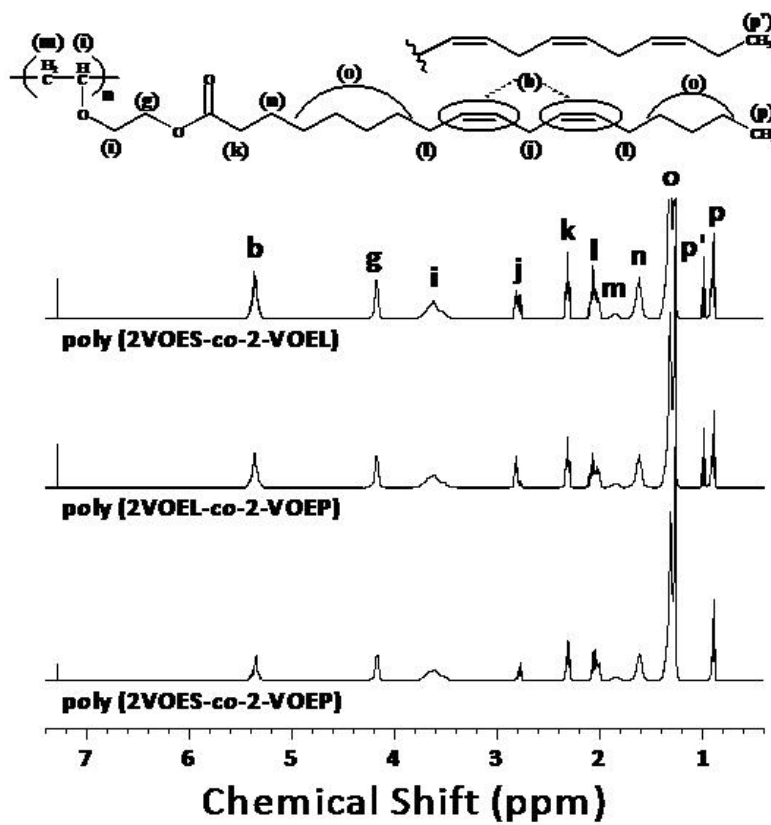


Figure 3.5. ^1H NMR spectrum of the poly(2-VOES-co-VOEL)-50/50, poly(2-VOES-co-VOEP)-50/50 and poly(2-VOEL-co-2-VOEP)-50/50 copolymers.

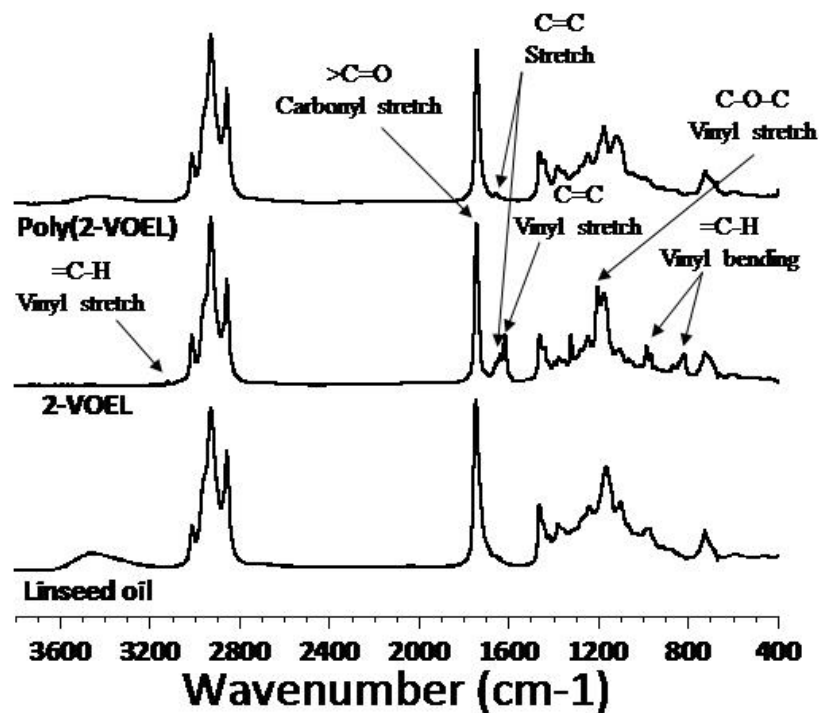


Figure 3.6. Characteristic FT-IR spectra of linseed oil, 2-VOEL and poly(2-VOEL).

Number average molecular weight and polydispersity index of the homopolymers and copolymers were evaluated using GPC and the results are reported in **Table 3.3**. As shown in **Table 3.3** for the series of poly(2-VOES) homopolymers experimental Mn values were very close to the targeted molecular weights. An increasing trend of PDI was observed with decreasing the Mn of poly(2-VOES) homopolymers, which was expected due to addition of higher initiator to monomer ratio, initiating increasing no of chains. A higher Mn and PDI for poly(2-VOES) produced from non-distilled 2-VOES might be due to presence of impurities resulting chain transfer. For copolymers targeted Mn was observed for 2-VOEL/2-VOES copolymer however, Mn decreased for copolymers produced with 2-VOEP as comonomer.

Table 3.3. Mn and PDI of the homopolymers and copolymers produced from POVEs.

Polymer	Mn (g/mol)	PDI
poly(2VOES), 6.9k	6,960	1.34
poly(2VOES), 7.3k	7,200	1.27
poly(2VOES), 9.1k	9,038	1.20
poly(2VOES), 18.9k	18,920	1.20
poly(2VOES), 23.9k	23,190	1.19
poly(2VOES), 33k	32,960	1.22
poly(2VOES), 54k	54,080	1.16
poly(2VOES), 12k (non-distilled)	12,073	1.32
Poly(2VOEL), 18k	17,924	1.31
Poly(2VOEL-co-2-VOES), 17k	17,050	1.23
Poly(2VOEL-co-2-VOEP), 14k	14,200	1.27
Poly(2VOES-co-2-VOEP), 11.2k	11,214	1.21

3.4.3. Visual and spectroscopic confirmation of removal of color impurities

Removal of the color impurities after distillation was confirmed by visual observation and taking UV-VIS absorption spectroscopy of monomers before and after distillation. As shown in **Figure 3.7**, two poly(2-VOES) with varying Mn (C and D) produced with distilled 2-VOES were surprisingly colorless, compare to poly(2-VOES) produced using non-distilled 2-VOES and linseed oil. Despite of the intense yellow color of linseed oil, almost colorless poly(2-VOEL) and its copolymers were synthesized and are shown in **Figure 3.8**, which makes them promising candidate as binder to produce white and light colors. This also confirmed that early removal of the color impurities at the monomer stage is very efficient to produce colorless polymer and the color does not redevelop during used cationic polymerization conditions.



Figure 3.7. Images that provide a comparison of the color difference between the (C) and (D) two poly(2-VOES) samples produced with purified 2-VOES to (A) linseed oil as well as a (C) poly(2-VOES) produced using non-purified 2-VOES.

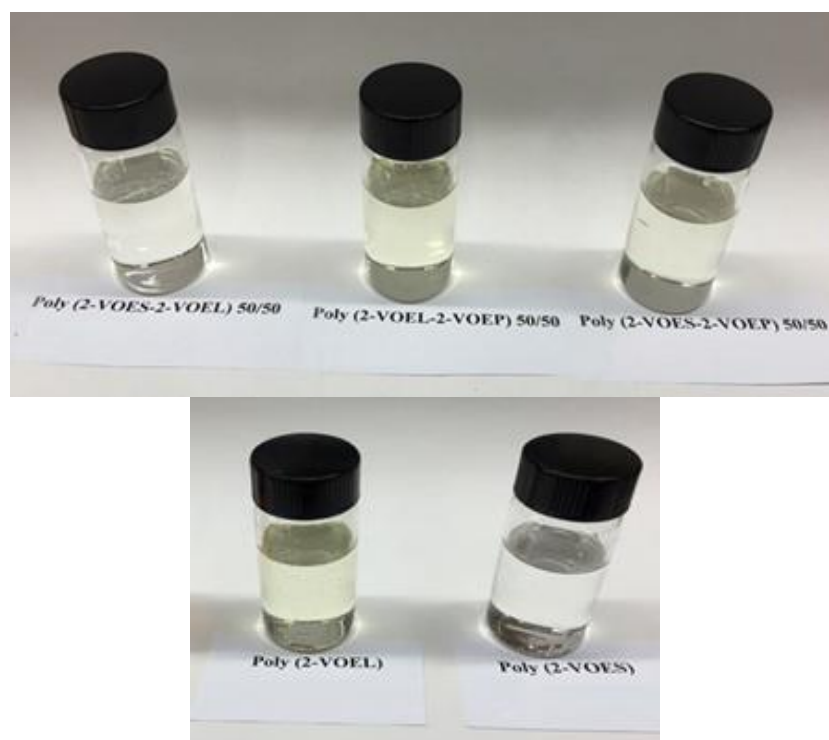


Figure 3.8. Images providing visual confirmation of the synthesis of essentially colorless homopolymers and copolymers from distilled POVE monomers.

Along with visual appearance, UV-VIS absorbance spectra for linseed oil and non-distilled 2-(VOES) monomer, as shown in **Figure 3.9**, clearly showed multiple signals between 260 to 360 nm which are mostly due to the presence of conjugated double bonds that might be resulted due to oxidation. However, UV-VIS absorbance spectra of 2-VOES monomer after distillation and its homopolymer confirms the removal of color impurities with the absence or significant reduction in intensity of these signals at higher wavelengths.

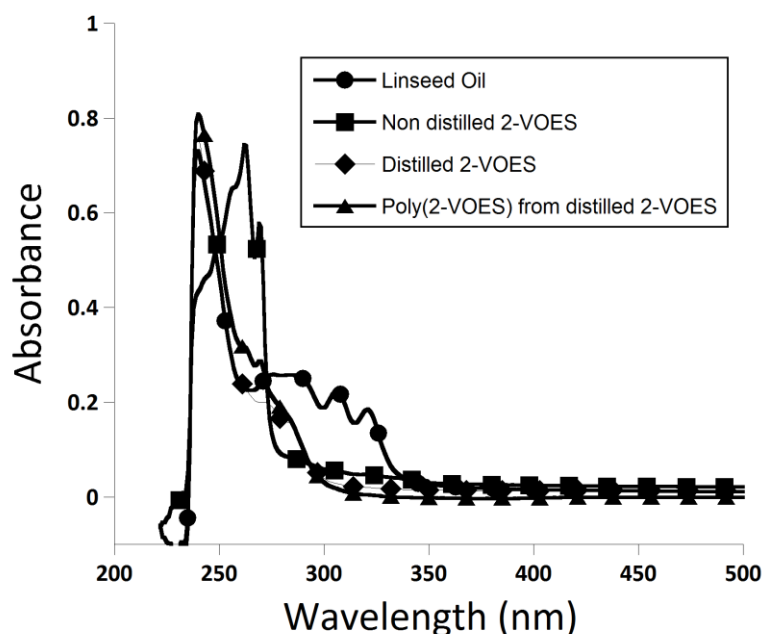


Figure 3.9. UV-VIS spectra of the linseed oil, non-distilled 2-VOES monomer, distilled 2-VOES and poly(2-VOES) from distilled monomer.

3.4.4. Thermal properties of homopolymers and copolymers

Characteristic DSC thermograms of poly(2-VOES), poly(2-VOEL), poly(2-VOES-co-2-VOEL)-50/50 along with linseed oil as reference are shown in **Figure 3.10**. Compare to linseed oil, POVE polymers represent very different thermal responses. DSC thermogram of linseed oil showed the presence of a glass transition temperature (T_g) at approximately $-137\text{ }^\circ\text{C}$ which is

followed by a broad endotherm with hysteresis at around $-77\text{ }^{\circ}\text{C}$ corresponding to the melting of the imperfect crystal domains; melting of these imperfect or low ordered crystal domains provides enough mobility to reorganize into perfect crystals. This phenomenon is supported by the presence of an immediate significant crystallization exotherm with peak maximum at $-62\text{ }^{\circ}\text{C}$ and two melting endotherms with the peak temperatures of -16 and $-75\text{ }^{\circ}\text{C}$.

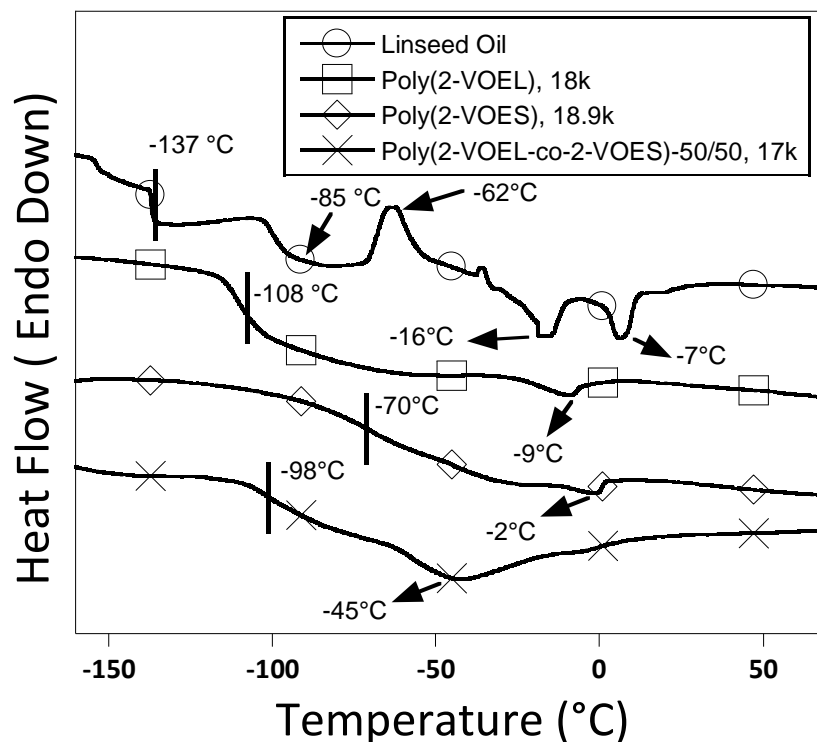


Figure 3.10. DSC thermograms for linseed oil, poly(2-VOEL), 18k, poly(2-VOES), 18.9k, and poly(2-VOES-co-2-VOES), 17k.

In contrast to linseed oil, poly(2-VOEL) and poly(2-VOES) showed T_g s around $-108\text{ }^{\circ}\text{C}$ and $-70\text{ }^{\circ}\text{C}$ respectively. The lower T_g of poly(2-VOEL) can be rationalized as an outcome of the presence of higher concentration of unsaturated fatty pendent chains than poly(2-VOES). Since all of the unsaturation in POVEs has cis configuration, each of these double bonds introduces a “kink” in the fatty acid chain, which significantly reduces the formation of intermolecular interactions such as Vander Waals interactions and increases the free volume. The presence of higher free

volume and lower interactions results in transition of the poly(2-VOEL) polymer chains at a lower temperature than poly(2-VOES). The DSC curve of poly(2-VOES-co-2-VOEL)-50/50 indicates similar behavior as the homopolymers, however, with a T_g at approximately -98 °C, which is intermediate of the T_g s from poly(2-VOEL) and poly(2-VOES).

3.4.5. Viscosity vs molecular weight (MW) of 2-VOES homopolymers

In the case of artist paints, the viscosity of the binder plays a critical role. Lower viscosity of the binder is desirable for higher pigment loading and mixing, while higher viscosity is required for obtaining the best film properties. So, the tunability of the binder viscosity is desirable which in case of traditional plant oil binders can only be achieved by varying the fatty chain unsaturation. So, an increase in viscosity of the drying oil (with high unsaturation) can be achieved by incorporating a nondrying oil (low unsaturation), however it will result in undesirable slow drying. In this study, we took a different approach of varying the viscosity by varying the MW of POVE polymer, since it has been extensively shown that log of viscosity of polymer varies linearly with log of MW until a critical MW above which viscosity increases with the 3.4 power of MW.^{28, 29}

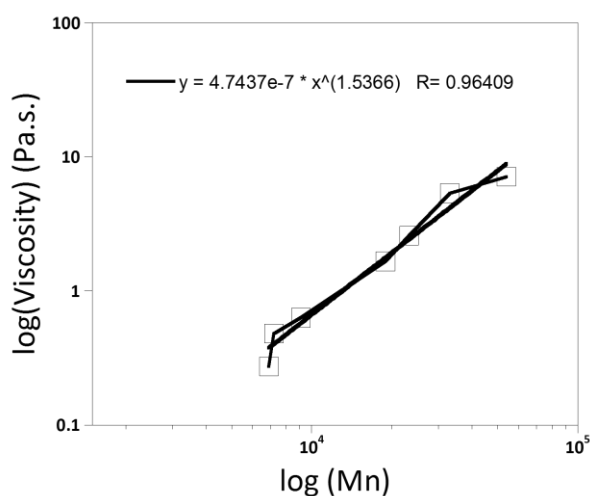


Figure 3.11. Viscosity at 23 °C as a function of MW for the poly(2-VOES) homo-polymers.

Figure 3.11 displays the dynamic viscosity at 23 °C as a function of polymer Mn in logarithmic scale for the seven 2-VOES homopolymers varying the MW from ~6 kDa to ~55 kDa. From **Figure 3.11** it is confirmed that viscosity of these 2-VOES homo-polymers increases with molecular weight linearly with a power of 1.53. This result suggests that the MW range selected for 2-VOES homo-polymers for this study was below the critical MW needed for the generation of polymer entanglements.

3.4.6. Characterization of coatings

3.4.6.1. Drying time measurements of polymers

Drying time measurements of the POVE based monomers and polymers were carried out to investigate the effect of both the polymer composition and MW on its drying behavior. Drying behavior of these polymers was studied without and also using a Co/Zr/Zn drier package. Drying time values recorded for 2-VOES homopolymers varying in MW and also for linseed oil as reference are shown in **Figure 3.12**. As shown in **Figure 3.12 (a)**, without a drier package, poly(2-VOES) homopolymers showed decrease in drying time with increasing the molecular weight and these values were 3 to 7 times shorter than linseed oil.

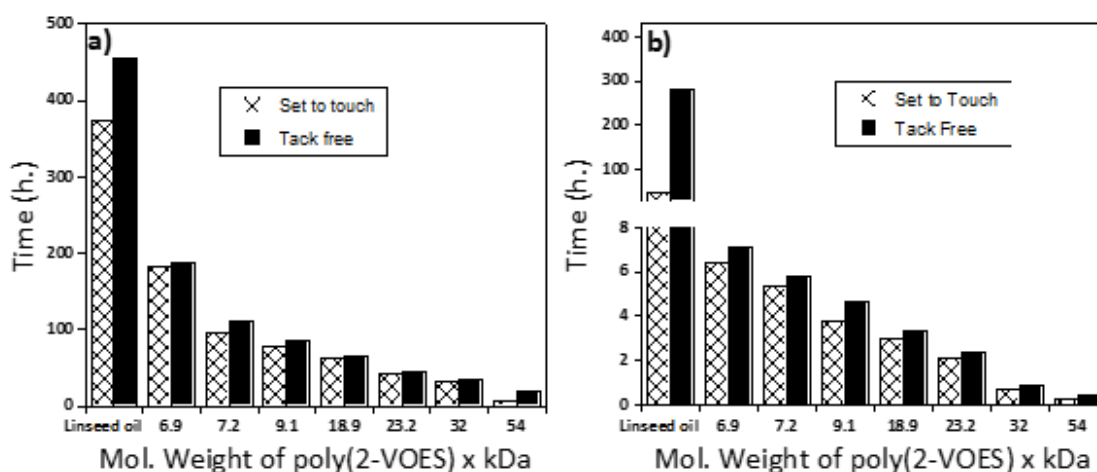


Figure 3.12. Drying time measurements of poly(2-VOES) homo-polymers (a) without drier package and (b) with drier package.

Linseed oil, being a drying oil, had a tack free time of approximately 450 h, however, poly(2-VOES) homo-polymer with a MW of ~7 kDa (linear polymer with approximately 20 pendent chain), being produced from soybean oil which is semi drying oil, showed a tack free time of 180 h which is less than half of the tack free time for linseed oil. This concludes that conversion of the triglyceride of a semi drying oil into a linear polymer with fatty pendent chains increases the functionality of the polymer thereby making it become tack free at shorter time than the drying oil. This effect increases exponentially with increasing the MW of the polymer. In presence of drier package both linseed oil and poly(2-VOES) homopolymers showed decrease in drying time [Figure 3.12 (b)]. However, this decrease in drying time was much intense (~25 times) for poly(2-VOES) homopolymers than linseed oil (~1.6 times) compared to their drying time without drier package. The magnitude of this effect increases with increasing the MW of the polymers. So, compared to linseed oil these POVE homo-polymers can provide a fast-drying system with an ability to tune the drying time by varying the MW.

Drying time values were also determined for homopolymers and copolymers of similar MW to investigate the effect of polymer composition on its drying behavior with and without drier catalyst and the results are shown in Figure 3.13. Linseed oil showed the longest ‘set to touch’ and ‘tack free’ time than the homopolymers and copolymers in presence and absence of drier package which which is attributed from its triglyceride nature having smaller number of functional groups per molecule compared to linear polymers. However, like poly(2-VOES), conversion of linseed oil triglyceride to a linear chain polymer shortened the drying time drastically and the even augmented in presence of drier catalyst. For homopolymers, shortest drying time was recorded for poly(2-VOEL) than poly(2-VOES) which is a direct reflection of the presence of higher amount of unsaturation (linolenic acid) in the parent oil. In case of copolymers an increase in drying time

was observed when 2-VOEP or 2-VOES was added as a comonomer to 2-VOEL, which is due to the dilution of pendent chains with more saturated fatty chains. However, a slightly shorter drying time of 2-VOEL co-polymer was recorded with 2-VOEP as a comonomer than 2-VOES, although 2-VOES has more unsaturated fatty concentration than 2-VOEP [Figure 3.13 (a)]. This slight inconsistency might be due to the ability of the saturated fatty chains to act as a plasticizer improving the mobility of the polymer chains near the gel point where, due to vitrification, the mobility of polymer segments become very slow.

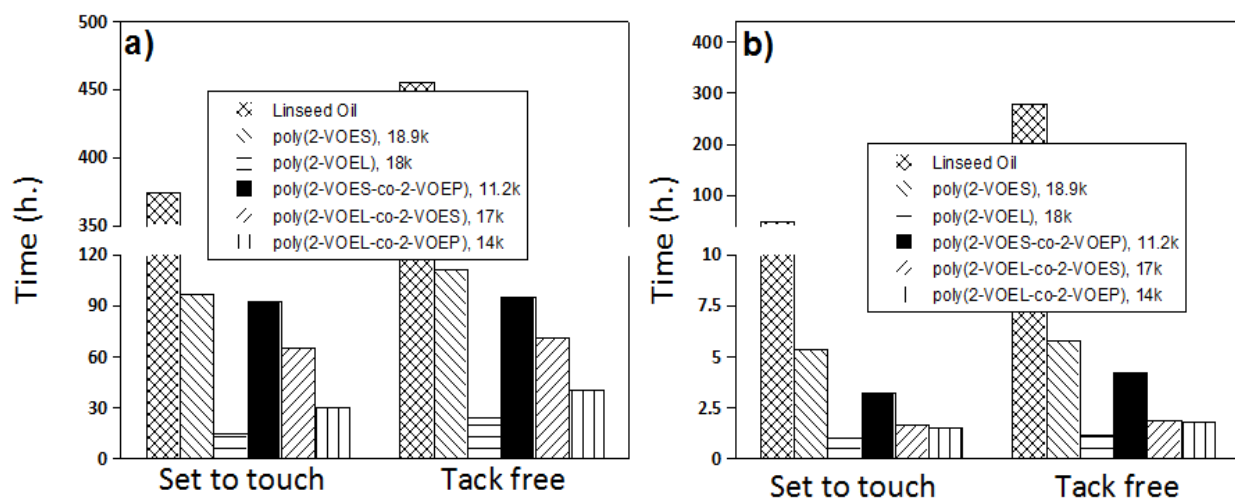


Figure 3.13. Drying time measurements of homo-polymers from 2-VOES, 2-VOEL and 50/50 wt.% co-polymers from 2-VOES, 2-VOEL and 2-VOEP (a) without and (b) with drier package.

3.4.6.2. Drying time measurements of polymers with pigment

Although the neat polymers synthesized from purified POVEs showed faster drying with tunability by varying the composition as well as the molecular weight of the linear polymer, to be able to use them as a binder for artist paint, evaluation of drying time in the presence of pigments is very important. The drying time behavior of poly(2-VOES) and linseed oil was evaluated with TiO₂ pigment without a drier package by using a pigment to binder weight ratio of 3:5. As shown in Table 3.4, the use of poly(2-VOES) as the binder reduced the drying time dramatically

compared to linseed oil. The set-to-touch time and tack-free time was reduced by as factor of 15.0 and 12.2, respectively.

Table 3.4. Drying time poly(2-VOES) and linseed oil in presence of TiO₂.

	Poly(2-VOES)/TiO₂	Linseed Oil/TiO₂
Set-to-touch (hours)	16	240
Tack-free (hours)	26	316

For artisan paints, the desired drying/curing time can vary depending on painting technique and preferences of the artist. As a result, it was of interest to investigate blends of poly(2-VOES) and linseed oil as the paint binder system. Thus, a series of white paints were prepared with a pigment to binder weight ratio of 3:5. The binders used were pure poly(2-VOES), pure linseed oil, or a blend of the two materials. **Figure 3.14** shows the data obtained with respect to drying/curing time. As shown in **Figure 3.14**, displacing just 10 weight percent of the linseed oil with poly(2-VOES) shortened the tack-free time by 60%.

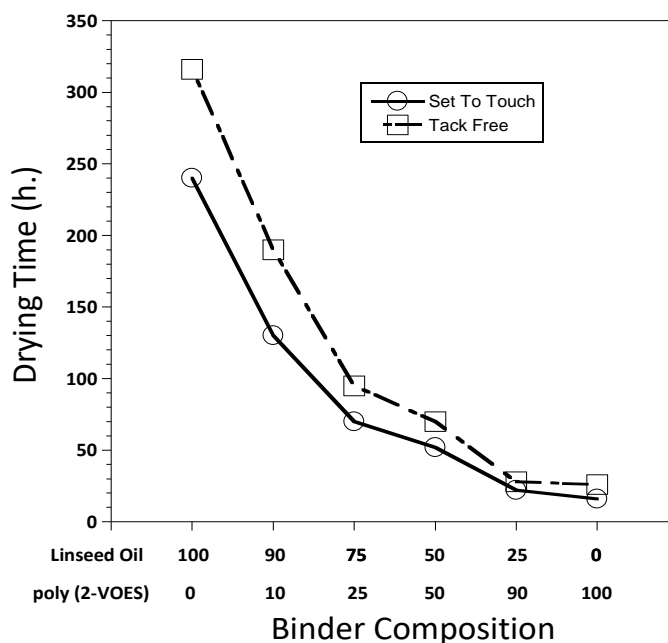


Figure 3.14. The drying/curing time for white paints based on blends of poly(2-VOES) and linseed oil as the binder.

Drying time of homopolymers and copolymers were also evaluated by producing paints with TiO₂ and ultramarine blue pigment without drier package. Pigment to binder weight ratio was 3:5. Recorded drying times with TiO₂ and ultramarine blue pigment are shown in **Figure 3.15** and **Figure 3.16** respectively. As shown in **Figure 6.15**, drying time of the coating produced from linseed was the shortest compared to the POVE homopolymers and copolymers. Although, shortening of drying time recorded for neat POVE copolymers had some inconsistency with increasing unsaturation however, in case of pigmented samples a nice trend of shortening drying time with increasing unsaturation concentration of the polymer composition i.e. poly(2-VOEL) < poly(2-VOEL-co-2-VOES) < poly(2-VOES) < poly(2-VOEL-co-2-VOEP) < poly(2-VOES-co-2-VOEP) has been observed for all the three levels of drying time measurements. Drying time of the specimens with the ultramarine blue pigment as shown in **Figure 3.16** had similar trend in drying time, however for each binder the drying time was slightly longer, which is not very surprising as pigments can vary the drying behavior of the binder based on their catalytic nature and also they are solid.³¹

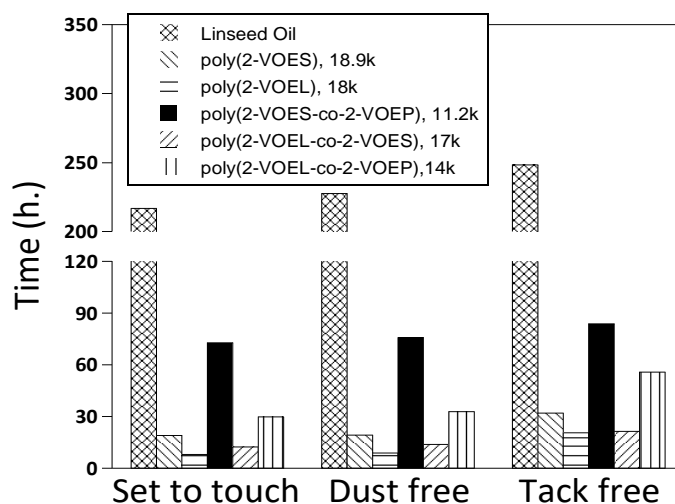


Figure 3.15. Drying time measurements of homo-polymers from 2-VOES, 2-VOEL and 50/50 wt.% co-polymers from 2-VOES, 2-VOEL and 2-VOEP with TiO₂ without drier package.

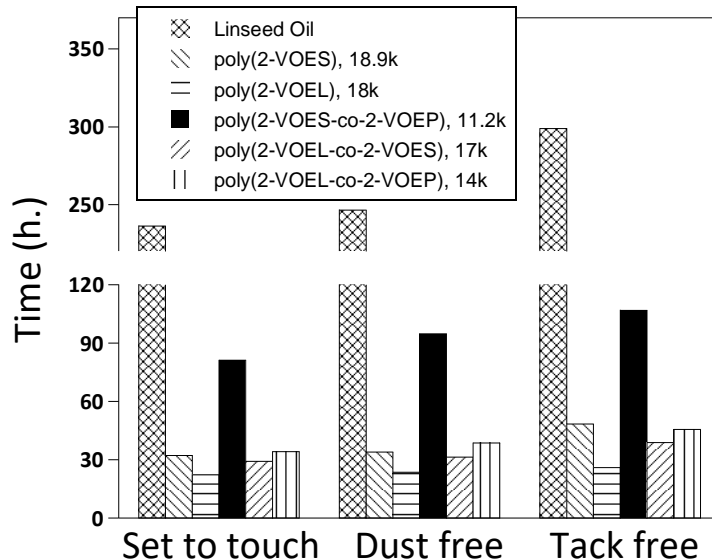


Figure 3.16. Drying time measurements of homo-polymers from 2-VOES, 2-VOEL and 50/50 wt.% co-polymers from 2-VOES, 2-VOEL and 2-VOEP with ultramarine blue pigment without drier package.

3.4.6.3. Qualitative and quantitative color evaluation of pigmented coatings

Along with drying behavior, evaluation of the color especially ‘yellowness’ of the pigmented coatings produced from purified POVEs polymers were carried out by measuring the L^* , a^* , b^* using a Macbeth Color Eye 7000 colorimeter. Two pigmented coatings were cast over LENETA (GARDCO) opacity charts using an 8 mil drawdown bar from poly(2-VOES), 18.9k with TiO_2 using a pigment to binder ratio of 3:5. For comparison a similar formulation from linseed oil was also prepared and two pigmented coatings were casted. One coating from each formulation was cured for 3 months at RT before the color evaluation. **Figure 3.17** provides images of sections of the coated charts after curing for 3 months at RT. As shown in **Figure 3.17**, the coating based on poly(2-VOES) was much whiter than the analogous coating based on linseed oil. Quantitative measure of color of these coatings were carried out and the L^* , a^* , b^* values are reported in **Table 3.5**. As reported in **Table 3.5**, the b^* value for the linseed oil/ TiO_2 coating showed number five

times higher than that for the poly(2-VOES)/TiO₂ coating, confirming that the former was much yellower in color than the latter cured at RT for 3 months.



Figure 3.17. Images that provide a comparison of the color difference between a white paint produced with poly(2-VOES) synthesized from 2-VOES that was purified by distillation to an analogous paint based on linseed oil.

In addition to evaluating the color of the cured coatings at RT for 3 months, one coating from each sample were heat aged at 120 °C for 5 h in an oven after cured for 1 month at RT. **Table 3.5** lists the L*, a*, b* values obtained from the two coatings after 2 months of heat aging. As shown in **Table 3.5**, the b* value for the linseed oil/TiO₂ coating increased by 3.7 units due to the heat aging, while the b* value for the poly(2-VOES)/TiO₂ coating increased by just 1.01 units which indicates that poly(2-VOES) has more color stability than linseed oil as a binder.

Table 3.5. L*, a*, b* values of the coatings prepared with TiO₂ containing paint films cured at RT and at 120 °C for 5h. (color was measured after 2 months).

	Poly(2-VOES) /TiO₂ (RT, 3 months)	Linseed Oil/TiO₂ (RT, 3 months)	Poly(2-VOES) /TiO₂ (120 °C, 5 h.)	Linseed /TiO₂ (120 °C, 5 h.)
L*	99.8	99.4	100	99.5
a*	0.98	1.13	0.92	1.58
b*	2.74	14.7	3.75	18.4

TiO₂ pigmented coatings were also produced from blends based on linseed oil to poly(2-VOES) at 90:10, 75:25, 50:50 and 25:75 using a pigment to binder ratio of 3:5 and cured for 3 months at RT before color evaluation. For comparison TiO₂ pigmented coatings were also produced from 100 % poly(2-VOES) and 100 % linseed oil using same pigment to binder ratio. **Figure 3.18** provides images of sections of the pigmented coatings. As shown in the **Figure 3.18**, the coating based on pure poly(2-VOES) as the binder appeared to be much whiter than the coating with pure linseed oil as the binder. Even incorporation 25 wt.% poly(2-VOES) to linseed oil tended to reduce the yellowness significantly.

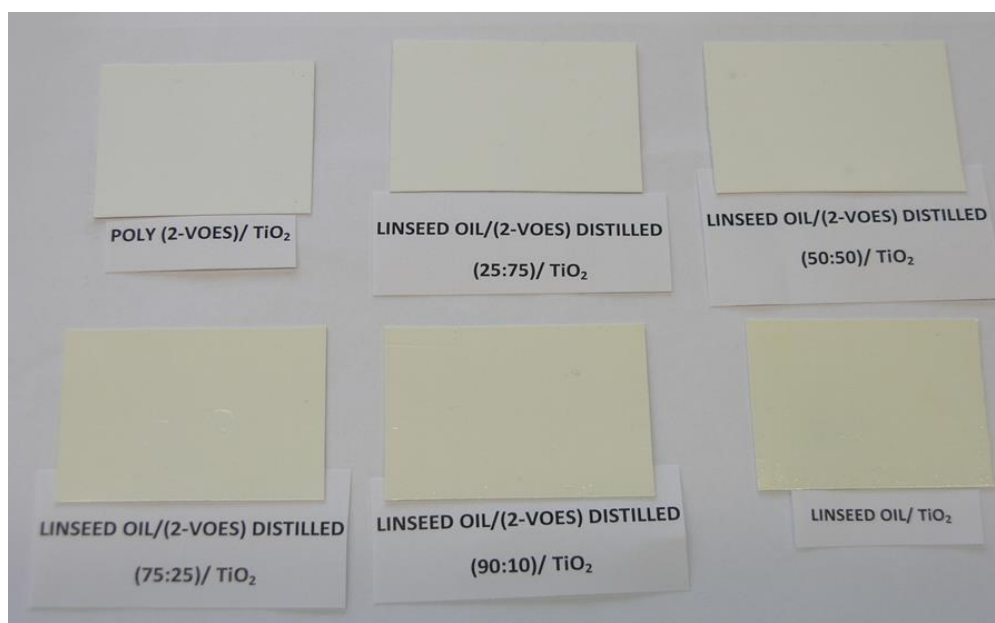


Figure 3.18. Images that provide a comparison of the color difference between a white paint produced with pure poly(2-VOES), pure linseed oil, or a blend of the two materials incorporated at different ratios.

For further confirmation L*, a*, b* values of these specimens were measured and the values are reported in **Table 3.6**. As reported in **Table 3.6**, Increasing the poly(2-VOES) amount up to 25 wt. %. resulted in a decrease in the b* value of the blend from 16 to 8 units, i.e. almost 50 %. Incorporation of poly(2-VOES) also increases the L* value i.e. coatings become brighter.

Table 3.6. L*, a*, b* values showing the color difference between TiO₂ pigmented produced from pure poly(2-VOES), pure linseed oil and their blend at different weight ratios.

Binder	L*	a*	b*
Linseed oil	98.40	1.57	15.14
Linseed oil : poly(2-VOES) = 90:10	99.35	1.81	14.59
Linseed oil : poly(2-VOES) = 75:25	99.55	1.71	8.67
Linseed oil : poly(2-VOES) = 50:50	99.75	1.62	5.40
Linseed oil : poly(2-VOES) = 25:75	99.36	1.72	4.43
Poly(2-VOES)	99.82	0.98	2.74

The same experiment was done using ultramarine blue pigment (custom product from Golden) both using a poly(2-VOES) and linseed oil. **Table 3.7** provides the drying/curing characteristics of the paints. As reported in **Table 3.7**, similar to the white paints, the blue paint based on poly(2-VOES) dried/cured dramatically faster than the linseed oil-based blue paint.

Table 3.7. The drying time of the ultramarine blue-containing paint films.

	Poly(2-VOES)/pigment	Linseed Oil/pigment
Set-to-touch (hours)	18	219
Tack-free (hours)	25	407

3.4.6.4. Evaluation of physical properties of cured coatings

Physical properties of the coatings produced from poly(2-VOES), 6.9k and linseed oil with TiO₂ pigment were measured after curing for 60 days at RT were evaluated using various ASTM methods and the values are reported in **Table 3.8** lists along with the results. The film hardness of the paint based on poly(2-VOES) was substantially higher than that for the linseed oil-based paint. Despite the higher hardness of the poly(2-VOES)-based paint, it exhibited excellent flexibility as indicated by the conical mandrel bend test and the reverse impact test. poly(2-VOES)-based paint also showed higher gloss than linseed oil paint.

Table 3.8. The physical properties of coatings produced from poly(2-VOES), 6.9k and linseed oil with TiO₂ pigment cured at RT for 60 Days without drier catalyst.

Coating properties	Poly(2-VOES)/TiO₂	Linseed Oil/TiO₂
König Pendulum Hardness (sec.), ASTM D4366	44 + 1	11 + 1
Pencil Hardness, ASTM D3363	HB	6B
Conical Mandrel Bend (%), ASTM D1737	100	100
Reverse Impact (in-lb), ASTM D2794	>172	>172
MEK Double Rubs, ASTM D4752	44 + 5	42 + 5
20° Gloss	47.3	22.2
60° Gloss	78.4	63.7
85° Gloss	91.1	73.0

Similarly, physical properties were also evaluated for coatings produced from homopolymers and copolymers with ultramarine blue pigment without drier package. The numbers are listed in **Table 3.9**. As shown in **Table 3.9**, both the chemical resistance and the hardness of the paint based on POVE homopolymers and copolymers had surprisingly higher numbers than linseed oil paints cured at RT. For the coatings cured at 150 °C for an hour showed numbers that are almost two times higher than RT curing, likewise the magnitude of difference between the POVE based polymers and linseed oil was substantially higher than that for the linseed oil-based paint. Despite the higher hardness of POVE-based paint, it also exhibited excellent flexibility like linseed oil as indicated by the conical mandrel bend results and the reverse/forward impact results.

Table 3.9. The physical properties of coatings produced from homopolymers (except poly(2-VOEP) and copolymers with ultramarine blue pigment without drier package.

	Curing temperature (°C)	Thickness (µm)	MEK double rubs	Konig pendulum hardness (sec.)	Mandrel Bend (0-32 %)	Reverse impact (in.lbs)	Reverse impact (in.lbs)
Linseed oil	25	107.7±5.5	78±8	18.3±1.5	32	173	173
	150	104±10	181±6	24.3±0.6	32	173	173
Poly(2-VOEL)	25	119±6	536±7	42±0.0	32	173	173
	150	100.7±3.3	1182±15	45.3±0.6	32	173	173
Poly(2-VOES)	25	106±5.6	239±8.3	43.6±0.6	32	173	173
	150	101±5.8	385/±8.6	45±0.0	32	173	173
Poly(2-VOEL/2-VOEP)-50/50 wt. %)	25	104±1.1	380±5	28.3±0.57	32	173	173
	150	100±2.2	533±7.5	30±0.0	32	173	173
Poly(2-VOEL/2-VOES)-50/50 wt. %)	25	111±6.1	430±8.1	33.3±1.1	32	173	173
	150	106±4.5	808±12	39±0.0	32	173	173
Poly(2-VOES/2-VOEP)-50/50 wt. %)	25	106±4.7	249±7	39±0.0	32	173	173
	150	102±2	255±4.5	43.3±0.57	32	173	173

3.5. Conclusions

The plant oil-based poly(vinyl ether)s (POVEs) provide several advantages over traditional drying oils as a binder for artist paint. POVEs produced from semi-drying oils, such as soybean oil, showed drying behavior faster than drying oils. POVEs can be easily distilled of resulting colorless products from which binders that have both dramatically lower color and faster drying than traditional drying oils was successfully produced. The viscosity of POVEs can be easily tailored by tailoring molecular weight without affecting other properties. In addition to tailoring viscosity, drying/curing time can be tailored by tailoring plant oil-based monomer composition. The higher molecular weight of POVEs as compared to plant oil triglycerides is expected to reduce cure shrinkage, which is expected to reduce stress cracking over time compared to drying oils. Also, the results obtained by studying the POVE homo- and co-polymers as a binder for TiO₂ white pigment and ultramarine blue pigment, we can conclude that these binders provide paints with high pigment loading, low yellowness and excellent coating properties than unmodified traditional oil.

3.6. References

1. M. Doerner, *The materials of the artist and their use in painting*, Harcourt Brace Jovanovich, San Diego, CA, First edn., 1984.
2. A. W. Arie, E. Hermens, and M. Peek, *Historical Painting Techniques, Materials, and Studio Practice*, Ed. E. Hermens, M. Peek, Allen Press, Inc., Leiden, the Netherlands, 1995, 38-48.
3. F. C. Izzo, *20th Century Artist's Oil Paints: A Chemical-Physical Survey*, 2011.
4. F. N Jones, W. Maoa, P. D. Ziemer, F. Xiao, J. Hayes and M. Golden, *Progress in Organic Coatings* 2005, **52**, 9-20.

5. J. Mallégol, J. L. Gardette and J. L. Gardette, *Progress in Organic Coatings* 2000, **39**, 107–113.
6. J. Mallegol, J. L. Gardette and J. Jacques, *Journal of the American Oil Chemists' Society*, 2000, **77**, 249-255.
7. T. Learner, *Analysis of Modern Paints*, Getty publications, Los Angeles, CA, 2004.
8. P. M. Whitmore, V. G. Colaluca and E. Farrell, *Studies in Conservation*, 1996, **41**, 250-255.
9. I. Ziraldo, K. Watts, A. Luk, A. F. Lagalante and R. C. Wolbers, *Studies in Conservation*, 2016, **61**, 209-221.
10. S. D. Peer, A. Bumstock, T. Leamer, H. Khanjian, F. Hoogland and J. Boon, *Studies in Conservation*, 2004, **49**, 202-207.
11. E. Jablonski, T. Learner, J. Hayes and M. Golden, *Studies in Conservation*, 2003, **48**, 3-12.
12. K. W. Evanson and M. W. Urban, *Journal of Applied Polymer Science*, 1991, **42**, 2287-2296.
13. P. A. Lovoi and M. A. Frank, International Technical Association, 4,588,885, May 13, 1986 .
14. A. Chernykh, S. Alam. A. Jayasooriya, J. Bahr and B. J. Chisholm, *Green Chemistry*, 2013, **15**, 1834-1838.
15. H. Kalita, A. Jayasooriya. S. Fernando and B. J. Chisholm, *Journal of Palm Oil Research*, 2015, **27**, 39-56.
16. H. Kalita, S. Alam, D. Kalita, A. Chernykh, I. Tarnavchyk, J. Bahr, S. Samanta, A. Jayasooriyama, S. Fernando, S. Selvakumar, A. Popadyuk, D. S. Wickramaratne, M. Sibi,

- A. Voronov, A. Bezbaruah and B. J. Chisholm, *ACS Symposium Series*, 2014, **1178**, 731-790.
17. S. Alam and B. J. Chisholm, *Journal of Coatings Technology and Research*, 2011, **8**, 671-683.
18. S. Alam, H. Kalita, O. Kudina, A. Popadyuk, B. J. Chisholm and A. Voronov, *ACS Sustainable Chemistry & Engineering*, 2013, **1**, 19-22.
19. S. Alam, H. Kalita, A. Jayasooriya, S. Samanta, J. Bahr, A. Chernykh, M. Weisz and B. J. Chisholm, *European Journal of Lipid Science and Technology*, 2014, **116**, 2-15.
20. A. Popadyuk, H. Kalita, B. J. Chisholm and A. Voronov, *International Journal of Cosmetic Science*, 2014, **36**, 547-555.
21. D. Kalita, I. Tarnavchyk, D. Sundquist, S. Samanta, J. Bahr, O. Shafranska, M. Sibi and B. Chisholm, "Novel biobased poly(vinyl ether)s for coating applications," *INFORM*, 26, 472-475 (2015). *INFORM*, 2015, **26**, 472-475
22. H. Kalita, S. Selvakumar, A. Jayasooriyamu, S. Fernando, S. Samanta, J. Bahr, S. Alam, M. Sibi, J. Vold, C. Ulven and B. J. Chisholm, *Green Chemistry*, 2014, **16**, 1974-1986.
23. D. K. Harjoyti Kalita, Samim Alam, Andrey Chernykh, Ihor Tarnavchyk, James Bahr, Satyabrata Samanta, Anurad Jayasooriyama, Shashi Fernando, Sermadurai Selvakumar, Dona Suranga Wickramaratne, Mukund Sibi and Bret J. Chisholm, *Biobased and Environmentally Benign Coatings*, Ed. A. G. A. Tiwari, M. D. soucek, Scrivener Publishing, Beverly, MA, 2016, 1-16
24. A. Popadyuk, H. Kalita, B. J. Chisholm and A. Voronov, *International Journal of Cosmetic Science*, 2014, **36**, 537-545.

25. S. Samanta, S. Selvakumar, J. Bahr, D. S. Wickramaratne, M. Sibi and B. J. Chisholm, *ACS Sustainable Chemistry and Engineering*, 2016, **4**, 6551-6561.
26. S. Aoshima and T. Higashimura, *Macromolecules*, 1989, **22**, 1009-1013.
27. R. Ploeger and O. Chiantore, *Smithsonian Contributions to Museum Conservatio*, Torino, 2012, 89-95.
28. T. G. Fox, *Bull. Am. Phys. Soc*, 1956, 123-124.
29. L. J. Fetters, *Journal of Research of the National Bureau of Standards – A. Physics and Chemistry*, 1965, **69A**, 33-37.
30. P. J. Flory, *Principles of Polymer Chemistry*, Cornell University Press, New York, 1953.
31. Saitzyk, S., *ART HARDWARE: The Definitive Guide to Artists' Materials*. June 1987: Watson-Guptill Publications.

CHAPTER 4. NOVEL BIO-BASED COATING RESINS PRODUCED FROM CARDANOL USING CATIONIC POLYMERIZATION AND THEIR POTENTIAL FOR ALKYD TYPE COATINGS

4.1. Abstract

A novel vinyl ether monomer was synthesized from cardanol (CEVE) using Williamson ether synthesis. CEVE homopolymer and copolymers with 25 and 50 wt.% cyclohexyl vinyl ether (CHVE) were produced. Cardanol-based coatings and free films were cured at room temperature (RT), 120 °C for one hour, or 150 °C for one hour before evaluating the coatings properties after seven days. The coatings were compared to coatings from two commercially available BECKOSOL alkyds, which followed the same curing regime. Evaluation of the coatings and free films cured at RT confirmed the formation of highly crosslinked networks, having higher elastic modulus, hardness and chemical resistance than the commercial alkyds. Curing at elevated temperatures further improved coating and film properties. Curing at elevated temperature improved adhesion for CEVE-based coatings, which showed lower values at RT compared to commercial alkyds. For copolymers, as expected, incorporation of CHVE repeat units from 25 to 50 wt.%, lowered the crosslink density due to dilution of reactive groups. However, the glass transition temperature (T_g), elastic modulus and elongation of the free films increased. Incorporation of CHVE repeat units also resulted in harder coatings with shorter drying time compared to coatings produced from poly(CEVE) and commercial alkyds due to their higher T_g , making the backbone chain more rigid. These results clearly indicate the tunability of these CEVE-based polymers as surface coatings, and potential candidates for producing alkyd type air drying coatings. However, unlike conventional alkyds, which require a high temperature melt process that have issues such as gelation, high polydispersity due to formation of monomers, dimers, trimers,

etc. that effect the physical properties and film formation, CEVE based polymers demonstrate advantages such as milder and energy efficient synthesis processes and low polydispersity with well-defined composition.

4.2. Introduction

Development of new environmentally friendly chemicals from renewable resources has become one of the prime objectives for green chemistry that can successfully act as substitutes for petroleum-derived monomers, of which we have a limited resource and often hostile to the environment.¹ Advancements in synthetic methodologies and potential application has led to the design and synthesis of novel, value added materials from renewable resources such as wood , crop etc. which otherwise would have just used for fuel, land filling etc. This awareness towards the use of sustainable materials is obvious, as approximately 25% of the 88 Presidential Green Chemistry Challenge winners can be directly correlated to the advancement in monomers and polymers from sustainable materials.²

Surprisingly, each year approximately 120 billion tons of carbon is produced by photosynthesis in biomass, which is equivalent to 80 billion tons of crude oil, of which only about 5% is used by humans.³ Among this small percentage, natural oil from renewables has become important raw materials to the chemical industry, mainly due to their vast application possibilities such as surfactants, lubricants, and coatings.⁴ Major vegetable oils had an annual global mass production up to 180 million metric tons in 2017, and they are considered as the most used bio-renewable resource. However, in the last few decades, researchers are exploring other resources mainly possessing phenolic moieties as structural units for the development of thermosets. One of the reasons for this drive is that despite the emergence of several new classes of thermosets, such as epoxies and polyimides; which show better performance in some superior engineering areas,

phenolic resins as prepared from phenol and formaldehyde retain industrial and commercial interest more than a century after their introduction.⁵ Although inherited with several desirable characteristics, such as superior mechanical strength, heat resistance and dimensional stability, as well as high resistance against various solvents, drawbacks such as acute toxicity causing necrotic skin lesions, fever, hypertension, adult respiratory distress syndrome (ARDS) etc. have been found from direct exposure to phenol- formaldehyde resins.^{6, 7} Among different renewable resources, liquid from the shells of cashew nut (CNSL), which was once considered an undesirable by-product of the cashew kernel industry located mostly in southern India, has been recognized as one of the major and economical resources of naturally occurring phenols which was also found to be nontoxic when tested on white mice in accordance with the method described by Hale et al.^{5, 8, 9} Diverse use of this CNSL as insulating varnishes, typewriter rolls, oil- and acid-proof cold setting cements, industrial floor tile, and automobile brake linings started in the early 19th century, when the United States imported approximately 27,000,000 pounds in 1937.

As shown in **Figure 4.1** CNSL contains four major components with an unsaturated C15-chain, namely, cardanol, cardol, anacardic acid and 2-methylcarbolic acid. With recent advances in synthetic chemistry and easy thermal decarboxylation of anacardic acid, pure cardanol with a yield of close to 50% was recovered from double vacuum distillation of CNSL.⁵ Development of novel monomers and polymers with crosslinkable groups that can be solubilized in common solvents has been a constant effort given by researchers.¹ These polymers have shown enormous utility in various coating applications like UV-curable coatings, inks, and IPNs. Design of low energy coatings and crosslinkable adhesives require the necessity of polymers that can be solution processed and crosslinked later with improved gloss and adhesion properties.¹⁰

Ikeda et al.¹¹ has reported the synthesis of linear crosslinkable polymers from cardanol via enzyme catalysis and oxidative crosslinking.¹² Polycardanol with molecular weight (MW) ranging from 4.8 kDa to 10 kDa was synthesized using soybean oil peroxidase. Autoxidation of as synthesized polycardanol with cobalt naphthenate (3 wt.%) resulted in rapid curing after 2 h with a pencil hardness of H. On the other hand, cardanol itself resulted in much inferior films due to slow rate of curing, which clearly illustrate the advantages of forming linear polymers.¹¹

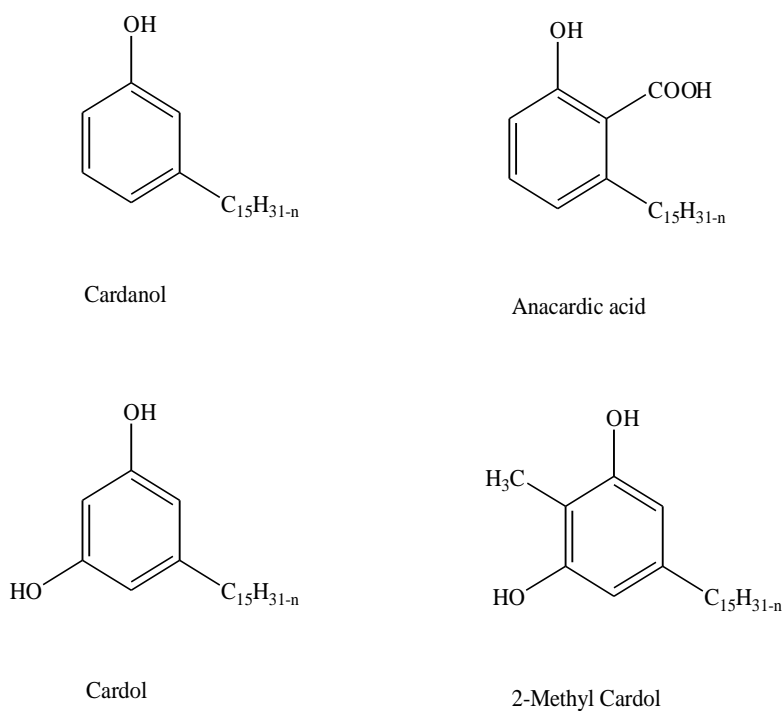


Figure 4.1. Natural compounds present in the cashew nut shell liquid anacardic acid (71.7%), cardanol (4.7%), traces of cardol (18.7%), 2-methylcardol (2.7%), and the remaining 2.2% is unidentified polymeric material.¹³ The side chain may be saturated, mono-olefinic, di-olefinic or tri-olefinic with a high percentage of the components having one or two double bonds per molecule of CNSL.⁵

In a separate work, John et al.¹⁴ reported the successful synthesis of cardanyl acrylate via base catalyzed reaction of cardanol with acryloyl chloride. However, copolymerization of cardanyl acrylate with methyl methacrylate via conventional free radical polymerization resulted in the formation of a crosslinked network rather than a linear polymer. Kattimuttathu et al.¹ overcame

this gelling issue using atom transfer radical polymerization (ATRP) and successfully synthesized linear polycardanyl acrylate and copolymer. However, one issue reported was the need of higher catalyst amount and its recovery from the product.

Alam et al.^{15, 16} reported the synthesis of vinyl ether monomers from soybean oil which was polymerized exclusively through the vinyl moiety, leaving the fatty unsaturation for further utilization in crosslinking. According to the authors, this as-synthesized polymer had a comb like structure where the fatty pendent chains were attached to the backbone, thereby increasing the functionality and exponentially decreasing the gel point. Previously, production of phenolic resins, epoxy resins, vinyl ester resins, phenalkamines, polyols¹⁷, non-isocyanate polyurethane¹⁸ using cardanol as renewable raw material has been reported. However, the synthesis of linear polymers from cardanol and their potential use in air drying coatings has not been reported.

In this chapter, the synthesis of cardanol vinyl ether (CEVE) monomer, its homopolymer, and copolymers of linear structure are reported. The ability of the cardanol to undergo autoxidation was previously reported by Krishnamoorthy et al.¹⁹ and Patel et al.²⁰, where it has been used in air drying polyurethane dispersions and antibacterial coatings. These developments have encouraged the evaluation of CEVE-based polymers as alkyd type coatings. Further investigation into the effect of incorporation of cyclohexyl vinyl ether (CHVE) on the properties of the cured coatings and films was conducted. Two commercial soy-based alkyds were used as a reference, since the overall goal is to use these as-synthesized polymers for surface coatings.

4.3. Materials and methods

4.3.1. Materials

The materials used for the study are described in **Table 4.1**. Unless specified otherwise, all materials were used as received.

Table 4.1. A description of the starting materials used for the study.

Chemical	Designation	Vendor
Cardolite LITE 2020	Cardanol	Cardolite Corporation, USA
2-Chloroethyl vinyl ether, >97%	2-Chloroethyl vinyl ether	TCI Chemicals
BECKOSOL® 1272	BECKOSOL® 1272	REICHHOLD
BECKOSOL® 10-539	BECKOSOL® 10-539	REICHHOLD
Potassium hydroxide, reagent grade, 90%, flakes	KOH	Sigma-Aldrich
Magnesium sulfate, anhydrous, ReagentPlus®, >99%	MgSO ₄	Alfa Aesar
Cyclohexyl vinyl ether	CHVE	BASF
Sodium hydroxide	NaOH	AMRESCO, LLC
Ethylaluminumsesquichloride, 97%	Et ₃ Al ₂ Cl ₃	Sigma-Aldrich
Methanol, 98%	Methanol	BDH Chemicals
Toluene	Toluene	BDH Chemicals
<i>n</i> -Hexane, 99%	<i>n</i> -Hexane	BDH Chemicals
Tetrahydrofuran, 99.0%	THF	J. T. Baker
Methyl ethyl ketone, 99%	MEK	Alfa Aesar
Cobalt 2-ethylhexanoate, 12% Cobalt	Cobalt octoate	OMG Americas
Zirconium 2-ethylhexanoate, 18% Zirconium	Zirconium octoate	OMG Americas
Zinc carboxylate in mineral spirits, 8%	Nuxtra® Zinc	OMG Americas

4.3.2. Synthesis of monomer

As illustrated in **Figure 4.2** novel vinyl ether monomer from cardanol (CEVE) was synthesized via Williamson ether synthesis, reacting cardanol with 2-chloroethyl vinyl ether in the presence of base catalyst. In a 2-neck 1L round bottom flask (rbf), 50 g of cardanol, 22 g of sodium hydroxide, and 300 mL of N,N-dimethylformamide were added. Nitrogen was bubbled for 10 minutes into the reaction mixture while stirring the reaction mixture using a magnetic stirrer bar. To the reaction mixture 24 g of 2-chloroethyl vinyl ether was added to under nitrogen. The reaction mixture was then heated to 80 °C using an oil bath and kept for 16 h, while stirring under a nitrogen blanket. After completion, the reaction mixture was cooled to room temperature and diluted with 250 mL of *n*-hexane. The mixture was washed two times with 200 mL DI water, two times with

100 mL of 2N hydrochloric acid (pH ~4.5) solution in DI water, and then one time with brine solution (200 mL). The hexane layer was dried over anhydrous MgSO_4 before being filtered. The filtered solution was then passed through a silica column. The product was isolated by removing the volatiles using a rotary evaporator under vacuum (5–7 mm of Hg) at 30 °C overnight. CEVE was characterized using proton nuclear magnetic resonance spectroscopy (^1H NMR), Fourier transform infrared spectroscopy (FTIR), and gel permeation chromatography (GPC).

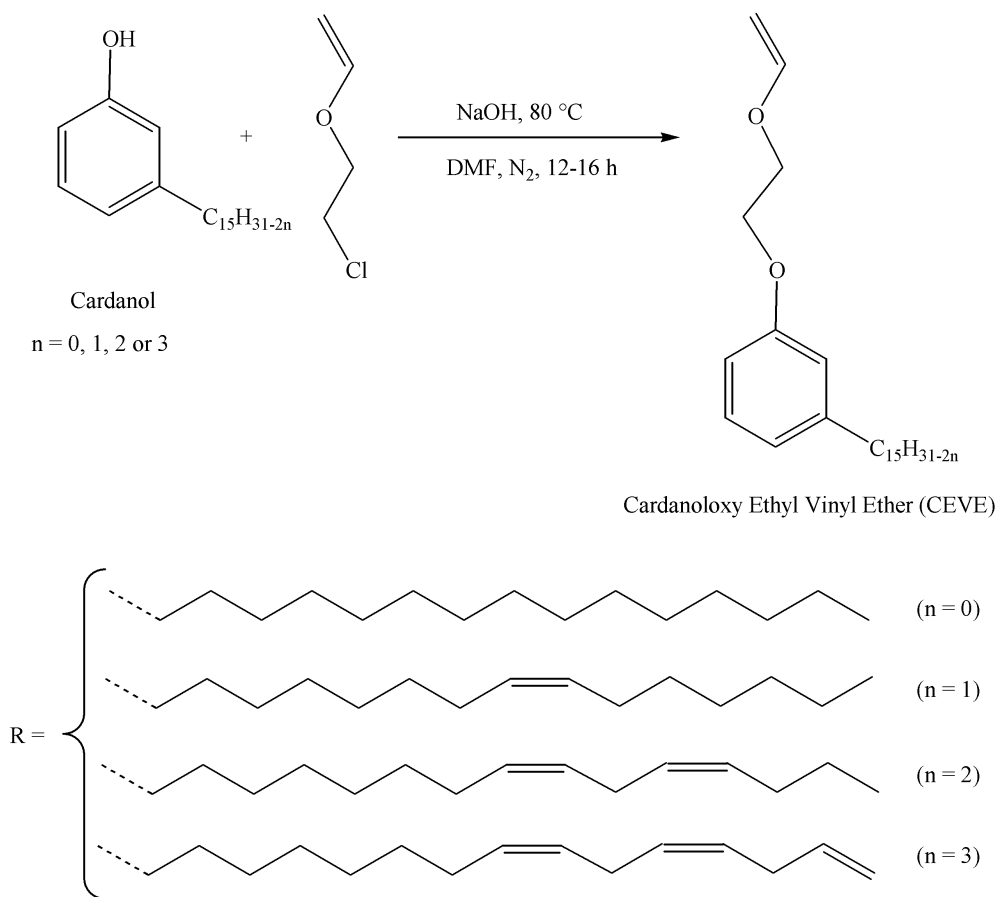


Figure 4.2. Schematic illustrating the synthesis of CEVE.

4.3.3. Synthesis of polymers

4.3.3.1. Synthesis of CEVE homopolymer

Poly(CEVE) was synthesized via carbocationic polymerization as shown in **Figure 4.3**. Initially, all glassware was dried at 200 °C for 2 h and then cooled by purging with N_2 to avoid

moisture condensation. Glassware was then immediately transferred inside the glove box with a custom built cold bath, where polymerizations were carried out. Toluene was distilled over calcium hydride and CEVE was dried with anhydrous magnesium sulfate prior to use. The cationogen, 1-isobutoxyethyl acetate (IBEA), was prepared using the procedure reported by Aoshima and Higashimura.²¹ In a 500 mL, 2-neck rbf, 30 g of dry CEVE and 59 mg of IBEA were dissolved in 100 mL of dry toluene and chilled to 0 °C using a heptane cold bath. Reaction mixture was continuously stirred with an overhead mechanical stirrer at 350 rpm. In a 100 mL closed glass container, 1.95 mL of coinitiator, Et₃Al₂Cl₃ (25 wt.% in toluene) was added to 50 mL of dry toluene and chilled to 0 °C. After 30 minutes of cooling, the polymerization was initiated by the addition of the co-initiator to the reaction mixture. The reaction was terminated after 2 h by the addition of 50 mL of chilled methanol. Polymer was precipitated by pouring the reaction mixture into 200 mL of methanol in a 500 mL glass bottle while stirring as to avoid entrapment of unreacted monomer by the polymer due to sudden precipitation. The copolymer was isolated and washed with methanol three times by re-dissolving in toluene. 100 mL of additional toluene was then added to dissolve the polymer. The trace methanol was collected after drying under vacuum (50–60 mm of Hg) at 30 °C for 3 hours. Homopolymer was characterized using ¹H NMR, FTIR and GPC.

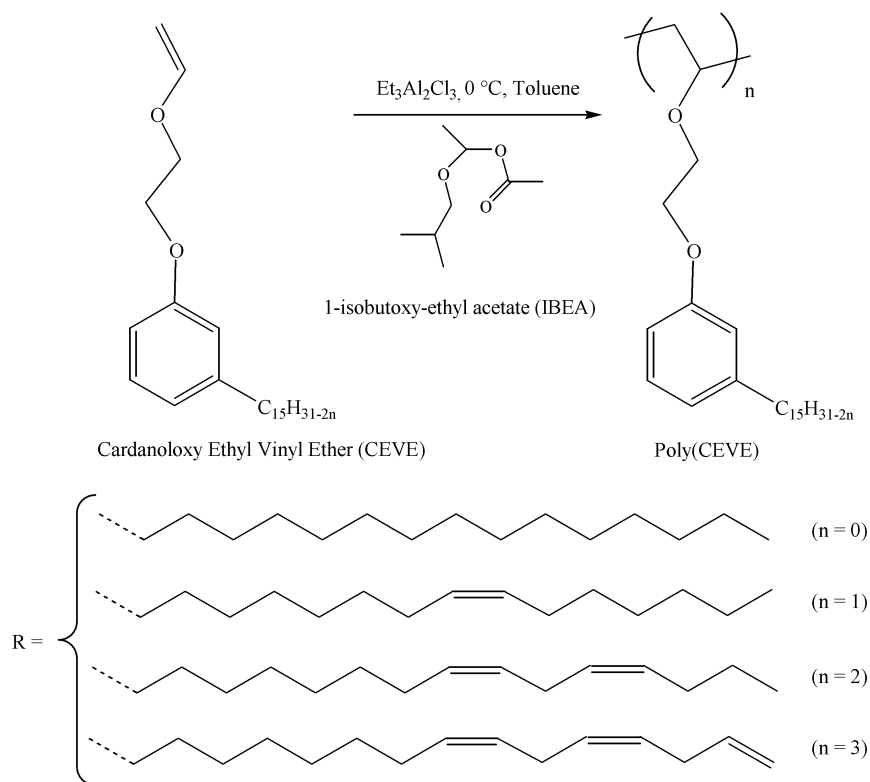


Figure 4.3. Schematic illustrating the synthesis of poly(CEVE).

4.3.3.2. Synthesis of CHVE homopolymer

Poly(CHVE) was synthesized on a smaller scale and the schematic is shown in **Figure 4.4**. CHVE was distilled over calcium hydride prior to the reaction to remove the stabilizer and residual moisture. Glassware was dried at 200 °C and cooled under N₂. In a 100 mL glass jar, 10 g of dry CHVE and 64 mg of IBEA were dissolved in 25 mL of dry toluene and chilled to 0 °C using custom made cooling blocks connected to a chiller with the cooling range up to - 20 °C. Reaction mixture was stirred with magnetic stirrer bar at 500 rpm by placing the cooling block on a magnetic stir plate inside the glove box operated under N₂. In a 40 mL vial, 2.25 mL of co-initiator, Et₃Al₂Cl₃ (25 wt.% in toluene) was added to 25 mL of dry toluene and chilled to 0 °C. After 60 minutes, the polymerization was initiated by the addition of the co-initiator to the reaction mixture with a transfer pipette. The reaction was terminated after 2 h by the addition of 10 mL of chilled methanol.

Polymer was precipitated and purified by pouring the reaction mixture to another 100 mL of methanol in a 250 mL glass bottle while stirring, and then washed with methanol three times by re-dissolving in toluene. Precipitated polymer was finally dissolved in 100 mL toluene and trace methanol was removed under vacuum (50-60 mm of Hg) at RT overnight. Homopolymer was characterized using ^1H NMR, FTIR and GPC.

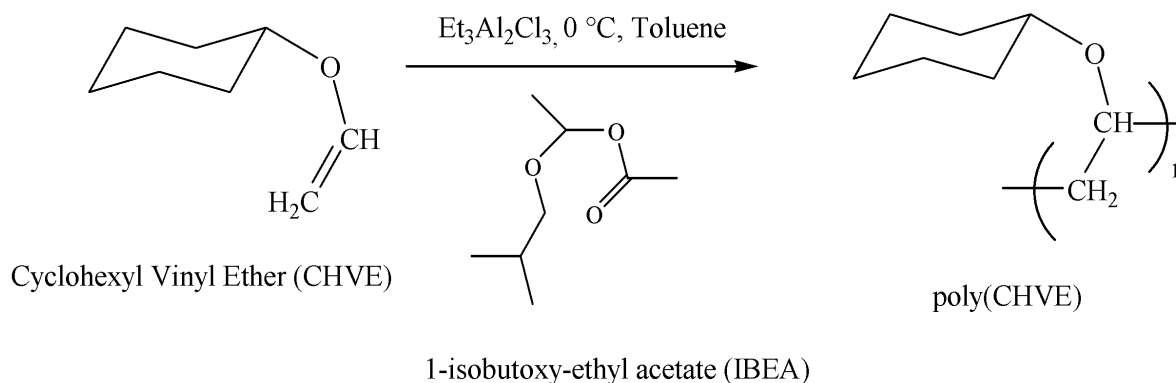


Figure 4.4. Schematic illustrating synthesis of poly(CHVE).

4.3.3.3. Synthesis of copolymer

As shown in **Figure 4.5** poly(CEVE-co-CHVE) was synthesized from CEVE and CHVE monomers using carbocationic polymerization with similar conditions for homopolymer synthesis. To investigate the effect of concentration of CHVE repeat units on the final coating properties, two different copolymers with 25 and 50 wt.% CHVE repeat units were synthesized. The compositions of the reaction mixtures are reported in **Table 4.2**. Copolymers were characterized using ^1H NMR, FTIR and GPC.

Table 4.2. Composition of the polymerization mixtures used to produce poly(CEVE-co-CHVE) copolymers.

Sample ID	CEVE, g	CHVE, g	IBEA, mg	Et ₃ Al ₂ Cl ₃ (25 wt.% in toluene), mL	Toluene, mL
poly(CEVE-co-CHVE)-75/25	30	10	122	4.34	300
poly(CEVE-co-CHVE)-50/50	20	20	195	5.55	300

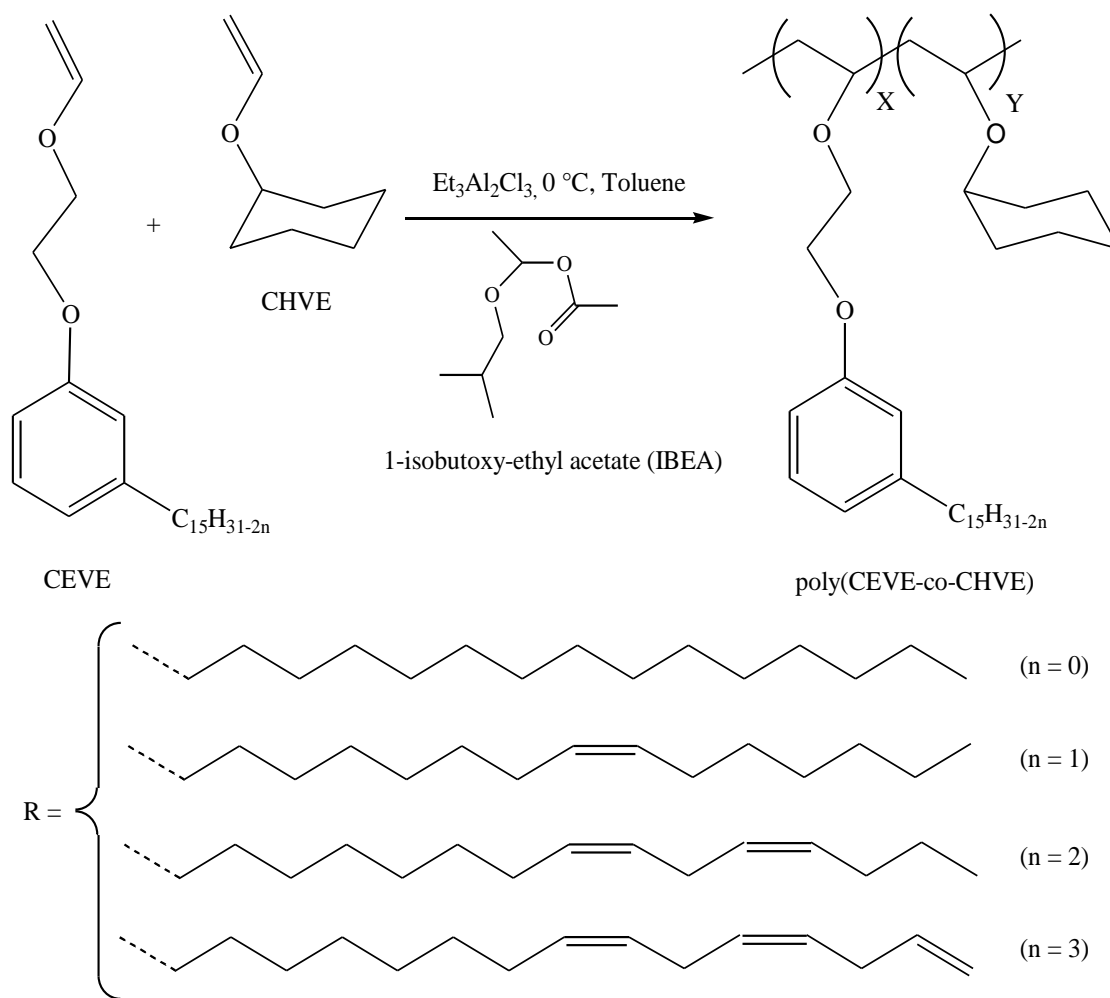


Figure 4.5. Schematic illustrating the synthesis of poly(CEVE-co-CHVE).

4.3.4. Commercial soy based alkyds for coating performance comparison

Polymers synthesized in this study are linear in nature with a carbon-carbon backbone chain ($-\text{[CH-CH}_2\text{]}_n-$) having pendent side chains consisting of C15 alkyl chain in meta position of the aromatic group. These alkyl chains consist of unsaturation similar to that present in fatty acids of triglycerides. In order to evaluate the feasibility of the coatings derived from these polymers as real-world air-drying coatings, two different commercial soy-based long oil alkyds, BECKOSOL1272 and BECKOSOL10-539 were chosen for comparison. Description of these alkyd resins are shown in **Table 4.3**.

Table 4.3. Descriptions of the BECKOSOL 1272 and BECKOSOL 10-539 as specified in the data sheet.

Sample ID	Description
BECKOSOL1272	100% solids, long oil soya alkyd
BECKOSOL10-539	High-solids (88-92%), long-oil alkyd in xylene/mineral spirit

4.3.5. Preparation of cured free films and coatings

Coatings and free films of poly(CEVE), two poly(CEVE-co-CHVE) copolymers and commercial alkyds were prepared by curing via autoxidation. To prepare coating formulations, 10 g of neat polymer was mixed with 8 mg of cobalt octoate, 40 mg of zirconium octoate, and 450 mg of Nuxtra® Zinc. using a FlackTek mixer operating at 3500 rpm for 30 seconds. Prior to making the formulations, BECKOSOL 10-539 and BECKOSOL 10-060 were dried using GeneVac EZ-2 plus centrifugal evaporator. All three commercial alkyds with 100 % solid content were mixed with drier package using a FlackTek mixer operating at 3500 rpm for 2 min. For the synthesized polymers 70% solid content solutions were prepared with toluene to which drier package was added and mixed using a FlackTek mixer operating at 3500 rpm for 30 sec. Liquid coating solutions were cast to steel-Q panels (0.2 x 3 x 6”, SAE1008 cold rolled steel panels pretreated with iron phosphate (Bonderite 1000) and Teflon®-laminated glass panels (0.5 x 4 x 8”), using a drawdown bar with 4 mil gap for commercial alkyds, and 6 mil gap for cardanol-based polymers to ensure similar dry film thickness for better comparison. Three different temperatures: room temperature (identified by using “RT” in the sample designation), 1 h at 120 °C, and 1 h at 150 °C (identified by using “120 °C” and “150 °C” in the sample designation respectively) were employed to cure five steel coated and one Teflon coated glass panels for each temperature, from each formulation. These panels were then kept at room temperature for one week in a well-

ventilated cabinet before testing. Coating on the Teflon®-laminated glass panel provided free film samples to be used for the characterization of mechanical and viscoelastic properties.

4.3.6. Methods and instrumentation

4.3.6.1. Nuclear magnetic resonance (NMR) spectroscopy

Proton nuclear magnetic resonance (^1H NMR) spectra were obtained using a 400 MHz Bruker 400 NMR spectrometer. Data acquisition was accomplished using 16 scans and CDCl_3 was used as the lock solvent.

4.3.6.2. Fourier transform resonance (FTIR) spectroscopy

Fourier transform infrared (FTIR) spectra were obtained with a Nicolet 8700 FTIR spectrometer operated with OMNIC software. Thin polymer films were solution cast onto a KBr disc, subsequently dried, and then scanned from $500\text{-}4000\text{ cm}^{-1}$ using 64 scans and 1.93 cm^{-1} data spacing.

4.3.6.3. Gel permeation chromatography (GPC)

MW and polydispersity index (PDI) of the polymers produced were characterized using gel permeation chromatography (GPC). For synthesized polymers an EcoSEC HLC-8320 GPC, Tosoh Bioscience, Japan with a differential refractometer (DRI) detector with Tetrahydrofuran (THF) as eluent at a flow rate of 0.35 mL min^{-1} was used. Samples were prepared at nominally 1 mg/mL in an aliquot of the eluent and allowed to dissolve at ambient temperature for several hours. The injection volume was $20\text{ }\mu\text{L}$ for each sample. Calibration was conducted using polystyrene standards (Agilent EasiVial PS-H 4ml). For commercial alkyds, Symyx Rapid-GPC with an evaporative light scattering detector (PL-ELS 1000) was used. Samples were prepared in THF at a concentration of 1 mg/mL . The molecular weight data were expressed relative to polystyrene standards.

4.3.6.4. Dynamic viscosity

Polymer viscosities were determined using an ARES Rheometer from TA Instruments. Samples were placed between two parallel plates with a 0.5 mm gap. Viscosity was measured by varying the shear rate from 1 to 100/min and the data at 10/min reported.

4.3.6.5. Dynamical mechanical analysis (DMA)

The viscoelastic properties of crosslinked free films were characterized using dynamic mechanical analysis (DMA) utilizing a Q800 dynamic mechanical thermal analyzer from TA Instruments in tension mode. For each cured system, specimens of 20 mm in length, 5 mm wide, and 0.08 to 0.10 mm thick were cut from free films. Temperature was ramped from -80 °C to 150 °C, except for samples from two poly(CEVE-co-CHVE) copolymers, where the ramp was from -50 to 150 °C at a heating rate of 5 °C/min. The frequency and strain rate were 1 Hz and 0.1%, respectively. T_g was reported as the peak maximum of the $\tan \delta$ response.

4.3.6.6. Differential scanning calorimetry (DSC)

Except for poly(CEVE), DSC experiments were performed using a Q1000 Modulated Differential Scanning Calorimeter from TA Instruments with a cooling limit of -90 °C. For poly(CEVE), a Q2000 Modulated Differential Scanning Calorimeter was used with a cooling limit of -200 °C. Helium (25 mL/min) was used as the purging gas. 7-10 mg samples were thoroughly dried prior to the measurement. For poly(CEVE), sample was first equilibrated at 23 °C and then the following heating and cooling regime used was used: cooled from 23 °C to -120 °C at 10 °C/minute (1st cooling cycle); held at -125 °C for 2 minutes; heated to 50 °C at 10 °C/minute (1st heating cycle); held at 50 °C for 2 minutes; cooled to -125 °C at 10 °C/minute (2nd cooling cycle); held at -125 °C for 2 minutes; heated to 120 °C at 20 °C/minute (2nd heating cycle). Similar method

was used for poly(CHVE), two poly(CEVE-co-CHVE) copolymers, and commercial alkyds, except confining the heating and cooling range from 90 °C to -90 °C.

4.3.6.7. Tensile testing

Dog bone shaped specimens were prepared (ASTM D638, Type V) from the films cured on Teflon® coated glass panels. An Instron 5545 tensile tester with 100 N load cell was used to carry out the tensile testing using a 1 mm/min displacement rate of the movable clamp. Five replicates were performed and the average and standard deviation are reported.

4.3.6.8. Swelling ratio

Swelling study of the crosslinked films were carried out according to ASTM D 3616. Samples were allowed to swell in toluene for 20 h before taking the mass of the swollen gel. Mettler Toledo precision balance was used for weight measurements. The values are reported in percent swelling ratio.

4.3.6.9. Drying time measurement

Drying times of homopolymers with varying molecular weights were recorded according to D1640/D1640M-14 (Method A).

4.3.6.10. Coating property measurement

Chemical resistance was performed with a modified version of ASTM D5402 in which double rubs were performed with a 2-lb ball peen hammer. The cotton cloth was fastened to the ball end of the hammer with a wire, which was dipped in methyl ethyl ketone (MEK) solvent every 25 rubs. Hardness was determined using König pendulum hardness test described in ASTM D4366-16. Impact resistance of the steel coated panels were performed according to ASTM D2794-93. The uncoated side of the panel received the impact (i.e. reverse impact). Flexibility was characterized using the conical mandrel bend test as described in ASTM D522.

4.4. Results and discussion

4.4.1. Synthesis and characterization of monomer and polymer

As illustrated in **Figure 4.2**, CEVE was synthesized via Williamson ether synthesis between cardanol and 2-chloroethyl vinyl ether. ^1H NMR spectra of the cardanol starting material, CEVE and poly(CEVE) homopolymer are shown in **Figure 4.6**. As shown in **Figure 4.6** the ^1H NMR spectrum of CEVE which showed resemblance to cardanol (starting material), except with four new signals assigned as “C” (δ 6.58-6.51, q, 1H, $\text{CH}_2=\text{CH-O-}$), “G” (4.26 and 4.07, dd, 1H, $\text{CH}_2=\text{CH-O-}$), “H” (4.24-4.18, q, 2H, $=\text{CH-O-CH}_2-$), and “I” (4.06-4.01, q, 2H, $-\text{CH}_2\text{-O-Ar}$) attributed from the ‘ethyl vinyl ether’ functionality along with the disappearance of the Ar-OH signal at δ 6.58 from cardanol. This confirmed the formation of CEVE monomer. Synthesis of poly(CEVE) via cationic polymerization is illustrated in **Figure 4.3**. ^1H NMR spectrum of poly(CEVE) shown in **Figure 4.6** confirms the disappearance of the “C” and “G” signals previously assigned to the vinyl protons of CEVE and the appearance of two broad signals assigned as “C” (3.8, m, 5H, $-\text{[CH}_2\text{-CH]}_n-$), and “G” (2.18, m, $-\text{[CH}_2\text{-CH]}_n-$), with downfield shift, confirming the incorporation of the vinyl group in the polymer backbone chain. Retention of the “E”, “J” and “L” signals clearly indicate that the polymerization went exclusively through vinyl double bond. Poly(CHVE) was synthesized from commercially available CHVE, and the reaction scheme is shown in **Figure 4.4**. ^1H NMR spectrum of poly(CHVE) is shown in **Figure 4.7**, where the signals “B” and “D” along with the signals from aromatic ring protons confirms the synthesis of poly(CHVE).

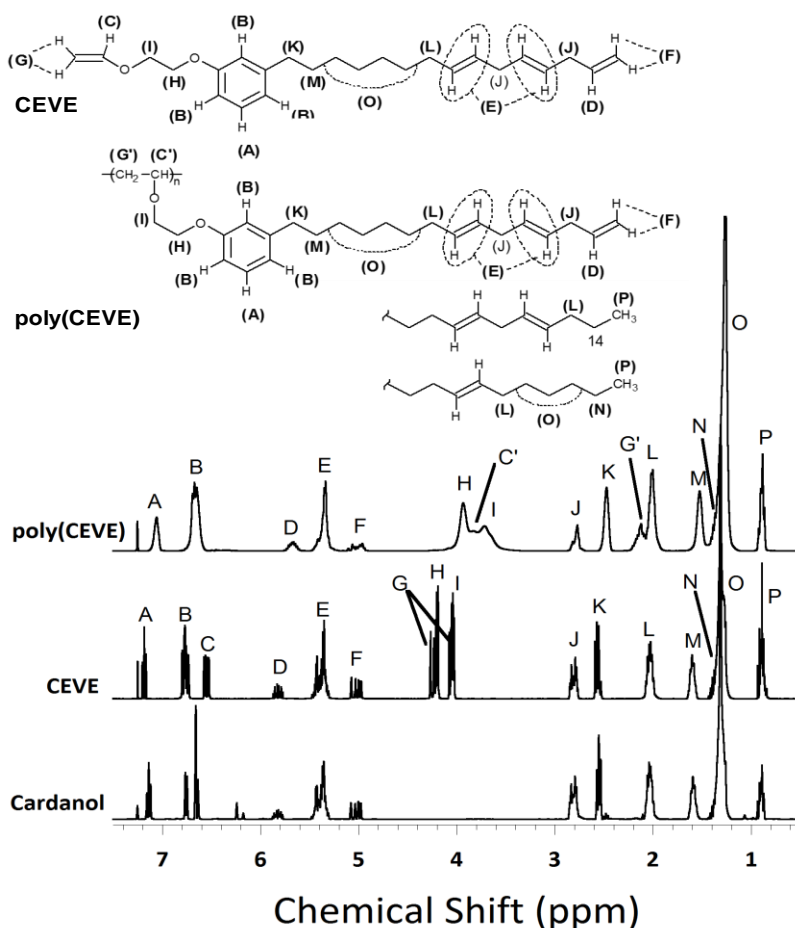


Figure 4.6. ^1H NMR spectrum of the cardanol, CEVE and poly(CEVE).

Copolymers with 25 and 50 wt.% nominal CHVE repeat unit incorporation using cationic polymerization were synthesized and the reaction scheme is shown in **Figure 4.5**. In **Figure 4.8** an ^1H NMR spectra of poly(CEVE-co-CHVE)-50/50 copolymer along with poly(CHVE) and poly(CEVE) are shown. The presence of all the signals associated with poly(CHVE) and poly(CEVE) confirms the formation of copolymers. Concentration of the incorporated CEVE and CHVE repeat units were calculated by integrating the nicely isolated signal at δ 6.68 designated as “B” from the CEVE alkyl chain and the peak at δ 3.31 designated as “S” signals from CHVE. Using these integration values, final composition of the poly(CEVE-co-CHVE)-75/25 and poly(CEVE-co-CHVE)-50/50 copolymers were found to be 69/31 and 48/52 wt.%, respectively.

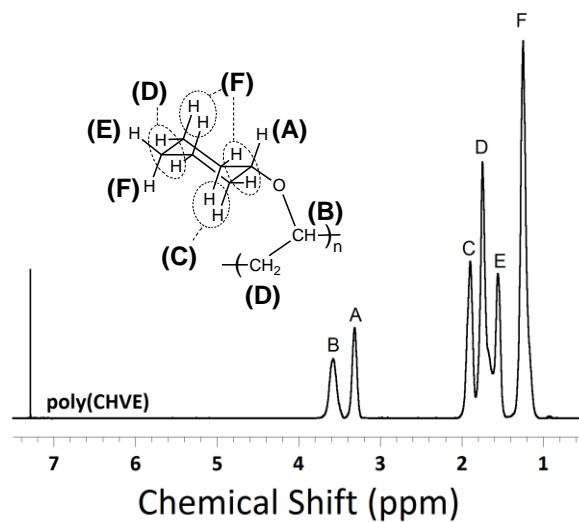


Figure 4.7. ¹H NMR spectrum of the poly(CHVE).

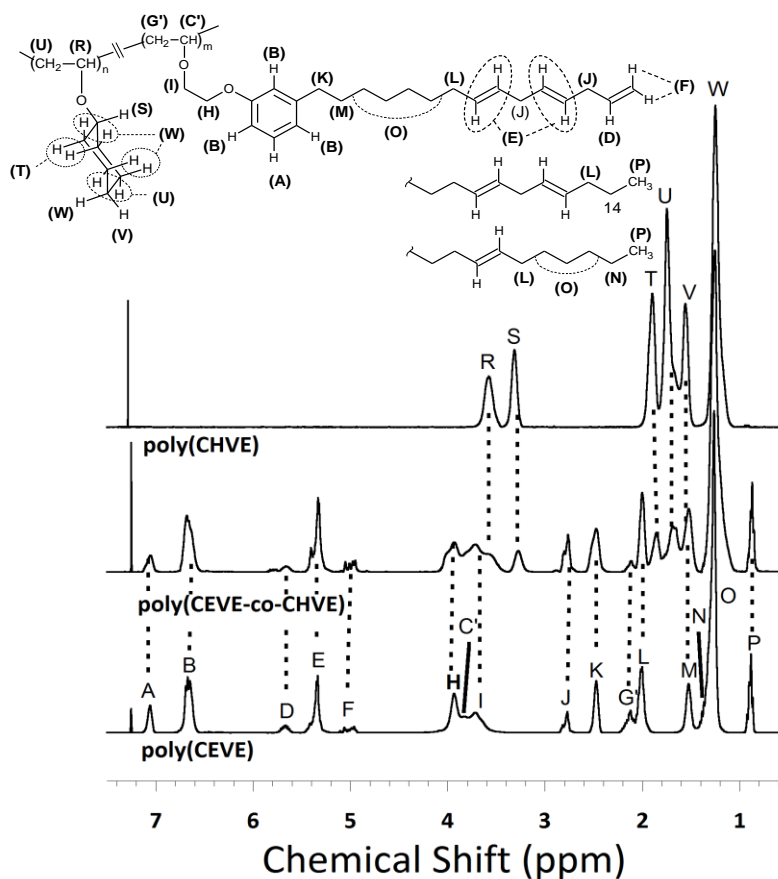


Figure 4.8. ¹H NMR spectrum of the characteristic poly(CEVE-co-CHVE) i.e. poly(CEVE-co-CHVE)-75/25 along with poly(CHVE) and poly(CHVE).

Normalized FTIR spectra of cardanol starting material, CEVE monomer, poly(CEVE) homopolymer and characteristic spectrum of poly(CEVE-co-CHVE) copolymer are shown in **Figure 4.9**. The successful synthesis of CEVE is confirmed by the absence of the broad peak at 3330 cm^{-1} , corresponding to the Ar-O-H functionality. Additionally, the appearance of medium, broad peak at 1615 cm^{-1} and a sharp peak at 1218 cm^{-1} corresponds to the incorporation of the vinyl group. Retention of the small intensity peak at 3077 cm^{-1} corresponding to Ar-C-H stretching along with two other peaks at 1615 and 1218 cm^{-1} , associated with aliphatic C=C unsaturation, has been observed from monomer to co-polymer. For poly(CEVE), disappearance of the peaks associated with the vinyl group and the data obtained from NMR study confirmed the fact that polymerization went exclusively through the vinyl group with the complete retention of the alkyl chain unsaturation. An increase in relative intensity of the sp^3 C-H bands at 2925 and 2850 cm^{-1} has been observed, demonstrating the incorporation of CHVE repeat units.

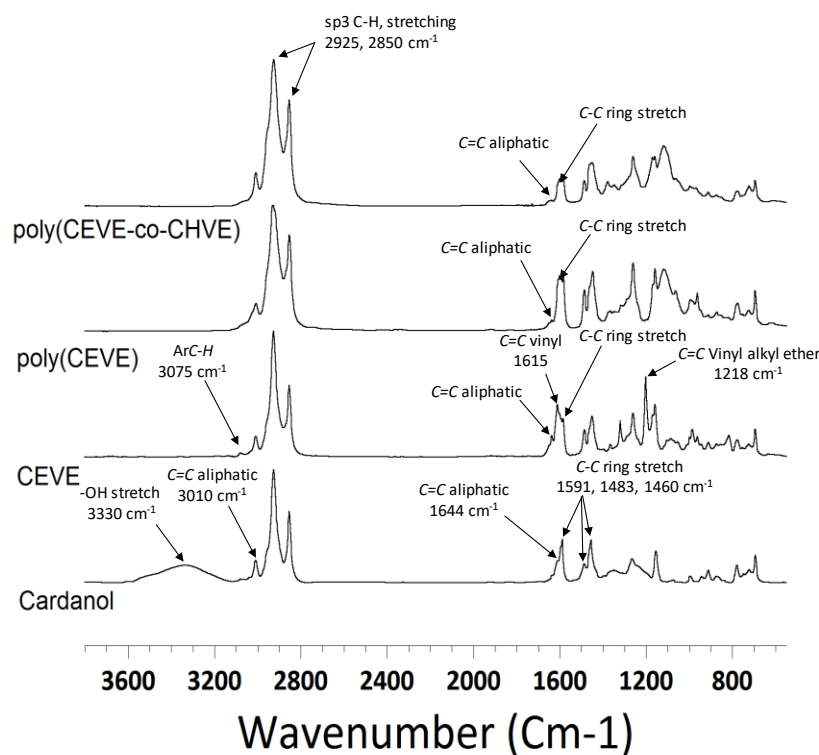


Figure 4.9. FTIR spectrums of cardanol, CEVE, poly(CEVE) and poly(CEVE-co-CHVE)-75/25.

Gel permeation chromatograms of the synthesized polymers and commercial alkyds are shown in **Figure 4.10**. The number-average molecular weight (M_n) and polydispersity index (PDI) of the synthesized polymers and commercial alkyds as expressed relative to polystyrene standards, are reported in **Table 4.4**.

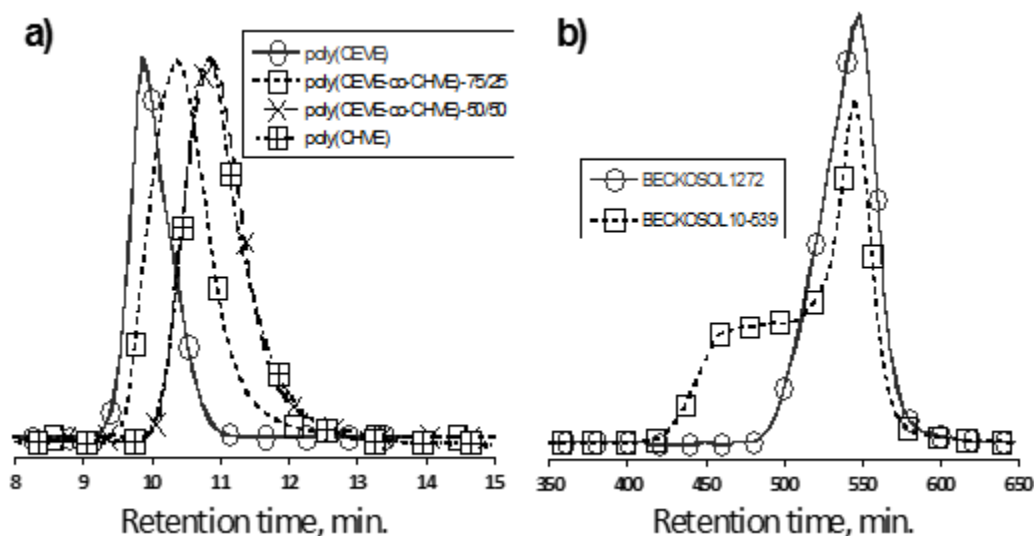


Figure 4.10. GPC chromatograms for (a) poly(CEVE), poly(CHVE) and poly(CEVE-co-CHVE) co-polymers and (b) BECKOSOL 1272, BECKOSOL10-539.

Table 4.4. M_n and PDI of the synthesized polymers and commercial alkyd resins measured using GPC.

Polymer ID	M_n (Da or g/mole)	PDI
poly(CEVE)	40,948	1.05
poly (CEVE-co-CHVE)-75/25	26,370	1.13
poly (CEVE-co-CHVE)-50/50	18,519	1.14
poly(CHVE)	19,786	1.25
BECKOSOL10-539	2,587 and 21,000	1.71 and 1.05
BECKOSOL1772	2,458	1.72

As shown in **Figure 4.10 (a)**, GPC chromatograms of as-synthesized homopolymers and copolymers were monomodal in nature with narrow distribution ($PDI < 1.2$). As reported in **Table 4.4** among the CEVE based polymers, poly(CEVE) showed the formation of polymer chains with very low PDI and highest M_n . For the copolymers, incorporation of CHVE repeat units resulted

in reducing the molecular weight while increasing the distribution of polymer chains. This observed trend can be justified by considering the fact that poly(CHVE) had molecular weight ~2 times lower than poly(CEVE) and medium distribution of polymer chains with PDI > 1.2. In case of commercial alkyds [Figure 4.10 (b)], BECKOSOL 1272 resulted monomodal chromatogram however, with high PDI of 1.72. This high polydispersity along with low molecular weight of ~2.45 kDa indicated that the chains were oligomeric in nature. Chromatogram from BECKOSOL 10-539 showed broad molecular weight distribution with main peak associated polymer chains having Mn ~2.58 kDa with a shoulder depicting the long chain polymers Mn ~21 kDa along with oligomers.

4.4.2. Thermal properties of polymers

Thermal properties of the homopolymers, copolymers and commercial alkyd resins were obtained using differential scanning calorimetry. As shown in Figure 4.11 (a), DSC thermogram of poly(CEVE) confirms the presence of a low T_g , around -76 °C, with a very weak and broad melting temperature at -26 °C. These findings agree with the previous work, where the T_g at approximately -98 °C was also observed for 2-vinyloxy ethyl soyate homopolymer.¹² This higher T_g for poly(CEVE) compared to poly(2-VOES) might be due to the presence of aromatic rings in the pendent chain resulting in some rigidity to the polymer chain, unlike the fatty ester pendent chains in poly(2-VOES). The observed weak melting endotherm was due to the presence of the long alkyl chains that can crystallize to some extent during cooling. As shown in Figure 4.11 (b), a much higher T_g of around 46 °C had been observed for poly(CHVE) without observing any melting endotherm. In case of poly(CHVE), the mobility of the polymer chains is much more restricted due to the presence of the cyclohexyl moiety directly linked to the backbone without any ethyl spacer. Absence of melting endotherm in poly(CHVE) augments the justification about the

side chain crystallization in case of poly(CEVE). Thermograms plotted in **Figure 4.11 (b)** for copolymers resulted in T_g s around $-50\text{ }^\circ\text{C}$ and $-30\text{ }^\circ\text{C}$ for poly(CEVE-co-CHVE)-75/25 and poly(CEVE-co-CHVE)-50/50, respectively, clearly indicating a positive effect of CHVE repeat units regarding increase in T_g compared to poly(CEVE). However, according to the Fox equation²², and assuming that the copolymers are statistical in nature, then the T_g s of the copolymers should have been $-55\text{ }^\circ\text{C}$ and $-30\text{ }^\circ\text{C}$ for poly(CEVE-co-CHVE)-75/25 and poly(CEVE-co-CHVE)-50/50, respectively. This slightly higher observed T_g for poly(CEVE-co-CHVE)-75/25 can be explained by considering the actual composition of the monomers poly(CEVE-co-CHVE)-69/31 corresponding to a T_g about $-49.6\text{ }^\circ\text{C}$ from the Fox equation. Unlike the homopolymer, both poly(CEVE-co-CHVE)-75/25 and poly(CEVE-co-CHVE)-50/50 were unable to show an endotherm corresponding to the side chain crystallization. Similar behavior of the side chain crystallinity had been observed in the previous work done by Alam et al.¹⁶ and Kalita et al.²² which can be explained using the melting point depression theory of copolymers by Flory.²³ Incorporation of CHVE repeat units in poly(CEVE) homopolymer reduces the uniformity of the backbone chain and acts as an impurity at the crystal growth front of CEVE pendent chains as they are not isomorphic. Also, unlike polymers with fatty acid pendent chains, where the presence of cis-double bonds affects the crystallization, CEVE-based polymers have an alkyl chain at the meta position of the aromatic ring along with unsaturation similar to fatty chains, making the spatial arrangements even more unfavorable for crystallization. Unlike the homopolymer, where polymer segments associated with relaxation has the same chemical composition, incorporation of CHVE repeat units also results in a broad distribution in the chemical composition of the polymer chains. This means a broad distribution of relaxation associated with these compositionally varying segments. This makes the relaxation not only broadening, but also difficult to perceive within the

same experimental conditions as applied to homopolymers. This might be the explanation for not observing a narrow and prominent T_g for poly(CEVE-co-CHVE)-50/50. DSC thermograms for commercial alkyds are shown in **Figure 4.11 (c)**. Transitions similar to poly(CEVE) were observed for BECKOSOL1272, which has a lower T_g at -44 °C and a sharp melting endotherm at -18 °C. However, for BECKOSOL10-539, the T_g was observed at approximately -19 °C without a melting endotherm. This observed behavior can be explained to a significant extent by considering the gel permeation chromatographs shown in **Figure 4.10 (b)**. In the case of BECKOSOL1272, T_g at lower temperatures within a narrow temperature range has been observed, due to the presence of short and narrowly dispersed polymer chains. On the other hand, BECKOSOL10-539 is highly polydispersed, resulting in a broad range of relaxations attained by varying chain segments. The higher T_g than BECKOSOL 10-539 corresponds to the fact that larger portions of the polymer chains are associated with much higher M_n , as reported in **Table 4.4**.

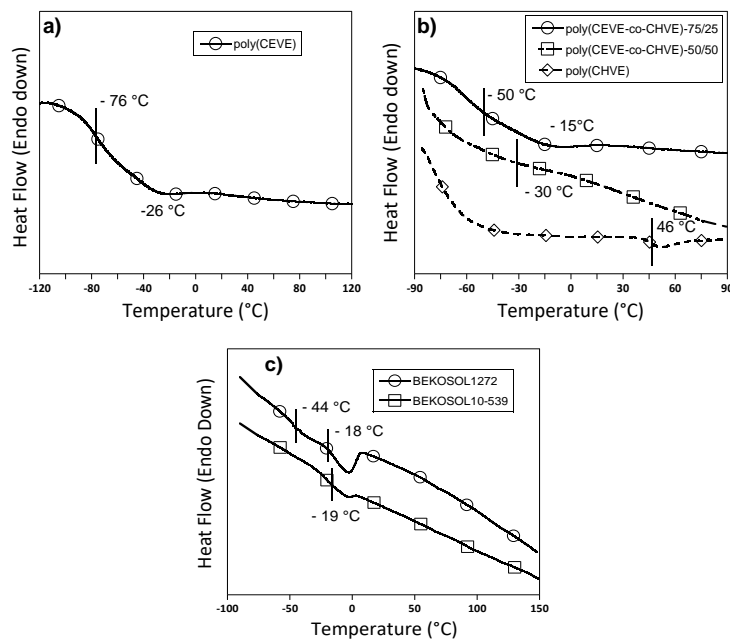


Figure 4.11. DSC thermograms for (a) poly(CEVE); (b) poly(CHVE), poly(CEVE-co-CHVE)-75/25 and poly(CEVE-co-CHVE)-50/50; (c) BECKOSOL 1272 and BECKOSOL10-539.

4.4.3. Drying time measurement

As reported in **Table 4.5**, the synthesized polymers showed significantly shorter drying times such as set to touch, dust free and dry to touch compared to the commercial alkyds. BECKOSOL1272, being oligomeric in nature, showed the highest tack free time near 2500 min (i.e. >40 h). Set-to-touch time for synthesized polymers decreased from 80 to 10 min with the incorporation of 50 wt. % CHVE repeat units to poly(CEVE), but the tack free time increased from 210 to 315 min. Incorporation of CHVE repeat units increases the T_g of the co-polymer (**Figure 4.11**) resulting in a harder, glassy surface thereby reducing the dry time set-to-touch, which depends on surface rather than bulk material properties. Incorporation of CHVE repeat units reduces the bulk curing compared to poly(CEVE) within the same curing time, resulting in longer dry to touch time.

Table 4.5. Drying time measurement data for polymers with drying catalyst.

Polymer	Set to touch time (min)	Dust free time (min)	Dry to touch time (min)
poly(CEVE)	80	140	210
poly(CEVE-co-CHVE)-75-25	22	85	275
poly(CEVE-co-CHVE)-50-50	10	26	315
BECKOSOL 1272	1740	2052	2532
BECKOSOL 10-539	412	652	832

4.4.4. Viscoelastic properties of crosslinked free-films

The viscoelastic properties of the crosslinked networks produced from poly(CEVE), copolymers, and the commercial alkyd resins were evaluated using DMA. The storage moduli plots of the cured films are shown in **Figure 4.12 (a-e)** and tangent δ responses are shown in **Figure 4.13 (a-e)** represents the, illustrating the effect of cure conditions and CHVE repeat unit content on viscoelastic responses.

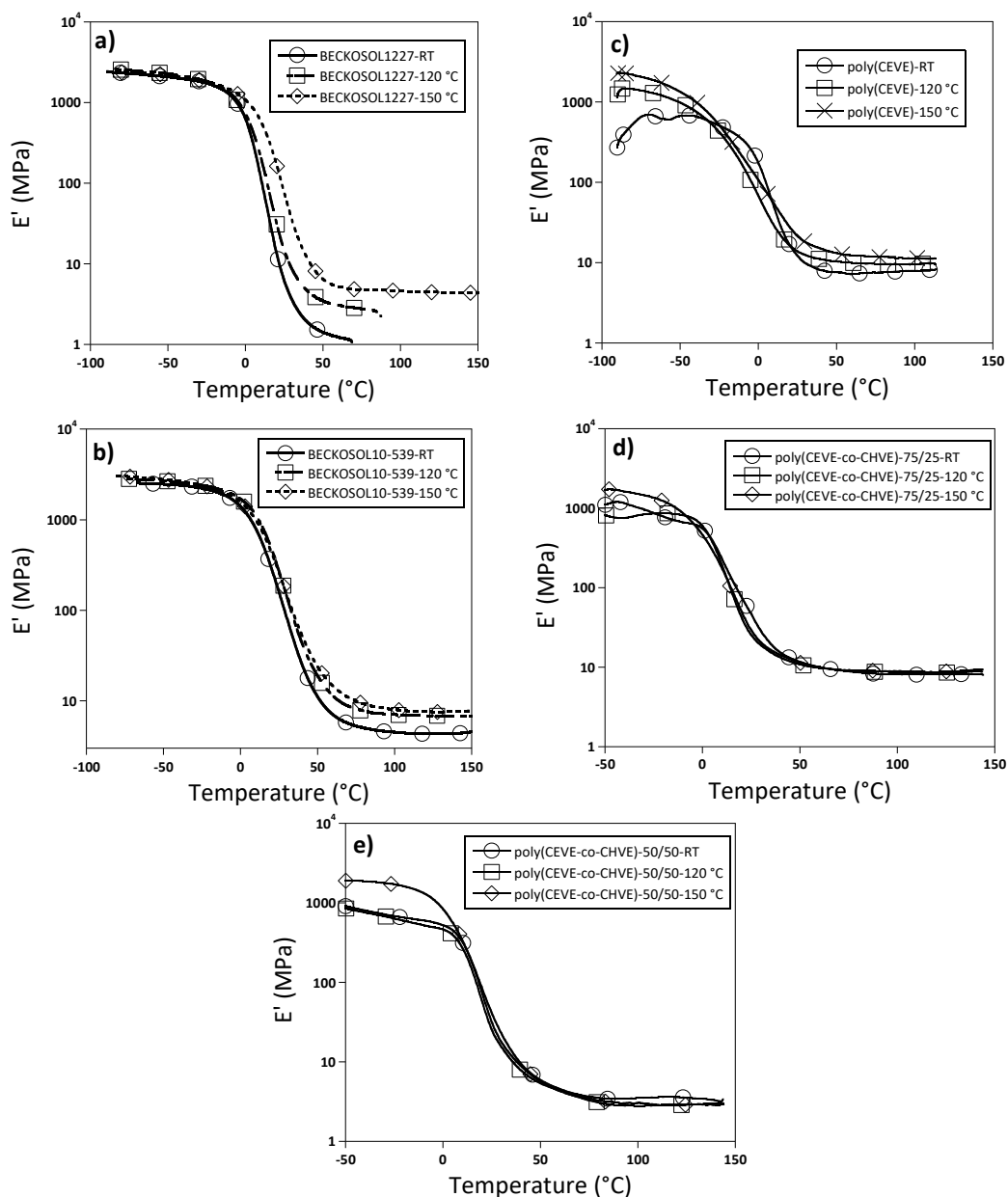


Figure 4.12. Representative storage modulus plots derived from (a)BECKOSO1272, (b) BECKOSOL 110-539, (c) poly(CEVE), (d) poly(CEVE-co-CHVE)-75/25 and (e) poly(CEVE-co-CHVE)-50/50 cured at RT, 120 for 1 h, and 150 $^{\circ}\text{C}$ for 1 h.

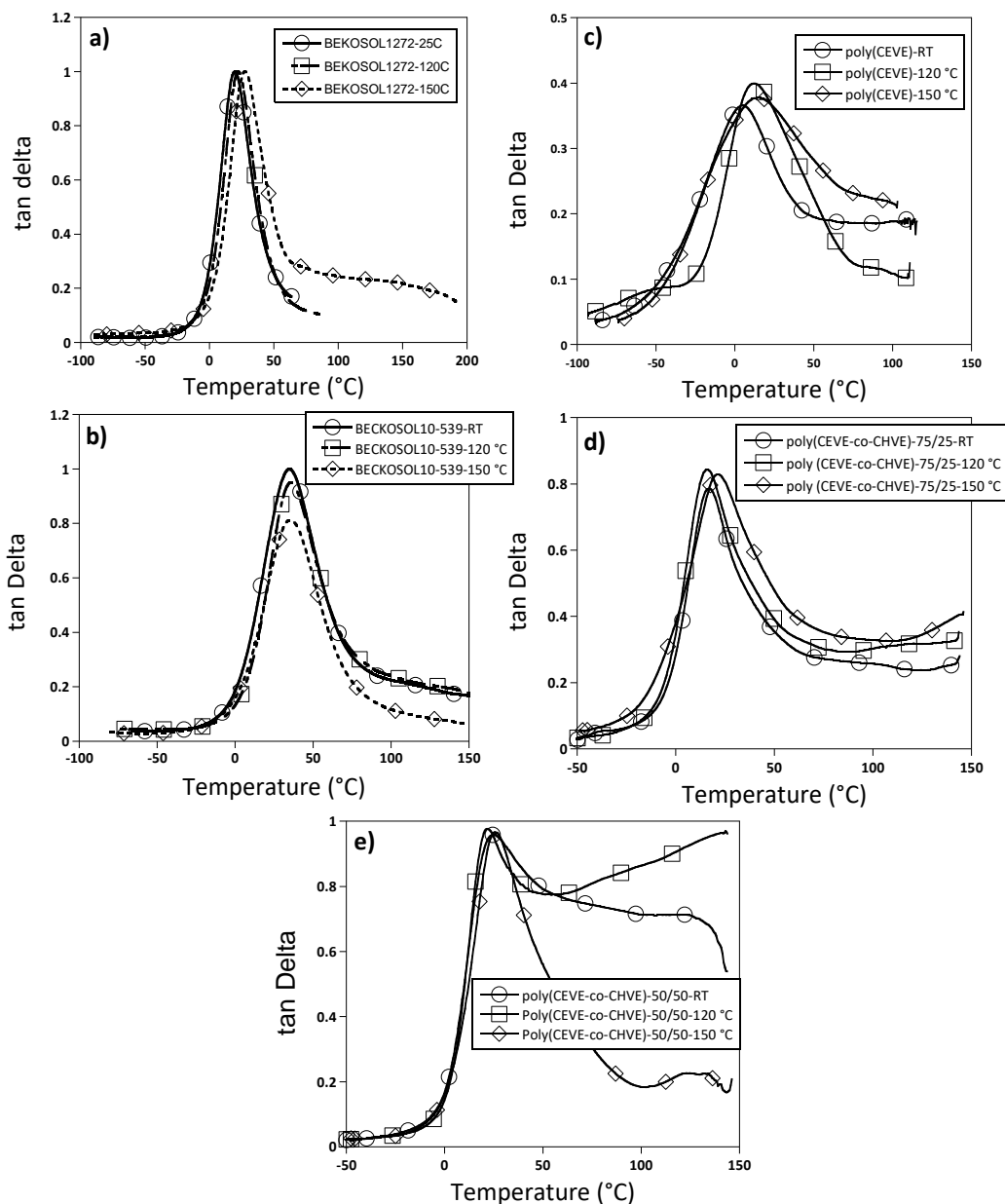


Figure 4.13. Representative $\tan \delta$ thermogram plots derived from (a) BEKOSOL1272, (b) BEKOSOL10-539, (c) poly(CEVE), (d) poly(CEVE-co-CHVE)-75/25 and (e) poly(CEVE-co-CHVE)-50/50 cured at RT, 120 for 1 h, and 150 °C for 1 h.

Two primary parameters, T_g and crosslink density (XLD) were obtained from the DMA thermograms. As shown in **Figure 4.12 (a-e)**, storage moduli (E') plots showed well defined rubbery plateau region above T_g , confirming the formation of a well crosslinked networks except

for BECKOSOL 1272 networks cured at RT and 120 °C. XLD was calculated by using the following equation (**Eq. 4.1**) in accordance with the theory of rubbery elasticity.^{44, 45} The value for storage modulus was taken at 60 °C above the T_g to measure crosslink density. XLD values for all the networks produced are reported in **Table 4.6**. As reported in **Table 4.6**, very low XLD values for BECKOSOL 1272 networks cured at RT and 120 °C might be the reason for not obtaining well defined rubbery plateau region.

$$\nu = E' / (3RT) \quad (4.1)$$

where, ν is the crosslink density, defined as the moles of crosslinks per unit volume of material, R is the universal gas constant, E' (Pa) is storage modulus in the rubbery plateau region, and T (K) is the temperature corresponding to the storage modulus value.

Table 4.6. Properties showing the T_g and XLD of the cured films produced from commercial alkyd resin, poly(CEVE), and poly(CEVE-co-CHVE) copolymer.

Sample	Curing temperature (°C)	T _g (°C)	XLD (moles/cm ³)	Swelling ratio (%)
BECKOSOL 1272	23 °C	19.5	1.12x10 ⁻⁴	-
	120 °C	22.4	2.90x10 ⁻⁴	-
	150 °C	27.4	4.39x10 ⁻⁴	-
BECKOSOL 10-539	23 °C	34.9	3.58x10 ⁻⁴	-
	120 °C	35.6	6.45x10 ⁻⁴	-
	150 °C	35.3	8.20x10 ⁻⁴	-
Poly(CEVE)	23 °C	5.6	10.48x10 ⁻⁴	17.0±1.9
	120 °C	11.2	13.65x10 ⁻⁴	13.5±2.2
	150 °C	25.8	16.60x10 ⁻⁴	12.2±1.5
Poly(CEVE-co-CHVE)-75/25	23 °C	16.3	12.14x10 ⁻⁴	15.9±1.7
	120 °C	16.4	12.50x10 ⁻⁴	15.0±2.4
	150 °C	21.4	14.36x10 ⁻⁴	13.9±2.0
Poly(CEVE-co-CHVE)-50/50	23 °C	24.5	4.65x10 ⁻⁴	21.0±4.5
	120 °C	21.3	4.47x10 ⁻⁴	23.2±3.5
	150 °C	25.8	3.92 x10 ⁻⁴	26.9±2.4

As reported in **Table 4.6**, XLD of the networks produced from CEVE based polymers were found to be higher than the commercial alkyds. However, a decreasing trend of XLD of the

networks with increasing CHVE repeat units in the copolymer was observed which was expected due to dilution of the reactive groups that can contribute to the crosslinked network. Increase in XLD with curing at elevated temperature 120 °C or 150 °C for an hour) was observed for networks derived from poly(CEVE), poly(CEVE-co-CHVE)-75/25 and the commercial alkyds. However, this effect tends to reduce with increasing CHVE repeat units and even a decrease in XLD with curing temperature was observed for networks derived from poly(CEVE-co-CHVE)-50/50.

Values for T_g of the crosslinked networks were obtained from the peak maximum of the $\tan \delta$ plots and are reported in **Table 4.6**. For poly(CEVE), film cured at RT, T_g was found to be ~6 °C and it increased to 25 °C when cured at 150 °C for an hour. Increase in T_g with curing temperature was also observed for films produced from poly(CEVE-co-CHVE)-75/25 and commercial alkyds however, the increment was not as prominent as that was observed for poly(CEVE). Commercial alkyds showed slightly higher T_g s than CEVE derived networks. A linear relationship between T_g and XLD (**Figure 4.14**) with correlation coefficient $r^2 > 0.98$ was obtained for the networks except poly(CEVE-co-CHVE)-50/50. In spite of low XLD, networks derived from poly(CEVE-co-CHVE)-50/50 resulted higher T_g s around 21 to 25 °C which must be attributed from the rigidity of the backbone chains provided by the cyclohexyl groups directly attached to them.

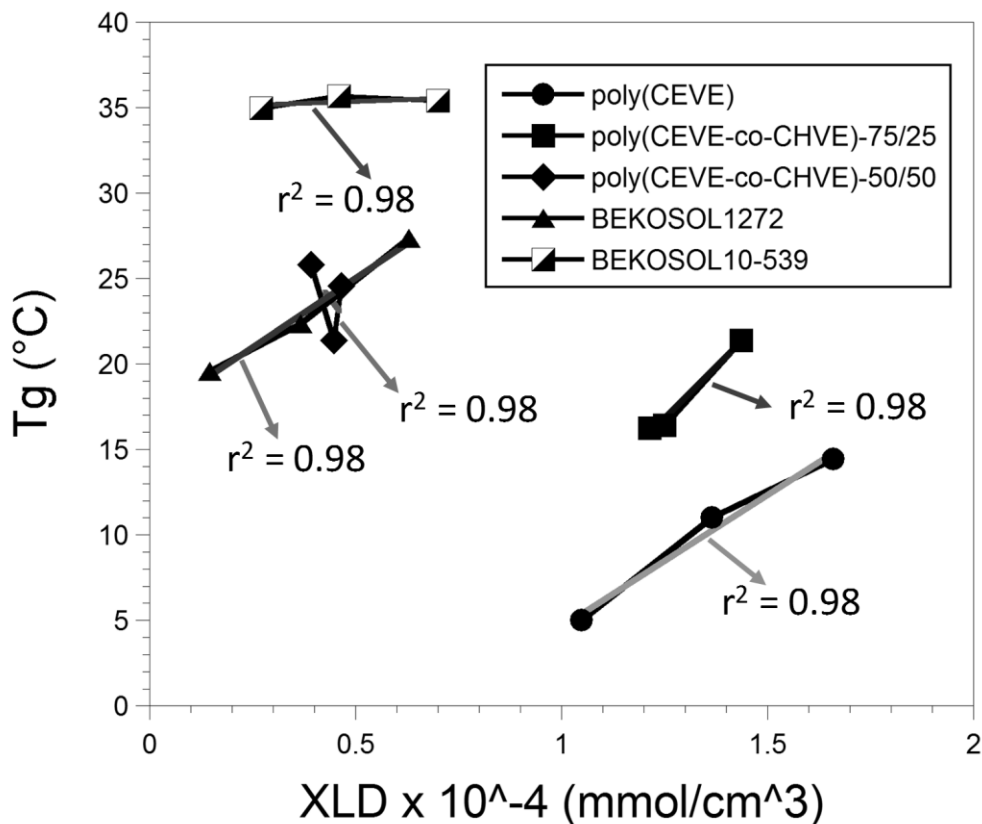


Figure 4.14. Plots showing linear relationship between Tg and XLD of the networks produced from CEVE based polymers and commercial alkyds.

4.4.5. Swelling study of crosslinked films

Swelling study of the crosslinked networks from poly(CEVE) and poly(CEVE-co-CHVE) copolymer networks were carried out to cross verify the crosslink density values obtained by considering the rubbery plateau modulus. According to the theory, a higher crosslink density should result in less swelling when submerged in a good solvent, as it reduces the free volume for the solvent to diffuse in. Swelling of the networks was achieved by dipping the cured free film in toluene and the results are reported in **Table 4.6**. For poly(CEVE), increasing the curing temperature significantly reduces the percent swelling from 17 ± 1.9 (RT) to 12 ± 1.5 (150 °C) confirming the formation of higher crosslink density networks. Incorporation of CHVE repeat units increased the swelling and the values are significantly higher for 50 wt.% CHVE incorporated

networks. For poly(CEVE-co-CHVE)-75/25 networks at RT had lower swelling than poly(CEVE) which is actually in accordance with the crosslink density values obtained from storage modulus plots and the theory of rubber elasticity. Curing temperature had a significant impact on the poly(CEVE) and poly(CEVE-co-CHVE)-75/25 networks, decreasing with curing temperature. This effect is prominent in the case of poly(CEVE-co-CHVE)-50/50 networks where a slightly higher swelling was observed with curing temperature, which is in accordance with the crosslink density values.

4.4.6. Mechanical properties of cured films

Bulk mechanical properties of the thermosets were determined by stamping out dog bone type samples from the free films and analyzing their tensile behavior. Stress-strain curves of the cured films from CEVE-based polymers and commercial alkyds are shown in **Figure 4.15 (a-e)**. The nature of these tensile stress-strain curves varies significantly with the composition and curing temperature. Networks derived from poly(CEVE) showed brittle characteristics with stress increasing linearly with strain until fracture. However, networks derived from CHVE copolymers tend to show ductile deformation along with strain hardening. This transformation is highest for poly(CEVE-co-CHVE)-50/50 networks. This ductile behavior also results in higher failure strain for poly(CEVE-co-CHVE)-50/50 networks, which is approximately 5-6 times higher than for poly(CEVE) networks cured at RT. Networks derived from poly(CEVE-co-CHVE)-75/25 also showed similar behavior. This transition from brittle to ductile behavior of the networks with incorporation of CHVE repeat units is due to the dilution of the reactive groups resulting in a network with relatively lower crosslink density. Networks derived from poly(CEVE) and poly(CEVE-co-CHVE)-75/25, because of the presence of higher CEVE repeat units, possess higher crosslink density. A higher crosslink density resulted restrained segmental movement of

polymer chains during deformation resulting as observed brittle failure. Incorporation of 50 wt.% CHVE was sufficient to provide ductile behavior. Networks derived from commercial alkyds showed similar ductile stress-strain behavior except for BECKOSOL 1272, which had brittle failure. Values for Young's modulus, elongation at break, and toughness for all the crosslinked networks are shown in **Figure 4.16**. For poly(CEVE) and poly(CEVE-co-CHVE)-75/25 networks, the measurement temperature at around 23 °C was significantly higher than the T_g of the networks, implying networks have rubbery behavior, which explains the observed increase in Young's modulus values with curing temperature due to the increase in crosslink density. Instead of lower crosslink density for poly(CEVE-co-CHVE)-50/50 networks, Young's modulus values were calculated to be higher than other networks which might be due to the glassy nature of these networks as the T_g s of the networks were slightly higher or near the measurement temperature. This also explains an increase in Young's modulus with curing temperature mainly because of increasing the T_g of the networks. Networks derived from BECKOSOL1272 showed the lowest Young's modulus as expected because of its very low crosslink density.

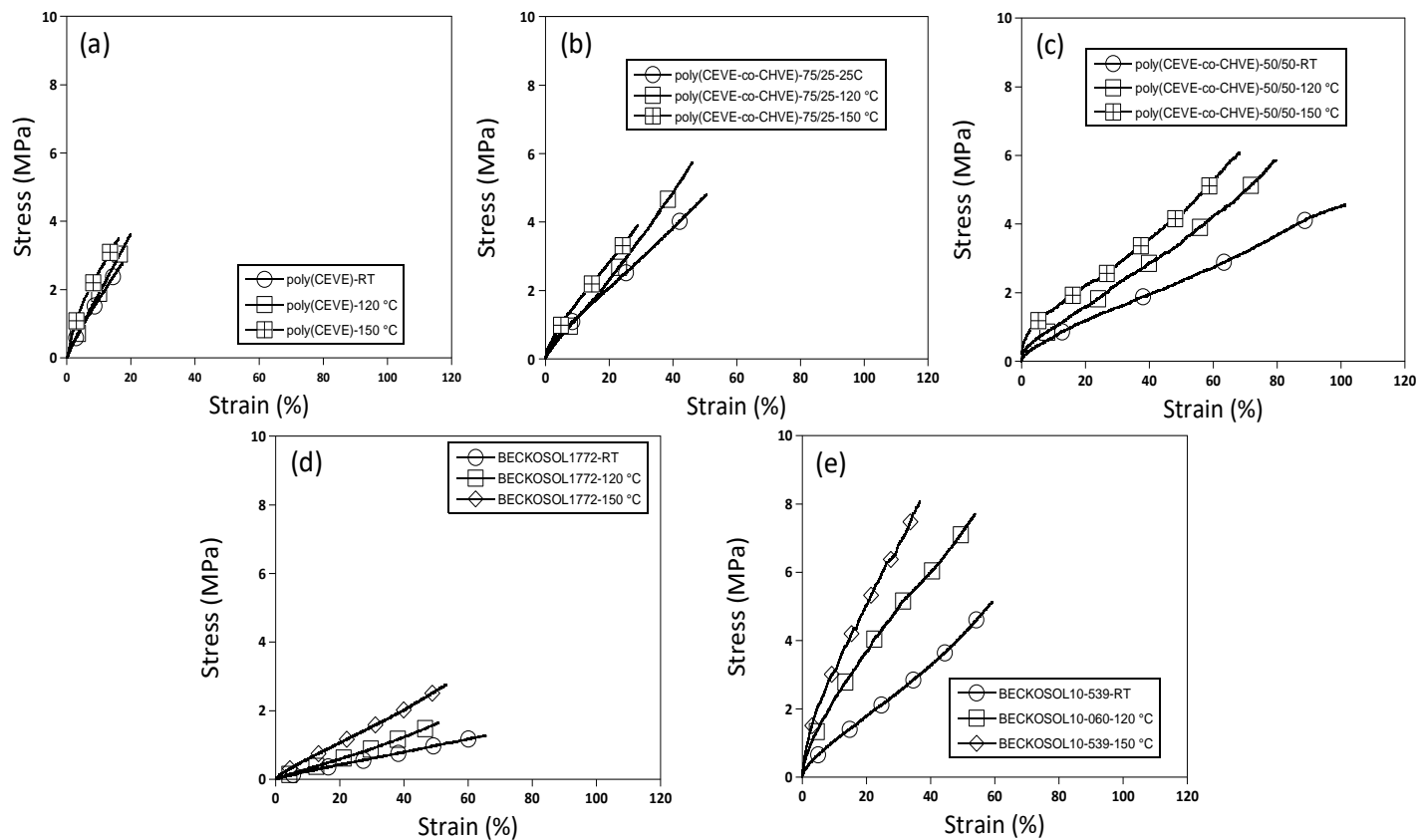


Figure 4.15. Representative stress-strain curves obtained for the fifteen different crosslinked networks derived from (a) poly(CEVE), (b) poly(CEVE-co-CHVE)-75/25, (c) poly(CEVE-co-CHVE)-50/50, (d) BECKOSOL1772, and (e) BECKOSOL10-539 cured at RT, 120 °C for 1 h and 150 °C for 1 h.

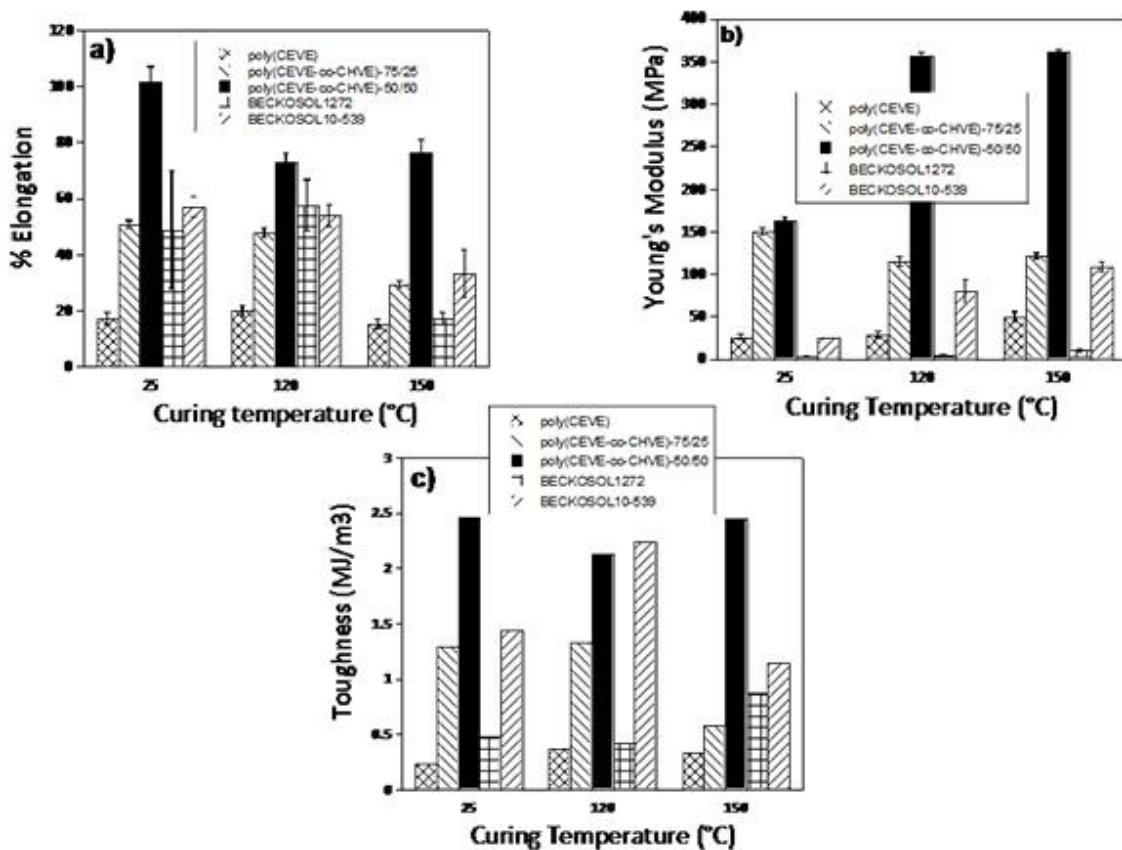


Figure 4.16. Average values of (a) Young's modulus, (b) elongation at break, and (c) toughness for the fifteen crosslinked networks produced for the study.

Poly(CEVE) copolymer networks cured at RT and 120 °C showed higher modulus than commercial alkyds, however, due to higher T_g and sufficiently higher crosslink density BECKOSOL10-539 networks cured at 150 °C, resulted in still a slightly higher Young's modulus. Elongation at break of the networks increased with increasing CHVE content and for a composition with certain amount of CHVE, elongation decreased with increasing curing temperature, which is mainly due to relative variations in crosslink density. Networks from the commercial alkyds showed similar elongation behavior. The values were higher than the synthesized polymer networks which might be due to the lower crosslink density and the better uniformity of the networks as seen from tangent δ plots (Figure 4.13).

4.4.7. Coatings properties

Each of the three synthesized polymers and commercial alkyd resins were coated onto steel substrates and cured using three different curing temperatures. The adhesion, hardness (pencil and pendulum), flexibility, chemical resistance, and impact strength were determined using industry standard methods. The flexibility and impact resistance were characterized using the conical mandrel bend test (ASTM D522) and reverse impact test (ASTM D2794). All fifteen coatings exhibited excellent flexibility (32%), as well as 172 in-lbs impact maxima as evidenced from the lack of cracking or delamination. This excellent impact resistance and flexibility might be the result of T_g s below or near RT and the presence of long pendent chains which have enough segmental mobility to dissipate the impact energy within the timeframe of the event. **Figure 4.17** displays the results obtained from the other coatings tests. In general, all of the coating properties varied significantly with both polymer composition and cure temperature.

Figure 4.17 (a) shows the variation in coating adhesion with polymer composition and cure temperature. The test method used to determine adhesion was the crosshatch adhesion method (ASTM D3359). With this method, the degree of adhesion is assessed visually by rating the amount of coating removed from the crosshatched area. A rating of “5B” indicates no coating removal; a rating of “0B” indicates greater than 65 % coating removal; and ratings between 0B and 5B indicate intermediate levels of coating removal between these two extremes. As shown in **Figure 4.17 (a)**, increase in CHVE units in the copolymer and the curing temperature generally increased the degree of adhesion. This might be due to the formation of lower density networks with incorporation of CEVE, resulting in lower volume shrinkage and greater polymer chain segmental mobility with higher curing temperature. This suggests a higher number of thermodynamically favorable coating/substrate interactions form, which in turn can increase the adhesion.²⁶ All the

commercial alkyds showed 5B crosshatch adhesion which might be due to its polyester backbone with ester functionality that can form electrostatic interactions with the steel substrate.

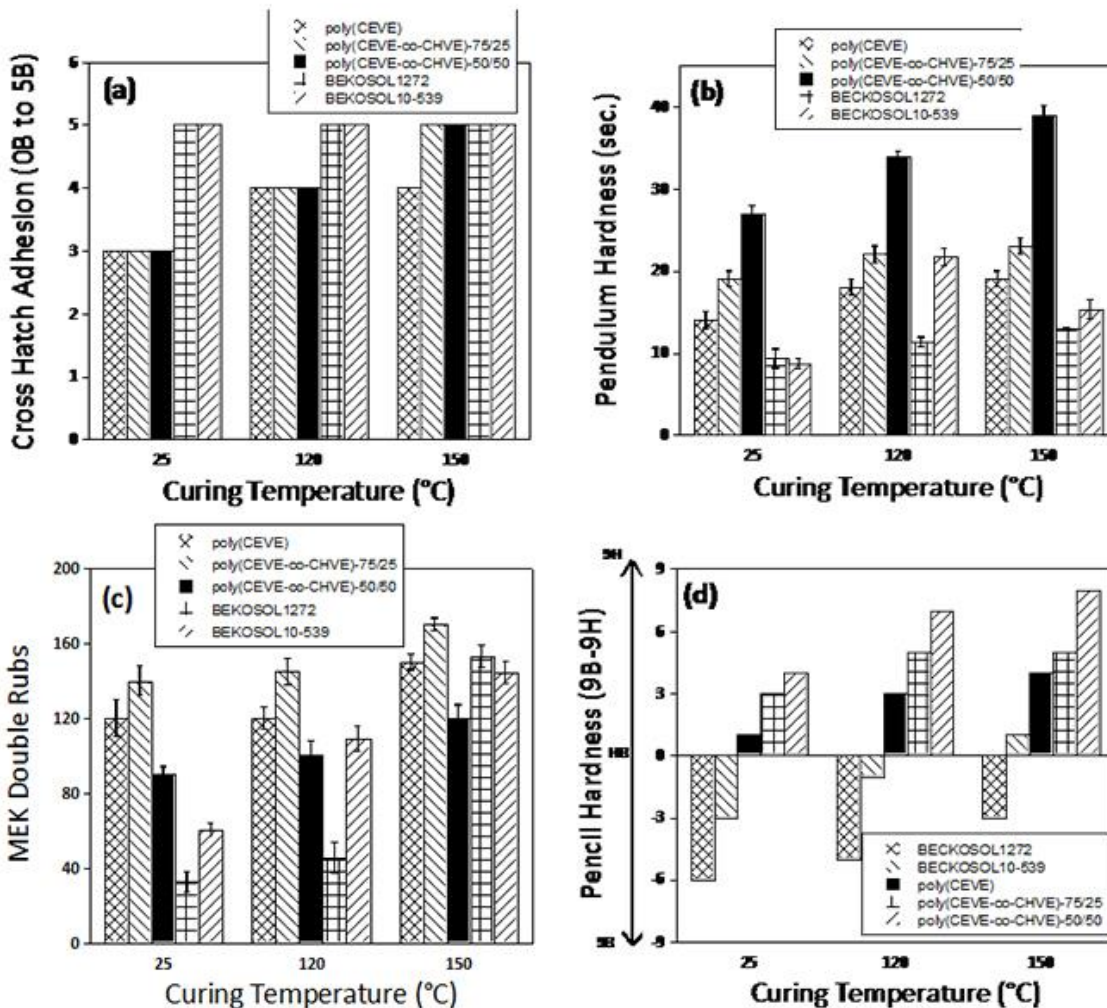


Figure 4.17. Plots describing the properties of coatings derived from the polymers of interest (a) Cross hatch adhesion, (b) pendulum hardness, (c) chemical resistance and (d) pencil hardness.

The trends observed with respect to pendulum hardness and impact resistance were very interesting. Pendulum hardness involves the measurement of the amount of time required to dissipate the rocking motion of two stainless steel balls put into motion by releasing a pendulum. Thus, pendulum hardness is essentially a measurement of the viscoelastic properties of the coating. Coatings exhibiting a relatively high viscous response to the stress induced by the steel balls would

be expected to more effectively dissipate that stress, resulting in a relatively low pendulum hardness value. Therefore, coatings with higher crosslink density should have better pendulum hardness as higher crosslinking will reduce the segmental movement i.e. less damping. Using this information, an expected trend will be poly(CEVE) > poly(CEVE-co-CHVE)-75/25 > poly(CEVE-co-CHVE)-50/50 > BEKCKOSOL10-539 > BECKOSOL1272. However, as shown in **Figure 4.17 (b)**, an opposite trend was observed for poly(CEVE), poly(CEVE-co-CHVE)-75/25 and poly(CEVE-co-CHVE)-50/50, where pendulum hardness increased with incorporation of CHVE repeat units. This anomaly can be explained by considering the glass transition values from tangent δ plots. As shown in **Figure 4.13**, T_g of poly(CEVE) are 10 to 20 °C below RT at which the measurements are done, which indicate that these coatings have higher values of loss modulus (E'') than poly(CEVE-co-CHVE) coatings which have T_g s near or higher than RT. Again, if we consider the Williams-Landel-Ferry principle of time-temperature superposition, according to which an increase in frequency by a decade is equivalent to an increase in temperature of about 6-7 °C.²³ Considering the frequency of pendulum was much higher than 1 Hz used for the DMA measurements, then the T_g of poly(CEVE) will shift closer to RT while the T_g s for the copolymers will shift upwards, ultimately leaving more glassy coatings at RT, and therefore harder coatings. Similar behavior was observed from the pencil hardness results. Coatings from commercial alkyd resins were much softer than the coatings derived from synthesized polymers for this study.

Chemical resistance of the coatings evaluated using MEK double rub method (ASTM D5402) showed impact from both the amount of incorporated CHVE and curing temperature. The results are shown in **Figure 4. 17 (c)**. At the same curing condition, coatings from CEVE polymers showed significantly higher solvent resistance than commercial alkyds. In the cases of commercial alkyds solvent resistance showed good agreement with the crosslink density increasing with curing

temperature. Incorporation of 25 wt.% CHVE in poly(CEVE) slightly improved the solvent resistance and was consistent with curing temperatures. This higher solvent resistance at elevated temperature, compared to poly(CEVE) networks with higher crosslink density, might be explained by considering both crosslink density and swelling ratio data. Higher swelling resistance of the rigid poly(CEVE-co-CHVE) coatings might be able to compensate for the reduced crosslink density due to incorporation of 25 wt.% CHVE. However, in the case of poly(CEVE-co-CHVE)-50/50, the loss in crosslink density is much higher making these coatings unable to compensate for swelling, resulting in reduced solvent resistance, but is still higher than commercial alkyds at RT and 120 °C curing conditions.

4.5. Conclusions

As expected, polymerization of CEVE and copolymerization with CHVE provided coating resins that enabled crosslinked networks with a significantly higher chemical resistance and hardness as compared to commercial alkyds, which exhibit excellent flexibility and impact resistance. Overall, it was found that both polymer composition and cure temperature significantly affected coatings properties. With regard to polymer composition, the results indicate that an optimum balance between thermal, mechanical, and physical properties can be obtained by tuning the ratio of CEVE and CHVE in the copolymer. For example, incorporation of 25 % in the copolymer improves the T_g and hardness. A transition from brittle to ductile mechanical behavior of the free films was observed with incorporation of CHVE repeat units; however, increasing the CHVE content to 50 wt.% produced low crosslink density networks resulting in poor solvent resistance performance while increasing the adhesion. Coatings derived from CEVE polymers showed better coating properties than commercial alkyd resins and excluded issues like high

energy polymerization process, presence of monomer and oligomers that can affect the coating properties, and gelation during resin synthesis.

4.6. References

1. K. I. Suresh and M. Jaikrishna, *Journal of Polymer Science Part A: Polymer Chemistry*, 2005, **43**, 5953-5961.
2. S. A. Miller, *ACS Macro Letters*, 2013, **2**, 550-554.
3. S. L. Kristufek, K. T. Wacker, Y. Y. T. Tsao, L. Su and K. L. Wooley, *Natural Product Reports*, 2017, **34**, 433-459.
4. U. Biermann, U. Bornscheuer, M. A. R. Meier, J. O. Metzger and H. J. Schafer., *Angew. Chem.*, 2011, **50**, 3854–3871
5. J. M. Raquez , M. Deleglisea, M. F. Lacrampea and P. Krawczak, *Progress in Polymer Science* 2010, **35**, 487–509.
6. N. Cohen, D. modai, A. Khahil and A. Golik, *Hum Toxicol.* , 1989, **8**, 247-250.
7. B. Schoenberg and C. A. Mitchell, *Arch Environ Health*, 1975, **30**, 574-577.
8. M. T. Harvey and S. Caplan, *Industrial and Engineering Chemistry*, 1940, **32**, 1306–1310.
9. W. Hale, *Hygienic Lab. Bull.* 88, U.S. Pub. Health Service, Hygienic Lab, 1913.
10. R. Nagelsdiek, M. Mennicken, B. Maier, H. Keul and H. Hocker, *Macromolecules*, 2004, **37**, 8923-8932.
11. R. Ikeda, H. tanaka, H. Uyama and S. Kobayashi, *polymer preprints*, 2000, **41**, 83-84.
12. H. Tonami, H. Uyama, S. Kobayashi and M. Kubota, *Macromolecular Chemistry and Physics*, 1999, **200**, 2365-2371.
13. B. Lochab, S. Shukla and I. K. Varma, *RSC Advances*, 2014, **4**, 21712-21752.

14. G. John, S. K. Thomas and C. K. S. Pillai, *Journal of Applied polymer science*, 1994, **53**, 1415-1423.
15. S. Alam and B. C. Chisholm, *Journal of Coatings Technology and Research*, 2011, **8**, 671-683.
16. S. Alam, H. Kalita, A. Jayasooriya, S. Samanta, J. Bahr, A. Chernykh, M. Weisz and B. J. Chisholm, *European Journal of Lipid Science and Technology*, 2014, **116**, 2-15.
17. M. Kathalewar, A. Sabnis and D. DMelo, *Progress in Organic Coatings*, 2014, **77**, 616-626.
18. M. Kathalewar, A. Sabnis and D. Mello, *European Polymer Journal*, 2014, **57**, 99-108.
19. M. K. S. Lalitha, Y. S. Prasad, V. Sridharan, C. U. Maheswari, C. S. Srinandan and S. Nagarajan, *ACS Sustainable Chemistry & Engineering*, 2017, **5**, 436-449.
20. C. J. Patel and V. Mannari, *Progress in Organic Coatings*, 2014, **77**, 997-1006.
21. S. Aoshima and T. Higashimura, *Macromolecules*, 1989, **22**, 1009-1013.
22. H. Kalita, S. Alam, D. Kalita, A. Chernykh, I. Tarnavchyk, J. Bahr, S. Samanta, A. Jayasooriyama, S. Fernando, S. Selvakumar, A. Popadyuk, D. S.a Wickramaratne, M. Sibi, A. Voronov, A. Bezbaruah and B. J. Chisholm, *ACS Symposium Series*, 2014, **1178**, 731-790.
23. P. J. Flory, *Principles of Polymer Chemistry*, Cornell University Press, New York, 1953.
24. T. Murayama, *Dynamic Mechanical Analysis of Polymeric Materials*, Elsevier, Amsterdam, The Netherlands, 1978.
25. L. W. Hill, *J. Coat. Technol.*, 1992, **64**, 29-41.
26. R. A. Cairncross and C. J. Durning, *AIChE J.*, 1996, **42**, 2415-2425.
27. R. A. Cairncross, L. F. Francis and L. E. Scriven, *Drying Tech. J.*, 1992, **10**, 893-923.

28. D. A. Edward, *Chem. Eng. Corn.*, 1998, **166**, 201-216.
29. J. Crank and G. S. Park, *Trans. Farad. Soc.*, 1951, **47**, 1072-1084.
30. J. R. Collier and G. W. Powers, *Polymer Engr. Sci.*, 1990, **30**, 118- 123.

CHAPTER 5. POLY (VINYL ETHER)S BASED ON EUGENOL AND THEIR APPLICATION AS SURFACE COATINGS

5.1. Abstract

In this study, a vinyl ether monomer from eugenol, 2-eugenoloxyl ethyl vinyl ether (EEVE) was synthesized. Using carbocationic polymerization the homopolymer of EEVE and copolymers with varying amount of cyclohexyl vinyl ether CHVE were produced. The polymers were then used to produce coatings and free films cured via autoxidation at room temperature and elevated temperatures (120 ° and 150 °C for an hour). For comparison, coatings with the same curing regime were made from three commercial alkyds. Analysis of the thermal, mechanical, viscoelastic and physical properties of the coatings showed significantly higher chemical resistance and hardness, base resistance, T_g , modulus for the EEVE and EEVE/CHVE derived coatings as compared to the commercial alkyds. Overall, it was found that both polymer composition and cure temperature significantly affected coatings properties. With regard to polymer composition, the results indicated that an optimum balance between thermal, mechanical, and physical properties can be obtained by tuning the ratio of CEVE and CHVE in the copolymer. For example, incorporation of 25 wt.% CHVE in the copolymer improves the T_g , hardness, base resistance and ductility of the free films. However, mechanical behavior of the free films showed more brittleness with incorporation of 50 and higher wt.% of CHVE repeat units due to increase in the rigidity of the polymer chains and result in low crosslink density networks. Coatings derived from poly(EEVE) and copolymer with 25 wt.% CHVE repeat units resulted in better properties than commercial alkyd resins. Also, the polymerization technique used in this study was able to produce polymers that were free of oligomers and without any gelling issues which are some common issues associated with conventional alkyd synthesis via step growth polymerization at high temperature.

5.2. Introduction

Since solvents and other volatile organic compounds (VOCs) are a major source of air pollution, technology development over the past several decades within the coatings industry has been largely driven by the need to reduce VOCs. More recently, the coatings industry has put more emphasis on the total environmental impact of coatings.¹ As a result, life-cycle assessment tools have been utilized to quantify and compare the ecological impact of different coatings. One of the considerations in a life-cycle analysis is the source of carbon for the coating components. All other things being equal, the use of coating raw materials from renewable resources provides for a lower environmental impact. In addition, coating building blocks derived from renewable resources tend to be less toxic and more biodegradable than non-natural, petrochemical-based raw materials.

Within the coatings industry, the segment of the coatings market that utilizes the largest amount of renewable resources is the alkyd coating segment. Alkyds are essentially polyesters modified with fatty acid ester chains. Examples for sources of the fatty acid ester component include soybean oil, linseed oil, and tung oil. Using life-cycle assessment, low VOC versions of alkyd coatings were shown to be more environmentally friendly than waterborne acrylic paints.¹ Besides being partially based on renewable resources, alkyds have several other desirable features including versatility, ease-of-use, and low cost. The versatility of alkyd coatings can be attributed to the tremendous chemical diversity of alkyd resin chemistry, while ease-of-use can be largely attributed to the ability to produce one-component, ambient-cured coatings. The one-component, ambient-cure nature of alkyd coatings is a result of the curing mechanism associated with the fatty acid ester component. When the alkyd resin contains polyunsaturated fatty acid ester chains, curing can be accomplished through the process of autoxidation.²⁻⁴

Probably the most widely used renewable resource for thermoset material applications is the plant oil triglyceride.^{5,6} The utility of plant oil triglycerides stem from their relatively low cost and presence of unsaturation. Besides curing by autoxidation, the unsaturation enables crosslinking/curing through other mechanisms by derivatization of the double bonds. For example, epoxidized soybean oil, acrylated epoxidized soybean oil, and soybean oil-based polyols are all commercially available.⁷⁻¹¹ A major limitation of the use of plant oil triglycerides and chemically-modified plant oil triglycerides is their relatively high molecular flexibility resulting from the long fatty alkyl chains. As a result of the extensive molecular mobility of triglyceride-based materials, they are not very useful for applications that require high glass transition temperatures (T_g s), moduli, tensile strength, and hardness. To obtain thermoset materials with high T_g s, moduli, tensile strength, and hardness, starting materials that possess aromatic and/or cycloaliphatic groups are typically required.

Nature provides several sources of compounds with aromatic or cycloaliphatic moieties. Renewable sources for cycloaliphatic groups include polysaccharides, sugars, and terpenes.¹²⁻¹⁴ The most abundant renewable resource for aromatic compounds is lignin. Lignin is the second most abundant renewable resource on the planet and consists of a crosslinked network of ring-substituted phenols.^{12,13,15-19} A tremendous amount of research and development is being focused on the depolymerization of lignin to produce low-cost, useful aromatic chemicals.^{16,20-23}

Eugenol is a biobased compound that can potentially be obtained from lignin, however, currently, it is most easily isolated from other renewable resources such as clove oil, nutmeg, cinnamon, and basil.²⁴ As shown in **Figure 5.1**, eugenol is a phenol with a methoxy group in the ortho-position of the aromatic ring and an allyl group in the para-position. Since eugenol is a bifunctional molecule, it is easy to envision it as a substrate for the generation of a number of

potentially useful new compounds and materials. Kaufman recently reviewed the literature pertaining to transformations of eugenol into a large variety of other natural products and analogs of natural products as well as bioactive compounds, monomers, and polymers.²⁴

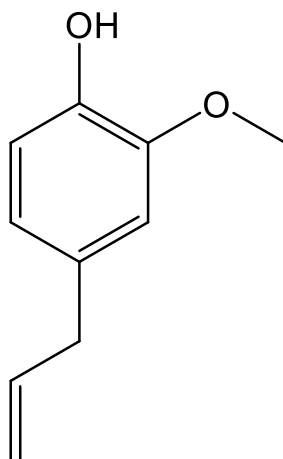


Figure 5.1. The chemical structure of eugenol.

Chisholm et al.^{9, 10, 25-34} have extensively investigated the use of specific cationic polymerization systems to produce novel polymers derived from plant oils containing mono and polyunsaturated fatty acid esters. By generating vinyl ether monomers from plant oil triglycerides with moderate to high levels of unsaturation, homopolymers and copolymers were produced that readily crosslinked at ambient conditions through the process of autoxidation. It was shown that the use of an appropriate cationic polymerization system enabled polymerizations that were essentially free of chain transfer and termination reactions. In fact, living polymerization was demonstrated for a vinyl ether monomer derived from soybean oil.

5.3. Experimental

5.3.1. Materials

The materials used for the study are described in **Table 5.1**. Unless specified otherwise, all materials were used as received.

Table 5.1. A description of the starting materials used for the study.

Chemical	Designation	Vendor
4-Allyl-2-methoxyphenol, 99%	Eugenol	Alfa Aesar
2-Chloroethyl vinyl ether	2-Chloroethyl vinyl ether	TCI
3-Chloroperoxybenzoic acid, $\leq 77\%$	mCPBA	Sigma-Aldrich
BECKOSOL 1272	BECKOSOL 1272	REICHHOLD
BECKOSOL 10-539	BECKOSOL 10-539	REICHHOLD
BECKOSOL 10-060	BECKOSOL 10-060	REICHHOLD
Cyclohexyl vinyl ether	CHVE	BASF
Potassium hydroxide, 90%, flakes	KOH	VWR
Magnesium sulfate	MgSO ₄	Alfa Aesar
Anhydrous calcium sulfate	DRIERITE® Absorbent	Millipore Sigma
Ethylaluminumsesquichloride, 97%	Et ₃ Al ₂ Cl ₃	Sigma-Aldrich
Methanol, 98%	Methanol	BDH Chemicals
Toluene	Toluene	BDH Chemicals
n-Hexane	n-Hexane	Sigma-Aldrich
Tetrahydrofuran, 99.0%	THF	J. T. Baker
Methyl ethyl ketone, 99%	MEK	Alfa Aesar
N,N-Dimethyl formamide, 99.8%	DMF	VWR
Teflon films	Teflon	McMaster-Carr
Cobalt 2-ethylhexanoate, 12% Cobalt	Cobalt octoate	OMG Americas
Zirconium 2-ethylhexanoate, 18% Zirconium	Zirconium octoate	OMG Americas
Zinc carboxylate in mineral spirits, 8%	Nuxtra® Zinc	OMG Americas
steel panels 4"×8"	steel panels	Q-LAB

5.3.2. Synthesis of 2-eugenoxethyl vinyl ether (EEVE)

2-Eugenoxethyl vinyl ether (EEVE) was successfully produced using Williamson ether synthesis and the synthetic scheme is shown in **Figure 5.2**. Initially, 50 g (0.47 mole) of 2-chloroethyl vinyl ether was mixed with 150 mL of N,N-dimethylformamide in a 500 mL round-bottom flask (rbf) equipped with a reflux condenser and a magnetic stirrer bar. To this reaction mixture, 78 g of eugenol (0.46 mol.), 26.4 g of potassium hydroxide was added and heated to 80 °C using an oil bath and kept for 16 hours, while stirring under nitrogen blanket. After completion, the reaction mixture was cooled down to room temperature and diluted with 250 mL of n-hexane.

Next, the solution was transferred to a separatory funnel and washed three times with 100 mL of 2N potassium hydroxide in deionized (DI) water to remove excess eugenol. After washing with potassium hydroxide, the organic layer was washed multiple times with DI water until the pH reached ~7 as indicated by litmus paper. Finally, the organic layer was dried over anhydrous magnesium sulfate and filtered. Filtrate was then kept in refrigerator at 5-7 °C overnight resulting in crystallization of EEVE. Supernatant n-hexane was then decanted and the remaining volatiles were stripped out using rotary evaporator at room temperature for 12 hours at 5-8 mbar. EEVE was characterized using ^1H NMR and FTIR spectroscopy.

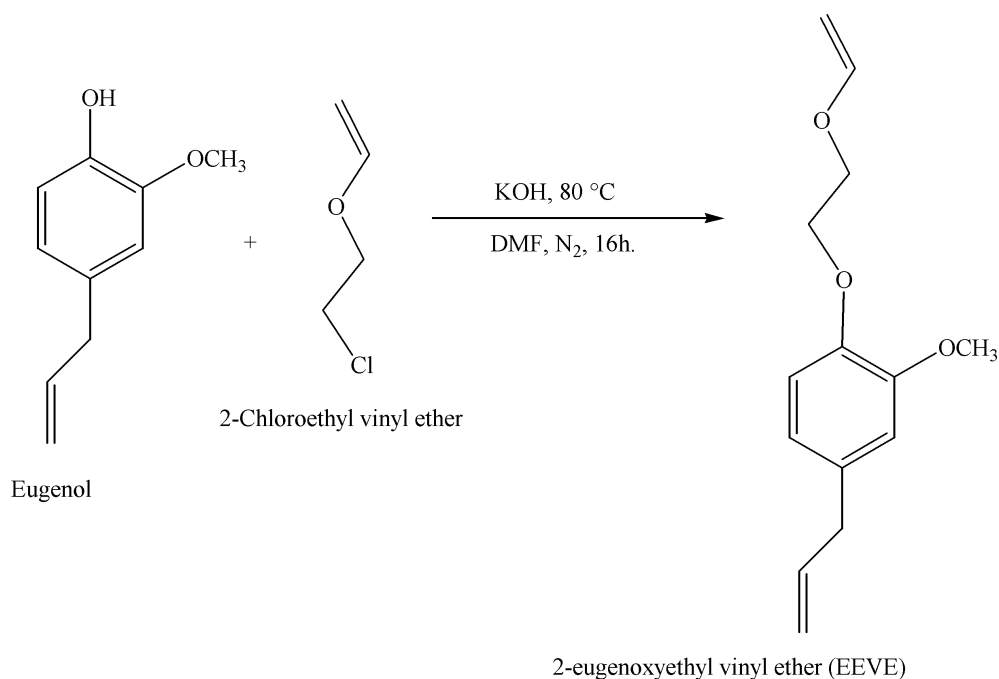


Figure 5.2. Synthesis of 2-eugenoxylethyl vinyl ether (EEVE).

5.3.3. Synthesis of poly (2-eugenoxylethyl vinyl ether), poly(EEVE)

Polymerization of EEVE is shown in **Figures 5.3**. All glassware was baked at 200 °C for 2 h and then cooled down by purging N₂ to avoid moisture condensation. Glassware was then immediately transferred inside the glove box with a custom build cold bath where polymerization was carried out. Toluene was distilled over calcium hydride immediately prior to use. 1-

Isobutoxyethyl acetate (IBEA) was synthesized and dried according to the procedure described by Aoshima and Higashimura.³⁵ Ethyl aluminum sesquichloride was diluted with distilled toluene to produce a 25 wt.% solution. In a 500 mL, two neck round bottom flask 50 g of dry EEVE and 170 mg of IBEA were dissolved in 150 mL of dry toluene and chilled to 0 °C using a heptane cold bath. Reaction mixture was continuously stirred with an overhead mechanical stirrer at 350 rpm. In a 100 mL closed glass container 6.07 mL of coiniciator, Et₃Al₂Cl₃ (25 wt.% in toluene) was added to 50 mL of dry toluene and chilled to 0 °C. A monomer:initiator:co-initiator ratio of 200:1:5 was used. After 30 minutes of cooling the polymerization was initiated by the addition of the co-initiator to the reaction mixture. The reaction was terminated after 2 hours by the addition of 50 mL of chilled methanol. Polymer was precipitated by pouring the reaction mixture into 200 mL of methanol in a 500 mL glass bottle while stirring to avoid entrapment of unreacted monomer by polymer due to sudden precipitation. The copolymer was reprecipitated three times from toluene by adding methanol and re-dissolved in 100 mL of toluene. Trace methanol was removed under vacuum (50–60 mm of Hg) at 30 °C for 3 h. Poly(EEVE) was characterized using ¹H NMR, FTIR, GPC and DSC.

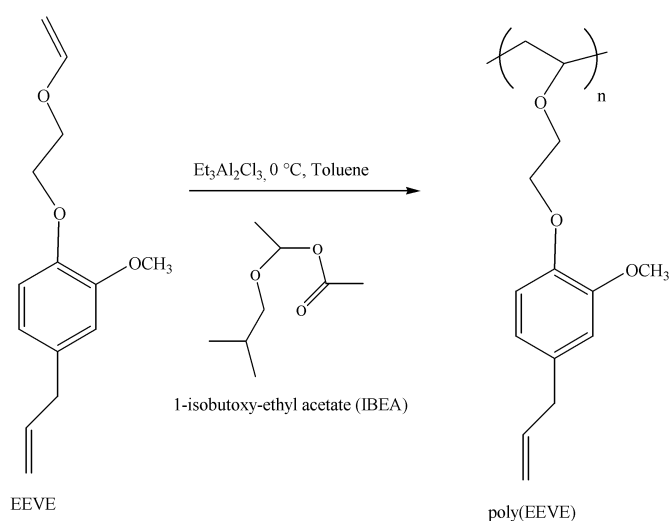


Figure 5.3. Synthesis of poly(EEVE).

5.3.4. Synthesis of EEVE and cyclohexyl vinyl ether (CHVE) copolymers

As shown in **Figure 5.4** copolymers were synthesized from EEVE and CHVE monomers using carbocationic polymerization previously used for homopolymer synthesis (**section 5.3.3**). To investigate the effect of concentration of CHVE repeat units on the final coating properties, three copolymers with 25, 50 and 75 wt.% CHVE repeat units were synthesized. The compositions of the reaction mixtures are reported in **Table 5.2**. Copolymers were characterized using ^1H NMR, FTIR and GPC.

Table 5.2. Composition of the polymerization mixtures used to produce poly(EEVE-co-CHVE) copolymers and poly(CHVE).

Sample ID	EEVE, g	CHVE, g	IBEA, mg	Et ₃ Al ₂ Cl ₃ (25 wt.% in toluene), mL	Toluene, mL
poly(EEVE-co-CHVE)-75/25	37.5	12.5	319	7.89	300
poly(EEVE-co-CHVE)-50/50	25	25	375	9.28	300
poly(EEVE-co-CHVE)-25/75	12.5	37.5	431	10.67	300

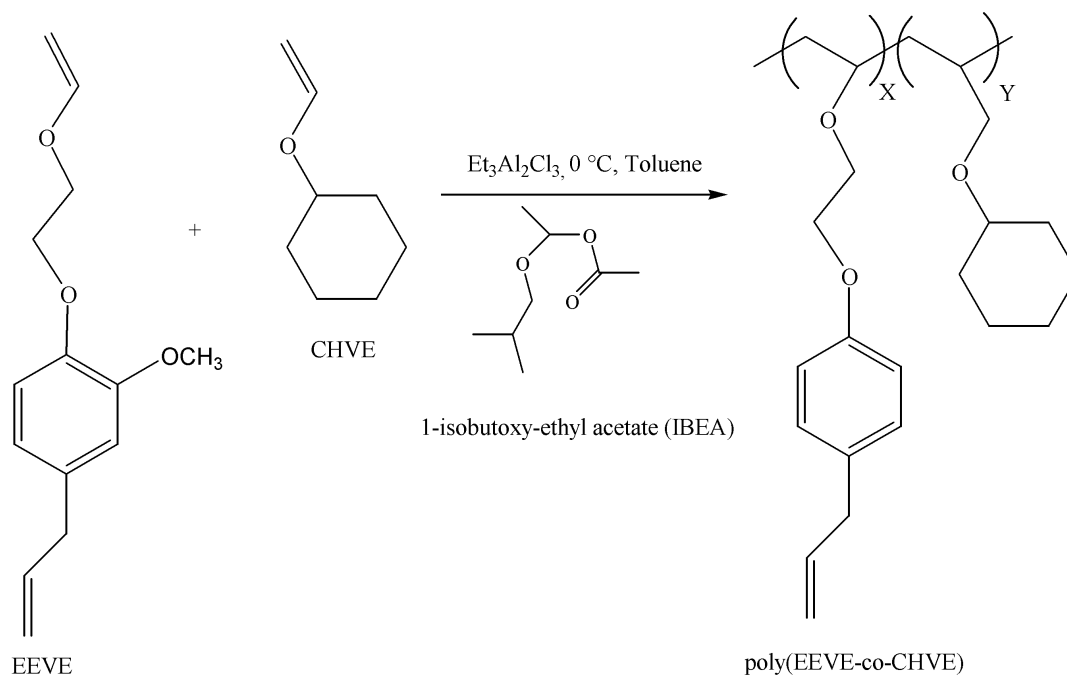


Figure 5.4. Schematic illustrating the synthesis of poly(EEVE-co-CHVE) copolymers.

5.3.5. Synthesis of CHVE homopolymer

Poly(CHVE) was synthesized on a smaller scale following the procedure used for the synthesis of poly(E EVE) homopolymer (section 5.3.3) and the schematic is shown in Figure 5.5. Prior to the use CHVE was distilled over calcium hydride to remove the stabilizer and residual moisture. For this synthesis instead of heptane cold bath, custom made cooling blocks connected to a chiller with the cooling range up to $-20\text{ }^{\circ}\text{C}$ was used and the reaction mixture was stirred with magnetic stirrer bar at 500 rpm by placing the cooling block on a magnetic stir plate. The composition of the reaction mixture is reported in Table 5.2. Homopolymer was characterized using ^1H NMR, FTIR and GPC.

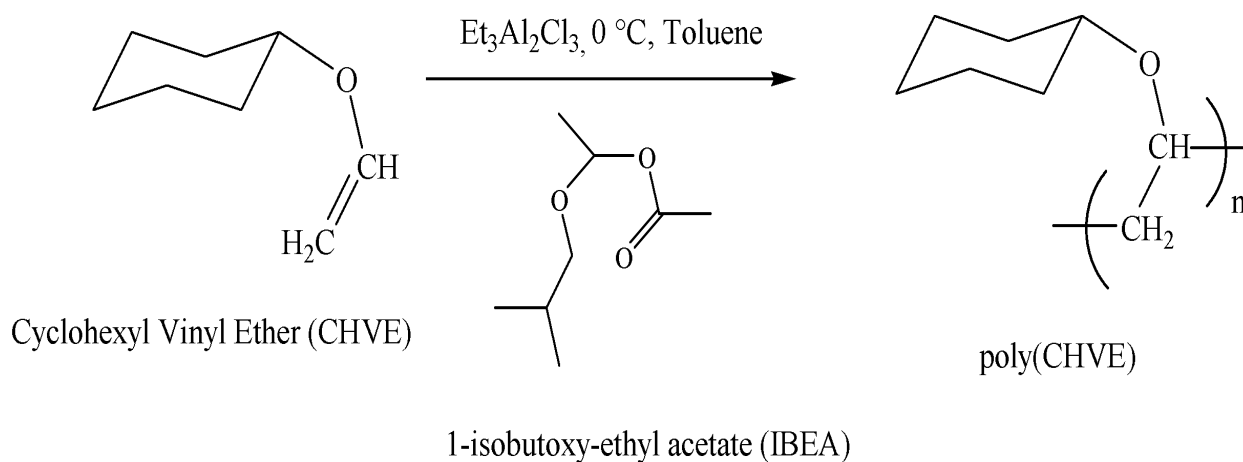


Figure 5.5. Schematic illustrating synthesis of poly cyclohexyl vinyl ether [poly(CHVE)].

5.3.6. Commercial soy-based alkyds for coating performance comparison

Polymers synthesized in this study are linear in nature with a carbon-carbon backbone chain ($-\text{[CH-CH}_2\text{]}_n-$) having pendent side chains with phenyl ring substituted with methoxy and allyl groups in the meta- and para- positions. In order to evaluate the feasibility of the coatings derived from these polymers as real-world air-drying coatings, three commercial soy-based long oil alkyds, BECKOSOL 1272, BECKOSOL 10-060 and BECKOSOL 10-539 were chosen for comparison. Descriptions of these alkyd resins are shown in Table 5.3.

Table 5.3. Descriptions of the commercial alkyds as specified in the data sheet.

Sample ID	Description
BECKOSOL 1272	100% solids, Soy based long oil alkyd
BECKOSOL 10-539	High-solids (88-92%), Soy based long-oil alkyd in xylene/mineral spirit
BECKOSOL 10-060	Solids (69-71%), Soy based long-oil alkyd in mineral spirit

5.3.7. Preparation of cured free films and coatings

Coatings and free films of poly(E EVE), three poly(E EVE-co-CHVE) copolymers and commercial alkyds were prepared by curing via autoxidation. To prepare coating formulations, 10 g of neat polymer was mixed with 8 mg of cobalt octoate, 40 mg of zirconium octoate, and 450 mg of Nuxtra® Zinc. using a FlackTek mixer operating at 3500 rpm for 30 seconds. Prior to making the formulations, BECKOSOL 10-539 and BECKOSOL 10-060 were dried using GeneVac EZ-2 plus centrifugal evaporator. All three commercial alkyds with 100 % solid content were mixed with drier package using a FlackTek mixer operating at 3500 rpm for 2 min. For the synthesized polymers 70% solid content solutions were prepared with toluene to which drier package was added and mixed using a FlackTek mixer operating at 3500 rpm for 30 sec. Liquid coating solutions were cast to steelQ-panels (0.2 x 3 x 6”, SAE1008 cold rolled steel panels pretreated with iron phosphated (Bonderite 1000) and Teflon®-laminated glass panels (0.5 x 4 x 8”), using a drawdown bar with 4 mil gap for commercial alkyds, and 6 mil gap for EEVE based polymers to ensure similar dry film thickness for better comparison. Three different temperatures: room temperature (identified by using “RT” in the sample designation), 1 h at 120 °C, and 1 h at 150 °C (identified by using “120 °C” and “150 °C” in the sample designation respectively) were employed to cure five steel and one Teflon coated glass panels for each temperature, from each formulation. These panels were then kept at room temperature for four weeks in a well-ventilated

glass cabinet before testing. Coatings on the Teflon®-laminated glass panels provided free film samples to be used for the characterization of mechanical and viscoelastic properties.

5.3.8. Methods and instrumentation

5.3.8.1. Nuclear magnetic resonance (NMR) spectroscopy

Proton nuclear magnetic resonance (^1H NMR) spectra were obtained using a 400 MHz Bruker 400 NMR spectrometer. Data acquisition was accomplished using 16 scans and CDCl_3 was used as the lock solvent.

5.3.8.2. Fourier transform resonance (FTIR) spectroscopy

Fourier transform infrared (FTIR) spectra were obtained with a Nicolet 8700 FTIR spectrometer operated with OMNIC software. Thin polymer films were solution cast onto a KBr disc, subsequently dried, and then scanned from $500\text{-}4000\text{ cm}^{-1}$ using 64 scans and 1.93 cm^{-1} data spacing.

5.3.8.3. Gel permeation chromatography (GPC)

MW and polydispersity index (PDI) of the polymers produced were characterized using gel permeation chromatography (GPC). For synthesized polymers EcoSEC HLC-8320 GPC, Tosoh Bioscience, Japan with a differential refractometer (DRI) detector with tetrahydrofuran (THF) as eluent at a flow rate of 0.35 mL min^{-1} was used. Samples were prepared at nominally 1 mg/mL in an aliquot of the eluent and allowed to dissolve at ambient temperature for several hours. The injection volume was $20\mu\text{L}$ for each sample. Calibration was conducted using polystyrene standards (Agilent EasiVial PS-H 4ml). For commercial alkyds, Symyx Rapid-GPC with an evaporative light scattering detector (PL-ELS 1000) was used. Samples were prepared in THF at a concentration of 1 mg/mL . The molecular weight data were expressed relative to polystyrene standards.

5.3.8.4. Dynamical mechanical analysis (DMA)

The viscoelastic properties of crosslinked free films were characterized using dynamic mechanical analysis (DMA) utilizing a Q800 dynamic mechanical thermal analyzer from TA Instruments in tension mode. For each cured system, specimens of 20 mm in length, 5 mm wide, and 0.08 to 0.10 mm thick were cut from free films. Temperature was ramped at 5 °C/min. The frequency and strain rate were 1 Hz and 0.1%, respectively. T_g was reported as the peak maximum of the tangent δ response.

5.3.8.5. Differential scanning calorimetry (DSC)

Except for poly(CEVE), DSC experiments were performed using a Q1000 Modulated Differential Scanning Calorimeter from TA Instruments with a cooling limit of -90 °C. For poly(CEVE), a Q2000 Modulated Differential Scanning Calorimeter was used with a cooling limit of -200 °C. Helium (25mL/min) was used as the purging gas. 7-10 mg samples were thoroughly dried prior to the measurement. Samples were first equilibrated at 23 °C and then the following heating and cooling regime used was used: cooled from 23 °C to -80 °C at 10 °C/minute (1st cooling cycle); held at -80 °C for 2 minutes; heated to 50 °C at 10 °C/minute (1st heating cycle); held at 50 °C for 2 minutes; cooled to -80 °C at 10 °C/minute (2nd cooling cycle); held at -80 °C for 2 minutes; heated to 90 °C at 10 °C/minute (2nd heating cycle).

5.3.8.6. Tensile testing

Dog bone shaped specimens were prepared (ASTM D638, Type V) from the films cured on Teflon® coated glass panels. Instron 5545 tensile tester with 100 N load cell was used to carry out the tensile testing using a 1 mm/min displacement rate of the movable clamp. Five replicates were performed to generate the reported data.

5.3.8.7. Thermogravimetric analysis (TGA)

Thermogravimetric analysis (TGA) was carried out using a Q500 from TA Instruments. Sample sizes ranged from 22 to 25 mg. Heating ramp from 25 °C to 700 °C at 10 °/min was used. Nitrogen was used as purging gas.

5.3.8.8. Gel content

Free film specimens and a Soxhlet extraction method were used to measure the gel content of crosslinked networks. A known amount of free film specimen was placed in a pre-weighed cellulose extraction thimble obtained from Whatman® and the thimble containing the sample placed in the Soxhlet extraction apparatus. The extraction apparatus was equipped with a round bottom flask containing 400 mL of toluene and a condenser. The toluene was heated to reflux and the extraction run overnight. The weight of the thimble and sample after extraction was determined after they had been dried in a vacuum oven. Gel content was expressed as the percent weight of the toluene insoluble fraction of the material.

5.3.8.9. Drying time measurement

Drying times of homopolymers with varying molecular weights were recorded according to D1640/D1640M-14 (Method A).

5.3.8.10. Coating property measurement

Chemical resistance was performed with a modified version of ASTM D5402 in which double rubs were performed with a 2-lb ball peen hammer. The cotton cloth was fastened to the ball end of the hammer with a wire, which was dipped in solvent every 25 rubs. Hardness was determined using König pendulum hardness test described in ASTM D4366-16. Impact resistance of the steel coated panels were performed according to ASTM D2794-93. The uncoated side of the panel received the impact (i.e. reverse impact). Flexibility was characterized using the conical

mandrel bend test as described in ASTM D522. Base resistance study was carried out in aq. 3% NaOH solution according to ASTM D1647-89.

5.4. Results and discussion

5.4.1. Synthesis and characterization of monomer and polymer

Synthesis of EEVE was carried out according to Williamson ether synthesis and the schematic is shown in Figure 5.2. Synthesis of EEVE was confirmed from the ^1H NMR spectra shown in Figure 5.6 (a). As shown in Figure 5.6 (a), signals assigned as “K”, $\delta = 6.54$ (q, 1H, $\text{CH}_2=\text{CH-O-}$) and “J”, $\delta = 4.24, 4.08$ (dd, 2H, $\text{CH}_2=\text{CH-O-}$) corresponding to vinyl protons along with “G” and “F” signals at $\delta = 4.05$ (m, 2H, $-\text{O-CH}_2\text{-CH}_2\text{-O-}$) and $\delta = 4.05$ (m, 2H, $-\text{O-CH}_2\text{-CH}_2\text{-O-Ar}$) corresponding the ethyl spacer confirms synthesis of EEVE. Absence of the eugenol starting material was confirmed from the complete disappearance of the Ar-OH signal. FTIR spectra further verified EEVE synthesis and is shown in Figure 5.7 (b). Disappearance of the $-\text{OH}$ signal at around 3455 cm^{-1} along with appearance of the signal at $1618, 1036$ and 850 cm^{-1} corresponding to C=C vinyl stretch, vinyl alkyl ether (C=C-O-C-) symmetric and asymmetric stretch respectively, confirms the successful vinyl functionalization of eugenol.

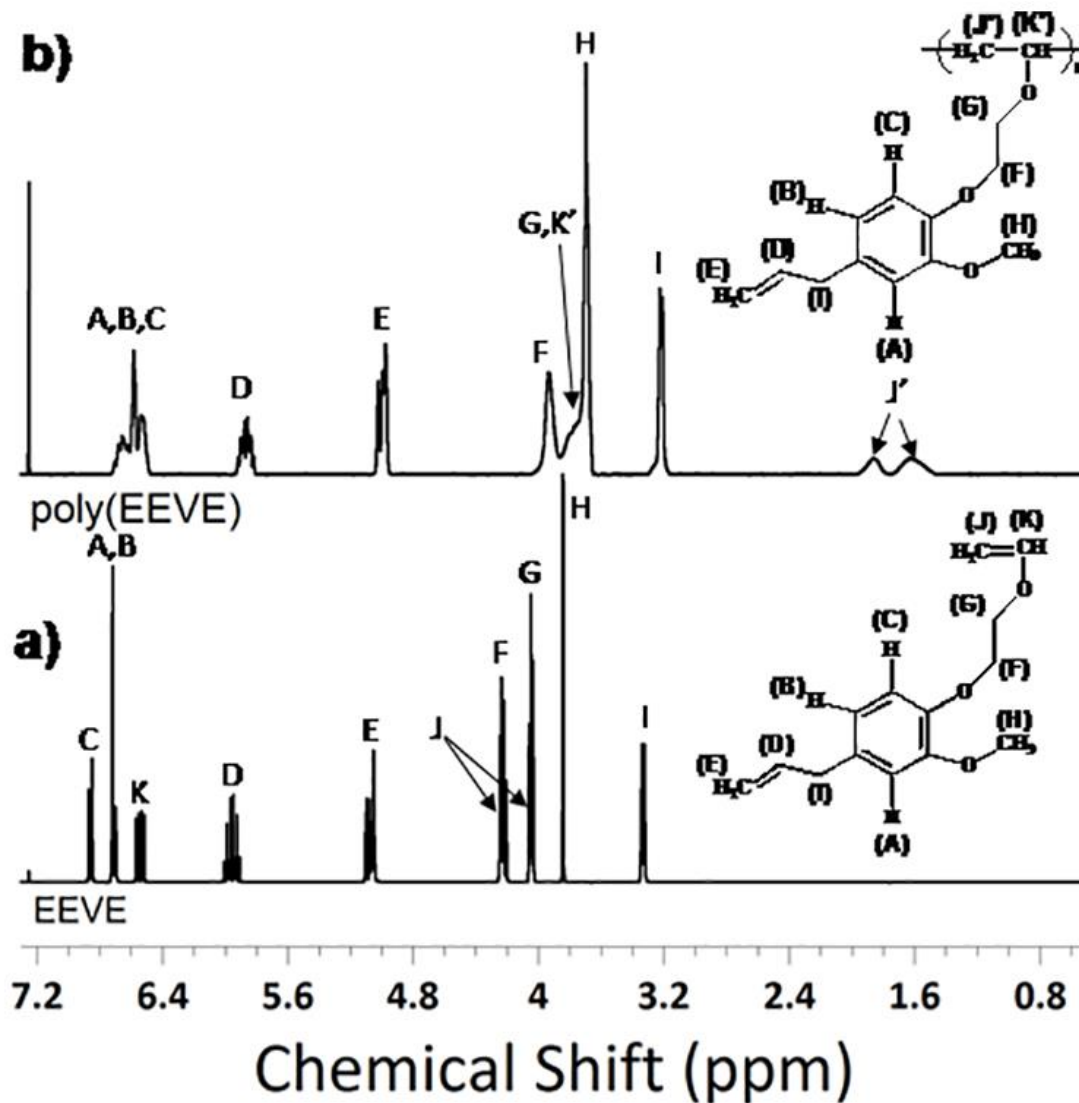


Figure 5.6. ^1H NMR spectra of (a) EEVE and (b) poly(EEVE).

It has been shown by Chernykh et al.³⁴ that utilizing an appropriate cationic polymerization system vinyl ether monomers from plant oil could be polymerized exclusively through the vinyl ether functionality resulting in linear polymers with complete retention of fatty unsaturation. The ability to produce linear bio-based polymers with pendent unsaturation was shown to be very useful for the production of thermoset coatings.^{10, 27-32, 36-39} For example, polymers derived from 2-(vinylloxy)ethyl soyate produced thermoset coatings that cured by autoxidation, due to the presence of the unsaturated fatty acid ester side-chains. Based on this previous work, it was of

interest to utilize a similar approach to produce poly(EEVE) leaving the allylic functionality in each repeat unit. The reaction scheme is shown in **Figure 5.3**. The successful synthesis of poly(EEVE) was confirmed from ^1H NMR and FTIR. ^1H NMR spectrum [**Figure 5.6 (b)**] of poly(EEVE) confirmed the downfield shift and broadening of the “J” and “K” signals to $\delta \sim 1.74$ and 3.87 respectively, these newly appeared signals assigned as “J” and “K” confirms the incorporation of vinyl double bond in the polymer backbone chain. ^1H NMR was also used to determine the occurrence of any side reactions during the polymerization involving the allylic substituent on the aromatic ring of EEVE. Specifically, chemical shifts and integration values associated with peaks “I,” “E,” and “D” were determined before and after polymerization. For a highly reactive carbocation, it might be expected that addition to the allyl double or hydride abstraction from the allyl methylene group would be possible side reactions. ^1H NMR results showed that these side reactions were not significant, indicating that carbocations generated during the polymerization were sufficiently stabilized to prevent these side reactions. FTIR spectrum of poly(EEVE) shown in **Figure 5.7 (c)** confirms the disappearance of the peaks at 1618 cm^{-1} (vinyl $C=C$ stretch), 1036 (vinyl alkyl ether, asymmetric) and 850 cm^{-1} (vinyl alkyl ether, symmetric) and retention of the peaks at 1637 cm^{-1} (allyl $C=C$ stretch); 1590 , 1513 , 1463 and 1452 cm^{-1} (aromatic $C=C$ stretch) confirmed the successful synthesis of poly(EEVE) exclusively through the vinyl ether group.

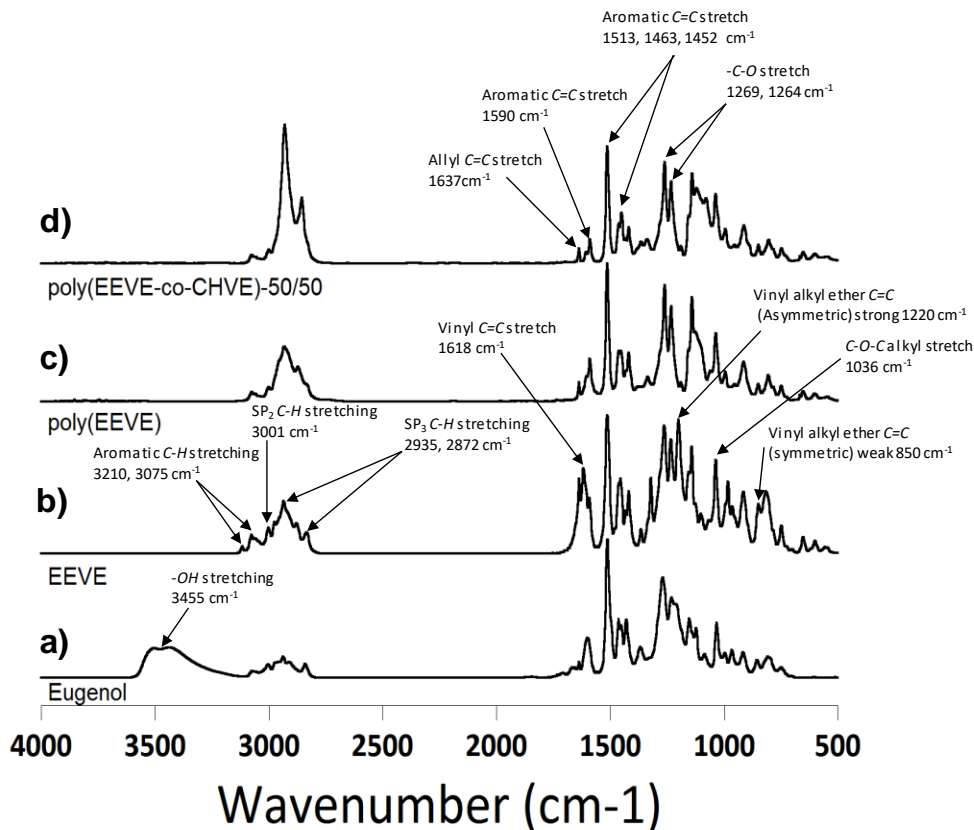


Figure 5.7. FTIR spectra of (a) eugenol, (b) EEVE, (c) poly(EEVE) and (d) poly(EEVE-co-CHVE)-50/50.

Three statistical copolymers were produced using cationic polymerization with CHVE as a comonomer using the reaction scheme shown in **Figure 5.4**. CHVE was selected as a comonomer since it is commercially available and expected to provide more rigidity than EEVE repeat unit to the backbone chain due to the absence of the ethyl spacer which can provide some flexibility. Although, promising in increasing the rigidity thereby T_g of the polymers incorporation of higher amount of CHVE repeat units might result in less crosslinked networks with poor film and coating properties. Therefore, a proper balance between EEVE repeat units (to provide crosslinking) and CHVE (T_g) was important. Three different copolymers with varying compositions reported in **Table 5.2** was synthesized to investigate the effect of incorporation CHVE repeat units in the final coating and film properties.

In **Figure 5.8** characteristic ^1H NMR spectrum of poly(CEVE-co-CHVE) copolymers are shown and the presence of signals associated with poly(EEVE) especially allylic protons (“E”, “D” and “J”) and poly(CHVE) along with backbone proton signals (“L”, “G” and “I”) confirms the formation of copolymers. Concentration of the incorporated EEVE and CHVE repeat units were calculated by integrating the well-resolved signal at δ 5.01 designated as “E” from the EEVE allyl group and the signal at δ 1.19 designated as “N” signals from CHVE. Using these integration values, final composition of the poly(EEVE-co-CHVE)-75/25, poly(EEVE-co-CHVE)-50/50 and poly(EEVE-co-CHVE)-25/75 copolymers were found to be 73/27 and 46/54 and 22/78 wt.% respectively.

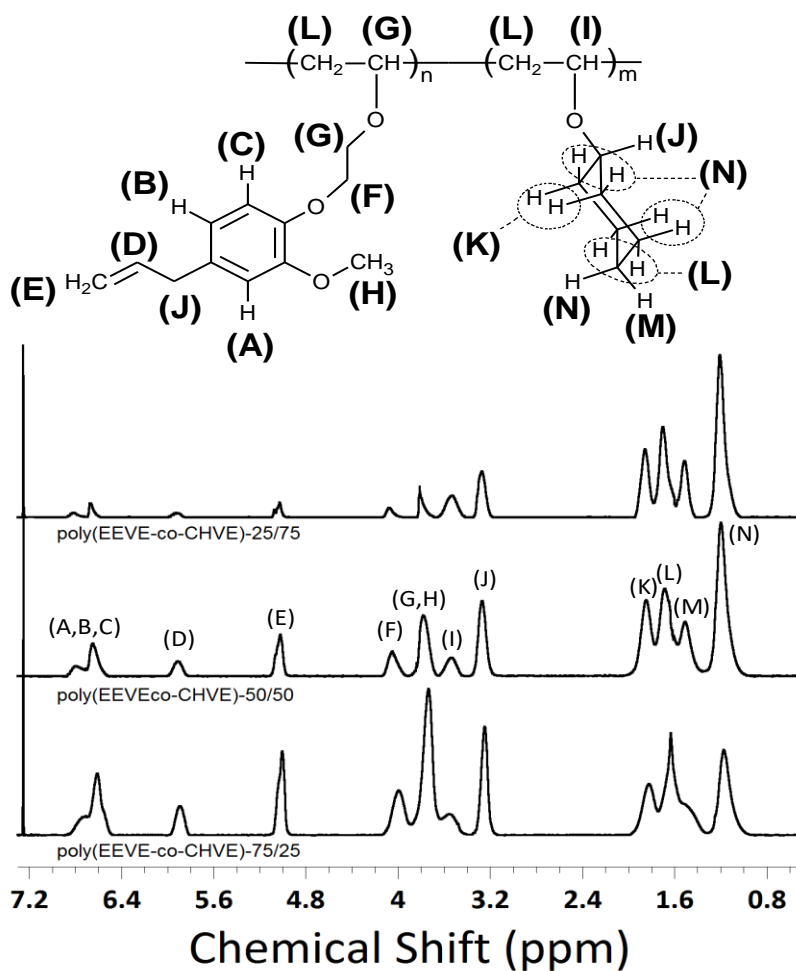


Figure 5.8. ^1H NMR spectra of the three copolymers of EEVE and CHVE.

Successful synthesis of copolymers was also confirmed from FTIR analysis. An FTIR spectrum of poly(E EVE-co-CHVE)-50/50 is shown in **Figure 5.7** (d) which confirms the presence of EEVE repeat units due to the signals at 1637 cm^{-1} (allyl $C=C$ stretch); 1590 , 1513 , 1463 and 1452 cm^{-1} (aromatic $C=C$ stretch) and CHVE repeat units due to significantly high normalized intensity of the sp^2 C-H stretching signals at 2985 and 2872 cm^{-1} compared to poly(E EVE) normalized signals.

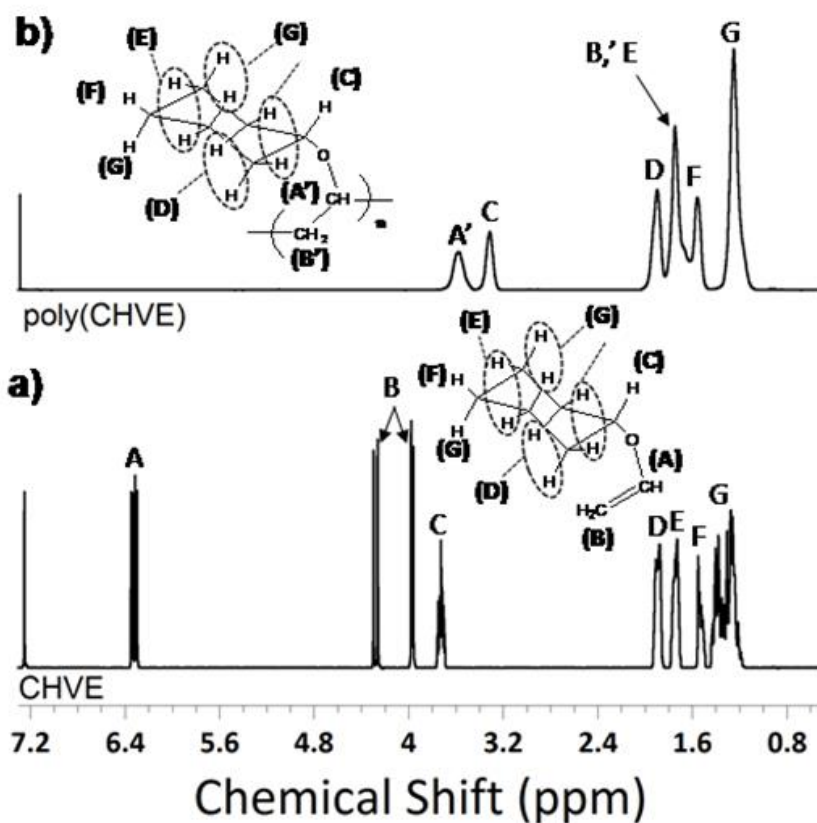


Figure 5.9. ^1H NMR spectra of (a) CHVE and (b) poly(CHVE).

Successful synthesis of poly(CHVE) was confirmed from ^1H NMR shown in **Figure 5.9** (b). As shown in **Figure 5.9** (b), the ^1H NMR spectrum of poly(CHVE) confirmed the disappearance of “A” and “B” signals corresponding to the CHVE [**Figure 5.9** (a)] vinyl protons signals (**Figure 5.7**) and appearance of the “A” and “B” backbone proton signals with retention of the proton signals associated with cyclohexyl ring.

5.4.2. GPC analysis

Both number average molecular weight (M_n) and polydispersity index of the five polymers were measured and the values are reported in **Table 5.4**. As reported in **Table 5.4** polymers possessed a monomodal [**Figure 5.10 (a)**], very narrow polydispersity index (PDI) (i.e. $PDI < 1.1$). The M_n s of all four polymers was very similar and ranged from 24.6 kDa to 30.3 kDa, which was similar to the target molecular weight of 30 kDa. Although specific experiments to determine if the polymerizations were living polymerizations were not carried out, the high yields ($>95\%$), narrow PDIs, and consistency between the actual M_n and predicted M_n based on monomer to initiator ratio suggest living polymerizations or at least long-lived polymerizations.

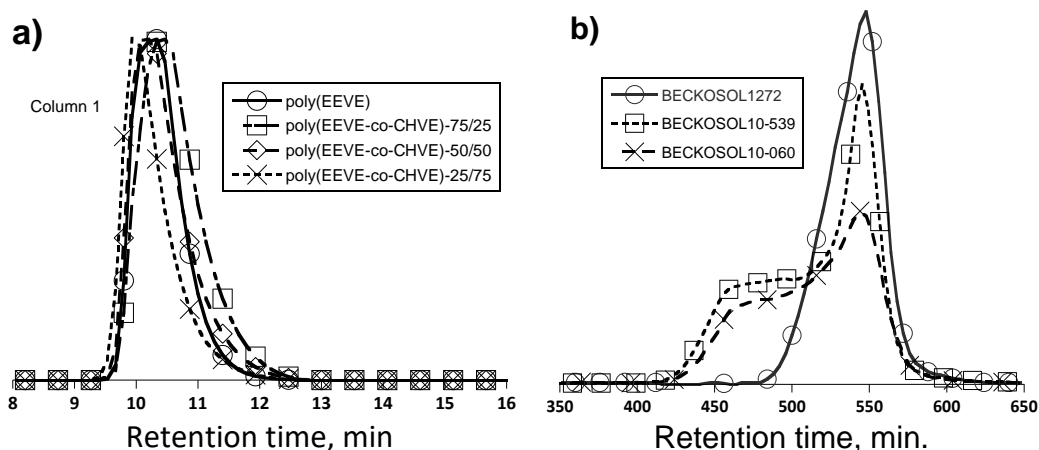


Figure 5.10. GPC chromatograms for poly(EEVE), (a) poly(CEVE-co-CHVE) copolymers, and (b) three commercial alkyds.

In case of commercial alkyds [**Figure 4.10 (b)**], chromatograms from BECKOSOL 10-539 and BECKOSOL 10-060 showed broad molecular weight distributions. Both chromatograms showed a main peak associated with short oligomeric polymer chains $M_n \sim 2.58$ kDa and a shoulder depicting the presence of longer chain polymers with M_n from 20 to 21 kDa. Presence of polymer chains with wide range of molecular weights from 2.5 to 21 kDa resulted in broad polydispersity. BECKOSOL 1272 resulted a monomodal chromatogram however, with high PDI of 1.72. This

high polydispersity along with low molecular weight of ~2.45 kDa indicated that the chains were oligomeric in nature.

Table 5.4. Mn and PDI of the synthesized polymers and commercial alkyd resins.

Polymer ID	Mn (Da or g/mole)	PDI
poly(E EVE)	27,578	1.06
poly(E EVE-co-CHVE)-75/25	24,645	1.09
poly(E EVE-co-CHVE)-50/50	26,568	1.05
poly(E EVE-co-CHVE)-25/75	30,300	1.07
BECKOSOL 10-539	2,587 and 21,000	1.71 and 1.05
BECKOSOL 10-060	2,356 and 20,562	1.80 and 1.06
BECKOSOL1772	2,458	1.72

5.4.3. Thermal properties of EEVE monomer and polymers

DSC thermogram of EEVE (**Figure 5.11**) resulted in two melting points at around 17 °C and 26 °C confirming the crystallinity of EEVE monomers. The early melting with an onset at 9 °C might due to the presence of imperfect crystals.

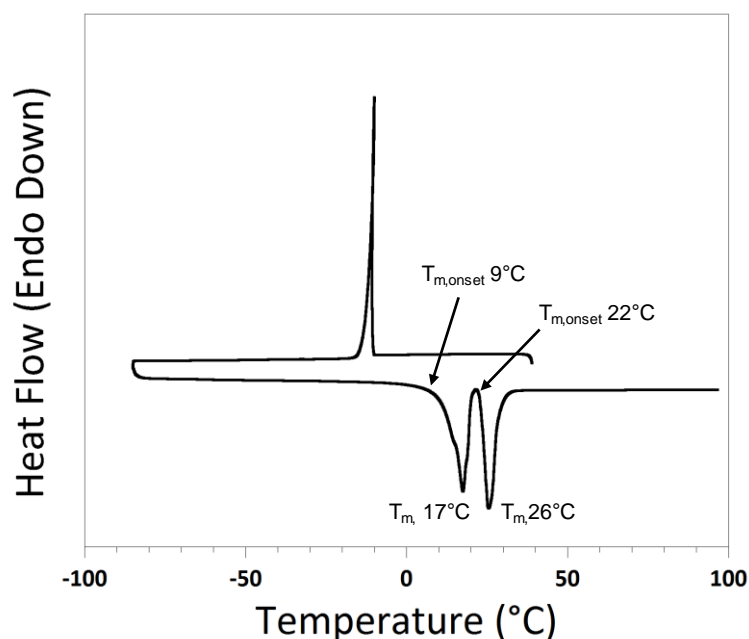


Figure 5.11. DSC thermogram of 2-vinyloxy ethyl vinyl ether (EEVE).

The thermal properties of the polymers were characterized using DSC and TGA. For comparison purposes, a poly(CHVE) sample was also produced and characterized. **Figure 5.12**

(a) displays the DSC thermograms obtained and the T_g s measured. These thermograms show that the T_g of the copolymers increase with increasing concentration of CHVE repeat units. This trend is consistent with expectations based on the T_g s calculated from Fox equation using the T_g s of the two homopolymers, poly(E EVE) and poly(CHVE). Clearly the ethyl spacer between the poly(vinyl ether) backbone and the eugenol pendent group enables greater segment mobility of the polymer backbone than a cyclohexyl ring directly attached to the poly(vinyl ether) backbone. The T_g range of the polymers containing EEVE repeat units is similar to that of many crosslinkable polymers and oligomers used for surface coatings. Crosslinkable polymers/oligomers with T_g s in this range typically provide smooth, high-gloss coatings that have the potential to penetrate porous substrates and provide excellent adhesion when cast from solution.^{9, 10, 26, 27, 31, 37}

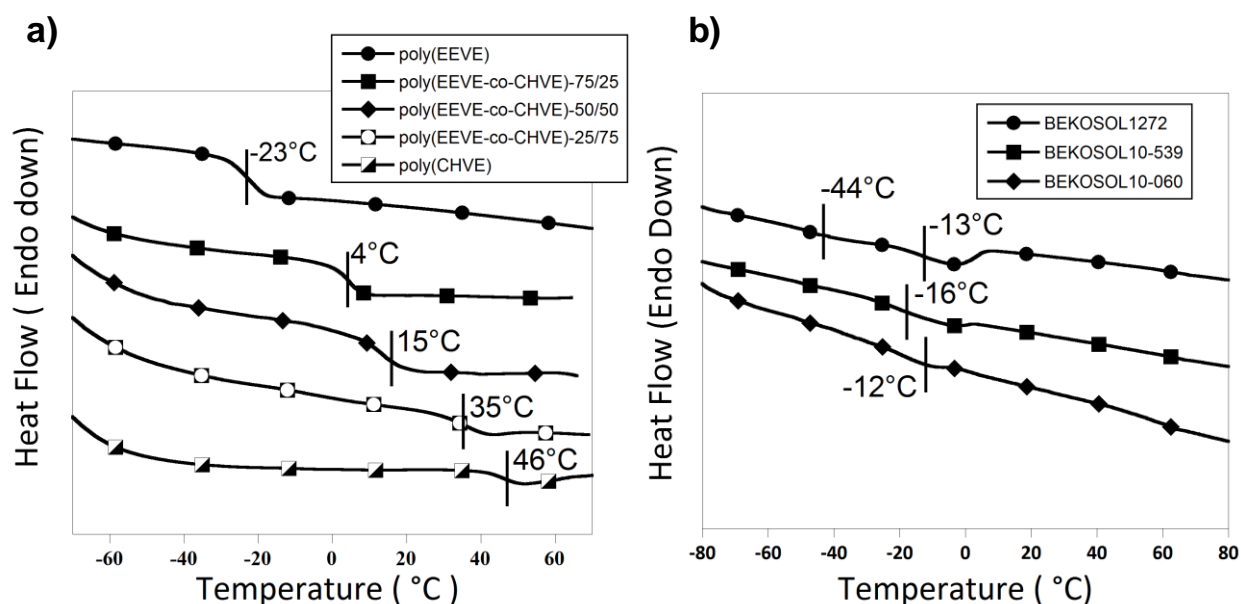


Figure 5.12. DSC thermograms obtained for all the (a) polymers produced and (b) commercial alkyds.

Thermal stability was characterized using TGA by heating samples in a nitrogen atmosphere. As shown in **Figure 5.13**, poly(CHVE) resulted 5% weight loss at 280 °C while poly(E EVE) showed higher thermal stability with 5% weight loss at 370 °C. Incorporation of CHVE

repeat units resulted in early degradation of the polymers i.e. lowering in thermal stability. This early degradation of copolymer might be attributed from the decomposition of CHVE around 280 °C to ethylene, butadiene, 1-hexene etc.⁴⁰

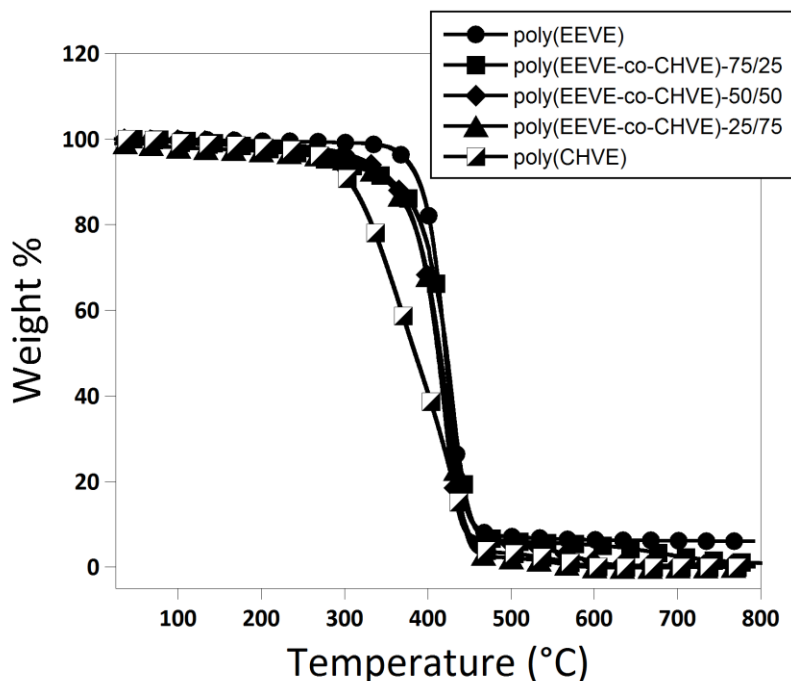


Figure 5.13. TGA thermograms for all of the polymers produced.

5.4.4. Study of autoxidation of poly(E EVE)

It was hypothesized that polymers derived from EEVE would be capable of crosslinking through autoxidation. As shown in **Figure 5.14**, abstraction of a proton from the allylic methylene of an EEVE repeat unit produces a free radical that is highly resonance stabilized. This is very similar to the situation that exists for the bis allylic hydrogen atoms in polyunsaturated fatty acid esters that have been identified as being critical for the relatively rapid crosslinking of alkyd coatings by autoxidation. Analogous to oxidative crosslinking of alkyd coatings this stabilized radical is expected react with oxygen in the atmosphere to produce a peroxide radical that subsequently undergoes that same propagation and termination reactions that result in a crosslinked network.

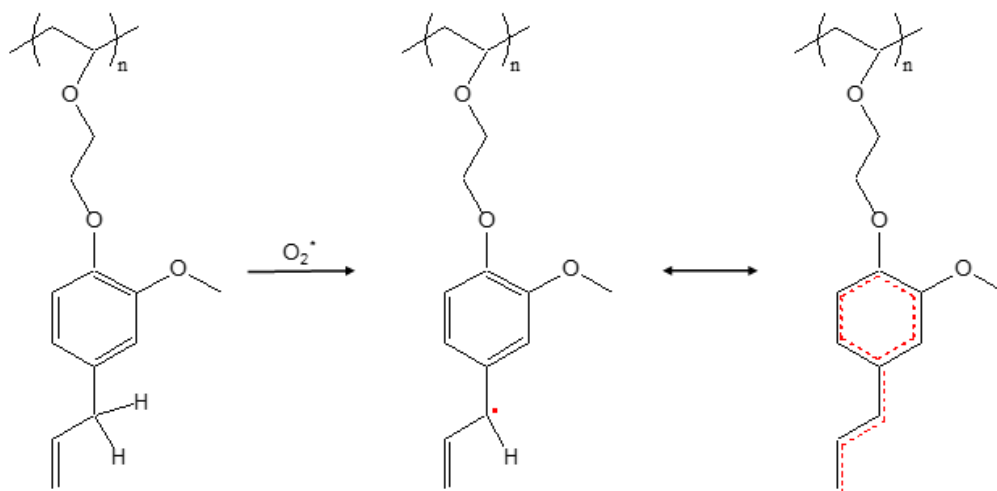


Figure 5.14. Illustration of resonance stabilization of a radical generated by hydrogen abstraction by singlet oxygen.

This hypothesis was confirmed by evaluating the FTIR spectra taken at different time intervals from the same poly(EEVE) sample mixed with drier package (Co, Zr and Zn based previously used to make coating formulation) casted on a KBr disk. FTIR spectra taken immediately after mixing poly(EEVE) with drier catalyst (zero hour), after 24, 72 h and normalized based on the peak at 1513 cm^{-1} corresponding to aromatic $C=C$ stretch are shown in **Figure 5.15**. The spectrum taken at zero time was subtracted from spectra taken at 24 and 72 h and from the resulting difference spectra (**Figure 5.15**) it could be confirmed that there was a decrease in the intensity of the signal corresponding to $C=C$ allylic stretch (1637 cm^{-1}). In addition, the appearance of signals characteristic for $-O-H/-O-O-H$ stretch (3412 cm^{-1}),⁴¹ alpha unsaturated ketone (1672 cm^{-1}),^{42,43} and $C-O$ stretch were also observed. These changes in signals can only be explained by considering an autoxidation mechanism where radicals formed due to abstraction of labile protons which then capture oxygen forms a peroxy radical. These peroxy radicals during propagation abstract another proton forming hydroperoxides which can break down to give products like ketone, aldehyde, alcohol etc.

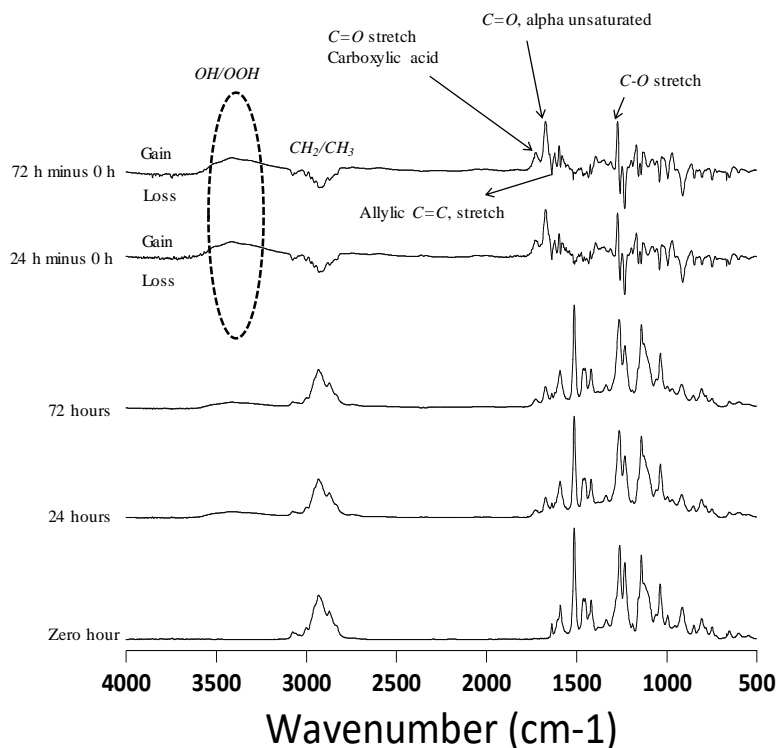


Figure 5.15. FTIR spectra of poly(E EVE) with catalyst taken at different time intervals along with difference spectra from the one taken at zero time.

5.4.5. Drying time measurements

As reported in **Table 5.5**, drying time of poly(E EVE) and poly(E EVE-co-CHVE) copolymers were significantly shorter than the commercial alkyds. **Poly(E EVE)** showed a tack free time of 1434 min which was very high compare to set to touch time which was only 21 min. This longer tack free time of poly(E EVE) might have attributed from its subzero T_g ($-23\text{ }^\circ\text{C}$) making it behave like sticky, viscous material. The tack free time of poly(E EVE) was reduced significantly to 163 min by incorporation 25 wt.% CHVE repeat units which had a T_g of $4\text{ }^\circ\text{C}$. Since incorporation of CHVE reduced the number of reactive functionality there by improving in drying time must have to be attributed from its improvement in T_g . Similarly, decreasing trend in drying time was observed with increasing CHVE repeat units in the copolymer i.e. increase in T_g . Among the commercial alkyds BECKOSOL 1272, being oligomeric in nature showed the longest

tack free time ~ 2500 min (i.e. >40 h). However, other two commercial alkyds BECKOSOL 10-539 and BECKOSOL 10-539 having longer polymeric chains (higher molecular weight) resulted shorter tack free time than BECKOSOL 1272 but still 10 to 15 times longer than poly (EEVE-co-CHVE)-50/50.

Table 5.5. Drying time measurement data for polymers with drying catalyst.

Polymer	Set to touch time (min.)	Dust free time (min.)	Tack free time (min.)
poly(EEVE)	21	57	1434
poly(EEVE-co-CHVE)-75/25	6	10	163
poly(EEVE-co-CHVE)-50/50	4	5	59
poly(EEVE-co-CHVE)-25/75	1	1	18
BECKOSOL 1227	1740	2052	2532
BECKOSOL 10-539	412	652	832
BECKOSOL 10-060	116	411	651

5.4.6. Viscoelastic properties of crosslinked free-films

The viscoelastic properties of the crosslinked networks produced from poly(EEVE), copolymers, and the commercial alkyd resins were evaluated using DMA. The storage moduli plots of the cured films are shown in **Figure 5.16 (a-f)** and tangent δ responses are shown in **Figure 5.17 (a-f)** represents the, illustrating the effect of cure conditions and CHVE repeat unit content on viscoelastic responses. Two primary parameters, T_g and crosslink density, were obtained from the DMA thermograms. For most of the networks, storage moduli (E') plots showed slight increase with temperature ($^{\circ}\text{C}$) after the transition which might be attributed from additional crosslinking as the crosslink density vs temperature plots [**Figure 5.18 (a-e)**] plots showed an increasing trend and is more prominent for films cured at elevated temperature and compositions with CHVE repeat units. This type of curing behavior during DMA analysis was previously reported by Soucek et al. for plant oil based air dried coatings.² Despite of it, networks clearly indicate the presence of plateau regions above T_g , confirming the formation of a well crosslinked network. Crosslink

density was calculated by using the following equation (Eq. 5.1) in accordance with the theory of rubbery elasticity.^{44, 45} The value for storage modulus was taken at 60 °C above the T_g to measure crosslink density. T_g and crosslink density values for all the networks produced are reported in

Table 5.6.

$$\nu = E'/(3RT) \quad (5.1)$$

Where, ν is the crosslink density, defined as the moles of crosslinks per unit volume of material, R is the universal gas constant, E' (Pa) is storage modulus in the rubbery plateau region, and T (K) is the temperature corresponding to the storage modulus value.

Table 5.6. Properties showing the T_g, XLD and gel content of the cured films produced from commercial alkyd resin, poly(E EVE), and poly(E EVE-co-CHVE) copolymer. One set of networks was produced by curing at ambient conditions for 4 weeks, while the other set was cured by heating for an hour at 120 °C and an hour at 150 °C then allowing the coatings to stand at ambient conditions for 4 weeks.

Sample	Curing temperature	T _g (°C)	XLD (moles/cm ³)	Gel content (%)
BECKOSOL 1272	23 °C	16.6	1.32x10 ⁻⁴	63.24± 7.0
	120 °C	19.0	3.10x10 ⁻⁴	78.16± 5.6
	150 °C	27.2	5.25x10 ⁻⁴	85.80±5.0
BECKOSOL 10-060	23 °C	32.3	2.24x10 ⁻⁴	64.59±6.2
	120 °C	34.7	3.85x10 ⁻⁴	84.50±7.5
	150 °C	39.6	8.86x10 ⁻⁴	86.12±6.3
BECKOSOL 10-539	23 °C	35.0	4.98x10 ⁻⁴	70.10±3.0
	120 °C	35.7	7.74x10 ⁻⁴	86.99±2.2
	150 °C	35.8	8.69x10 ⁻⁴	89.73±4.1
Poly(E EVE)	23 °C	42.6	2.88x10 ⁻⁴	67.65±1.6
	120 °C	47.2	10.07x10 ⁻⁴	77.53±2.5
	150 °C	55.5	15.45x10 ⁻⁴	94.96±1.8
Poly(E EVE-co-CHVE)-75/25	23 °C	47.4	2.08x10 ⁻⁴	83.02±1.7
	120 °C	42.4	2.98x10 ⁻⁴	83.15±2.4
	150 °C	39.1	3.27x10 ⁻⁴	84.82±2.0
Poly(E EVE-co-CHVE)-50/50	23 °C	46.7	1.09x10 ⁻⁴	21.79±1.0
	120 °C	42.6	0.27x10 ⁻⁴	26.97±1.5
	150 °C	36.0	-	28.11±2.4
Poly(E EVE-co-CHVE)-25/75	23 °C	-	-	1.88±0.3
	120 °C	-	-	1.92±0.5
	150 °C	-	-	1.98±0.6

As reported in **Table 5.6** both T_g and XLD for the commercial alkyds showed an increasing trend with curing temperature. Among the commercial alkyds BECKOSOL 1272 showed lowest T_g that might be resulted from its oligomeric nature. Compare to commercial alkyds cured films from poly(EEVE) showed higher T_g and its increased from ~ 42 °C to ~ 55 °C with increasing the curing temperature from RT to 150 °C. This higher T_g of poly(EEVE) networks was attributed from their comparatively higher crosslink density. However, higher T_g of poly(EEVE) network cured at RT compared to the BECKOSOL 10-060 and BECKOSOL 10-539 networks cured at elevated temperatures could not be justified based on XLD, as based on XLD this trend should have been other way round. This higher value of T_g associated with poly(EEVE) network at comparatively lower XLD might be due to the presence of phenyl rings as a part of the crosslinked networks providing rigidity to the crosslinked system compared to commercial alkyds with long fatty chains.

Further evaluation of the extent of crosslinking was carried out by measuring the gel contents of the cured films. For comparison purposes, data from commercial alkyd resins were also generated. The networks from poly(EEVE) showed gel content results (**Table 5.6**) that were essentially the same as that of the commercial alkyd, which indicates that the polymer is capable of forming crosslinked networks through the process of autoxidation. For the three EEVE-based copolymers, gel content was highly dependent on EEVE repeat unit content with gel content decreasing with decreasing EEVE repeat unit content. Since it is the EEVE repeat units that contain the chemical moieties that form the crosslinked network, this trend in gel content is not surprising. For the commercial alkyd and poly(EEVE) homopolymer, heating at 120 °C and 150 °C for one hour increased the gel content. In contrast, the gel content of networks derived from the EEVE/CHVE copolymers showed little to no increase in gel content when the curing included this

high temperature step. Increasing the CHVE repeat unit from 25 to 75 % drastically reduced the gel content along with decreasing the T_g . However, decrease in T_g was not so prominent as expected from reduced XLD which might be attributed from the rigidity of the backbone chains provided by the cyclohexyl groups directly attached to them. Similar effect was observed in case of T_g s of the neat EEVE/CHVE copolymers.

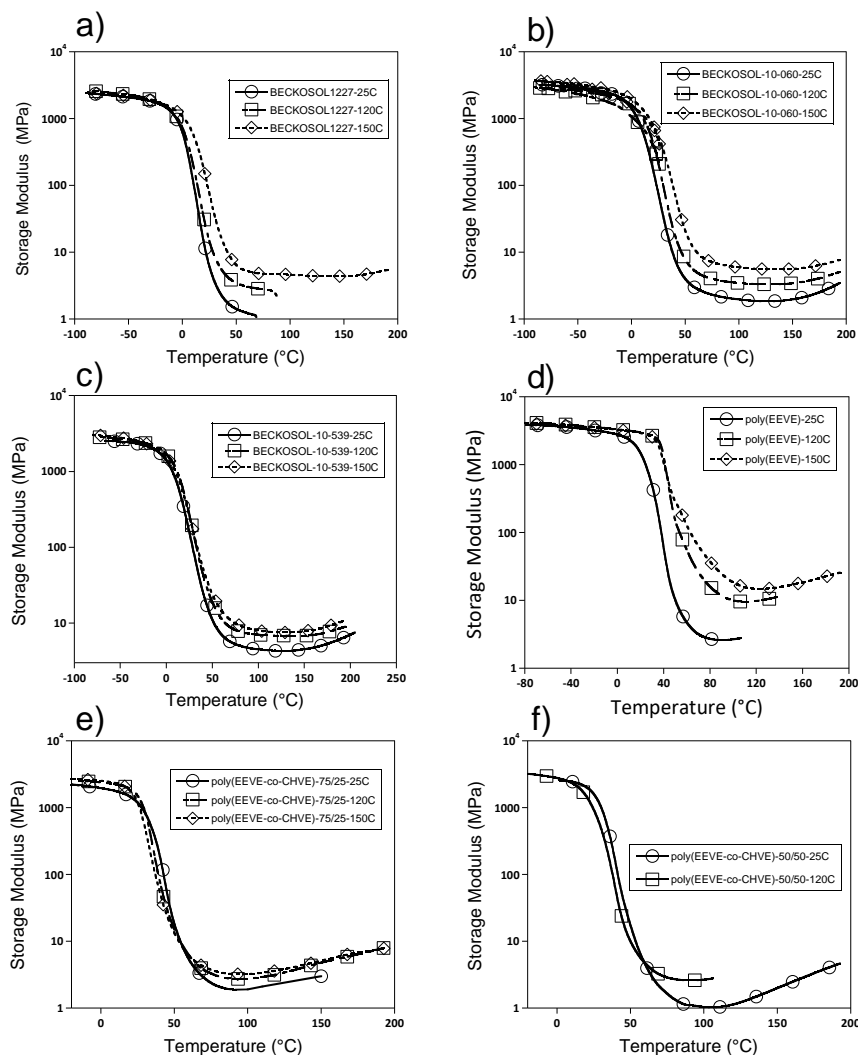


Figure 5.16. Representative storage modulus thermogram plots derived from (a) BECKOSO1272, (b) BECKOSO 10-539, (c) BECKOSO 10-539 (c), (d) poly(EEVE), (e) poly(EEVE-co-CHVE)-75/25 and (f) poly(EEVE-co-CHVE)-50/50 cured at RT, 120 for 1 h, and 150 °C for 1 h.

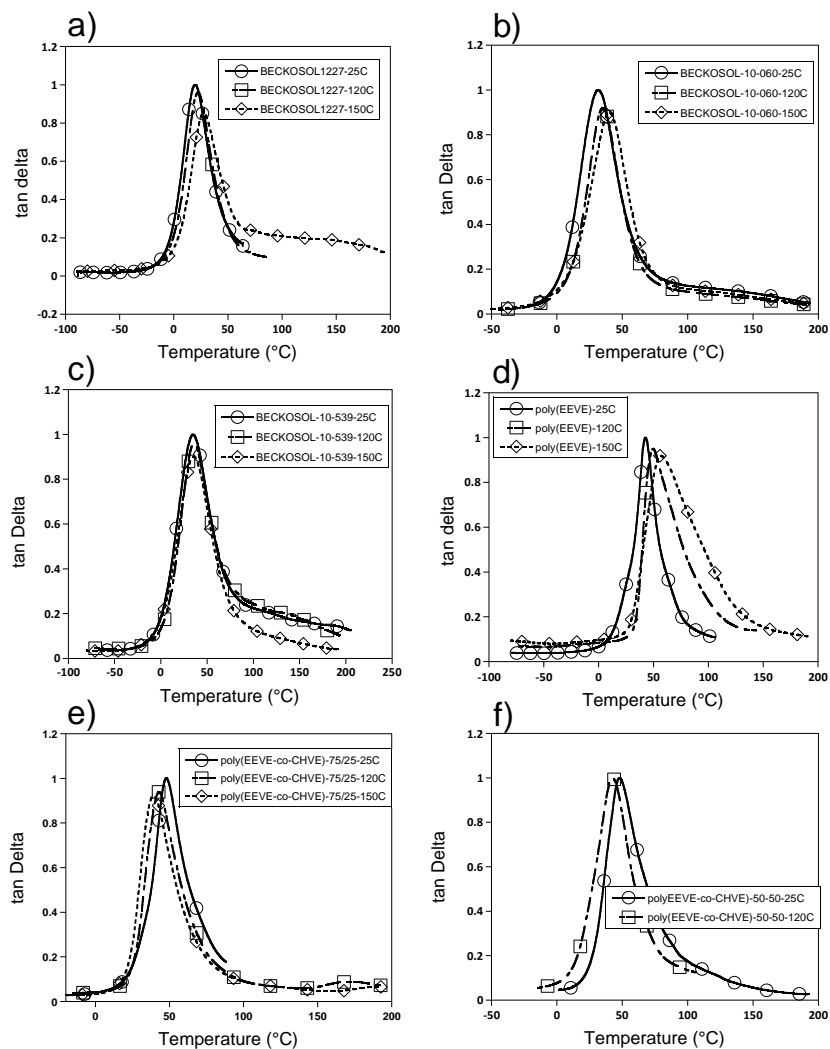


Figure 5.17. Representative $\tan \delta$ plots derived from (a) BECKOSO 1272, (b) BECKOSO 10-539, (c) BECKOSO 10-539 (c), (d) poly(E EVE), (e) poly(E EVE-co-CHVE)-75/25 and (f) poly(E EVE-co-CHVE)-50/50 cured at RT, 120 for 1 h, and 150 °C for 1 h.

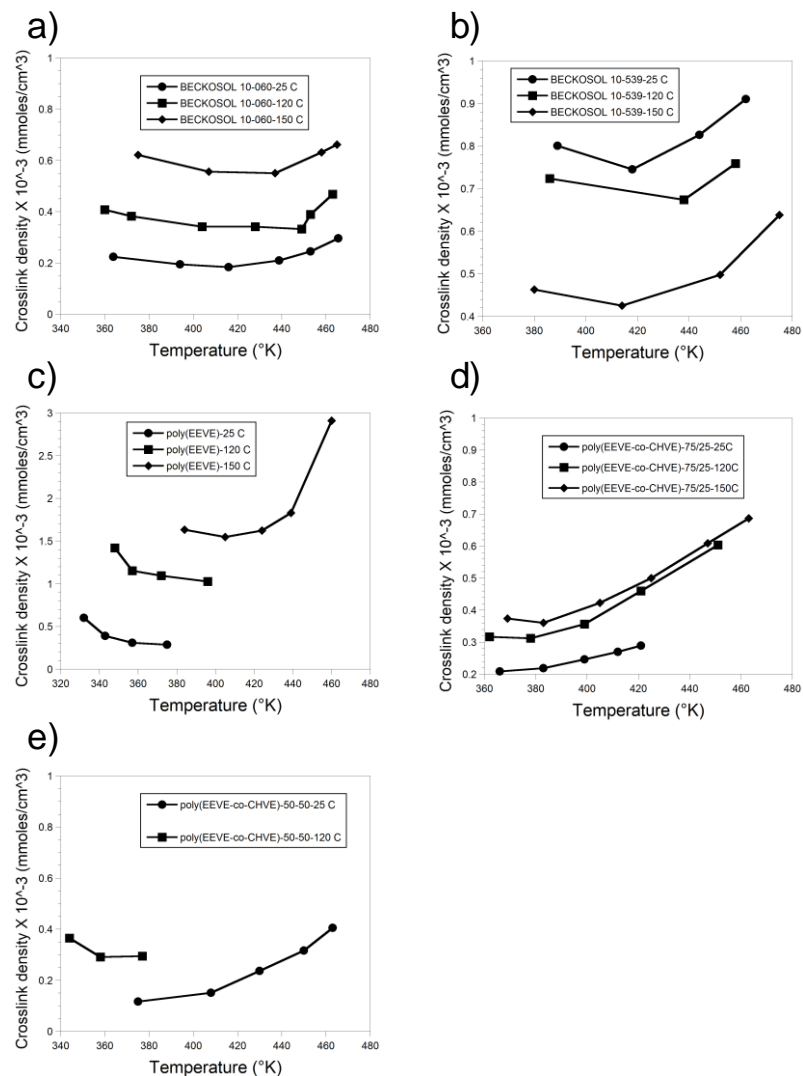


Figure 5.18. Plots showing variation in XLD with temperature during the DMA analysis for the films produced from (a) BECKOSO 10-060, (b) BECKOSO 10-539, (c) poly(E EVE), (d) poly(E EVE-co-CHVE)-75/25 and (e) poly(E EVE-co-CHVE)-50/50 cured at RT, 120 for 1 h, and 150 °C for 1 h.

5.4.7. Mechanical properties of cured films

Bulk mechanical properties of the thermosets were determined by stamping out dog bone type samples from the free films and analyzing their stress vs strain behavior. Representative stress-strain curves of the films from poly(E EVE), poly(E EVE-co-CHVE) copolymers and, for comparison, commercial alkyds cured at RT are shown in **Figure 5.19**. The nature of these tensile stress-strain curves varies significantly with varying the composition and curing temperature.

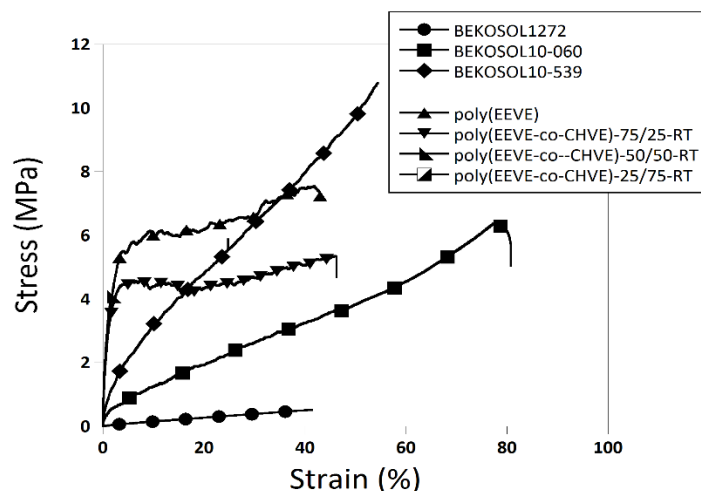


Figure 5.19. Stress as a function of elongation for representative crosslinked networks derived from the commercial alkyd resins, poly(E EVE), and poly(E EVE-co-CHVE) copolymers. All samples were cured at ambient conditions for 4 weeks before testing.

As shown in **Figure 5.19**, networks produced from BECKOSOL 10-539 and BECKOSOL 10-539 showed very high elasticity compared to BECKOSOL 1272 which showed soft, brittle failure. This high ductility of commercial alkyds had been attributed to their high crosslink density and long fatty chains allowing them to behave like rubbery material. Compared to commercial alkyd, networks derived from poly(E EVE) showed ductile nature with very high stiffness. As reported in **Table 5.7**, compared to commercial alkyds, poly(E EVE) network cured at RT resulted ~ 10 times higher Young's modulus which increased up to ~15 times for the networks when cured at 150 °C for an hour. This increase in modulus might be attributed to the formation of higher XLD networks which on the other hand reduced the elongation from ~ 40 to ~14 percent. However, networks derived from CHVE incorporated copolymers tend to show ductile deformation along with strain hardening. However, networks derived from 25 wt.% CHVE repeat units showed better ductility along with higher elongation. This increased ductility of the networks with incorporation of CHVE repeat units is due to the dilution of the reactive groups resulting in a network with relatively lower crosslink density. This dilution in XLD of the networks also result in decrease in Young's modulus to some extent.

Table 5.7. Young's modulus, tensile strength and elongation of the networks derived from the commercial alkyd resin, poly(EEVE), and poly(EEVE-co-CHVE) copolymer. One set of networks was produced by curing at ambient conditions for 4 weeks, while the other set was cured by heating for an hour at 120 °C and an hour at 150 °C then allowing the coatings to stand at ambient conditions for 4 weeks.

Sample	Curing temperature	Young's Modulus (MPa)	Tensile strength (MPa)	Elongation (%)
BECKOSOL 1272	23 °C	1.6±0.3	0.6±0.3	45.2±16.2
	120 °C	3.6±0.8	1.5±0.8	48.7±20.9
	150 °C	6.1±4.2	2.9±1.3	53.9±10.8
BECKOSOL 10-060	23 °C	25.1±3.9	6.7±0.5	83.9±8.5
	120 °C	34.5±14.7	13.4±0.9	76.1±2.3
	150 °C	41.2±18.9	14.0±2.1	77.8±6.1
BECKOSOL 10-539	23 °C	15.4±5.9	7.1±2.9	54.7±4.2
	120 °C	36.3±6.2	9.4±2.7	46.3±17.9
	150 °C	89.2±12.2	12.6±1.3	41.9±1.2
Poly(EEVE)	23 °C	485.5±84.3	7.5±0.9	40.1±9.6
	120 °C	889.9±67.5	13.4±0.9	15.6±1.8
	150 °C	619.4±95.0	10.2±0.1	14.6±5.6
Poly(EEVE-co-CHVE)-75/25	23 °C	477.0±44	5.8±1.2	59.1±17.5
	120 °C	491.7±35	7.3±0.9	55.2±7.3
	150 °C	472.4±59	6.9±1.2	46.1±14.5
Poly(EEVE-co-CHVE)-50/50	23 °C	671.3±160	4.1±0.6	2.3±0.1
	120 °C	867.2±125	6.2±0.8	1.7±0.6
	150 °C	887.1±177	7.0±1.2	1.6±0.3
Poly(EEVE-co-CHVE)-25/75	23 °C	862.3±64.5	2.6±0.2	0.6±0.2
	120 °C	1184.5±38.8	2.7±0.4	0.2±0.2
	150 °C	-	-	-

Compare to poly(E EVE) and 25 wt.% CHVE repeat unit incorporated networks which showed ductile nature, networks derived with 50 and 75 wt.% CHVE repeat units showed hard, brittle failure with very low elongation. This brittle nature of the films might be attributed from the very low crosslink density of the networks. Surprisingly, these networks resulted in very high Young's modulus which must be attributed from the rigidity of the networks attributed from the CHVE repeat units directly attached to the backbone chains.

5.4.8. Coatings properties

Each of the four synthesized polymers and commercial alkyd resins were coated onto steel substrates and cured using three different curing temperatures. The adhesion, hardness (pencil and pendulum), flexibility, chemical resistance, and impact strength were determined using industry standard methods. Development of solvent resistance as a function of time for coatings derived from the commercial alkyd resin, poly(E EVE), and poly(E EVE-co-CHVE) copolymers are shown in **Figure 5.20**. As shown in **Figure 5.20** MEK double rubs (MEK DRs) for the commercial alkyds increased linearly up to two weeks and then the values reached a plateau confirming very slow development of the crosslink density. On the other hand, networks derived from poly(E EVE) and poly(E EVE-co-CHVE) copolymers showed slow development of MEK DRs at the beginning similar to the commercial alkyds. However, unlike commercial alkyds these networks showed significant increase in MEK DRs after certain time period which might be consider as if the networks reached the gel point. This intensity of improvement in MEK DRs decreased with increasing the CHVE repeat units which might be due to decrease in no of reactive functionality however, the time of transition increased. Networks derived poly(E EVE) and poly(E EVE-co-CHVE)-75/25 resulted almost three times higher solvent resistance after 4 weeks compared to commercial alkyds.

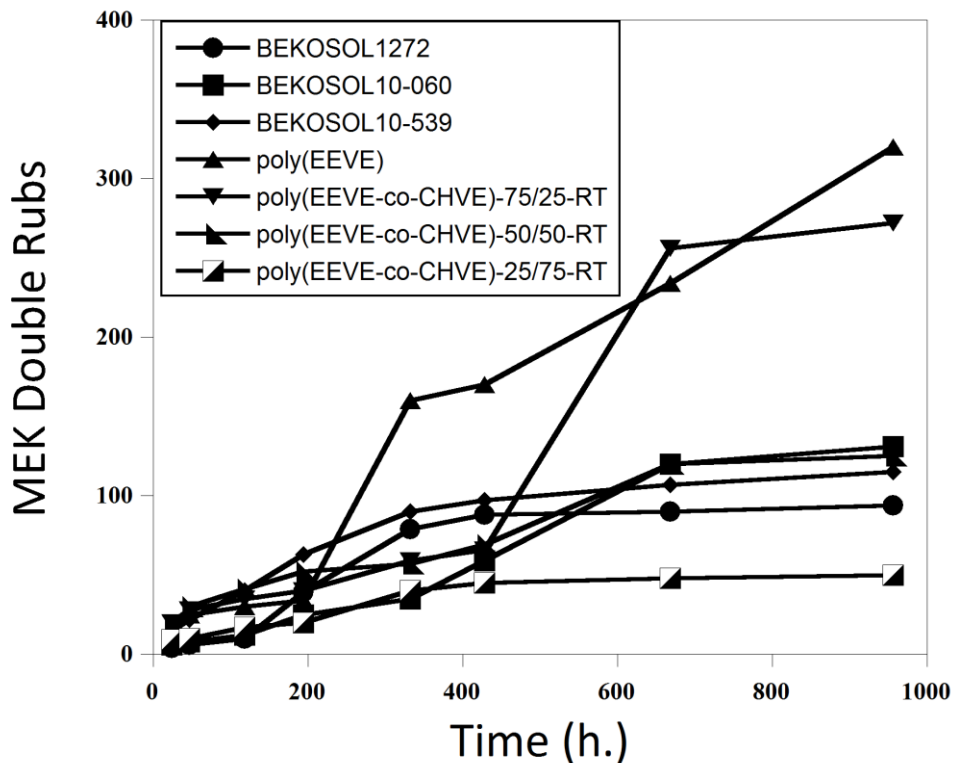


Figure 5.20. A comparison of the solvent resistance as a function of time for coatings derived from the commercial alkyd resin, poly(E EVE), and poly(E EVE-co-CHVE) copolymer. Solvent resistance was measured according to ASTM method D5420 (i.e. MEK double rub test).

The results from conical mandrel bend (ASTM D522) and reverse impact (ASTM D2794), crosshatch adhesion (ASTM D3359), König pendulum hardness (ASTM D4366-16) and MEK DRs (ASTM D5420) are reported in **Table 5.8**. Coatings derived from commercial alkyds showed very high flexibility (32%), as well as 172 in-lbs impact maxima as evidenced from the lack of cracking or delamination. This excellent impact resistance and flexibility might be the result of the presence of long pendent chains which have enough segmental mobility to dissipate the impact energy within the timeframe of the event. These coatings also showed very good cross hatch adhesion (5B).

As are reported in **Table 5.8**, both poly(E EVE) and poly(E EVE-co-CHVE)-75/25 networks showed crosshatch adhesion of 5B and flexibility slightly lower for coatings at RT

however, improved to 32% with curing at elevated temperatures. Flexibility showed a decreasing trend with increasing CHVE repeat units. Impact resistance of poly(E EVE) coatings were low for the coatings cured at RT which improved with increasing curing temperature. CHVE incorporated coatings resulted very low impact resistance which was expected due significantly decrease in XLD and glassy behavior at RT (T_g higher than RT).

The trends observed with respect to pendulum hardness and impact resistance were very interesting. Pendulum hardness involves the measurement of the amount of time required to dissipate the rocking motion of two stainless steel balls put into motion by releasing a pendulum. Thus, pendulum hardness is essentially a measurement of the viscoelastic properties of the coating. Coatings exhibiting a relatively high viscous response to the stress induced by the steel balls would be expected to more effectively dissipate that stress, resulting in a relatively low pendulum hardness value. Therefore, coatings with higher crosslink density should have better pendulum hardness as higher crosslinking will reduce the segmental movement i.e. less damping. Using this information, an expected trend will be poly(E EVE) > commercial alkyds > poly(E EVE-co-CHVE)-75/25 > poly(E EVE-co-CHVE)-50/50 > poly(E EVE-co-CHVE)-50/50. However, as reported in **Table 5.8**, an opposite trend of poly(E EVE) < poly(E EVE-co-CHVE)-75/25 < poly(E EVE-co-CHVE)-50/50 < poly(E EVE-co-CHVE)-25/75 was observed where, pendulum hardness increased with incorporation of CHVE repeat units. This anomaly can be explained by considering the fact that both poly(E EVE) and poly(E EVE-co-CHVE)-75/25 resulted networks which can undergo plastic deformation i.e. viscous compared to poly(E EVE-co-CHVE)-50/50 and poly(E EVE-co-CHVE)-25/75 networks which behave very brittle i.e. glassy. It is due to this glassy nature of the higher CHVE incorporated networks which is attributed to higher pendulum hardness.

Chemical resistance of the coatings evaluated using MEK double rub method showed impact from both the amount of incorporated CHVE and curing temperature. Compared to the commercial alkyds, poly(E EVE) networks cured at RT showed three times higher solvent resistance which increased doubly for the coatings cured at 150 °C. However, incorporation of CHVE repeat units tend to reduce solvent resistance due to decrease in crosslink density of the resulted networks. Incorporation of 25 wt.% resulted a threshold point up to networks could show better solvent resistance than commercial alkyds. Incorporation of higher amount of CHVE repeat units significantly decreased the solvent resistance further below the commercial alkyds.

Table 5.8. Properties of coatings derived from the commercial alkyd resin, poly(E EVE), and poly(E EVE-co-CHVE) copolymer.

Sample	Curing temperature	Thickness (µm)	Cross hatch Adhesion (0B-5B)	Conical mandrel bend (0%-32%)	MEK DRs (no)	König pendulum hardness (sec)	Reverse impact (in-lbs)
BECKOSOL 1272	23 °C	127±1.1	5	32	85±8	9±0.2	172
	120 °C	140±6.7	5	32	134±6	11±1.5	172
	150 °C	100±2.1	5	32	186±6	13±0.1	172
BECKOSOL 10-060	23 °C	94±6.8	5	32	155±9	18±4.4	172
	120 °C	110±1.6	5	32	177±8	23±2.1	172
	150 °C	105±3.1	5	32	254±5	25±1.2	172
BECKOSOL 10-539	23 °C	127±11.3	5	32	110±4	23±0.0	172
	120 °C	101±1.5	5	32	136±5	32±0.0	172
	150 °C	105±2.6	5	32	162±16	34±0.0	172
Poly(E EVE)	23 °C	129±6.7	5	17	405±5	24±0.6	8
	120 °C	127±5.1	5	32	1021±12	21±0.0	12
	150 °C	131±3.5	5	32	1528±25	33±2.6	20
Poly(E EVE-co-CHVE)-75/25	23 °C	141±2.1	5	13	287±2	28±1.2	6
	120 °C	141±3.7	5	32	176±15	21±0.0	4
	150 °C	117±2.2	5	32	273±6	44±2.0	4
Poly(E EVE-co-CHVE)-50/50	23 °C	123±6.4	5	12	123±6	46±0.6	4
	120 °C	139±0.4	4	8	69±2	60±1.7	4
	150 °C	126±2.5	4	8	86±6	63±5.5	4
Poly(E EVE-co-CHVE)-25/75	23 °C	133±5.5	4	1	49±2	70±0.0	4
	120 °C	138±0.8	3	1	49±4	161±2.9	4
	150 °C	135±1.2	3	1	48±3	173±3.8	4

Base resistance of the coatings derived poly(E EVE), poly(E EVE-co-CHVE) copolymers and commercial alkyds cured at RT were evaluated by exposing 3"x3" coating by masking the rest with tape to prevent any diffusion to an aq. 3% NaOH solution according to ASTM D1647-89. As shown in **Figure 5.21** commercial alkyd coatings dissolved after 15 min of exposure however, coatings derived from poly(E EVE) showed minor whitening after 24 h compared to poly(E EVE-co-CHVE) copolymers which did not show any whitening, blistering, color change even gloss loss after 24 h exposure to 3% NaOH solution. This high base resistance of EEVE or EEVE/CHVE derived coatings compared to alkyd coatings might be attributed from the chemically stable carbon-carbon backbone and ether linkages which is not susceptible to hydrolysis compared to polyester backbone.

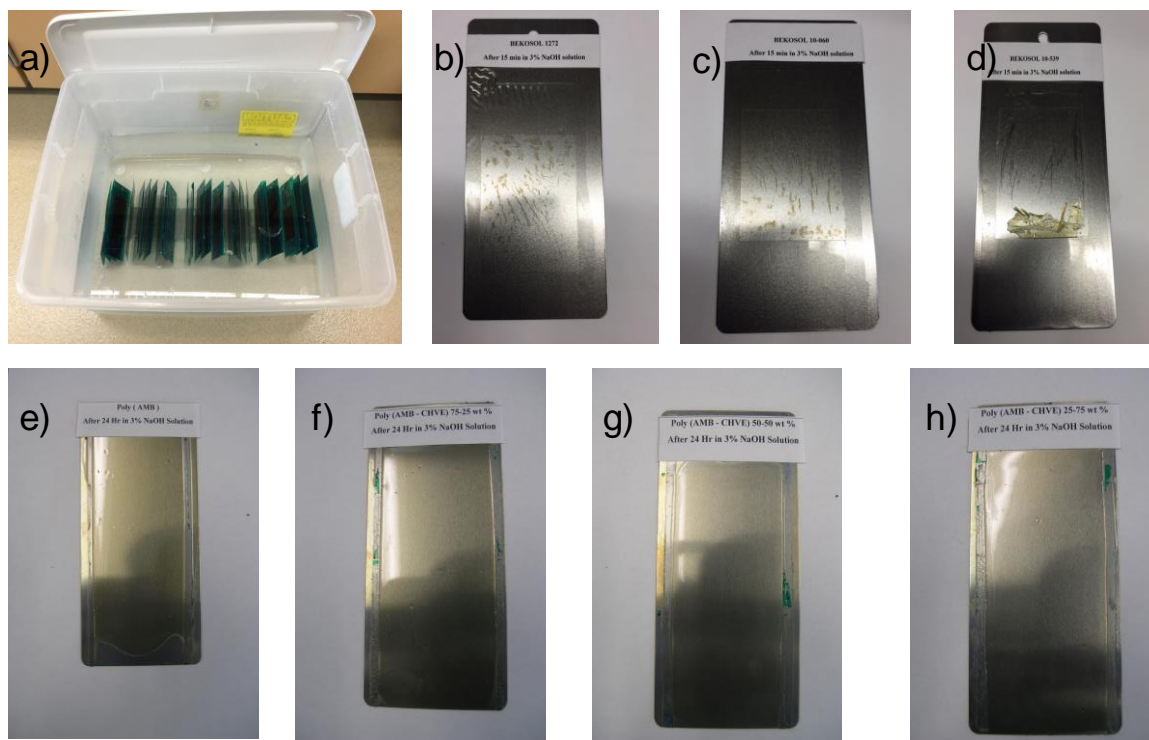


Figure 5.21. Picture of (a) Coatings exposed to 3% NaOH solution, (b) BECKOSOL 1272 coating after 15 min, (c) BECKOSOL 10-060 coating after 15 min, (d) BECKOSOL 10-539 coating after 15 min, (e) poly(E EVE) coating after 24 h, (f) poly(E EVE-co-CHVE)-75/25 coating after 24 h, (g) poly(E EVE-co-CHVE)-50/50 coating after 24 h, and (h) poly(E EVE-co-CHVE)-25/75 coating after 24 h.

5.5. Conclusions

As desired, polymerization of EEVE and copolymerization with CHVE provided coating resins that enabled crosslinked networks via autoxidation with a significantly higher chemical resistance and hardness, base resistance, T_g , modulus as compared to commercial alkyds. Overall, it was found that both polymer composition and cure temperature significantly affected coatings properties. With regard to polymer composition, the results indicate that an optimum balance between thermal, mechanical, and physical properties can be obtained by tuning the ratio of CEVE and CHVE in the copolymer. For example, increasing the CHVE repeat unit content from 0 to 25 % in the copolymer improves the T_g , hardness, base resistance and ductility of the free films. However, mechanical behavior of the free films showed ductile to brittle transition with incorporation of 50 and higher wt.% of CHVE repeat units due to increase the rigidity of the polymer chains and result in low crosslink density networks. Coatings derived from poly(EEVE) and copolymer with 25 wt.% CHVE repeat units resulted in better properties than commercial alkyd resins.

5.6. References

1. A. Hofland, *Progress in Organic Coatings*, 2012, **73**, 274-282.
2. M. D. Soucek, T. Khattab and J. Wu, *Prog. Org. Coat.*, 2012, **73**, 435-454
3. J. Mallegol, J. Lemaire and J. L. Gardette, *Progress in Organic Coatings* 2000, **39**, 107–113.
4. S. D. Hirahumira, *Journal of Polymer Science*, 1982, **21**, 35–74.
5. M. A. R. Meier, J. O. Metzger and U. S. Schubert, *Chemical Society Reviews*, 2007, **36**, 1788-1802.

6. M. Galia, L. M. D. Espinosa, J. C. Ronda, G. Lligadas and V. Cadiz, *Eur. J. Lipid Sci. Technol.*, 2010, **112**, 87–96.
7. S. J. Park, F. L. Jin and J. R. Lee, *Materials Science and Engineering: A*, 2004, **374**, 109-114.
8. E. Kaya, S. K. Mendon, D. Delatte, J. W. Rawlins and S. F. Thames, *Macromolecular Symposia*, 2013, **324**, 95-106.
9. H. Kalita, S. Alam, D. Kalita, A. Chernykh, I. Tarnavchyk, J. Bahr, S. Samanta, A. Jayasooriyama, S. Fernando, S. Selvakumar, A. Popadyuk, D. S. Wickramaratne, M. Sibi, A. Voronov, A. Bezbaruah and B. J. Chisholm, in *Soy-Based Chemicals and Materials*, American Chemical Society, 2014, **1178**, 371-390.
10. H. Kalita, S. Alam, D. Kalita, A. Chernykh, I. Tarnavchyk, J. Bahr, S. Samanta, A. Jayasooriyama, S. Fernando, S. Selvakumar, A. Popadyuk, D. S. Wickramaratne, M. Sibi, A. Voronov, A. Bezbaruah and B. J. Chisholm, *ACS Symposium Series*, 2014, **1178**, 731-790.
11. S. Grishchuk, J. K. Kocsis, *eXPRESS Polymer Letters* 2011, **5**, 2-11.
12. S. L. Kristufek, K. T. Wacker, Y. T. T. Tsao, L. Su and K. L. Wooley, *Natural Product Reports*, 2017, **34**, 433-459.
13. A. Gandini and T. M. Lacerda, *Progress in Polymer Science*, 2015, **48**, 1-39.
14. A. Gandini, T. M. Lacerda, A. J. F. Carvalho and E. Trovatti, *Chemical Reviews*, 2016, **116**, 1637-1669.
15. G. S. Martins, E. A. Vara and J. C. Duarte, *Ind. Crops Prod.*, 2008, **27**, 189-195.
16. M. P. Pandey and C. S. Kim, *Chemical Engineering & Technology*, 2011, **34**, 29-41.

17. A. L. Holmberg, K. H. Reno, N. A. Nguyen, R. P. Wool and T. H. Epps, *ACS Macro Letters*, 2016, **5**, 574-578.
18. H. Chung and N. R. Washburn, *Green Materials*, 2013, **1**, 137-160.
19. Z. Sun, B. Fridrich, A. D. Santi, S. Elangovan, and K. Barta, *Chemical Reviews Article ASAP*.
20. X. Huang, T. I. Korányi, M. D. Boot and E. J. M. Hensen, *ChemSusChem*, 2014, **7**, 2276-2288.
21. K. Okuda, M. Umetsu, S. Takami and T. Adschiri, *Fuel Processing Technology*, 2004, **85**, 803-813.
22. J. S. Dordick, M. A. Marletta and A. M. Klivanov, *Proceedings of the National Academy of Sciences*, 1986, **83**, 6255-6257.
23. P. J. Deuss, M. Scott, F. Tran, N. J. Westwood, J. G. de Vries and K. Barta, *Journal of the American Chemical Society*, 2015, **137**, 7456-7467.
24. T. S. Kaufman and *J. Braz. Chem. Soc.*, 2015, **26**, 1055-1085.
25. S. Samanta, S. Selvakumar, J. Bahr, D. S. Wickramaratne, M. Sibi and B. J. Chisholm, *ACS Sustainable Chemistry and Engineering*, 2016, **4**, 6551-6561.
26. S. Alam, H. Kalita, O. Kudina, A. Popadyuk, B. J. Chisholm and A. Voronov, *ACS Sustainable Chemistry & Engineering*, 2013, **1**, 19-22.
27. S. Alam, H. Kalita A. Jayasooriya, S. Samanta, J. Bahr, A. Chernykh, M. Weisz and B. J. Chisholm, *European Journal of Lipid Science and Technology*, 2014, **116**, 2-15.
28. S. Alam and B. J. Chisholm, *Journal of Coatings Technology and Research*, 2011, **8**, 671-683.

29. H. Kalita, S. Alam, D. Kalita, A. Chernykh, I. Tarnavchyk, J. Bahr, S. Samanta, A. Jayasooriyama, S. Fernando, S. Selvakumar, D. S. Wickramaratne, M. Sibi and B. J. Chisholm, *European Coatings Journal*, 2015, **6**, 26-29.
30. H. Kalita, A. Jayasooriyama, S. Fernando and B. J. Chisholm, *Journal of Palm Oil Research*, 2015, **27**, 39-56.
31. D. Kalita, I. Tarnavchyk, D. Sundquist, S. Samanta, J. Bahr, O. Shafranska, M. Sibi and B. Chisholm, "Novel biobased poly(vinyl ether)s for coating applications, *INFORM*, 2015, **26**, 472-475. 2014.
33. A. Popadyuk, H. Kalita, B. J. Chisholm and A. Voronov, *International Journal of Cosmetic Science*, 2014, **36**, 547-555.
34. A. Chernykh, S. Alam, A. Jayasooriya, J. Bahr and B. J. Chisholm, *Green Chemistry*, 2013, **15**, 1834-1838.
35. S. Aoshima and T. Higashimura, *Macromolecules*, 1989, **22**, 1009-1013.
36. H. Kalita, A. Jayasooriyamu, S. Fernando, S. Samanta, J. Bahr, S. Alam, M. Sibi. J. Vold, C. Ulven and B. J. Chisholm, *Green Chemistry*, 2014, **16**, 1974-1986.
37. H. kalita, S. Alam, A. Jayasooriyamu, S. Fernando, S. Samanta, J. Bahr, S. Selvakumar, M. Sibi, J. Vold, C. Ulven and B. J. Chisholm, *Journal of Coatings Technology and Research*, 2015, **12**, 633-646.
38. B. J. Chisholm, H. Kalita, D. Kalita, S. Alam, A. Chernykh, I. Tarnavchyk, J. Bahr, S. Samanta, A. Jayasooriyama, S. Fernando, S. Selvakumar, D. Suranga Wickramaratne and M. Sibi, *Coatings World*, 2015, **20**, 48-54.
39. R. V. Gorkum and E. Bouwman, *Coord. Chem. Rev.*, 2005, **249**, 1709-1728.
40. W. Tsang, *International Journal of chemical Kinetics* 1978, **10**, 1119-1138.

41. J. H. Hartshorn, *Journal of Coatings Technology*, 1982, **54**, 53-58.
42. R. V. Gorkum and E. Bouwman, *Coordination Chemistry Reviews*, 2005, **249**, 1709-1728.
43. C. W. Fritsch and F. E. Deatherage, *Journal of the American Oil Chemists Society*, 1956, **33**, 109-113.
44. T. Murayama, *Dynamic Mechanical Analysis of Polymeric Materials*, Elsevier, Amsterdam, The Netherlands, 1978.
45. L. W. Hill, *J. Coat. Technol.*, **64**, 29-41.

CHAPTER 6. A HIGH THROUGHPUT APPROACH TO STUDY THE EFFECT OF CURATIVES AND LEVELS OF EPOXIATION ON THE PROPERTIES OF THE COATINGS DERIVED FROM EUGENOL

6.1. Abstract

A novel bio-based vinyl ether monomer, 2-eugenoloxyl vinyl ether (EEVE), was synthesized from eugenol, a bifunctional bio-based molecule. The synthesis of the homopolymer from EEVE was carried out using cationic polymerization exclusively via the vinyl ether functionality leaving the allylic double bonds intact. The allylic double bonds were further converted to epoxide using *m*-chloroperoxybenzoic (mCPBA) acid using mild conditions. Usually, full conversion of the double bonds to epoxy functionality is a time-consuming process and prone to side reactions, so, in this study epoxidized poly(EEVE) were made with 3 levels of epoxidation: 30, 50 and 70 %, respectively. These polyepoxides were used to produce two-component, amine-cured coatings and their properties were compared to a reference coating based on the diglycidyl ether of bisphenol-A (DGEBA). Coatings were prepared via curing with twelve amine curatives of aliphatic, cycloaliphatic, aromatic and polyether nature. Cured coatings were then tested using “high throughput” methods such as dye extraction and nano-indentation to evaluate the structure-property relationships. Conventional coatings testing methods, mainly König pendulum hardness and differential scanning calorimetry (DSC), were used to cross verify the trends observed in high throughput experiments. In the case of epoxidized poly(EEVE) [Epoly(EEVE)] compounds coatings properties can be tuned from soft and elastic to hard and brittle by varying the extent of epoxidation as well as by varying the nature of curative from flexible aliphatic or polyether to rigid cycloaliphatic or aromatic amines. Both crosslink density and hardness values were higher for coatings prepared with Epoly(EEVE) resins with 50% or higher percent epoxidation than coatings

prepared from DGEBA resin using the same curative and curing regime. Thus, these environmentally friendly epoxy compounds have the potential to be competitive with DGEBA resin derived from petrochemicals in a number of potential applications.

6.2. Introduction

Recent years have witnessed the need for thermosetting resins which can provide improved chemical, thermal, mechanical and electrical properties etc. Among different thermosetting networks, epoxy resins have been considered as one of the most versatile thermosetting polymers in the world.¹ Epoxy networks have been extensively used in various applications such as coatings, adhesives, flooring and paving applications, materials for electronics, and high-performance composite materials.²⁻⁹ The properties of these thermosetting resins can be easily tailored to obtain the desired ultimate properties such as high modulus, strength, durability, thermal and chemical resistance as provided by high cross-link density.¹⁰⁻¹³ Due to their crosslinked networks thermosets cannot be reshaped.^{11, 14} Most of the epoxy networks are derived from petroleum origin and are often suspected of being hazardous.¹⁵ The diglycidyl ether of bisphenol A (DGEBA), which accounts for more than 90 % of the volume of epoxy resins, is produced by reacting bisphenol A (BPA) with epichlorohydrin. BPA and epichlorohydrin have been studied extensively for their toxicity and are found to be carcinogenic, mutagenic, and reprotoxic (CMR).¹⁶⁻¹⁸ BPA itself is suspected to be an endocrine disruptor making adverse effect to health and environment. yet it is produced at over one billion pounds per year in just the USA.^{19, 20} Recently, DGEBA has been recognized as a group 3 carcinogen classified by the International Agency for Research on Cancer.¹⁸ These adverse effects on health and environment along with their dependency on fossil fuels for raw materials which are depleting every day has pushed the scientific community to search for potential replacements of BPA based resins mainly with those made from sustainable

materials. A growing effort is being made particularly for the development of partially or fully bio-based epoxy thermosets.²¹

To, achieve properties similar to those provided by petroleum based compounds, researchers are constantly exploring renewable materials containing aromatic fragments such as cardanol,^{22, 23} vanillin and its derivatives,²⁴ lignin derivatives²⁵ and eugenol²⁶ as sustainable alternatives to DGEBA. Lignin, due to its complex phenolic structure has been considered as one of the most abundant substitutes for phenolic based resins. Being the cell-wall component, lignin provides well-known rigidity and impact resistance to the stems. Although, lignin is highly available as a waste by-product especially from the paper industries, so far only 1-2% of it has been utilized for specific applications whereas the rest has been used as (bio) fuel.²⁷

In recent years, eugenol has been extensively used in pharmaceutical industry, food industry, perfume industry and also as therapeutic medicine, antioxidant, food ingredient etc. due to its properties like reduction of blood sugar, triglyceride, cholesterol levels, aroma etc.²⁸⁻³¹ Mostly obtained from clove oil, it has an annual market value of US\$30-70 million per year which keeps increasing due to recent research showing its availability as a lignin derivative and potential to be obtained via enzymes.³²

With the need for the development of novel materials within a narrow timeline, researchers have developed new experimental methodologies involving the rapid synthesis and evaluation of large numbers of compounds in parallel using robotics, rapid analytical instrumentation, and data management software. Although, mostly used by the pharmaceutical industry for the development of new drugs to reduce the time and cost, these new high throughput methodologies have been adopted by the researchers in polymer and coating industry for materials development, and its use continues to increase.³³ High throughput experimentation has become a powerful tool to explore

large parameter spaces and to identify structure–property relationships.³⁴ Recently, Stafslie et al.³⁵ reported the development of novel surface coatings using a high throughput multiwell plate screening method to rapidly assess bacterial biofilm retention on antifouling surfaces. Evaluation of cross-linkers for polyurethane dispersions and in a separate study development of catalyst for and 1K PUR coatings utilizing dye extraction as a high throughput screening method was reported by Bach et al.^{36, 37} and was found to be very efficient. The relative difference in crosslink density between various crosslinked systems were evaluated by quantifying the amount of dye extracted from each system using an appropriate solvent for a definite period. Higher dye extraction indicates lower crosslink density. High throughput instrumentation such as depth-sensing indentation has been used extensively for probing of mechanical properties of surface coatings such as the elastic modulus and creep compliance. Depth sensing indentation, involves the measurement of penetration depth into a material surface by applying load on a rigid indenter. One of the advantages of this technique is the requirement of small amounts of sample material along with sequential measurements over one or many samples.^{34, 38}

In this work, the synthesis of a novel vinyl ether monomer from eugenol and its polymerization via a cationic mechanism is described. One of the advantages of this approach as reported previously by Alam et al.³⁹ is that the polymerization proceeds exclusively through the vinyl ether group leaving the allylic functionality for further derivatization. The synthesized homopolymer was converted to epoxy resins by taking advantage of the allylic double bond; the epoxidation was targeted at three different levels by varying the amount of reagent. The final properties of the coatings developed from epoxy resins are known to depend on the type of curatives and curing regime, therefore in this work the synthesized epoxy polymers were cured with twelve curatives using two temperatures and five curing times. Coatings were then evaluated

using both high throughput and conventional methods and were compared to the coatings derived from DEGBA using the same curatives and curing conditions.

6.3. Experimental

6.3.1. Materials

The materials used for the study are described in **Table 6.1**. Unless specified otherwise, all materials were used as received.

Table 6.1. A description of the starting materials used for the study.

Chemical	Designation	Vendor
4-Allyl-2-methoxyphenol, 99%	Eugenol	Alfa Aesar
2-Chloroethyl vinyl ether	2-Chloroethyl vinyl ether	TCI
3-Chloroperoxybenzoic acid, $\leq 77\%$	mCPBA	Sigma-Aldrich
Bisphenol A diglycidyl ether	EPON 828	Momentive
Perylene, 98+%	Perylene	Alfa Aesar
Potassium hydroxide, 90%, flakes	NaOH	VWR
Magnesium sulfate	MgSO ₄	Alfa Aesar
Anhydrous calcium sulfate	DRIERITE® Absorbent	Millipore Sigma
Ethylaluminumsesquichloride, 97%	Et ₃ Al ₂ Cl ₃	Sigma-Aldrich
Methanol, 98%	Methanol	BDH Chemicals
Toluene	Toluene	BDH Chemicals
n-Hexane	n-Hexane	Sigma-Aldrich
Tetrahydrofuran, 99.0%	THF	J. T. Baker
Methyl ethyl ketone, 99%	MEK	Alfa Aesar
N,N-Dimethyl formamide, 99.8%	DMF	VWR
Perylene, 98+%,	Perylene	Alfa Aesar
Teflon films	Teflon	McMaster-Carr
steel panels 4"×8"	steel panels	Q-LAB
polypropylene microtiter plates		Evergreen Scientific

6.3.2. Synthesis of 2-eugenoxethyl vinyl ether (EEVE)

2-Eugenoxethyl vinyl ether (EEVE) was successfully produced using Williamson ether synthesis and the synthetic scheme is shown in **Figure 6.1**. 50 g (0.47 mole) of 2-chloroethyl vinyl ether was mixed with 150 mL of N,N-dimethylformamide in a 500 mL round-bottom flask equipped with a reflux condenser and a magnetic stir bar. 78 g of eugenol (0.46 mol.), 26.4 g of

potassium hydroxide was added to the reaction mixture. The reaction mixture was then heated to 80 °C using an oil bath and kept for 16 hours, while stirring under a nitrogen blanket. After completion, the reaction mixture was cooled down to room temperature and diluted with 250 mL of n-hexane. Next, the solution was transferred to a separatory funnel and washed three times with 100 mL of 2N potassium hydroxide in deionized (DI) water to remove excess eugenol. After washing with potassium hydroxide, the organic layer was washed multiple times with DI water until the pH reached ~7 as indicated by litmus paper. Finally, the organic layer was dried over anhydrous magnesium sulfate and filtered. Filtrate was then kept in refrigerator at 5-7 °C overnight resulting in crystallization of EEVE. Supernatant n-hexane was then decanted and the remaining volatiles were stripped out using a rotary evaporator at room temperature for 12 hours at 5-8 mbar. EEVE was characterized using ¹H NMR and FTIR spectroscopy.

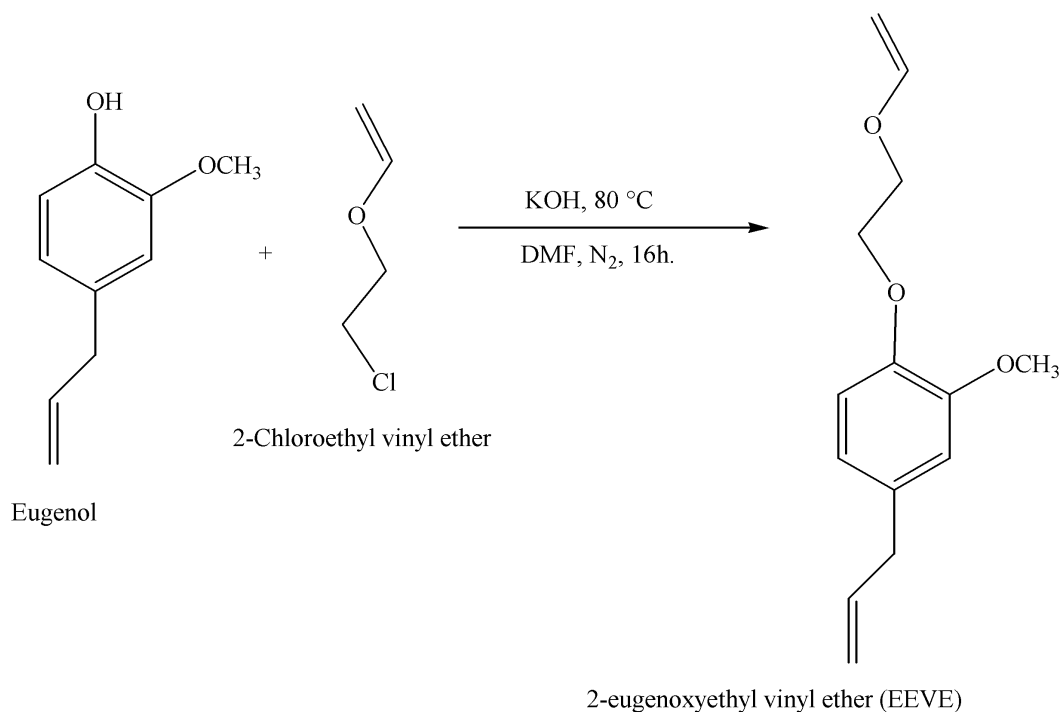


Figure 6.1. Synthesis of 2-eugenoloxyethyl vinyl ether (EEVE).

6.3.3. Synthesis of poly (2-eugenoxylethyl vinyl ether), poly(E EVE)

Polymerization of EEVE is shown in **Figure 6.2**. All glassware was baked at 200 °C for 2 h. and then cooled down by purging with N₂ to avoid moisture condensation. Glassware was then immediately transferred inside a glove box with a custom built cold bath where polymerization was carried out. Toluene was distilled over calcium hydride immediately prior to use. 1-Isobutoxyethyl acetate (IBEA) was synthesized and dried according to the procedure described by Aoshima and Higashimura.⁴⁰ Ethyl aluminum sesquichloride was diluted with distilled toluene to produce a 25 wt.% solution. In a 500 mL, two neck round bottom flask 50 g of dry EEVE and 170 mg of IBEA were dissolved in 150 mL of dry toluene and chilled to 0 °C using a heptane cold bath. The reaction mixture was continuously stirred with an overhead mechanical stirrer at 350 rpm. In a 100 mL closed glass container 6.07 mL of coinitiator, Et₃Al₂Cl₃ (25 wt.% in toluene) was added to 50 mL of dry toluene and chilled to 0 °C. A monomer:initiator:co-initiator ratio of 200:1:5 was used. After 30 minutes of cooling the polymerization was initiated by the addition of the co-initiator to the reaction mixture. The reaction was terminated after 2 hours by the addition of 50 mL of chilled methanol. Polymer was precipitated by pouring the reaction mixture into 200 mL of methanol in a 500 mL glass bottle while stirring to avoid entrapment of unreacted monomer by polymer due to sudden precipitation. The copolymer was reprecipitated three times from toluene by adding methanol and re-dissolved in 100 mL of toluene. Trace methanol was removed under vacuum (50–60 mm of Hg) at 30 °C for 3 h. Poly(E EVE) was characterized using ¹H NMR, FTIR, GPC and DSC.

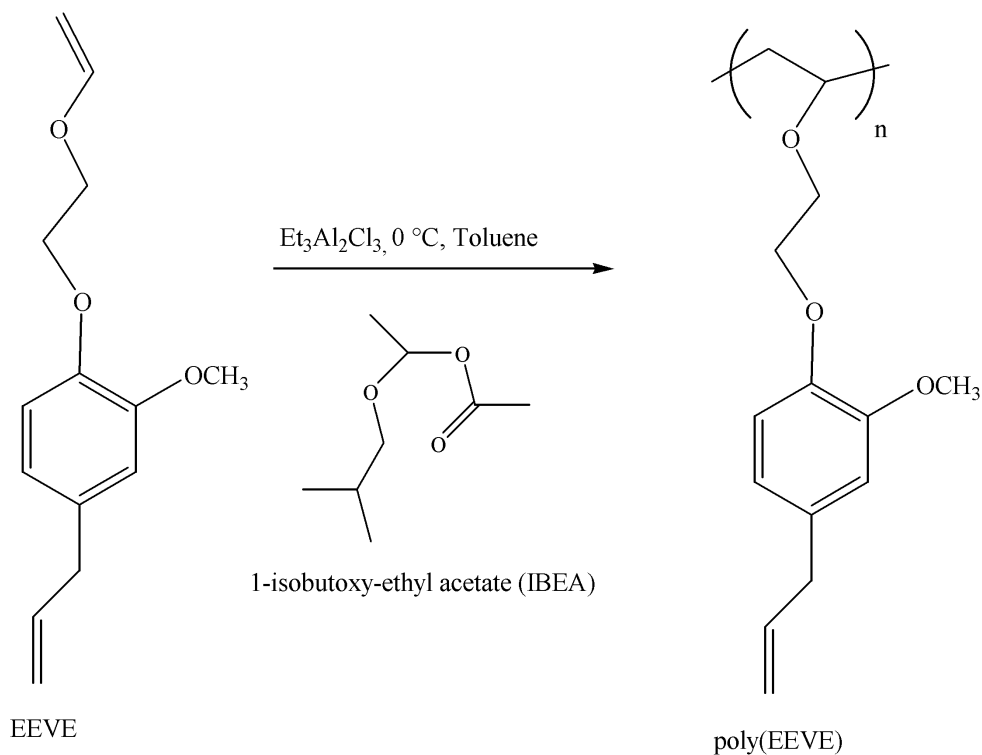


Figure 6.2. Synthesis of poly(E EVE).

6.3.4. Synthesis of epoxidized poly (2-eugenoxylethyl vinyl ether), Epoly(E EVE)

Epoxidation of poly(E EVE) was carried out using meta-chloroperoxybenzoic acid (mCPBA). Prior to use, mCPBA was purified according to the procedure reported by Kennedy et al.⁴¹ A detailed description is as follows: 30 g of m-chloroperoxybenzoic acid was purified by washing with 300 mL of phosphate buffer. Phosphate buffer was prepared by dissolving 33.55 g of $\text{Na}_2\text{HPO}_4 \cdot 7\text{H}_2\text{O}$ and 17 g of KH_2PO_4 in 500 mL of distilled water. After washing, purified mCPBA was transferred into 500 mL round bottom flask and dried overnight using a rotary evaporator at 5-8 mbar and room temperature (RT). To remove trace amount of water, mCPBA was further dried to constant weight over DRIERITE® absorbent in a vacuum desiccator. Recovery was 74.5%.

Epoxidation of poly(E EVE) was carried out using the purified mCPBA to produce Epoly(E EVE) resins with epoxidation levels of 30, 50 and 70% (Figure 6.3). Table 6.2 represents

the compositions for the reaction mixtures used to produce the Epoly(E EVE) resins. A representative procedure for Epoly(E EVE) attempted for 50% epoxidation is as follows:- 15 g of poly(E EVE) was transferred to a 250 mL round bottom flask and mixed with 50 mL of dichloromethane (CH_2Cl_2) using a magnetic stirrer bar. In a 100 mL beaker, 5.53 g of purified mCPBA was dissolved in 25 mL of CH_2Cl_2 and transferred to a 50 mL addition funnel which was then added dropwise over 30 min to the reaction mixture while stirring at room temperature. After addition, the reaction mixture was flushed with nitrogen and the reaction was carried out for 10-12 hours. Subsequently, the reaction mixture was concentrated by removing approximately 50 mL of CH_2Cl_2 using a rotary evaporator at 400 mbar and RT. After concentrating, the reaction mixture was poured into 150 mL of methanol where the epoxidized polymer precipitated out. The polymer was then redissolved with a minimal amount of CH_2Cl_2 and washed three times with methanol. Finally, the polymer was dissolved in 30 mL methyl ethyl ketone (MEK) and trace amount of methanol and CH_2Cl_2 was removed using rotary evaporator overnight at RT at 150 mbar. The synthesized Epoly(E EVE) was characterized using ^1H NMR, FTIR, GPC and DSC.

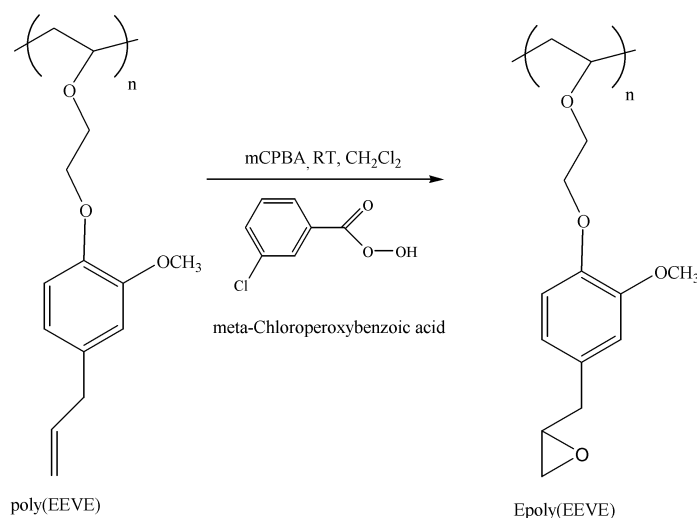


Figure 6.3. Schematic illustrating the synthesis of epoxy poly(2-eugenoxylethyl vinyl ether) i.e. Epoly(E EVE).

Table 6.2. Compositions for the reaction mixtures used to produce Epoly(E EVE) resins with epoxidation levels of 30, 50 and 70% and their percent conversion evaluated from titration and ¹H NMR.

Sample ID	EEVE, g, (moles)	mCPBA, g, (moles)	CH ₂ Cl ₂ , mL	Targeted % epoxidation	EEW, HBr titration (% epoxidation)	% epoxidation ¹ H NMR
Epoly(E EVE)-30%	15 (0.064)	3.32 (0.019)	3	30	248.31 (27.47)	27.01
Epoly(E EVE)-50%	15 (0.064)	5.53 (0.032)	75	50	504.35 (49.23)	48.75
Epoly(E EVE)-70%	15 (0.064)	7.743 (0.0448)	75	70	371.32 (66.87)	64.72

6.3.5. Preparation of thermosets

In his study, twelve formulations from each Epoly(E EVE) varying in epoxidation levels and with EPON 828 as a reference were prepared using twelve amine curatives. As shown in **Table 6.3**, four types of amine curatives: aliphatic, cycloaliphatic, aromatic and polyether were selected to evaluate the impact of the nature of amine curative on the properties of the cured coatings. To evaluate the relative performance of curatives towards crosslinking, the dye extraction method previously reported by Bach et al.^{36, 37} was used. Prior to making formulations, a 3 mM solution of perylene dye in toluene was prepared. A representative procedure for making dye incorporated formulation of EPON with isophorone diamine as curative is as follows: 1.14 g of EPON 828 resin was transferred into a 20 mL glass vial where 2.56 mL of MEK solvent and 202 μL of perylene dye solution were subsequently added and mixed using Teflon coated magnetic stir bar at 900 rpm on multi-position magnetic stirring plates for 25 min. Next, 0.26 g of isophorone diamine was added to the mixture and mixed for another 20 min prior to deposition on primed aluminum discs. Epoxy to amine ratio was 1:1 for all the 48 formulations and the amount of dye per formulation unit volume was kept constant.

Table 6.3. List of amine curatives used to study structure-property relationships.

Type	Name of curative	Designation	Amine hydrogen equivalent weight (AHEW)
Aliphatic	Priamine 1075	Priamine	267
	1,8-Diaminooctane	1,8-DA Octane	36.07
	Diethylenetriamine	DETA	20.63
	Tetraethylenepentamine	TEPA	24.37
Aromatic	m-Xylylenediamine	Xylene DA	34.05
Cycloaliphatic	1,3-Bis(Aminomethyl)cyclohexane	1,3 BAC	35.55
	Isophorone diamine	IPDA	42.68
	bis(p-aminocyclohexyl) methane	PACM	52.5
Polyether	JEFFAMINE EDR-148 (XTJ-504)	XTJ-504	37.05
	JEFFAMINE D-400	Jeff. D-400	115
	JEFFAMINE D-230	Jeff. D-230	60
	JEFFAMINE T-403	Jeff. t-403	81

6.3.6. Methods and instrumentation

6.3.6.1. Dye extraction

Preparation for the dye extraction method was carried out by punching out 10 mm epoxy primed aluminum discs and affixing them to a 4" × 8" aluminum panel in a 6 × 11 array format. 75 µL of each formulation (**section 6.3.5**) was deposited on six discs using an Eppendorf repeat pipettor. Coatings were then allowed to cure overnight under ambient conditions. Array panels were then cured further at room temperature for 7 days and at 80 °C using a preheated oven for 30 min, 1 h, 3 h or 6 h. After curing, three discs from each set (same formulation and curing regime) were transferred into 24 well (6x4) polypropylene microtiter plates, each row of wells containing two sets of discs. The discs were affixed to the bottom of each well with double-sided tape and were allowed to adhere for 18 to 20 hours prior to dye extraction.

Dye extraction was performed by adding 500 µL of toluene to each well of the microtiter plate using an Eppendorf repeat pipettor. The toluene was quickly added to each row of the microtiter plate with 15 s intervals between the rows. The formulations were allowed to soak for

10 min on an orbital shaker, then 150 μ L of each extraction sample was collected and transferred to a 96 well microtiter plate using a 6-channel, adjustable spacing, multichannel pipette. Each row of two sets with three replicates was collected at the same time, aspirating twice to ensure a homogenous mixture. The timing of collection for each individual formulation was held to 15 second intervals to ensure that the soaking time was precise. Fluorescence measurements (415ex/471em) of all extraction samples using a TECAN Saffire2 plate reader were taken immediately following collection. An illustration of the overall extraction procedure is shown in

Figure 6.4.

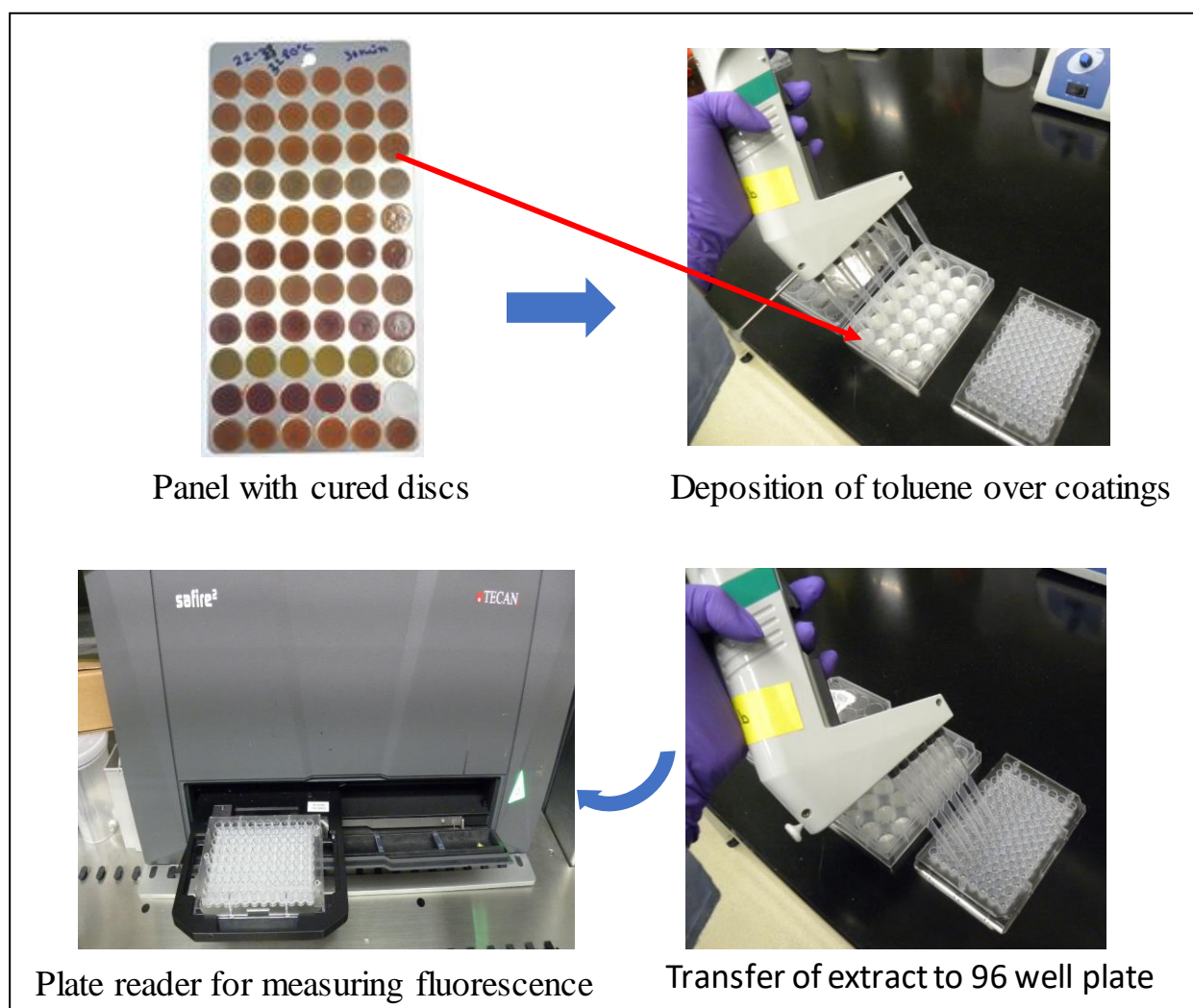


Figure 6.4. Illustration of the dye extraction method

6.3.6.2. Nanoindentation

Depth sensing indentation, also called instrumented indentation or nanoindentation was performed using a Hysitron TriboIndenter with automation (9 samples per run) using a diamond Berkovich tip. Since accurate determination of the elastic modulus from the indentation load-displacement responses requires flat sample surfaces, indentation was performed mostly near the center of the coated discs. Before every indent, the indenter was held in contact with the surface, to allow for piezoactuator stabilization (35 s) and drift correction (40 s), at a contact load of only 0.5 mN to prevent any deformation prior to the indentation experiment. The drift rate (typically 0.1 nm s⁻¹) was automatically determined over the last 20 s of the 40 s period. After lifting the tip up to 30 nm and reapproaching the surface (surface detection at a load of 0.5 mN), the tip was loaded to maximum load of 300 μ N in 5 s, held at maximum load for 5 s and unloaded in 5 s. Nine measurements with a spacing of 60 μ m apart were performed per sample and the first one was left out from the analysis to further reduce the influence of drift.

6.3.6.3. Differential scanning calorimetry

Thermal properties of the polymers and cured coatings were characterized using a Q1000 Modulated Differential Scanning Calorimeter from TA Instruments with a cooling limit up to -90 °C. For the polymers, 7-10 mg of samples were thoroughly dried prior to the measurement. For EEVE, the sample was first equilibrated at 23 °C and then cooled from 23 °C to -90 °C at 10 °C/minute, held at -90 °C for 3 minutes and heated to 100 °C at 10 °C/minute. For poly(EEVE) and Epoly(EEVE) samples the following heating and cooling regime was used: sample was first equilibrated at 23 °C and then heated from 23 °C to 50 °C at 10 °C/minute (1st heating cycle); held at 50 °C for 2 minutes and cooled to -60 °C at 10 °C/minute (1st cooling cycle); and heated to 80 °C at 10 °C/minute (2nd heating cycle). DSC thermograms are reported from the second heating

cycle. For the cured coatings, the following heat/cool/heat regime was used: the sample was first equilibrated at 23 °C and then heated to 50 °C at 10 °C/minute, held at 50 °C for 2 minutes, cooled to -30 °C at 10 °C/minute, and heated to 150 °C at 20 °C/minute.

6.3.6.4. Thermogravimetric analysis (TGA)

Thermogravimetric analysis was carried out using a Q500 Thermogravimetric analyzer from TA Instruments equipped with a responsive low-mass furnace, sensitive thermobalance, and efficient horizontal purge gas system and a temperature range from 25 to 1000 °C. Thermogravimetric analysis (TGA) was carried out by heating the sample at 10 °C /min from 25 to 800 °C under nitrogen. The sample sizes ranged from 22 to 25 mg.

6.3.6.5. Nuclear magnetic resonance (NMR) spectroscopy

Proton nuclear magnetic resonance (¹H NMR) spectra were obtained using a 400 MHz Bruker 400 NMR spectrometer. Data acquisition was accomplished using 16 scans and CDCl₃ was used as the lock solvent.

6.3.6.6. Gel permeation chromatography (GPC)

Molecular weight (MW) and polydispersity index (PDI) of the polymers were determined using gel permeation chromatography. EcoSEC HLC-8320GPC from Tosoh Bioscience, equipped with a differential refractometer detector was used. Two different columns were used depending on the targeted MW of the polymers. For polymers with an targeted MW below 15,000 g/mol, two TSKgel SuperH3000 columns were used, while two TSKgel SuperHM columns were used for polymers with an targeted MW above 15,000 g/mol. THF was used as the mobile phase, the flow rate was 0.35 ml/min, and the operating temperature of the columns and detector was 40 °C. Samples were prepared in THF at a nominal concentration of 1 mg/ml and the sample injection

volume was 20 μ L. A calibration curve was produced using polystyrene standards (Agilent EasiVial PS-H 4mL).

6.3.6.7. Fourier transform resonance (FTIR) spectroscopy

Fourier transform infrared spectra were obtained with a Nicolet 8700 FTIR spectrometer operated with OMNIC software. Thin polymer films were solution cast onto a KBr disc, subsequently dried, and then scanned from 500-4000 cm^{-1} using 64 scans and 1.93 cm^{-1} data spacing.

6.3.6.8. König pendulum hardness

König pendulum hardness was measured according to ASTM D 4366-16 by sticking two cured coated discs on a steel panel on top of which steel balls of the pendulum were placed; the results were reported in seconds.

6.3.6.9. Measurement of epoxy equivalent weight

Epoxy equivalent weight (EEW, g/eq.) of the epoxy products was evaluated by titrating epoxy samples with 0.0925 N solution of HBr in glacial acetic acid; 1 wt.% solution of crystal violet in acetic acid was used as an indicator. EEW value was calculated using the **Eq. 6.1**, where W is the sample mass in grams, N is the normality of HBr solution, and V is the volume of HBr solution used for titration in mL.

$$EEW = \frac{100 \times W}{N \times V} \quad (6.1)$$

6.4. Results and discussion

6.4.1. Synthesis and characterization of EEVE and poly(EEVE)

Synthesis of EEVE was carried out according to Williamson ether synthesis and the schematic is shown in **Figure 6.1**. The synthesis of EEVE was confirmed from the ^1H NMR spectrum shown in **Figure 6.5 (a)**. As shown in **Figure 6.5 (a)**, signals assigned as “K”, $\delta = 6.54$

(q, 1H, CH₂=CH-O-) and “J”, $\delta = 4.24, 4.08$ (dd, 2H, CH₂=CH-O-) corresponding to vinyl protons along with “G” and “F” signals at $\delta = 4.05$ (m, 2H, -O-CH₂-CH₂-O-) and $\delta = 4.05$ (m, 2H, -O-CH₂-CH₂-O-Ar) corresponding the ethyl spacer confirms the successful synthesis of EEVE. The absence of the eugenol starting material was confirmed from the complete disappearance of the Ar-OH signal. FTIR further verified EEVE synthesis and is shown in **Figure 6.6 (b)**. Disappearance of the -OH signal at around 3455 cm⁻¹ along with appearance of the signal at 1618, 1036 and 850 cm⁻¹ corresponding to C=C vinyl, vinyl alkyl ether (C=C-O-C-) symmetric and asymmetric stretch respectively, confirms the successful vinyl functionalization of eugenol.

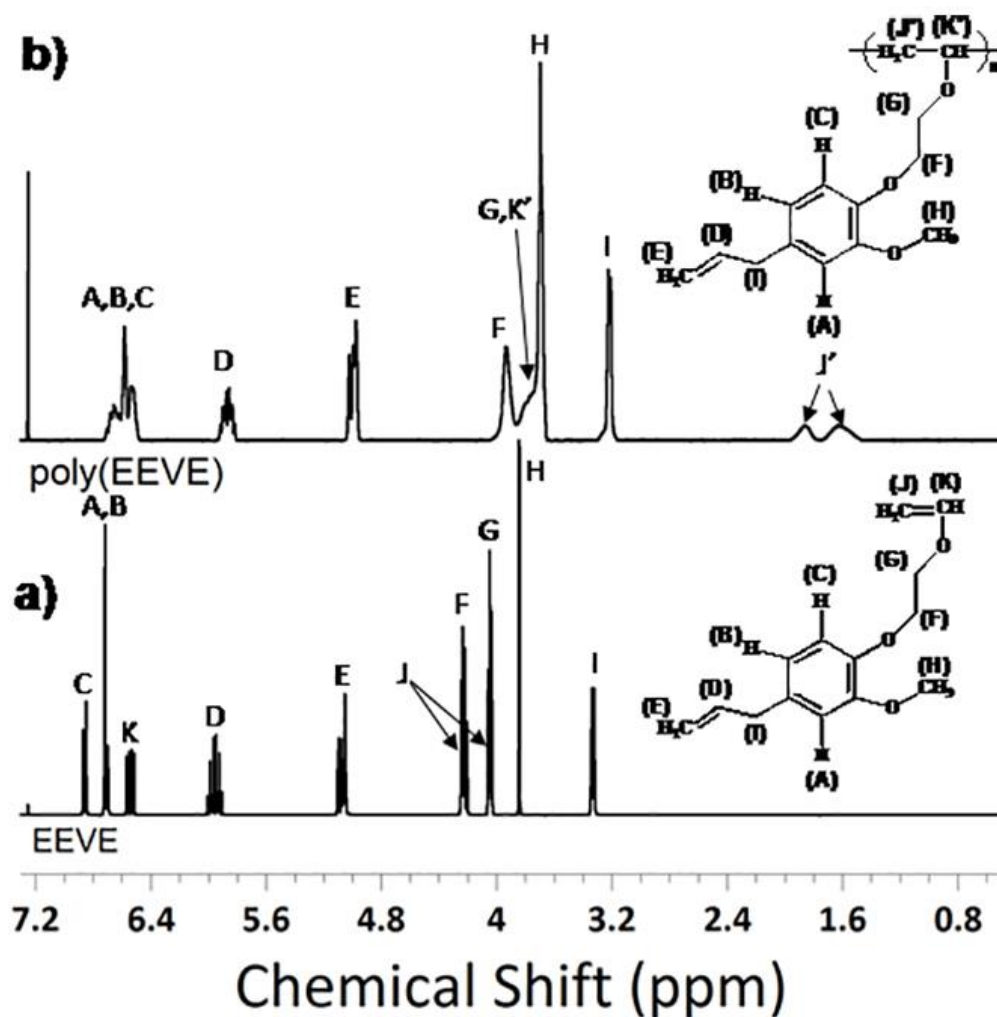


Figure 6.5. ¹H NMR spectrum of (a) EEVE (bottom) and (b) poly(EEVE) (top).

It has been shown by Chernykh et al.⁴² that utilizing appropriate cationic polymerization system vinyl ether monomers from plant oils could be polymerized exclusively through the vinyl ether functionality resulting in linear polymers with complete retention of fatty unsaturation. The ability to produce linear bio-based polymers with pendent unsaturation was shown to be very useful for the production of thermoset coatings.^{39, 43-52} For example, polymers derived from 2-(vinylloxy)ethyl soyate produced thermoset coatings that cured by autoxidation, due to the presence of the unsaturated fatty acid ester side-chains. Based on this previous work, it was of interest to utilize a similar approach to produce poly(E EVE) leaving the allylic functionality in each repeat unit. The reaction scheme is shown in **Figure 6.2**. The successful synthesis of poly(E EVE) was confirmed from ¹H NMR and FTIR. ¹H NMR spectrum of poly(E EVE) [**Figure 6.5 (b)**] confirmed the downfield shift and broadening of the “J” and “K” signals to $\delta \sim 1.74$ and 3.87 respectively, these newly appeared signals assigned as “J” and “K” confirms the incorporation of vinyl double bond in the polymer backbone chain. Retention of the “D” and “E” signals clearly indicate the ability of the used cationic polymerization technique to proceed exclusively through the vinyl double bond. FTIR spectrum of poly(E EVE) shown in **Figure 6.5 (c)** and confirms the disappearance of the peaks at 1618 cm⁻¹ (vinyl C=C stretch), 1036 (vinyl alkyl ether, asymmetric) and 850 cm⁻¹ (vinyl alkyl ether, symmetric) and retention of the peaks at 1637 cm⁻¹ (allyl C=C stretch); 1590, 1513, 1463 and 1452 cm⁻¹ (aromatic C=C stretch) confirmed the successful synthesis of poly(E EVE) exclusively through the vinyl group.

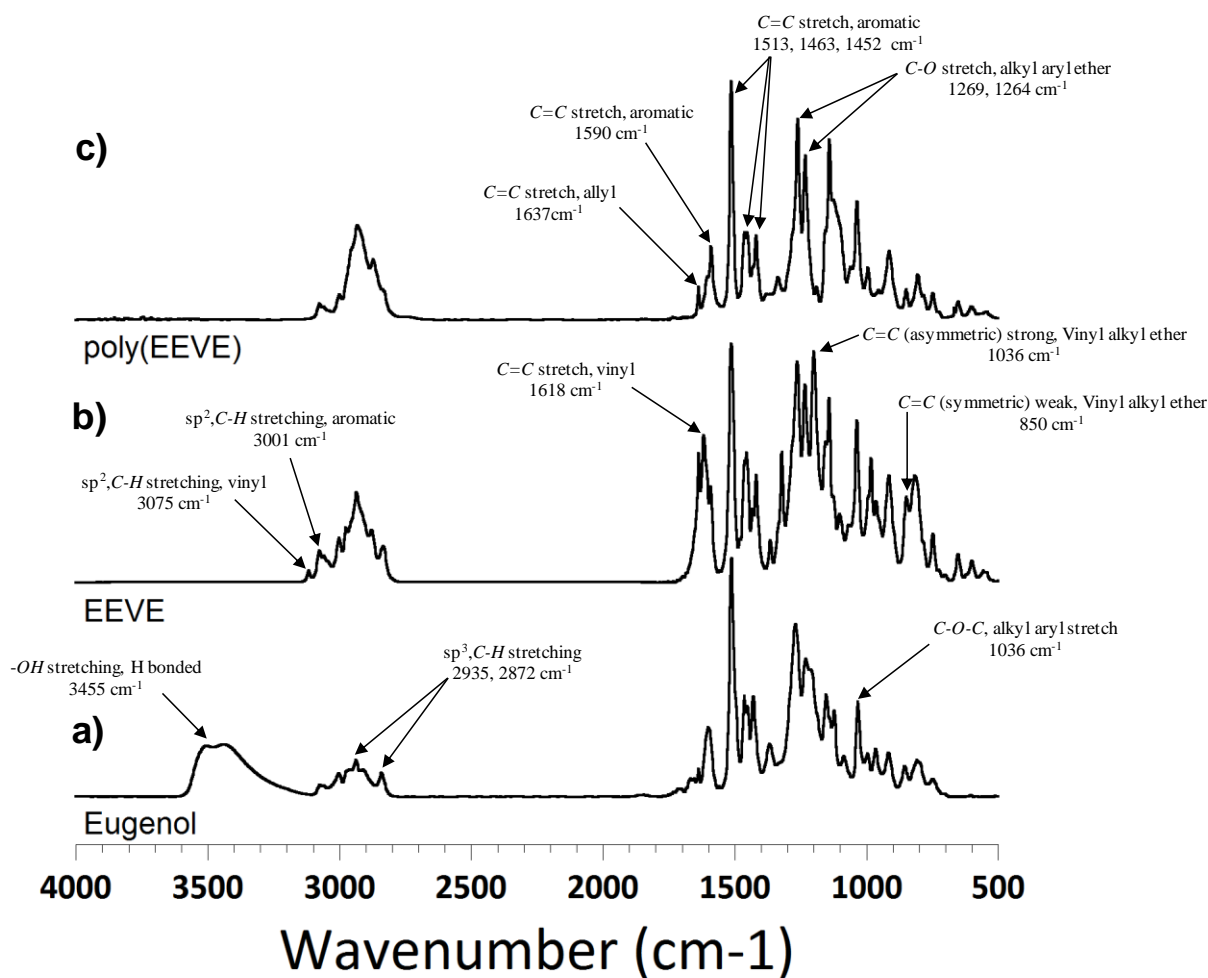


Figure 6.6. FTIR spectra of (a) eugenol (bottom), (b) EEVE (middle) and (c) poly(EEVE) (top).

6.4.2. Synthesis and characterization of Epoly(EEVE)

Epoxidation of poly(EEVE) was carried out using the purified mCPBA and three Epoly(EEVE) with varying in level of epoxidation of 30, 50 and 70% were produced. ^1H NMR of the Epoly(EEVE)-50%, shown in **Figure 6.7**. As shown in **Figure 6.7**, reduction of the normalized intensity of the “E” and “D” signals corresponding to allylic protons was observed. Simultaneously, appearance of three new signals assigned as “X”, “Y” and “Z” corresponding to the oxirane ring protons was also observed which confirmed the conversion of allylic double bond to epoxy functionality. FTIR spectra of Epoly(EEVE)-50% [**Figure 6.8 (b)**] also confirmed the

reduction of normalized intensity of the peak at 1637 cm^{-1} (allyl $\text{C}=\text{C}$ stretch) and the appearance of two sharp signals at 941 and 833 cm^{-1} (asymmetric and symmetric $\text{C}-\text{O}-\text{C}$ ring deformation).

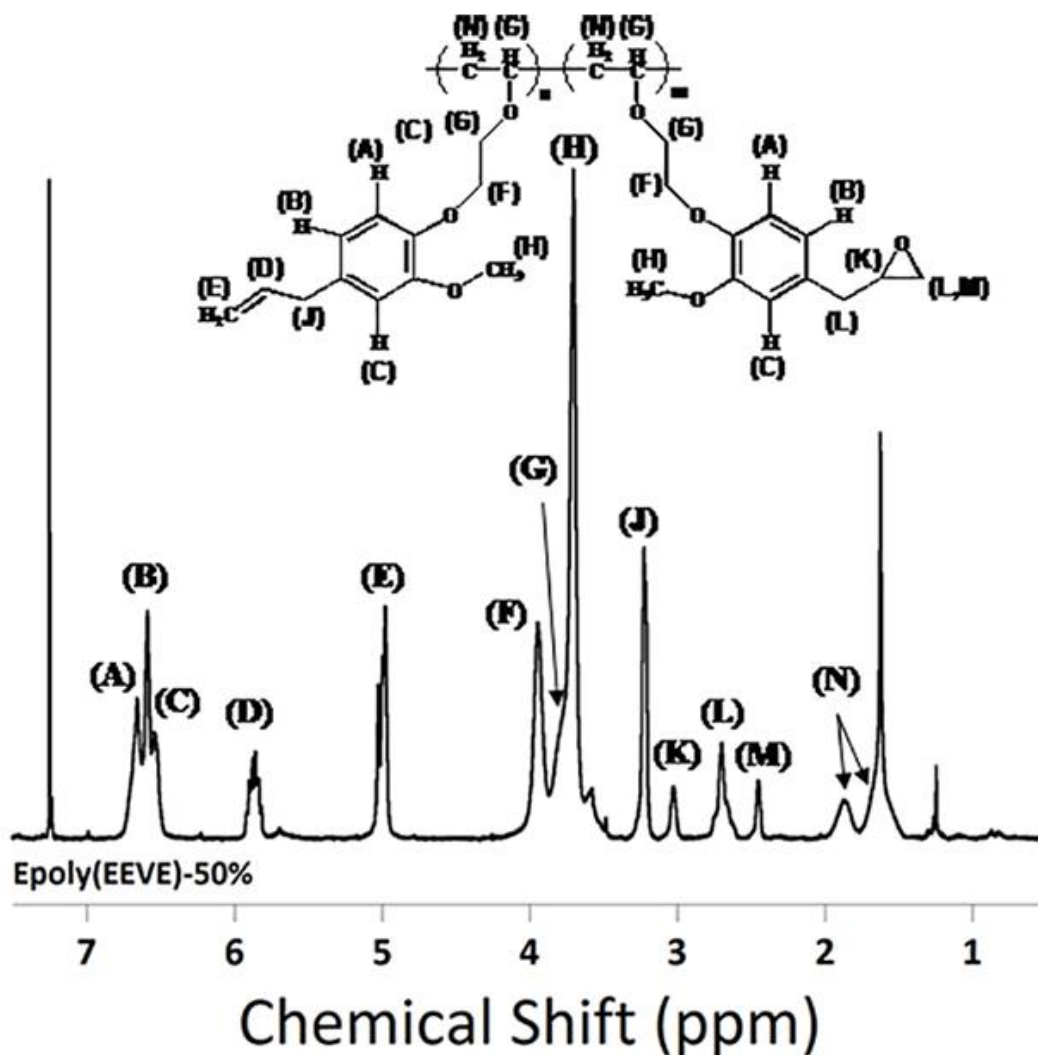


Figure 6.7. ^1H NMR spectrum of Epoly(E EVE)-50%.

Epoxy equivalent weight (EEW) of the as-synthesized Epoly(E EVE) resins were evaluated by titrating with hydrobromide solution (0.0925 N). Calculated EEWs and percent epoxidation values are reported in **Table 6.2**. Calculated percent epoxy values were found to be close to the expected values except for the 70% epoxidation sample, which might be due to decreases in the rate of epoxidation with reduction of the concentration of allylic double bonds and the reagent. Percent epoxy values obtained from HBr titration was cross-verified by calculating the values from

^1H NMR using (Eq. 6.2). The values matched within an error < 5%. EEWs calculated from the HBr titration was considered for making the coating formulations.

$$\% \text{ epoxidation} = 100 \times \frac{\text{Integration value of the "J" peak}}{\text{Integration value of the "K" peak}} \quad (6.2)$$

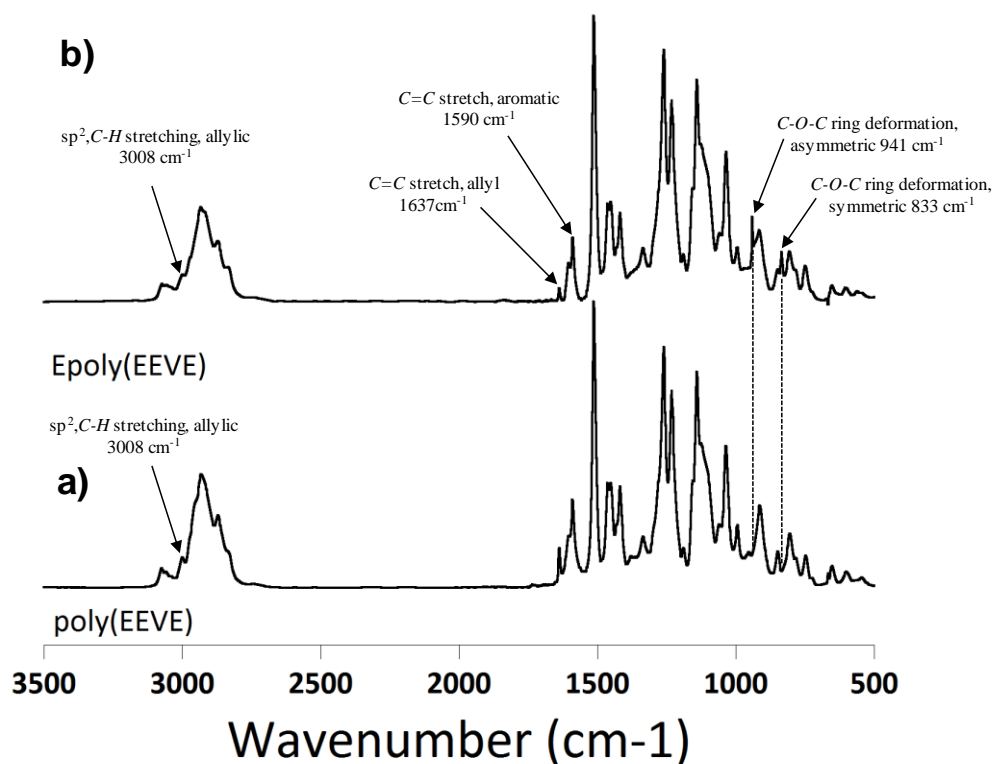


Figure 6.8. FTIR spectra of (a) poly(E EVE) and (b) Epoly(E EVE).

6.4.3. Thermal properties of EEVE, poly(E EVE) and Epoly(E EVE)

The thermal properties of the monomer and polymers were evaluated by using DSC. DSC thermogram of EEVE (Figure 6.9) indicated two melting points at around 17 °C and 26 °C, confirming the crystallinity of the EEVE monomer. The lower melting point with an onset at 9 °C might due to the presence of imperfect crystals. DSC thermograms of the poly(E EVE) and Epoly(E EVE) resins are shown in Figure 6.10. DSC thermogram of poly(E EVE) showed a glass transition temperature (T_g) at around -22 °C well below the room temperature making it a very

viscous and sticky material. Also, the absence of any melting endotherm confirms that the polymer did not form any crystalline phase at subzero temperature. On the other hand, thermograms of the Epoly(E EVE) resins showed interesting results, where, an increase in T_g was observed with increasing the % epoxidation value. As shown in **Figure 6.10**, T_g increases from -22 to -18 °C with approximately 30 % epoxidation of poly(E EVE) which increased up to -10 °C with 70 % epoxidation. This increase in T_g with increasing percent epoxidation can be explained by considering the fact that, T_g increases with increasing polarity within a group of polymers, with the same or similar backbone flexibility. These polar interactions act like friction during relaxation thereby delaying the process and hence increase the T_g . A study carried by Agapov et al.⁵³ showed that the T_g of a polymer varies in a complex way when a polar group is positioned away from the polymer backbone rather than when the polar group is directly attached to the backbone when both fragility and T_g increase. An increase in T_g from 372 to 394 °C was observed for polystyrene when a chlorine atom was placed in the para position. In case of poly(E EVE) the epoxy functionality increases the dipole moment thereby increases the cohesive energy which ultimately leads to increase in T_g .

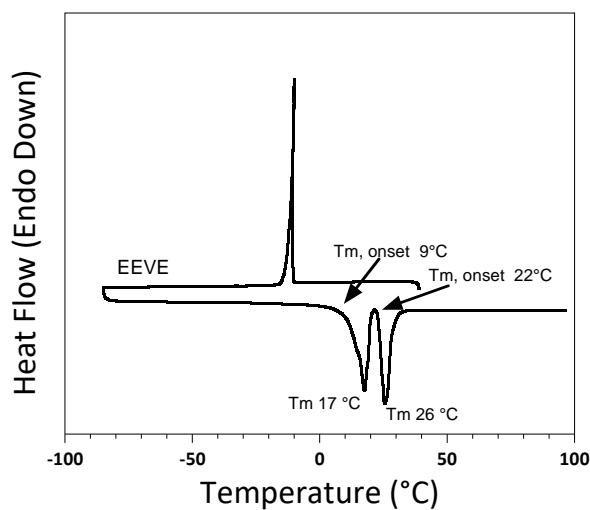


Figure 6.9. DSC thermogram of EEVE.

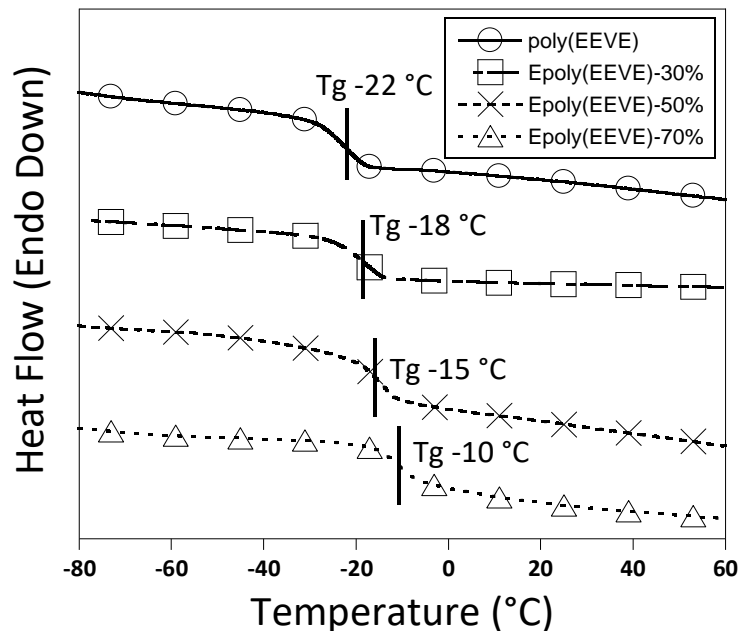


Figure 6.10. DSC thermograms of poly(E EVE), Epoly(E EVE)-30%, Epoly(E EVE)-50% and Epoly(E EVE)-70%.

6.4.4. Molecular weight and polydispersity index analysis

The number average molecular weight (M_n) and polydispersity index of poly(E EVE) and Epoly(E EVE) resins were determined using GPC analysis and the chromatograms are shown in **Figure 6.11**. Obtained M_n and PDI values are reported in **Table 6.4**. From the numbers in **Table 6.4** it is clear that with increasing the level of epoxidation both M_n and PDI increased. One of the reason of this increase in M_n might be due to incorporation of oxygen atoms in epoxy functionality and since this functionalization is randomized per polymer molecule is also lead to increase in polydispersity. Incorporation of 50% epoxy functionality leads to an increase in M_n from approximately 17.5 kDa to 19 kDa with a change in PDI from 1.20 to 1.23.

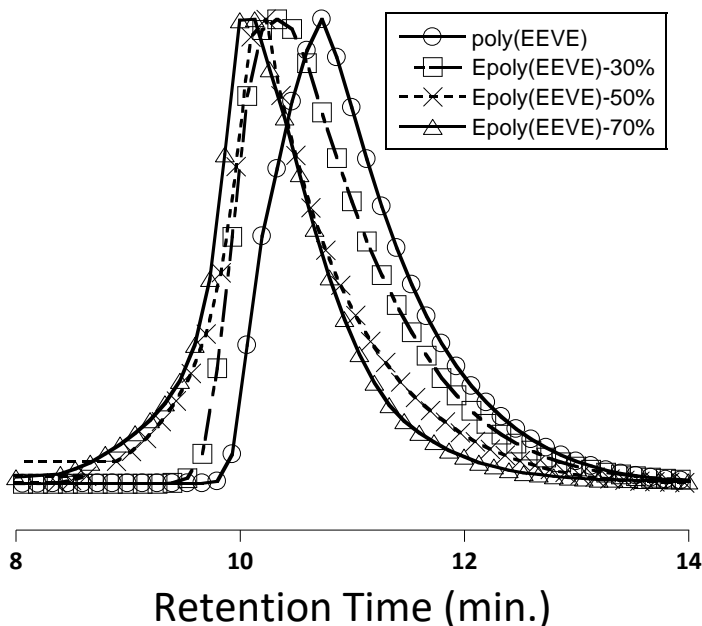


Figure 6.11. GPC chromatograms for a) poly(E EVE), Epoly(CHVE)-30%, Epoly(CHVE)-50%, and Epoly(CHVE)-70%.

Table 6.4. Mn and PDI of the synthesized poly(E EVE) homo-polymers and its epoxy functionalized polymers with three levels of epoxidation. All values are expressed relative to polystyrene standards.

Polymer ID	Mn (Da or g/mole)	PDI
poly(E EVE)	17,429	1.20
Epoly(E EVE)-30%	18,963	1.23
Epoly(E EVE)-50%	19,500	1.26
Epoly(E EVE)-70%	21,860	1.27

6.4.5. Properties of cured coatings

Properties of the cured coatings were evaluated using high throughput dye extraction and nanoindentation to evaluate relative crosslink density and elastic modulus along with hardness, respectively. DSC of the cured coatings were determined using DSC to compare the trend of hardness obtained from indentation and the glass transition temperature which usually a function of crosslink density and the rigidity of the components.

6.4.5.1. Dye extraction

Figure 6.12 shows the dye extraction data plotted in the form of “heat maps” for each of the Epoly(E EVE) resins and EPON 828 resin where the values are color-coded according to relative values; color intensity is lower with higher dye extraction i.e. lower crosslink density. In each individual figure, the “X” axis represents the curing regime and the “Y” axis represents the amine curatives. From the color differences of the individual heat maps we can conclude that for a given amine curative and curing regime increasing the percent epoxidation of Epoly(E EVE) resin results in lower dye extraction. In comparison to EPON resin both Epoly(E EVE)-50% and Epoly(E EVE)-70% resins resulted in lower dye extraction irrespective of amine curative and curing conditions, however, Epoly(E EVE)-30% resulted in higher dye extraction. According to the previous work by Bach et al.,^{36, 37} this indicates that Epoly(E EVE)-50% and Epoly(E EVE)-70% form relatively denser networks than EPON resin. A relatively higher dye extraction of Epoly(E EVE)-30% indicates that about 50% epoxidation is required to provide networks with comparable crosslink density to the networks formed by EPON resin. Regarding the effect of amine curatives, overall it can be concluded that both cycloaliphatic and aromatic type amine curatives resulted in higher crosslink density networks than the aliphatic and polyether type for a given resin and curing conditions, however, this variation decreases with increasing the percent epoxidation of the Epoly(E EVE) resin. A closer look at the “heat maps” further reveals that with EPON resin, polyether type curatives resulted in higher crosslinked density networks than aliphatic type curatives whereas the reverse trend was observed in the case of Epoly(E EVE) resins. Small difference in dye extraction values between Epoly(E EVE)-50% and Epoly(E EVE)-70% networks implied that 50% epoxidation could result in sufficiently crosslinked networks. Besides the nature of the amine curatives curing time and temperature plays a major role in the formation of

crosslinked networks. At a lower level of epoxy functionality (30%), curing at room temperature for a week resulted in networks comparable to those cured at 80 °C for 1h which increases to 3h for di- and trifunctional polyether curatives. Among the aliphatic curatives, Priamine with highest AHEW resulted in lowest crosslink density networks. With Epoly(E EVE) resins Priamine resulted in smooth coatings, however, surface roughness and phase separation were observed with EPON. With DETA and TEPA curatives coatings cured for 3 h. at 80 °C significantly lower dye extraction than coatings cured at RT, 0.5 and 1 h at 80 C. This lower reactivity at RT and over short curing period at elevated temperature might due to the presence of secondary N-H which usually has lower reactivity however, reacted after curing for 3 h at 80 °C.

minimum
maximum

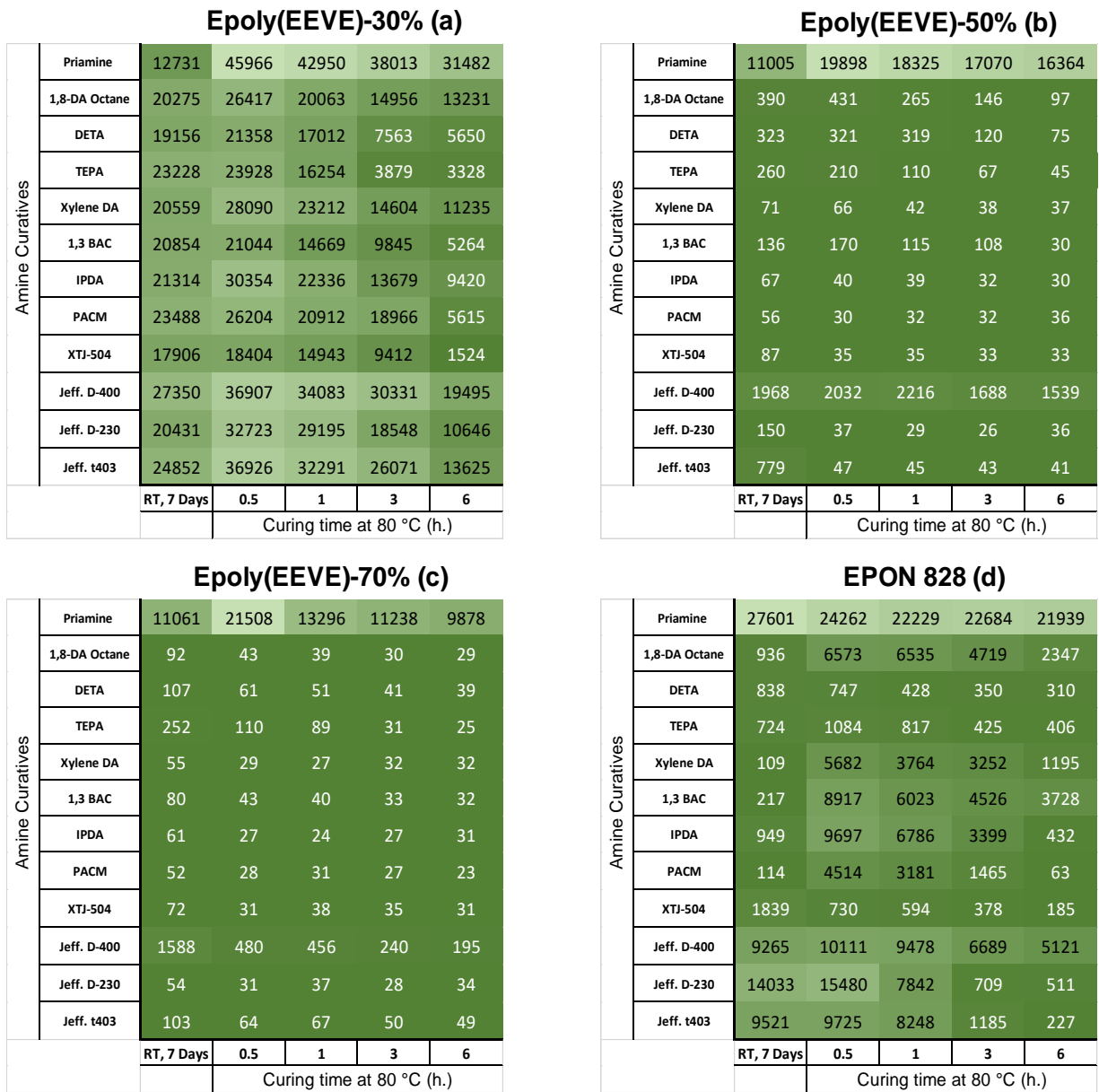


Figure 6.12. Dye extraction” heat maps” for perylene incorporated coatings; Epoly(E EVE)-30% (a), Epoly(E EVE)-50% (b), Epoly(E EVE)-70% (c) and EPON 828 (d). A three scale color coding was used.

6.4.5.2. Differential scanning calorimetry (DSC)

The glass transition temperature of the cured coatings on selective coatings was measured using differential scanning calorimetry and the results shown in **Figure 6.13**. Overall, an

increasing trend of T_g was observed for the coatings prepared from Epoly(E EVE) resins with increasing percent epoxidation. This increment is up to 40 °C with the percent epoxidation increasing from 30 to 50%. However, this improvement in T_g was only 5 to 10 °C for coatings prepared from 70% epoxidized poly(E EVE) compare to 50%. This tends to indicate that coatings prepared with 50 % epoxidized Epoly(E EVE) resulted in highly crosslinked networks after which formation of more crosslinks had a small impact on the segmental mobility of the networks with temperature. The glass transition temperature of the coatings prepared with EPON 828 showed lower T_g than coatings prepared with Epoly(E EVE) with 50 and 70% epoxidation. The glass transition temperature referred to the long-range mobility of the polymer crosslink networks thereby it depends on both crosslink density and composition of the networks. For a given network system increasing the crosslinks also reduces the free volume for the movement of the networks there by increasing the T_g . As EPON 828 resin has a more rigid structure than Epoly(E EVE) polymer, so the higher T_g associated with 50 and 70 % epoxidized poly(E EVE) must be attributed from the formation of higher crosslink density networks.

The effect of curing time has more impact on the T_g for the Epoly(E EVE)-30% whereas, both Epoly(E EVE)-50% and Epoly(E EVE)-70% showed a slight increase in T_g for the coatings cured at 80 °C for 3h compared to 1 h. Also, interestingly T_g for coatings cured at RT for a week showed similar values for coatings cured at 80 °C for 1 h and up to 3 h with polyether curatives. Coatings cured with cycloaliphatic curatives resulted higher T_g than aliphatic and polyether curatives and is more prominent for coatings with increasing curing time.

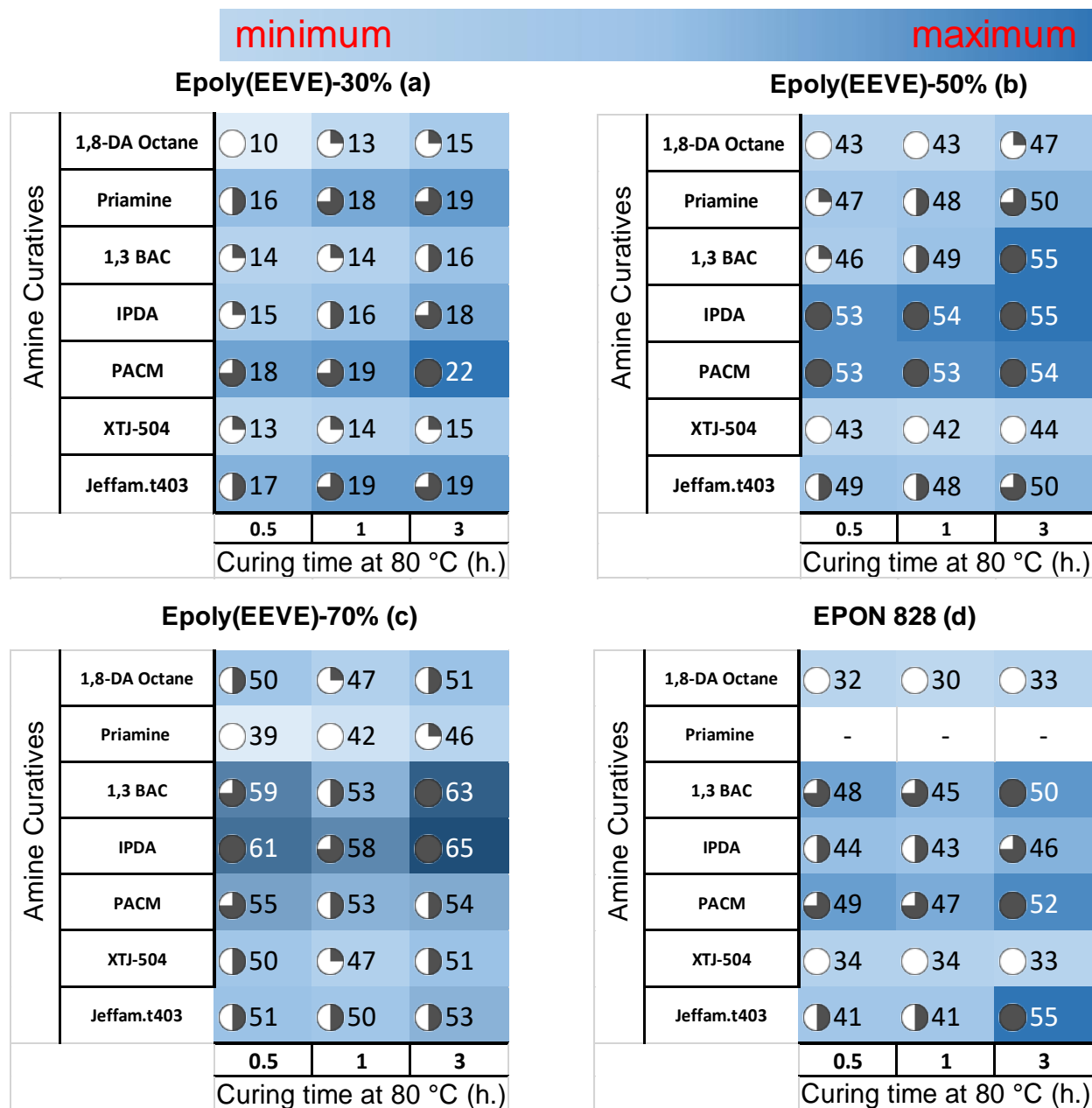


Figure 6.13. Glass transition temperature (°C) heat maps (a) Epoly(E EVE)-30%, (b) Epoly(E EVE)-50%, (c) Epoly(E EVE)-70% and d) EPON 828. A three-scale color-coding was used for individual map. Another icon scale is used where each 20 % increment in value is represented with an additional black quarter of the circle.

6.4.5.3. König pendulum hardness (KPH)

Results from the KPH are reported in **Figure 6.14**. The values clearly indicate an effect of curatives and curing regime. In general, it is obvious from color coding that increasing the curing

time results in increasing the hardness attributed to the increase in crosslink density estimated from the dye extraction. Pendulum hardness is the measurement of the amount of time required to dissipate the rocking motion of two stainless steel balls put into motion by releasing a pendulum. Thus, coatings exhibiting a highly crosslinked network have a less viscous response to the stress induced by the steel balls, thereby dissipating the stress less effectively resulting in higher pendulum hardness. In the case of Epoly(E EVE) resins, for a given curative and curing regime increasing the percent epoxidation resulted in coatings with increasing hardness which was expected due to increase in functionality. Significant improvement in hardness ~ 20% had been observed for coatings derived from Epoly(E EVE)-50% than Epoly(E EVE)-30% which could be justified by considering the T_g values shown in **Figure 6.13**. As shown in **Figure 6.13**, T_g of the coatings derived from Epoly(E EVE)-30% were below RT at which the pendulum hardness was measured, which results in coatings to behave more viscous than glassy allowing them to dissipate the energy from the rocking motion of the pendulum in a shorter period of time. In case of Epoly(E EVE)-30% and Epoly(E EVE)-50% hardness increases gradually with curing time however, for Epoly(E EVE)-70% a plateau had been observed after 3 h resulting in a slight improvement in T_g for curing up to 6 h. This observed behavior of hardness reaching a plateau might be due to the fact that increasing the percent epoxidation from 50 to 70 resulted relatively highly crosslinked networks mostly curing after 1 h. With similar crosslink density, both aromatic and cycloaliphatic curatives resulted in harder coatings than aliphatic and polyether curatives which must be attributed from their comparatively rigid structures. However, coatings from EPON resin cured at RT with polyether curatives showed higher hardness than cycloaliphatic and aromatic type curative. This might be due to fact that unlike Epoly(E EVE) resin, EPON having rigid structure and forming comparatively dense networks with polyether curatives can

compensate for the flexible nature. For both aliphatic and polyether curatives increasing the functionality for example, from DETA or Jeffamine di-functional D-230 to TEPA or trifunctional Jeffamine T-403 resulted in an increase in hardness. Similar results were obtained within a group of curatives where decreasing the spacer between amine functional groups resulted in an increase in hardness. For example, compared to XTJ-504, which has a linear oxyethylene structure, Jeffamine D-400 with a polypropylene structure showed a significant increase in hardness, which indicate that having the methyl side group increases the rigidity. Even decreasing the average polypropylene spacer from approximately 6.1 (Jeffamine D-400) to 2.5 (Jeffamine D-230) able to increase the hardness to some extent. Overall, coatings derived from 50 or 70% epoxidized Epoly(E EVE) resins could result in coatings with hardness comparable to EPON resin

minimum

maximum

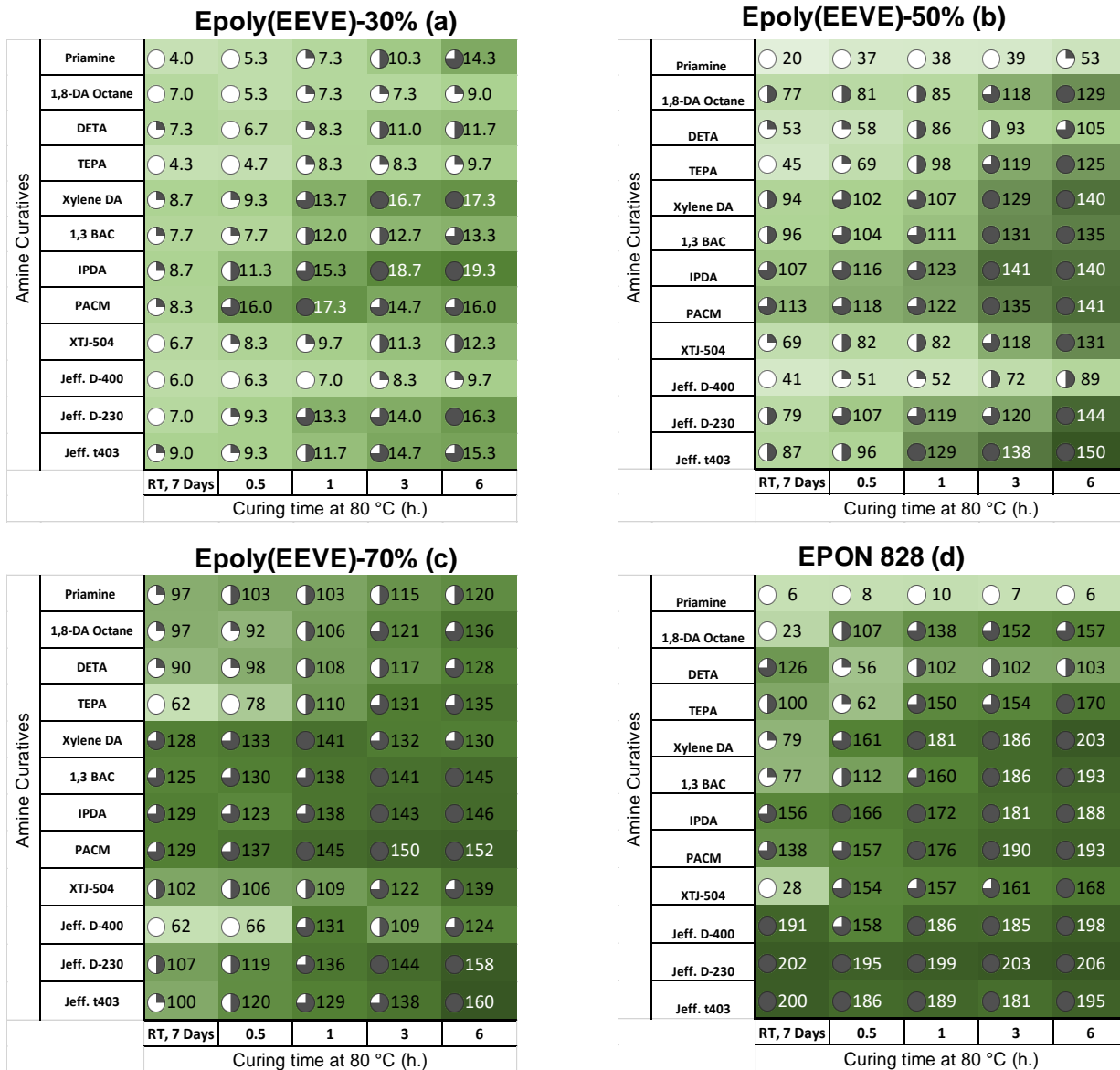


Figure 6.14. König pendulum hardness (sec.) heat maps (a) Epoly(E EVE)-30%, (b) Epoly(E EVE)-50%, (c) Epoly(E EVE)-70% and d) EPON 828. A three-scale color-coding was used for individual map to perceive the variation in a better way. Another icon scale is used where each 20 % increment in value is represented with an additional black quarter of the circle.

6.4.5.4. Nanoindentation

Hardness and elastic modulus were also determined using nanoindentation as a high throughput method and the values are reported as “Heat maps” in **Figures 6.15** and **Figure 6.16**,

respectively. It is worth mentioning that polymeric materials create several challenges during accurate measurements of the elastic modulus.⁵⁴ Even in some extreme cases when the coating is too soft, the values cannot be measured or become negative due to low compliance of the system. As shown in **Figure 6.15** coatings hardness were influenced by percent epoxidation [Epoxy(EEVE) resins], the nature of the curatives and the curing regime for each epoxy resin including EPON 828. In the case of Epoxy(EEVE)-30% coatings were soft irrespective of the curatives. However, hardness increased 4 to 25 times depending on the curative when cured at 80 °C for 3 h compared to those cured at 80 °C for 1h and RT for a week. Within a certain type of curative hardness seems to increase with increasing the functionality of the curatives. For example, TEPA showed higher hardness than DETA, likewise Jeffamine T-403 has higher hardness than Jeffamine D-230 and Jeffamine D-400. EPON 828 showed the similar behavior however, the hardness is lower than Epoxy(EEVE)-50% and Epoxy(EEVE)-70%. Coatings cured with aromatic and cycloaliphatic amine curatives are harder than aliphatic and polyether type curatives. Similar results were observed from the pendulum hardness and is mainly attributed to the rigid nature of the curatives leading to higher T_g thereby behaving more glassy at the experimental temperature. TEPA and Jeffamine D-230 formed harder coatings than other curatives of their types mainly due to their high functionality and lower flexibility oxypropyl chain backbone, respectively.

Elastic modulus values obtained from nanoindentation (**Figure 6.16**) showed unusual trend of decrease in modulus with increase in epoxy content of the resin i.e. increase in relative crosslink density. Coatings derived from Epoxy(EEVE) resins with 50 and 70 % epoxidation showed modulus values in the range of ~2.5 to 12 GPa which can be considered as practical based on the previous work carried on polymeric materials.^{34, 54, 55} Surprisingly, coatings produced from Epoxy(EEVE)-30% showed elastic modulus in the range of 30 to 200 GPa. This unexpected higher

modulus might be due to the limitations associated with nanoindentation experimentation for soft coatings compared to the reference used for calibration (quartz glass). Compared to coatings derived from 50 and 70 % epoxidized resins and EPON resin for which the indentation depth was in the range of ~350 to 900 nm, Epoly(E EVE)-30% derived coatings had displacement up to 4000 nm. This higher indentation of the tip due to softness of the coatings might also result in excessive creep that might not be overcome with 5 s loading at max force. This creep behavior can affect the initial unloading segment of the load– displacement plot which would lead to errors in computing the correct contact stiffness.⁵⁶ This overestimation might also be attributed from the material pile-up and the viscoelastic behavior which is a common problem for indentation testing of very soft coatings.⁵⁷

Values for coatings produced from Epoly(E EVE)-50% and Epoly(E EVE)-70% showed numbers in the range similar to those calculated from EPON resin. EPON resin coatings with Priamine were not tested due to their phase separation. Although coatings with aliphatic curatives showed lower numbers, an increasing trend has been observed with curing compared to coatings with aromatic, cycloaliphatic and polyether curatives which on the other hand resulted a decreasing trend with increasing curing time. These results showed that although nanoindentation is useful tool to study the hardness of polymeric coatings however, measurement of elastic modulus of relatively soft organic coatings might be tricky due to deficiencies associated with the instrumentation and also calculation assumption used in the software.⁵⁴

minimum

maximum

Epoly(E EVE)-30% (a)

Amine Curatives	Priamine	7.0	3.0	5.0	20.0
	1,8-DA Octane	5.0	5.0	3.2	27.0
	DETA	2.3	1.6	2.1	69.0
	TEPA	3.0	1.8	2.2	84.0
	Xylene DA	5.8	6.4	4.2	60.1
	1,3 BAC	3.0	2.3	4.0	85.0
	IPDA	1.9	3.2	5.7	77.0
	PACM	2.9	50.7	67.0	50.0
	XTJ-504	2.8	2.0	2.5	30.0
	Jeff. D-400	5.0	3.0	3.3	45.1
	Jeff. D-230	6.3	2.0	6.0	63.6
	Jeff. t403	9.0	1.9	3.7	95.4
		RT, 7 Days	0.5	1	3
		Curing time at 80 °C (h.)			

Epoly(E EVE)-50% (b)

Amine Curatives	Priamine	53	67	57	58
	1,8-DA Octane	168	199	243	357
	DETA	93	157	216	312
	TEPA	116	224	287	350
	Xylene DA	215	336	350	367
	1,3 BAC	236	312	363	432
	IPDA	273	300	343	355
	PACM	237	348	409	437
	XTJ-504	197	100	177	217
	Jeff. D-400	154	241	255	263
	Jeff. D-230	259	168	219	419
	Jeff. t403	200	215	275	368
		RT, 7 Days	0.5	1	3
		Curing time at 80 °C (h.)			

Epoly(E EVE)-70% (c)

Amine Curatives	Priamine	148	167	173	199
	1,8-DA Octane	185	315	369	318
	DETA	162	262	242	387
	TEPA	167	377	417	487
	Xylene DA	236	248	396	861
	1,3 BAC	298	385	482	514
	IPDA	229	423	485	573
	PACM	222	498	548	632
	XTJ-504	308	285	333	353
	Jeff. D-400	213	249	232	312
	Jeff. D-230	242	306	326	424
	Jeff. t403	235	216	299	369
		RT, 7 Days	0.5	1	3
		Curing time at 80 °C (h.)			

EPON 828 (d)

Amine Curatives	Priamine	-	-	-	-	
	1,8-DA Octane	75	229	273	245	252
	DETA	125	236	255	285	299
	TEPA	145	282	289	295	310
	Xylene DA	397	277	283	285	298
	1,3 BAC	417	291	284	288	308
	IPDA	342	262	290	354	376
	PACM	347	286	290	299	335
	XTJ-504	132	162	230	216	242
	Jeff. D-400	214	201	267	197	248
	Jeff. D-230	293	243	249	261	294
	Jeff. t403	282	259	246	249	281
		RT, 7 Days	0.5	1	3	6
		Curing time at 80 °C (h.)				

Figure 6.15. “Heat maps” for hardness (GPa) values of (a) Epoly(E EVE)-30%, (b) Epoly(E EVE)-50%, (c) Epoly(E EVE)-70% and (d) EPON 828. Coatings of Epoly(E EVE) cured for 6h. was not included in the experiment.

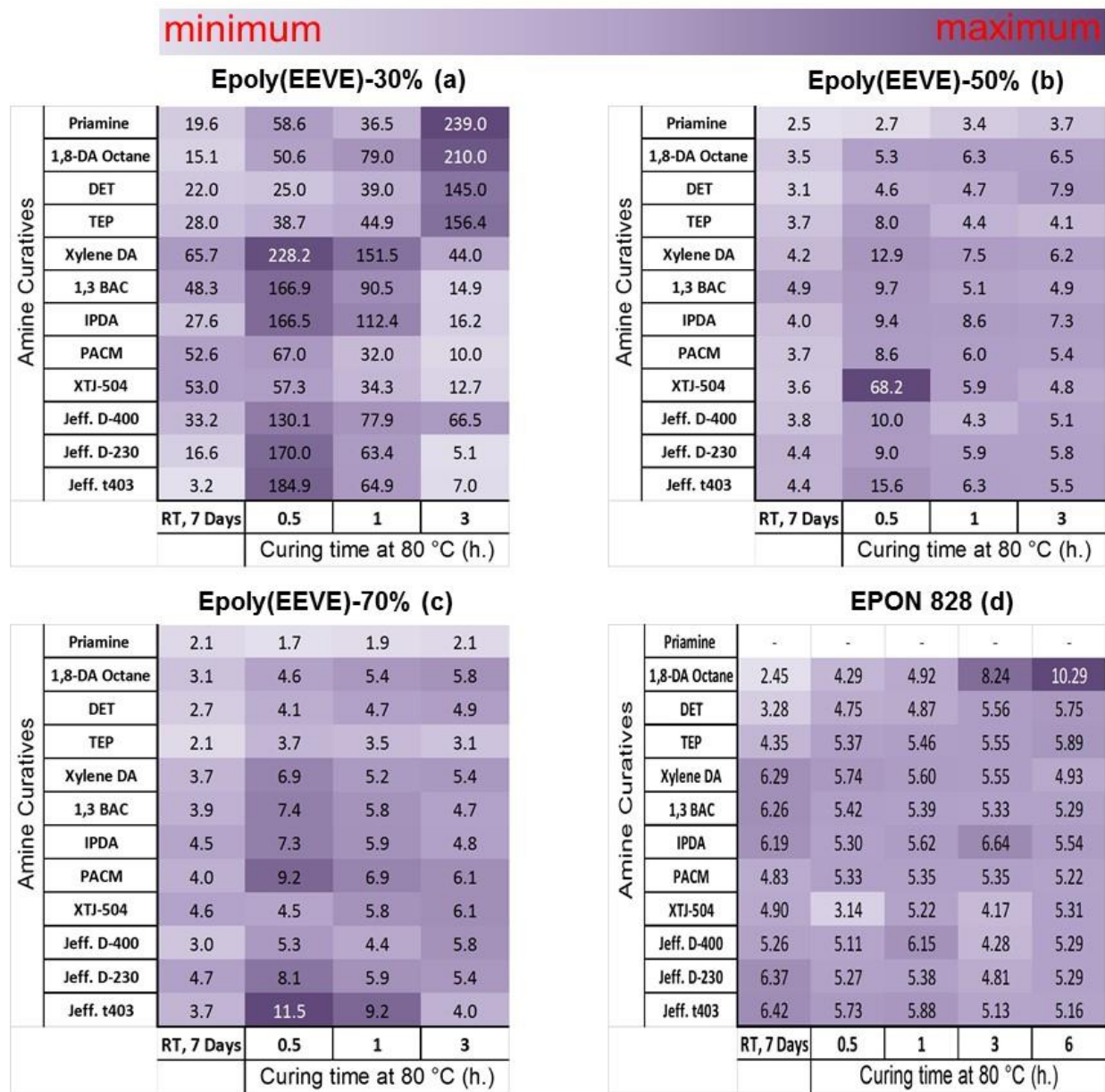


Figure 6.16. “Heat maps” for elastic modulus (GPa) values of (a) Epoly(E EVE)-30%, (b) Epoly(E EVE)-50%, (c) Epoly(E EVE)-70% and (d) EPON 828. Coatings of Epoly(E EVE) cured for 6 hours was not included in the experiment.

6.5. Conclusions

A novel bio-based vinyl ether monomer, 2-eugenoloxyl vinyl ether (EEVE) was synthesized from eugenol. Homopolymer of EEVE [poly(EEVE)] was synthesized using cationic polymerization, which derivatized to produce epoxy resins of varying amount of epoxidation from

30, 50 to 70%. Epoxidation was done using m-chloroperoxybenzoic acid under mild conditions through the allylic double bond. Quantitative conversion (error <5%) of allylic double bonds to epoxy functionality was observed. Structure-property relationships of the novel Epoly(E EVE) resins and EPON resin (reference) were evaluated via curing with twelve amine curatives. From the dye extraction results it can be concluded that compared to 30 % epoxidized resin, both 50 and 70 % epoxidized resins showed higher crosslinked density networks. This relative crosslink density of 50 % epoxidized resin was found to be slightly higher than EPON resin while keeping the curative and curing regime same. This clearly removes the necessity of high epoxy conversion for poly(E EVE) resin which usually takes significantly longer reaction time and also lead to side reactions. Hardness values obtained from both Koenig pendulum hardness and nanoindentation showed that 50 % epoxidized resin can also result in sufficiently harder coatings compared to EPON resin. Again, properties of the coatings produced from Epoly(E EVE) resins can also be tailored from soft to hard by varying the nature of amine curatives from aliphatic, polyether to cycloaliphatic, aromatic. and, or the amount of epoxy functionality. This tendency was not observed for EPON resin where coatings resulted similar hardness irrespective of curatives. Although, unexpected trend for elastic modulus was observed mostly for the coatings from 30 % epoxidized poly(E EVE) resin however, the values were found to be slightly higher for coatings from 50 % epoxidized resin with polyether and cycloaliphatic type curatives than the EPON resin for the same types of curatives.

6.6. References

1. J. M. Raquez, M. Deléglisea, M. F. Lacrampea and P. Krawczak, *Progress in Polymer Science* 2010, **35**, 487–509.

2. S. C. R. Auvergne, G. David, B. Boutevin and J. P. Pascault., *Chem. Rev.*, 2014, **114**, 1082–1115.
3. I. Novak, I. Krupa and I. Chodak, *European Polymer Journal*, 2003, **39**, 585-592.
4. M. M. Davoodi, S. M. Sapuan, D. Ahmad, A. Ali, A. Khalina and M. Jonoobi, *Materials & Design*, 2010, **31**, 4927-4932.
5. C. S. Kovash, E. Pavlacky, S. Selvakumar, M. P. Sibi and D. C. Webster, *ChemSusChem*, 2014, **7**, 2289-2294.
6. X. Pan, P. Sengupta and D. C. Webster, *green chemistry*, 2011, **13**, 965-975.
7. X. Pan, P. Sengupta and D. C. Webster, *Biomacromolecules*, 2011, **12**, 2416-2428.
8. S. Rimdusit and H. Ishida, *Polymer*, 2000, **41**, 7941-7949.
9. L. C. Salazar, M. A. G. Domingo and D. Guimaraens, *Contact Dermatitis*, 1994, **31**, 157-160.
10. C. Chen, R. S. Justice, D. W. Schaefer and J. W. Baur, *Polymer*, 2008, **49**, 3805-3815.
11. K. Mimura, H. Ito and H. Fujioka, *Polymer*, 2000, **41**, 4451-4459.
12. S. J. Park, F.-L. Jin and J. R. Lee, *Materials Science and Engineering: A*, 2004, **374**, 109-114.
13. M. Tomita and M. Murakami, *Physica C: Superconductivity*, 2000, **341-348**, 2443-2444.
14. J. M. Raquez, M. Deleglise, M. F. Lacrampe and P. Krawczak, *Progress in Polymer Science*, 2010, **35**, 487-509.
15. H. Q. Pham and M. J. Marks, in *Kirk-Othmer Encyclopedia of Chemical Technology*, John Wiley & Sons, Inc., 2000.
16. I. Faye, M. Decostanzi, Y. Ecochard and S. Caillol, *Green Chemistry*, 2017, **19**, 5236-5242.

17. T. N. Inguan and E. H. Silaka. Bisphenol A, National Institute of Health, Research Triangle Park, North Carolina, 2010.
18. A. D. C. Buff and M. Ibert, Rowuette Freres, Lestrem, France, US 2017/0002132 A1, 2017, pp 8.
19. L. N. Vandenberg, R. Hauser, M. Marcus, N. Olea and W. V. Welshons, *Reprod. Toxicol.*, 2007, **24**, 139-177.
20. E. A. Baroncini, S. K. Yadav, G. R. Palmese and J. F. Stanzione, *Journal of Applied polymer science*, 2016, **133**, 44103-44122.
21. C. Aouf, H. Nouailhas, C. L. Guerneve, S. Caillol, B. Boutevin and H. Fulcrand., *J. Polym. Sci., Part A: Polym. Chem. Eng. Corn.*, 2011, **49**, 2261–2270.
22. E. Darroman, N. Durand., B. Boutevin and S. Caillol, *Prog. Org. Coat.*, 2016, **91**, 9-16.
23. C. Voirin, S. Caillol, N. V. Sadavarte, B. V. Tawade, B. Boutevin and P. P. Wadgaonkar, *Polym. Chem.*, 2014, **5**, 3142-3162.
24. M. Fache, B. Boutevin and S. Caillol, *Eur. Polym. J.*, 2015, **68**, 488–502.
25. J. R. Mauck, S. K. Yadav, J. M. Sadler, J. J. La Scala, G. R. Palmese, K. M. Schmalbach and J. F. Stanzione, *Macromol. Chem. Phys.*, 2017, **218**, 1700013–1700022.
26. B. G. Harvey, C. M. Cahagun, A. J. Guenther, T. J. Groshens, L. R. Cambrea, J. T. Reams and J. M. Mabry, *ChemSusChem*, 2014, **7**, 1964–1969.
27. G. S. Martin, E. A. Vara and J. C. Duarte, *Ind. Crops Prod.*, 2008, **27**, 189-195.
28. P. Prakash and A. N. Gupta, *Indian J Physiol Pharmacol.*, 2005, **49**, 125–131.
29. G. W. Gould, *Journal of Food Protection*, 1996, **59**, 82-86.
30. W. G. Larsen, *Journal of the American Academy of Dermatology*, **12**, 1-9, 1985.

31. S. R. Shanthun-Al-Arefin, S. Rahman, M. Akter, M. Munmun and M. A. Kalpana, *Advances in Natural and Applied Sciences*, 2012, **6**, 1496-1507.
32. Z. Sun, B. Fridrich, A. D. Santi, S. Elangovan and K. Barta, *Chemical Reviews Article ASAP*.
33. B. J. Chisholm and D. C. Webster, *Journal of Coatings Technology and Research*, 2007, **4**, 1-12.
34. J. M. Kranenburg, C. A. Tweedie, R. Hoogenboom, F. Wiesbrock, H. M. L. Thijs, C. E. Hendriks, K. J. Van Vliet and U. S. Schubert, *Journal of Materials Chemistry*, 2007, **17**, 2713-2721.
35. S. Stafslie, J. Daniels, B. Chisholm and D. Christianson, *Biofouling*, 2007, **23**, 37-44.
36. H. Bach, C. Gurtler and S. Nowak, *Farbe Lack*, 2002, **108**, 30.
37. H. Bach, C. A. Gambino, P. D. Lunney and D. A. Wicks, in *High-Throughput Analysis: A Tool for Combinatorial Materials Science*, eds. R. A. Potyrailo and E. J. Amis, Springer, US, Boston, MA, 2003, pp. 525-549.
38. J. M. Kranenburg, H. M. L. Thijs, C. A. Tweedie, S. Hoepfener, F. Wiesbrock, R. Hoogenboom, K. J. Van Vliet and U. S. Schubert, *Journal of Materials Chemistry*, 2009, **19**, 222-229.
39. S. Alam and B. J. Chisholm, *Journal of Coatings Technology and Research*, 2011, **8**, 671-683.
40. S. Aoshima and T. Higashimura, *Macromolecules*, 1989, **22**, 1009-1013.
41. P. Drefuss and J. P. Kennedy, *Analytical Chemistry*, 1975, **47**, 771-774.
42. A. Chernykh, S. Alam, A. Jayasooriya, J. Bahr and B. J. Chisholm, *Green Chemistry*, 2013, **15**, 1834-1838.

43. S. Alam, H. Kalita, A. Jayasooriya, S. Samanta, J. Bahr, A. Chernykh, M. Weisz and B. J. Chisholm, *European Journal of Lipid Science and Technology*, 2014, **116**, 2-15.
44. H. Kalita, S. Samanta, A. Jayasooriyamu, S. Fernando, S. Samanta, J. Bahr, S. Alam, M. Sibi, J. Vold, C. Ulven and B. J. Chisholm, *Green Chemistry*, 2014, **16**, 1974-1986.
45. H. Kalita, S. Alam, A. Jayasooriyamu, S. Fernando, S. Samanta, J. Bahr, S. Selvakumar, M. Sibi, J. Vold, C. Ulven and B. J. Chisholm, *Journal of Coatings Technology and Research*, 2015, **12**, 633-646.
46. H. Kalita, S. Alam, D. Kalita, A. Chernykh, I. Tarnavchyk, J. Bahr, S. Samanta, A. Jayasooriyama, S. Fernando, S. Selvakumar, D. S. Wickramaratne, M. Sibi and Bret J. Chisholm, *European Coatings Journal*, 2015, **6**, 26-29.
47. H. Kalita, A. Jayasooriyama S. Fernando and B. J. Chisholm, *Journal of Palm Oil Research*, 2015, **27**, 39-56.
48. D. Kalita, I. Tarnavchyk, D. Sundquist, S. Samanta, J. Bahr, O. Shafranska, M. Sibi and B. Chisholm, "Novel biobased poly(vinyl ether)s for coating applications, *INFORM*, 2015, **26**, 472-475
49. B. J. Chisholm, H. Kalita, D. Kalita, S. Alam, A. Chernykh, I. Tarnavchyk, J. Bahr, S. Samanta, A. Jayasooriyama, S. Fernando, S. Selvakumar, D. S. Wickramaratne and M. Sibi, *Coatings World*, 2015, **20**, 48-54.
50. H. Kalita, S. Alam, D. Kalita, A. Chernykh, I. Tarnavchyk, J. Bahr, S. Samanta, A. Jayasooriyama, S. Fernando, S. Selvakumar, A. Popadyuk, D. S. Wickramaratne, M. Sibi, A. Voronov, A. Bezbaruah and B. J. Chisholm, *ACS Symposium Series*, 2014, **1178**, 731-790.

51. J. M. Kranenburg, H. M. L. Thijs, C. A. Tweedie, S. Hoepfener, F. Wiesbrock, R. Hoogenboom, K. J. Van Vliet and U. S. Schubert, *Journal of Materials Chemistry*, 2009, **19**, 222-229.
52. R. V. Gorkum and E. Bouwman, *Coord. Chem. Rev.*, 2005, **249**, 1709-1728.
53. A. L. Agapov, Y. Wang, K. Kunal, C. G. Robertson and A. P. Sokolov, *Macromolecules*, 2012, **45**, 8430-8437.
54. M. R. V. Landingham, J. S. Villarrubia, W. F. Guthrie and G. F. Meyers, *Macromolecular Symposia*, 2001, **167**, 15-44.
55. B. Lucas, C. Rosenmayer and W. Oliver, Materials Research Society proceedings, **97**, San Francisco Marriott Hotel, San Francisco, California, 1997.
56. Y. C. Lu, G. P. Tandon, D. C. Jones and G. A. Schoeppner, *Mechanics of Time-Dependent Materials*, 2009, **13**, 245-260.
57. M. Hardiman, T. J. Vaughan and C. T. McCarthy, *Polymer Testing*, 2016, **52**, 157-166.

CHAPTER 7. CONCLUSIONS AND FUTURE DIRECTIONS

7.1. Conclusions

Novel linear chain growth polymers have been synthesized from vinyl ether monomers developed from renewable resources having pendent groups with functionality that can be used for post curing.

Novel plant oil based vinyl ether (POVE) monomers from soybean, linseed and camelina oil were synthesized and a series of homopolymers varying in molecular weight and composition were synthesized using cationic polymerization. A decreasing trend of viscosity was observed with increasing the PO unsaturation due to their *cis* configuration. Study of the viscoelastic properties and mechanical properties of the cured films produced from relatively moderate and relatively high MW polymers resulted that at a given polymer MW, T_g , XLD, Young's modulus, and tensile strength all increased with increasing unsaturation in the parent PO. For example, films derived from poly(2VOES) with M_n 14kDa resulted T_g , plateau modulus and XLD of -14.5 °C, 1.242 MPa and 1.926×10^{-4} cm³/mole whereas, cured films from poly(2VOEL) with M_n 14kDa showed numbers -7 °C, 3.138 MPa, 4.73×10^{-4} cm³/mole respectively. Similar trend in coating hardness, solvent resistance, and impact resistance had been observed with unsaturation in fatty acid composition of parent oil and were consistent with the viscoelastic property results.

Another set of colorless poly(POVEs) has been produced from linseed oil, soybean oil and palm oil by distilling the POVE monomers removing the colored impurities. These polymers then evaluated as a binder (drying time and yellowness) for artist paint to generate coatings with white or pale colorant compare to linseed oil. As derived poly(vinyl ether)s (POVEs) provides several advantages over traditional drying oils as a binder. Poly(POVE)s produced from semi-drying oils, such as soybean oil, palm oil showed faster dry/cure along with dramatically lower yellowness

than linseed oil. The viscosity and drying time of poly(POVE)s can be easily tailored by tailoring molecular weight without affecting other properties.

Novel, vinyl ether monomers were also produced cardanol (CEVE) and eugenol (EEVE), renewables with phenolic functionality. Homopolymers of CEVE and EEVE were synthesized using cationic polymerization and their T_g s were confirmed at subzero temperatures. Copolymers with 25 and 50 wt.% cyclohexyl vinyl ether (CHVE) were produced to improve the T_g s and was found successful. For the first time, ability of poly(EEVE) and copolymers to undergo autoxidation through allylic functionality has been demonstrated using FTIR. Coatings and free films cured via autoxidation at RT and elevated temperatures were prepared from the polymers and their properties were compared commercial alkyds. Evaluation of the coatings and free films cured at RT, confirmed the formation of highly crosslinked networks attributing to higher elastic modulus and hardness increasing with amount of CHVE comonomer and curing temperature than commercial alkyds. Surprisingly higher solvent resistance and hydrolytic stability were reported than alkyd coatings, and is attributed to the presence of aromatic functionality and carbon-carbon backbone rather than polyester backbone of alkyds. Curing at elevated temperatures further improved coating and film properties. These results clearly indicate the potential of these polymers for producing alkyd type air drying coatings with higher end performance.

Epoxidized poly(EEVE) was produced with varying epoxy levels (30%, 50% and 70%) via derivatizing allylic double bond. These novel epoxy polymers were cured with twelve different amine curatives and their properties were screened using high throughput experimentation. For comparison similar experimentations were performed with BPA based epoxy resin and the results showed that depending of the epoxidation level and structural feature of the amine curative coatings with varying crosslink density, hardness (pendulum and reduced), elastic modulus and T_g

can be obtained from poly(EEVE) based epoxies and most of the formulations with epoxy level 50 to 70 % showed better results than BPA based epoxy resin. Also, coatings from the EPON were much brittle with very less tunability of properties using various crosslinker.

7.2. Future research directions

Research work presented in this dissertation can provide a platform for future researches that can expand beyond air drying and epoxy amine cured coatings.

1. Synthesis of copolymers from POVEs with various suitable comonomers such as maleic anhydride, acrylonitrile etc. via free radical polymerization technique and their study for air drying coating. These monomers should increase the modulus of the free films and also hardness of the coatings and also adhesion due to presence of polar groups.
2. Copolymerization of POVEs with poly(ethylene glycol) ethyl vinyl ether and their application in waterborne coating.
3. Synthesis of vinyl ether monomers from lignin derived phenolic materials such as guaiacol and syringol and their utilization as rigid comonomer instead of CHVE with EEVE to increase the bio-based content and study of their air-drying coating. Both syringol and guaiacol are commercially available from lignin which makes them economically viable.
4. Epoxidation of copolymers derived from EEVE with guaiacol or syringol vinyl ether and study of their amine, anhydride cured coatings. Also, synthesis of polyols from these copolymers and formation of polyurethane networks using isocyanate curing agents.

5. Further validation of high throughput methods to evaluate coating properties with small amount of materials.